Unraveling EWS/FLI1 Protein Turnover: Therapeutic Potential of the Ubiquitin System in Ewing Sarcoma Pathogenesis

---

Dissertation

zur

Erlangung der naturwissenschaftlichen Doktorwürde
(Dr. sc. nat.)

vorgelegt der

Mathematisch-naturwissenschaftlichen Fakultät

der

Universität Zürich

von

Maria Elka Gierisch

aus

Deutschland

Promotionskomitee

Prof. Dr. Beat W. Schäfer (Vorsitz)

PD Dr. Stefano Ferrari

Prof. Dr. Felix K. Niggli

Zürich, 2016

To Lina and her family.

Table of contents

Summary 6
Zusammenfassung 8
1. Introduction 10
1.1. Pediatric cancers 11
1.1.1. Cancer in childhood and adolescents – epidemiology, incidence and survival 11
1.1.2. Childhood cancer survivors 13
1.1.3. The genomic landscape of pediatric tumors 13
1.1.4. Translocation derived tumors 14
1.1.5. Sarcoma – epidemiology, classification and treatment 14
1.1.6. Targeted therapies in sarcoma 16
1.2. Ewing sarcoma 17
1.2.1. Epidemiology and survival 17
1.2.2. Treatment modalities 17
1.2.2.1. Prognostic markers 18
1.2.2.2. Clinical trials 19
1.2.2.3. EWING2008- the largest European study 20
1.2.3. Underlying genetics of Ewing sarcoma tumors 20
1.2.3.1. The EWS/FLI1 fusion protein 22
1.2.3.2. EWS/FLI1 target genes 22
1.2.4. Cell cycle deregulation in Ewing sarcoma 23
1.2.5. EWS/FLI1 interacting proteins 24
1.2.6. The ETS family and cancer 25
1.2.7. The ETS member FLI1 25
1.2.8. EWSR1 full length protein 26
1.2.9. The Ewing sarcoma cell of origin and tumor models 26
1.2.10. Drug screenings to identify new therapeutic targets for Ewing sarcoma treatment 27
1.2.11. Challenges and opportunities for novel treatment strategies 28
1.2.12. Turnover in Ewing sarcoma pathogenesis 29
1.3. The ubiquitin proteasome system 30
1.3.1. A historical overview 30
1.3.2. Mechanism of intracellular proteolysis 31
1.3.3. Proteasomal degradation 31
1.3.4. The process of protein ubiquitination 31

1.3.5. The ubiquitin code ... 33
1.3.6. E3 ligases ... 34
1.3.6.1. Cullin-RING ligases ... 34
1.3.6.2. HECT E3 ligases ... 34
1.3.6.3. WWP1 ... 35
1.3.6.4. U-box domain E3 ligases ... 35
1.3.7. Deubiquitinating enzymes ... 36
1.3.8. Ubiquitin specific protease 19 (USP19) ... 38
1.4. The role of the ubiquitin system in cancer ... 39
1.4.1. Deregulation of UPS components in cancer ... 39
1.4.2. UPS associated targeting for cancer therapy ... 40
1.4.3. Inhibitors of the ubiquitin system in clinics ... 42
1.4.4. Degradation of fusion proteins as a novel strategy in targeted therapy ... 43
1.4.4.1. Degradation of ERG and ERG fusions in prostate cancer ... 43
1.4.4.2. Selective degradation of PML/RARα in acute promyelocytic leukemia therapy ... 44
1.4.5. Ewing sarcoma – therapeutic potential of UPS targeted therapy ... 45
2. Aims ... 46
3. Results ... 48
4. Manuscript I ... 49
Abstract ... 51
Introduction ... 51
Results ... 52
Discussion ... 54
Experimental procedure ... 56
References ... 59
Figure Legends ... 63
Figures ... 65
Supplementary information ... 71
5. Manuscript II ... 78
Abstract ... 79
Introduction ... 80
Materials and Methods ... 81
Results ... 83
Discussion ... 86
References ... 88

Figures 90
Supplementary tables 95
6. Manuscript III 96
Abstract 98
Introduction 99
Material and methods 100
Results 103
Discussion 106
References: 109
Figures and Figure Legends 111
Supplementary figures 119
Supplementary tables 125
7. Discussion 127
7.1. Targeting the ubiquitin system – current state and future opportunities 128
7.1.1. The developing field of ubiquitin drug targets 128
7.1.2. Chemical inducers of protein degradation 129
7.1.3. Therapy induced targeting – PML/RARα as a model for EWS/FLI1 131
7.2. EWS/FLI1 stability and turnover 133
7.2.1. Global Protein Stability profiling to dissect proteolytic turnover 133
7.2.2. Proteasomal degradation of EWS/FLI1 – common for other ETS members? 134
7.2.3. Control of TFs by the proteasome system 135
7.3. Identification of relevant Ewing sarcoma targets for ubiquitin-based drug treatments 137
7.3.1. EWS/FLI1 regulation by E3 ligases and their potential for therapy 137
7.3.2. Destabilization of proteins – DUB inhibition as a promising approach? 137
7.4. A novel therapeutic strategy: degradation of EWS/FLI1 protein 139
8. References 140
9. Acknowledgements 165
10. Appendix 167

Summary

Ewing sarcoma is a rare pediatric bone and soft tissue tumor with an aggressive behavior and a prevalence to metastasize. The 5-year survival rate for the localized disease is around 70% while for patients with metastasis it is less than 40%. Ewing sarcoma is characterized by a balanced translocation of the *EWSR1* gene on chromosome 22 and *FLI1* gene on chromosome 11 leading to expression of the aberrant EWS/FLI1 oncoprotein. Sequencing of Ewing sarcoma tumors revealed that the fusion protein is the only consistent genetic alteration despite apart from few secondary mutations. The EWS/FLI1 protein modulates a variety of target genes and protein-protein interactions. As the transcription factor is unique for Ewing sarcoma cells, it serves as an ideal therapeutic target. Protein turnover is mainly mediated by the ubiquitin proteasome system. An enzymatic cascade of three enzymes transfers a ubiquitin to a target protein. The linkage of the polyubiquitin chain determines if proteins are degraded by the proteasome or involved in signaling events. The chains can be modified or removed by deubiquitinating enzymes. EWS/FLI1 ubiquitination has barely been investigated even though it might be of therapeutic relevance. In this thesis, we aim to investigate the mechanisms of EWS/FLI1 degradation and identify regulators of the ubiquitin pathway as targets for therapeutic interventions.

We first characterized EWS/FLI1 as a polyubiquitinated substrate of the proteasome system. By using Global Protein Stability profiling, we determined the turnover rate of EWS/FLI1 as faster compared to both full length proteins EWSR1 and FLI1. Mass spectrometry analysis revealed two ubiquitin acceptor sites within EWS/FLI1 of which only mutation of the K380 residue in the DNA-binding domain abolished ubiquitination and posttranslationally stabilized the protein. By comparing the transcriptional activation properties of wild type EWS/FLI1 and its turnover deficient mutant, we identified the majority of target genes as saturated. Further, one subgroup of target genes was increased by higher fusion protein levels whereas a second subgroup was partly dependent on continuous fusion protein turnover. Both subgroups were consisting of protein and RNA coding genes. We identified EWS/FLI1 turnover as an important and critical pathway for Ewing sarcoma pathogenesis.

We then aimed at understand how EWS/FLI1 is ubiquitinated and which E3 ligase(s) mediate stability. We identified the N-terminal PPxY motif as critical for E3 ligase binding. Mutation of this site decreased ubiquitination and stabilized the fusion protein. As only NEDD4 family members, a subgroup of HECT E3 ligases, are binding this motif, we screened all members for their ability to destabilize EWS/FLI1. Most consistently, WWP1 negatively regulated EWS/FLI1 protein levels. This interaction was partly abolished upon mutation of the PPxY domain. On a physiological level, WWP1 overexpression slightly decreased Ewing sarcoma cell growth and colony formation. Hence, we characterized a novel E3 ligase binding motif in the fusion protein leading to deepen our understanding of the molecular mechanisms underlying EWS/FLI1 turnover.

To identify potential inhibitory targets within the EWS/FLI1 turnover machinery, we screened for deubiquitinating enzymes capable to mediate fusion protein stability. We identified ubiquitin specific protease 19 as a main candidate. Depletion of USP19 directly destabilized the protein and modulated a subset of target genes. This effect was accompanied by an increase in EWS/FLI1 ubiquitination. On a cellular level, USP19 knockdown delayed tumor growth both *in vitro* and *in vivo*. Hence, we

demonstrate that destabilization of EWS/FLI1 can be achieved by inhibition of deubiquitinating enzymes which is a new and promising strategy for Ewing sarcoma therapy.
Within these studies, we unraveled the turnover of the EWS/FLI1 fusion protein and identified the E3 ligase WWP1 and the deubiquitinating enzyme USP19 as potential targets for novel therapeutic strategies. As current treatment protocols include only non specific chemotherapeutics, combinations with agents directly destabilizing the main driver EWS/FLI1 present a promising approach and another step towards targeted therapies in Ewing sarcoma.

Zusammenfassung

Ewing Sarkoma ist ein seltener pädiatrischer Knochen- oder Weichegewebetumor, der ein aggressives Verhalten zeigt und häufig metastasiert. Die 5-Jahres Überlebensrate liegt für einen begrenzten Tumor bei ungefähr 70% gegenüber 40% für Patienten mit Metastasen. Ewing Sarkoma zeichnet sich durch eine ausbalancierte Translokation des *EWSR1* Gens auf Chromosom 22 und des *FLI1* Gens auf Chromosom 11 aus, das zur Expression des abnormalen EWS/FLI1 Onkoproteins führt. Sequenzierungen von Ewing Sarkoma Tumoren haben ergeben, dass das Fusionsprotein neben einigen wenigen sekundären Mutationen die einzige konsistente gentische Veränderung darstellt. Das EWS/FLI1 Protein reguliert eine Vielzahl an Zielgenen und Protein-Protein-Interaktionen. Da der Transkriptionsfaktor einzigartig ist für Ewing Sarkoma Zellen, stellt es ein ideales Ziel dar. Der Proteinabbau ist hauptsächlich über das Ubiquitin-Proteasome-System reguliert. Eine enzymatische Kaskade von drei Enzymen überführt ein Ubiquitin auf das Substratprotein. Die Verbindung der Multiubiquitinketten bestimmt, ob das Protein über das Proteasom abgebaut wird oder sich an Signaltransduktionen beteiligt. Die Ketten können von Hydrolasen verändert oder entfernt werden. Die EWS/FLI1 Ubiquitinierung wurde bis jetzt kaum erforscht, obwohl es von potenzieller therapeutischer Relevanz ist. In dieser Dissertation beabsichtigen wir die Mechanismen des EWS/FLI1 Proteinabbaus zu untersuchen und mögliche Regulatoren aus der Ubiquitingruppe für therapeutische Ziele zu identifizieren.

Zuerst haben wir das EWS/FLI1 Protein als multiubiquitiniertes Substrat des Proteasome Systems charakterisiert. Durch die Globale-Protein-Stabilitätsanalyse konnten wir eine schnellere Abbaurate von EWS/FLI1 gegenüber den vollständigen EWSR1 und FLI1 Proteinen zeigen. Die Massenspektrometrie Analyse ergab, dass EWS/FLI1 an zwei Stellen Ubiquitin binden kann. Nur eine Mutation der K380 Seite in der DNS-Bindungsdomäne beseitigt die Ubiquitinierung und führt zu einer posttranslationalen Stabilisierung des Proteins. Ein Vergleich der transkriptionalen Aktivität vom Wildtypprotein und der Abbaumutante ergab, dass der Grossteil der Zielgene in einem gesättigten Zustand vorliegt. Weiterhin gibt es jedoch eine Untergruppe von Zielgenen, deren Expressionen nur bei hohem Proteinniveau erhöht ist sowie eine zweite Untergruppe, die von konstanten EWS/FLI1 Abbauraten abhängig ist. Beide Untergruppen bestehen aus Protein kodierenden und RNS kodierenden Genen. Zusammenfassend haben wir den Abbau des EWS/FLI1 Proteins als wichtigen und kritischen Weg in der Ewing Sarkoma Krankheitsentstehung beschrieben.

Als nächstes haben wir versucht zu verstehen, wie das EWS/FLI1 Protein ubiquitiniert und durch welche E3 Ligase(n) die Stabilität beeinflussen wird. Dazu haben wir das N-terminale PPxY Motiv als kritische E3 Bindungsstelle gefunden. Eine Mutation dieser Seite verringert die Ubiquitinierung und stabilisiert das Fusionsprotein. Da nur die NEDD4 Proteinfamily als Untergruppe der HECT E3 Ligasen an dieses Motiv binden, haben wir alle Mitglieder auf ihre destabilisierende Wirkung für das EWS/FLI1 Protein überprüft. Am konsistentesten regulierte WWP1 die EWS/FLI1 Proteinlevel. Diese Interaktion konnte teilweise verhindert werden, wenn das PPxY Motiv mutiert vorlag. Physiologisch wird durch eine WWP1 Überexpression das Ewing Sarkoma Zellwachstum und die Koloniebildung leicht vermindert. Daher konnten wir ein neues E3 Ligase Bindungsmotiv für das Fusionsprotein beschreiben, dass das Verständnis für Abbauvorgänge des EWS/FLI1 Proteins klar vertieft.

Um nun potenzielle hemmende Ziele im Abbaumechanismus des EWS/FLI1 Proteins zu finden, haben wir die Hydrolase gesucht, die die Stabilität des Fusionsproteins beeinflusst und so die Hydrolase USP19 als Hauptkandidat gefunden. Die USP19 Hemmung führt zur direkten Destabilisierung des Proteins und verändert so auch die Expression von Zielgenen. Dieser Effekt wurde begleitet von einer erhöhten Ubiquitinierung des Fusionsproteins. Auf zellulärer Ebene führt die USP19 Reduzierung zu einem verminderten Tumorwachstum *in vitro* und *in vivo*. Damit zeigen wir auf, dass die Destabilisierung des EWS/FLI1 Proteins durch Hemmung von

Hydrolasen erreicht werden kann. Dies stellt eine neue und vielversprechende Strategie in der Ewing Sarkoma Therapie dar.

Mit diesen Studien konnten wir die Abbauprozesse des EWS/FLI1 Fusionsproteins detailliert aufzeigen und haben die E3 Ligase WWP1 sowie die Hydrolase USP19 als potentielle Ziele einer neuen therapeutischen Strategie identifiziert. Da aktuelle Behandlungsprotokolle nur unspezifische Chemotherapeutika beinhalten, würde die Kombinationen mit Mitteln, die das Hauptprotein EWS/FLI1 direkt destabilisieren, einen weiteren wichtigen Schritt zu einer zielgerichteten Therapie in Ewing Sarkoma darstellen.

1. Introduction

1.1. Pediatric cancers

1.1.1. Cancer in childhood and adolescents – epidemiology, incidence and survival

Cancer is a global and heterogeneous disease with many faces. It generally does not discriminate between age, country, race or gender (with the exception of reproductive system specific tumors). A total of 1'658'370 new cancer cases and 589'430 cancer deaths have been reported in the United States in 2015 (1). In Switzerland, around 35'000 people are diagnosed with cancer and more than 16'000 cases result in death per year (2). However, around 1% of all newly diagnosed cases occur in children and adolescents in developed countries (3). In Switzerland, about 170 cases with various cancer subtypes are diagnosed every year in children and 37 cancer-related deaths are reported (Fig. 1A, registered by the Federal Statistical Office (FSO), the National Institute for Cancer Epidemiology and Registration (NICER) and the Swiss Childhood Cancer Registry (SCCR)). Despite the low total numbers, pediatric cancers are the second most common cause of death in children only outreached by accidents (1, 3), (4). In the US, the overall incidence rate over the last five years (reported for 2007-2011) for all cancers declined by 1.8% per year in men, remained stable in woman and adolescents while it increased in children by 0.6% (1).

The spectrum of cancer is fairly different between children, adolescents and adults (Fig. 1B). While carcinomas like breast, lung, prostate, and colorectal cancers are predominant in adults; especially leukemia, brain and solid tumors arise most commonly in children (2, 4). Although acute lymphoblastic leukemia can occur in all age groups, it is presenting with specific subtypes and with high incidence rates in children (1, 5). Further, medulloblastoma or a variety of predominantly pediatric sarcoma subtypes like rhabdomyosarcoma, Ewing sarcoma, osteosarcoma and Wilms tumor can arise in adults, but are extremely rare (6).
Pediatric cancers are classified into twelve subgroups (Fig. 1C). The most common subtypes in the age range from 1-14 years are acute lymphoblastic leukemia (26%), tumors of the central nervous system (21%), neuroblastoma (7%) and non-Hodgkin lymphoma (6%) (5). Similar numbers and incidences have been reported for Switzerland by the most recent SCCR report (SCCR report 2014). In adolescents (15-19 years), Hodgkin lymphoma (15%), thyroid tumors (11%) and tumors of the brain and the central nervous system (10%) are predominant (5, 7). Furthermore, the outcome of several cancers as acute lymphoblastic leukemia, Ewing sarcoma or kidney tumors are worse than for the younger age group (7).

The survival rate for pediatric cancers is with around 80% much higher than in adults. The 5-year relative survival rate for children and adolescents for all cancers combined has dramatically increased from 61.7% in 1975–1977 to 81.4% in 1999–2006 analyzed by the SEER (Surveillance, Epidemiology and End Results) program of the National Cancer Institute (seer.cancer.gov). However, the outcome is still very heterogeneous within pediatric tumors (Fig. 1D) and highly depends on the disease state, genetic abnormalities and the age of the patient (8). Best survival rates with ≥90% have been reported for acute lymphoblastic leukemia, non-Hodgkin lymphoma and Hodgkin lymphoma (9). Even though

the survival rate is still improving for leukemia and lymphomas, the rates for solid tumors have reached a plateau since ten years (5). Ewing sarcoma stagnates at a survival rate of 72% and even lower numbers are reported for osteosarcoma (71%) and rhabdomyosarcoma (64%) (1, 5, 9).

Treatment of pediatric patients generally includes cytotoxic chemotherapy, radiotherapy and surgery in the case of solid tumors. However, the exact treatment protocols are tumor-type dependent and can slightly vary between Europe and the US. The good survival rates for most pediatric cancers result from continuous efforts of prospective clinical trials, improved risk assessment and supportive care (8). However, treatment related toxicity and adverse side effects are still the most challenging problems for childhood cancer survivors.

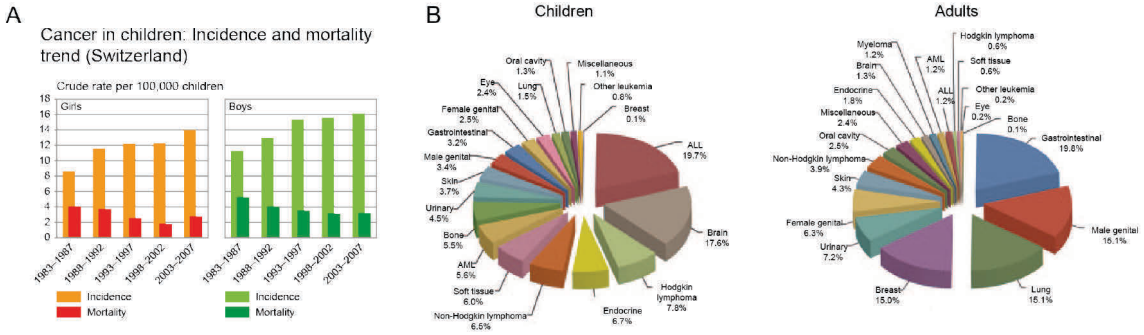

D Pediatric Cancer 5-Year Observed Survival Rates <19years (SEER statistics, US)

	YEAR OF DIAGNOSIS	
	1975-1979	2003-2009
All ICCC sites	**63%**	**83%**
Leukemia	48%	84%
Acute lymphocytic leukemia	57%	90%
Acute myeloid leukemia	21%	64%
Lymphoma	72%	91%
Hodgkin lymphoma	87%	97%
Non-Hodgkin lymphoma	47%	85%
Barin and central nervous system	59%	75%
Ependymoma	37%	81%
Astrocytoma	69%	85%
Medulloblastoma	47%	70%
Neuroblastoma	54%	79%
Retinoblastoma	92%	99%
Wilms tumor	75%	90%
Hepatic tumor	25%	74%
Bone tumor	49%	73%
Osteosarcoma	45%	71%
Ewing sarcoma	42%	72%
Rhabdomyosarcoma	49%	64%
Thyroid carcinoma	99%	98%
Melanoma	83%	95%

Fig. 1: The distribution, incidence and survival rates of pediatric cancers. (A) The incidence of childhood cancer is increasing from the early 1990s till 2007 for both genders while the mortality rate is dropping in Switzerland (modified after (2, 4)). (B) The spectrum of tumors highly differs between children (left) and adults (right). The graph chart represents the cancer distribution of the 2012 SEER data (6). (C) Childhood cancer distribution within the age groups in Switzerland. Cancers are classified within nine subgroups. The surfaces are proportional to the number of cases (modified after (2, 4)). (D) Comparison of 5-year survival rates for pediatric cancers for two time periods, data include 9 SEER registries until 2010 (5). ICCC=International Classification of Childhood Cancers.

1.1.2. Childhood cancer survivors

Children who survived a pediatric cancer may still be influenced many years after diagnosis by treatment related long-term side effects. Secondary malignant neoplasms are much more likely for childhood cancer survivors than in adult cancer patients. A 30 year follow-up study (1970-1986) of the Childhood Cancer Survivor Study (CCSS) cohort in the US was showing a generally increased incidence of 9.3% for secondary malignancies (10). However, the risk highly depends on the subtype of the primary cancer and the use of radiotherapy in first line treatment. Another study of the CCSS cohort assessed the risk of late mortality for childhood cancer survivors. Generally, the incidence of mortality caused by recurrence or the primary disease declined while death rates increased due to secondary neoplasms, cardiac death and other treatment related causes. The overall cumulative mortality rate at 30 years after diagnoses was 18.1%, identifying long-term morbidity as a serious issue for later life (11).

Clinically focused monitoring of childhood cancer survivors is highly necessary for secondary malignancies and general health issues as results of cancer treatment early in life. It is hoped that improved treatment protocols and newly discovered chemotherapies will decrease the risk for secondary malignancies and health problems in the future.

1.1.3. The genomic landscape of pediatric tumors

Cancer genomes are largely characterized by genomic instability, accumulation of gene mutations and epigenetic changes driving tumor initiation, progression and maintenance. The hallmarks of cancer are summarizing the most crucial pathways manipulated by tumor cells to ensure their own survival and spreading throughout the human body (12, 13). In most adult cancers, an accumulation of mutations is giving rise to tumor formation (14). It has been shown first for colorectal cancer that a sequential series of mutations resulting in activated oncogenes or loss of critical tumor suppressor genes leads to the progression of benign lesions to a malignant phenotype (15). Since then, various efforts have been done to characterize the human cancer genome. The identification of numerous different mutations even within the same tumor subtype revealed that not all mutations are causing cancer. So-called “driver” mutations conferred a growth advantage to cancer cells whereas “passenger” mutations do not (14, 16). Driver mutations are found with a high incidence in distinct tumor entities, but are more infrequent in others suggesting certain heterogeneity in adult cancers (17, 18). Nevertheless, there is a clear variation in the mutational landscape of all tumor types. Tumors such as gastric, lung or colorectal cancer are highly subjected to exogenous mutagen exposure. They exhibit a high prevalence for accumulation of somatic mutations due to their high cellular turnover rate and an epithelial surface. Several melanoma and lung cancer subtypes display more than 1000 mutations per mega base (Mb) DNA (18, 19).

In contrast, pediatric cancers are characterized by a low frequency of mutations with usually less than one mutation/ Mb DNA (Fig. 2A). Ewing sarcoma has one of the lowest mutation frequencies of all pediatric cancers with less than 0.1 mutation/ Mb DNA (16, 19). The Pediatric Cancer Genome Project reported that mainly structural alterations such as inter- and intrachromosomal rearrangements are

common mechanism of mutagenesis in pediatric leukemia and solid tumors rather than accumulation of several mutational events. Further, whole-genome sequencing revealed that the spectrum of mutations underlying pediatric cancers is very different from adult cancer, even though they may have a similar histology (6). Overall, the genomics of pediatric cancers are highly distinct from adult cancers. While an accumulation of driver mutations is most commonly the cause of adult tumor development, pediatric lesions are thought to arise within developing tissues with high frequency of chromosomal rearrangements.

1.1.4. Translocation derived tumors

The Philadelphia chromosome in chronic myelogenous leukemia was the first described chromosomal rearrangement (20, 21). Later, it was precisely characterized as a reciprocal translocation involving chromosomes 9 and 22 leading to the BCR/ABL fusion gene (22). Generally, translocations and gene fusions are prominent in pediatric leukemias and solid tumors, but can also occur in carcinomas. A total of 352 gene fusions have been detected and characterized so far among all cancer subtypes with highest frequencies in hematological tumor subtypes like acute lymphoblastic leukemia or mature B-cell neoplasm (Fig. 2B) (23).

Translocations are also typical for mesenchymal cancers. In malignant solid tumors, fusion positive cancers account for less than 1% of all cases while 5-20% of bone and soft tissue tumors harbor a characteristic hybrid gene (23, 24). Here, balanced as well as unbalanced translocations are distinct for a certain tumor type and correlate with specific clinical features (25). In prostate cancers, gene fusions of E26-transformation-specific (ETS) family proteins are fused to ubiquitously expressed promoters or 5' untranslated regions. This translocation event is leading to a deregulated protein expression than a classical fusion protein (26). These tumors also display a characteristic global gene expression profile as for acute lymphoblastic leukemia or fusion positive rhabdomyosarcoma (27, 28).
Translocations are known to occur at any time, any age and cancer type. In adult cancers, chromosomal breakpoints can arise as a result of external inducing agents. Certain breakpoint hotspots in the genome are more prone to chromosomal instability than other regions. However, there is so far little evidence for any hypothesis why and how fusion positive cancer are created (23). For pediatric malignancies, translocation based tumors are suspected to arise already prenatally during fetal hematopoiesis as shown for several leukemia (29, 30). Several studies of monozygotic twins with the same subtype of pediatric leukemia support the *in-utero* hypothesis (31).

1.1.5. Sarcoma – epidemiology, classification and treatment

Sarcomas are classified into bone and soft tissue tumors with several distinct subtypes (32). The underlying genetic events of all sarcomas are either tumor-specific translocations or complex tumor karyotypes with severe genetic and chromosomal instabilities (33).

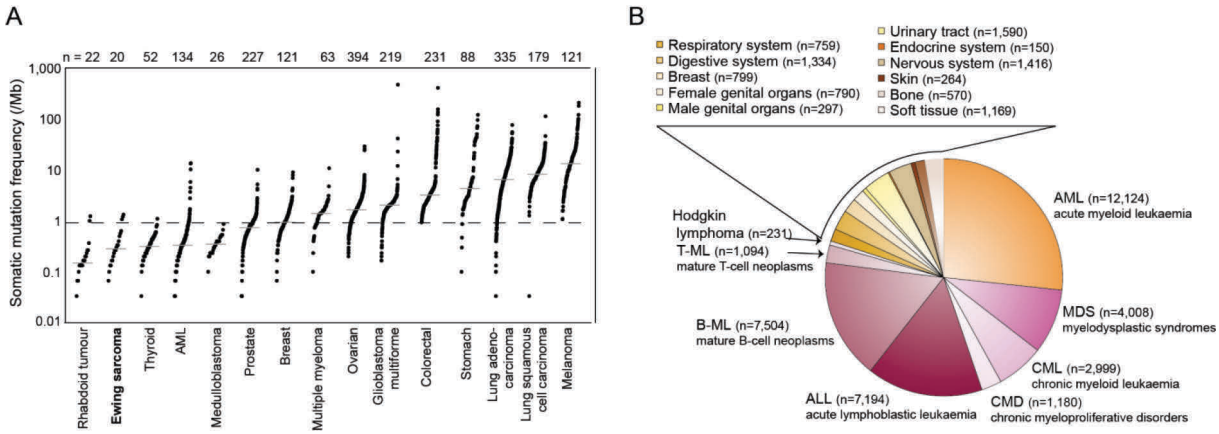

Fig. 2: The genomic landscape of tumors. (A) Somatic mutation frequencies are shown for selected cancers with the lowest to highest frequencies from the left to the right panel. The dots represent the mutation frequency in exomes from tumor versus normal pairs. Mutation frequencies highly vary between different caners, pediatric cancers cluster on the left site (modified after (19)). Mb= mega base (B) The distribution of gene rearrangements within fusion-positive cancers. A total of 45'472 cytogenetically abnormal malignant disorders reported by literature were included in the graph (modified after (23)).

Soft tissue sarcomas can be divided into more than 50 histological subtypes with a unique pattern. Most importantly, soft tissue sarcoma can be discriminated into a benign and malignant subtype. The benign form includes lipomas, fibrohistiocytic and fibrous tumors or vascular tumors and has a rather high incidence of 300 cases/100'000 people per year. They are 99% superficial, in 95% with <5mm in diameter, present mostly without pain and are very uncommon in children (34). In contrary, malignant soft tissue sarcomas have an incidence of 3 cases/100'000 people per year which is generally increasing by age (32, 35). They are ubiquitously located to 75% in the extremities and mostly include malignant forms of high grade pleomorphic sarcoma, liposarcoma, leiomyosarcoma and synovial sarcoma (36). Pediatric forms are rhabdomyosarcoma, infantile fibrosarcoma and synovial sarcoma (37-39). Treatment includes surgery as first bases whereas the use of radiotherapy and chemotherapy is non standardized for all forms (40) and rather depends on resection of a non compartmented tumor (36, 39).

Bone tumors divide into the main subtypes of osteosarcoma, chondrosarcoma and Ewing sarcoma. The incidence presents with 0.8 cases/100'000 people per year. The tumors mostly display a bimodal distribution peaking in the second decade of life and again at >60 years of age especially for osteosarcoma. Clinical features are rather non-specific with located constant pain as the major criteria, followed by regional swelling, general discomfort and fractures. Bone tissue tumors arise in pelvic bones, extremities, ribs and vertebral columns (32, 35, 41). Bone sarcomas are diagnosed by radiography, magnetic resonance imaging (MRI) and computer tomography (CT-) based methods respectively (42). Most frequently, cancer cells metastasize to the lung, bones and bone marrow (43). Treatment includes surgery and tumor-type specific established chemotherapy treatment protocols (41).

1.1.6. Targeted therapies in sarcoma

Classical chemotherapeutics are still the standard of care in most bone and soft tissue sarcomas. Several clinically relevant anti-tumor agents have been developed over the years and are currently under FDA (Food and Drug Administration, US) approval or in clinical trials (Table 1) (44-46). Targeted therapy is most commonly based either on the presence of a molecular marker serving as a target or functional differences of cancer cells versus non tumorigenic cells. Several relevant targets have been investigated including receptors and growth factors (IGF1R, PDGF, c-kit), signaling pathways (mTOR), cell cycle regulators (CDKs) or angiogenic factors (VEGF, VEGFR) and brought to clinical trials (47). Over the last two decades, there was only little improvement in survival rates for children with pediatric sarcoma like rhabdomyosarcoma, osteosarcoma or Ewing sarcoma. A lack of interest by industrial companies needs to be compensated by academic research. However, translating research discoveries into clinics is even more challenging due to limited resources to conduct clinical trials and the low number of patients for trials in general.

Table 1: Targets and targeted agents in sarcoma (modified after (44)).

Disease	Agents	Targets
Gastrointestinal stromal tumor	Imatinib, sunitinib, sorafenib, regorafenib	c-kit, platelet-derived growth factor receptor alpha
Chordoma	Imatinib	Platelet-derived growth factor receptor alpha
Alveolar soft part sarcoma	Sunitinib, cediranib	Alveolar soft part sarcoma/ transcription factor E3
Angiosarcoma	Sorafenib, bevacizumab	Vascular endothelial growth factor
Nonadipocytic sarcomas	Pazopanib	Vascular endothelial growth factor
Ewing sarcoma	Ganitumab, figitumumab	Insulin-like growth factor 1 receptor
Liposarcoma	PD03329919	Cdk4
Chondrosarcoma	GDC0449, RO4929097	Hedgehog, Notch

1.2. Ewing sarcoma

1.2.1. Epidemiology and survival

In 1921, James Ewing described a series of adolescent tumors as diffuse endothelioma of bone which were highly distinct from osteosarcoma in their histology, appearance in the bone and sensitivity towards radiation (48). A few years later, the Boston surgeon Ernest Codman named the cancer after James Ewing (historical review Fig. 3, by (49)). Histologically, it is a blue small round cell and undifferentiated tumor with a characteristic rearrangement.

Ewing sarcoma is the second most common bone tumor in the pediatric population with a general incidence of 0.3 cases /100'000 people per year with stable incidence numbers over the last decades (32, 50). It arises in bone and soft tissue with an age dependent distribution (Fig. 4A). The incidence peaks during the second decade of life in adolescence for the bone subtype. Further, a predilection for males with the ratio of 1.4 to 1 has been reported (32, 51). A racial difference in incidences of Ewing sarcoma has been observed throughout several studies and in the SEER registry with Caucasians to be more affected than other races (52). No racial differences have been observed for other tumors with a similar chromosomal rearrangement (53).

The 5-year survival rate for localized disease is between 60%- 70%, with 68% reported for the SEER registries between 1973-2004 and with 39% for patients with metastasis at initial diagnosis (Fig. 4B). Tumor cells were migrating to the lung in 10% of patients, to the bone and bone marrow for another 10% and to other locations for 5% of all cases (41, 50). Further, relapse patients have even a worse outcome and only 13.3% of those patients achieve a second complete remission (54). Secondary malignancies show a high rate for secondary bone or soft-tissue sarcomas, also carcinomas and hematologic malignancies have been reported (various studies are summarized by (55)).

1.2.2. Treatment modalities

First general symptoms of a bone tumor are pain and a mass in the involved area which can be accompanied by fever, anemia, leukocytosis and an increase in sedimentation. The tumor itself is tan–grey, often necrotic and hemorrhagic (32). Ewing sarcoma most commonly arises in the diaphysis or metaphyseal-diaphyseal portion of long bones, pelvis and ribs (Fig. 4C). The skull, vertebra, scapula, and short tubular bones of hands and feet are rarely involved (32, 56).
Standard imaging procedures of lesions include whole body MRI or CT scans (Fig. 4D). Diagnosis of Ewing sarcoma is performed by biopsy and the rearrangement detected by cytogenic fluorescence in situ hybridization (FISH) method on paraffin embedded tissue or by quantitative real time PCR (qRT-PCR) from frozen sections. Further, a hematoxylin and eosin (H&E) and CD99 marker stain is used for immunohistochemical analysis (41).

Current treatment protocols include local neo-adjuvant chemotherapy and surgery. In case of an unfavorable location of the tumor, unfeasible surgery or for high-risk patients, radiotherapy with 45–60Gy is given post-operationally. Next, chemotherapy combinations are given consisting of doxorubicin, ifosfamide, vincristine, and actinomycin (VAIA) for standard risk patients with a localized disease in 3-6 cycles in 2-3 week intervals for 10-12 month. High risk patients additionally receive etoposide (32, 41, 56). Chemotherapy for relapse patients are commonly based on cyclophosphamide, high-dose ifosfamide in combination with etoposide or irinotecan with temozolomide or gemcitabine with docetaxel (57, 58).

1.2.2.1. Prognostic markers

For many years, the only relevant predictor of outcome was the presence of metastasis with an unfavorable prognosis (59). Later, outcome could also be linked to the location of the primary tumor site and the age at presentation with the disease. Generally, treatment of younger patients achieves better disease control and subsequently outcome (60, 61). Patients with Ewing sarcoma over the age of 40 display much lower survival rates and have more likely an extraskeletal or axial primary tumor and a tendency to metastasize (62). A most current study identified discrete prognostic groups based on age, race and if the disease was localized or recurrent. In two independent cohorts, best outcome in overall survival was achieved for localized and non-pelvic tumors in patients with an age below 18 while increasing age and metastasis lowered the prognosis significantly (Fig. 4D) (63).

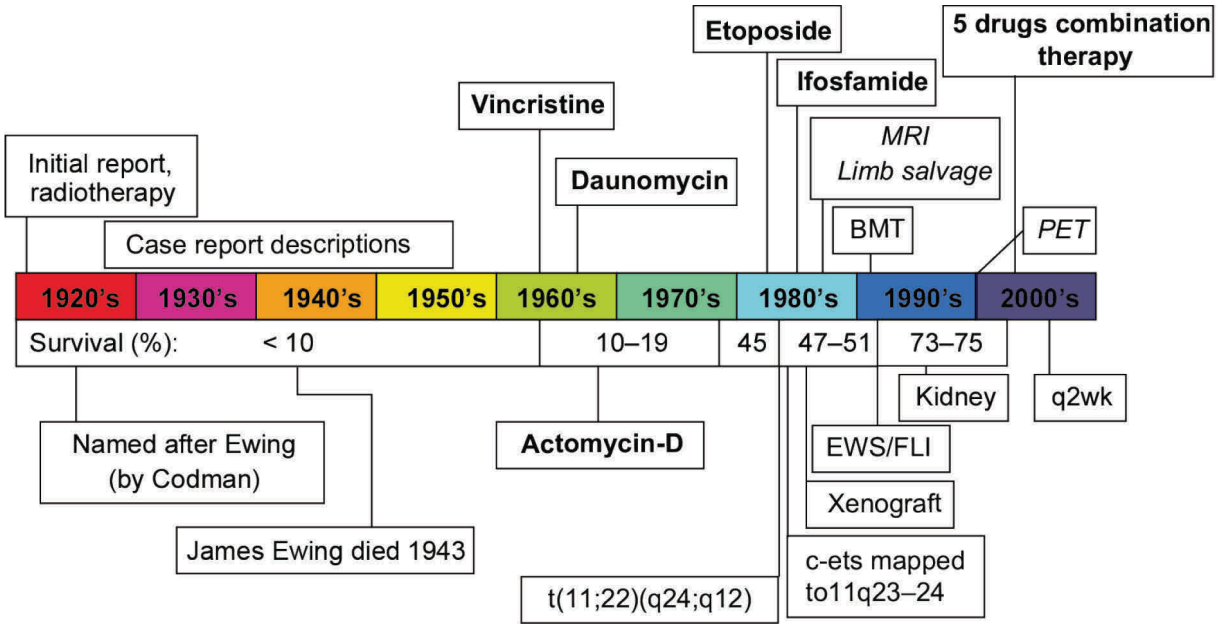

Fig. 3: Timeline of historical milestones for Ewing sarcoma (modified after (49)).

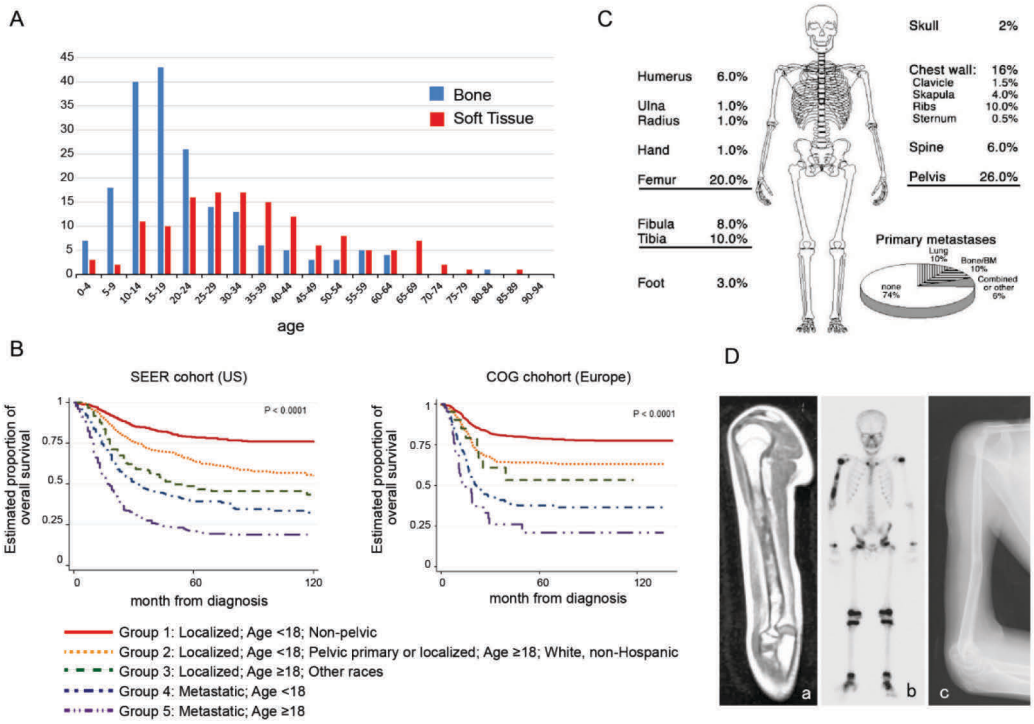

Fig. 4: Pediatric Ewing sarcoma. (A) Age distribution of patients with either bone or soft-tissue Ewing sarcoma in the Japanese population (51). (B) Kaplan–Meier estimates of overall survival for the European COG and US SEER cohorts according to the prognostic group (modified after (63)). (C) Ewing sarcoma primary sites of the tumor according to data from 1'426 patients of the European Intergroup Cooperative Ewing Sarcoma Studies (56). (D) Patient with Ewing sarcoma of the right humerus. MRI shows the position of the tumor and a bone scan with a high isotope uptake in the tumorigenic region. After surgery and several cycles of chemotherapy, the humerus was tumor free (51).

1.2.2.2. Clinical trials

The first selected chemotherapeutic for Ewing patients was cyclophosphamide in the 1960s. Then, a study was conducted with combinational chemotherapeutic treatment including cyclophosphamide and vincristine in addition to radiotherapy (summarized by (56)). IESS-I was the first large US study gathered from 1972 to 1978 demonstrating a strong advantage in survival by adding doxorubicin to the current three drug chemotherapeutics including cyclophosphamide, vincristine and actinomycin (VAC plus radiotherapy). Long-term follow-up studies revealed a dramatic increase of the 5-year survival rate from 24% (three drugs and radiotherapy) or 44% (three drugs and bilateral pulmonary radiation) to 60%. Further, a decreased number of patients developed metastasis (64). Following this, IESS-II was conducted from 1978 to 1982 and revealed a better outcome for patients treated with a higher dose of actinomycin (65, 66). Even though treatment protocols did not change dramatically over the next years, addition of ifosfamide and etoposide to the treatment protocol increased the 5-year survival rate again from 54% to 69% for non-metastatic disease (67). However, an evaluation of metastatic Ewing sarcoma revealed no beneficial impact due to the treatment change (68). Higher chemotherapeutic doses only increased the risk for secondary malignancies due to high toxicity while the event-free survival was not improving (69). Later, a comparison of ifosfamide and cyclophosphamide in patients with localized Ewing sarcoma could show that both drugs have the

same effect with less toxicity effects for ifosfamide (70, 71). An increased dose of ifosfamide was given to patients with metastatic disease and showed no improvement of survival (58, 72).

1.2.2.3. EWING2008- the largest European study

The EWING2008 trail aims to investigate better tolerable treatment doses and protocol arms for Ewing sarcoma patients. Initially, patients receive six cycles of standard chemotherapy consisting of vincristine, ifosfamide, doxorubicin and etoposide. Then, patients are subdivided into three groups): Standard risk patients (group 1) are good responders with localized disease. They receive additionally eight cycles of chemotherapy composed of vincristine and actinomycin with cyclophosphamide for females or ifosfamide for males. They are randomized to receive add-on treatment with fenretinide, zoledronic acid, fenretinide plus zoledronic acid, or no add-on treatment. High risk patients (group 2) are poor responders with a localized disease and additionally receive eight cycles of vincristine, actinomycin and ifosfamide chemotherapy or high-dose treatment with busulfan-melphalan. Patients with metastasis are in high risk group 3 and are randomized to either continued treatment with eight cycles of vincristine, actinomycin and cyclophosphamide or high-dose treosulfan-melphalan (73).

Euro-Ewing 2012 is the second large following Phase III study for Ewing sarcoma patients. Here, the use of radiotherapy and peripheral stem cell transplantation in addition to different combinations of chemotherapeutics will be investigated. Study results are not yet published as both trials are still recruiting patients (source: euroewing.eu).

1.2.3. Underlying genetics of Ewing sarcoma tumors

Ewing sarcoma tumors harbor a balanced translocation of the chromosomes 11 and 22 leading to expression of the EWS/FLI1 fusion protein (74). This translocation occurs in 85% of all Ewing sarcoma cases, only 15% harbor EWSR1 fused to another member of the ETS family, most commonly ERG (75, 76). Many more different fusions with other ETS superfamily members have been reported (reviewed by (77)).

As described before, Ewing sarcoma has one of the lowest mutation frequencies with 0.1 mutations/ Mb DNA (19). Besides the primary EWSR1-ETS translocation, the genomic landscape of Ewing sarcoma tumors is genetic rally rather normal with less than 15% of tumors displaying additional mutational events (Fig. 5A) (78). Secondary events driving tumor formation are subject of extensive sequencing efforts of pediatric tumor samples and established cell lines. Early studies by comparative genome hybridization revealed gain of chromosome 8 (35% of cases), chromosome 1 (25%) and chromosome 12 (25%) (79). With improving methods over the years, it has been shown that chromosome 8 and especially chromosome 1q gain are indeed the major detected copy number alteration (80-83). Next generation sequencing revealed in more detail that STAG2 (17%), CDKN2A (12%) and TP53 (7%) point mutations, rearrangements or other non-genetic mechanism are the major secondary events in Ewing sarcoma tumors (Fig. 5A) (78, 83, 84). Other less frequent mutations are

occurring in epigenetic regulators (83). Importantly, patients treated with common chemotherapeutics display increased somatic aberrations in their tumor genome (Fig. 5B) (83). Thus, the only consistent alteration found in all patient samples is the EWS/FLI1 fusion gene, or other EWS-ETS rearrangements.

Chromosome 1q gain has been associated with poor outcome as well as rare chromosomal loss, like 16q which was also linked to worse survival rate (Fig. 5C-D) (80-83). Several groups reported that especially TP53 inactivation is a prognostic marker for poor outcome (81, 85-87). Studies with larger cohorts like the Children's Oncology Group could not confirm a prognostic relevance (88) or only in combination with STAG2 mutations (Fig. 5D) (83).

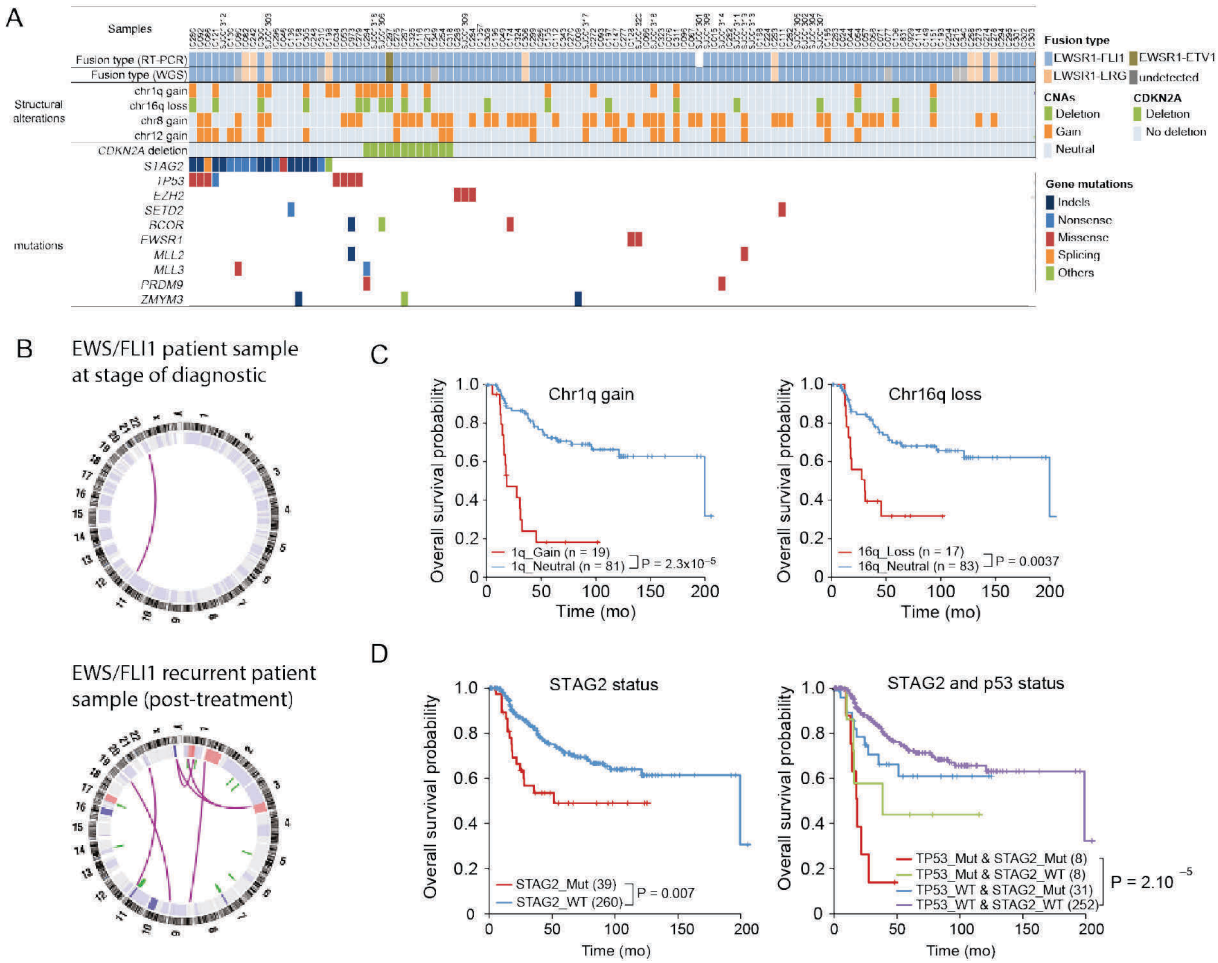

Fig. 5: Genomic landscape of Ewing sarcoma tumors. (A) Profile of recurrent abnormalities in Ewing sarcoma detected by massively parallel sequencing (modified after (83)). (B) Circo plots of a primary and a recurrent tumor analyzed by whole exome sequencing. Cytobands are showing segmented copy number variations. Chromosomes are arranged end-to-end. Interchromosomal rearrangements are displayed as purple arcs (78). (C-D) Prognostic significance of copy number alterations of chromosome 1q gain and chromosome 16q loss by Kaplan-Meier curves. Overall survival curves of patients according to the STAG2 mutation status and in combination with p53 using Kaplan-Meier curves (83).

1.2.3.1. The EWS/FLI1 fusion protein

The balanced translocation t(11;22)(q24;q12) resulting in the EWS/FLI1 fusion protein has been discovered as the main genetic alteration for Ewing sarcoma. The N-terminal part of EWSR1 is fused to the C-terminal part of FLI1 (Fig. 6A) (74). Most commonly the EWSR1 exons 1 to 7 are fused to exons 6 to 9 of FLI1. This type 1 translocation occurs in 85% whereas in type 2 exon 7/5 fusions are present in 10% of all cases (Fig. 6B) (75). Many more infrequent variants have been described as well as several other ETS family fusion partners for EWSR1 (76, 89). In diagnostics, fusion based EWSR1 translocations are detected by FISH analysis (Fig. 6C).

In the 1990s, first indications suggested that patients with a type 1 translocations had an advantage over type 2 and other infrequent variants (90). However, analysis of the EURO-E.W.I.N.G.99 study cohort revealed that current treatment protocols have no prognostic benefit for any translocation type (91, 92).

The EWS/FLI1 protein is indispensable for Ewing sarcoma pathogenesis as shown by antisense cDNA or antisense oligodeoxynucleotides towards the breakpoint region resulting in growth inhibition, decreased proliferation and viability (93-95). EWS/FLI1 is an aberrant transcription factor and a potent transcriptional modulator due to its DNA-binding domain (96, 97). The transforming capacity is more powerful than for FLI1 as it harbors a stronger transactivation domain in its N-terminal part (98). Even though DNA-binding of EWS/FLI1 and wild-type FLI1 occurs with the same sequence specificity, transcriptional activation properties are altered for EWS/FLI1 possibly due to its dependency on the EWSR1 activation domain (99). Differences in DNA-binding ability have also been reported for members of the ETS superfamily. ETS-binding profiles are clustering into four distinct classes, and all cancer associated members ERG, ETV1, ETV4 and FLI1 are clustering together indicating that a similar defined activation pattern is cancerogenous (100).

The structure of the ETS domain of EWS/FLI1 consists of three α-helices and four stranded anti-parallel β-sheets when bound to DNA. It belongs to the class of helix-turn-helix proteins. Defined residues in the DNA-binding domain are necessary for the DNA interaction including arginine 386 (respectively arginine 340 for FLI1) (101, 102). EWS/FLI1 protein carrying point mutations in the ETS domain fails to interact with DNA, and these cells are subsequently incapable of tumor growth. However, DNA-binding independent properties are also contributing to the malignant phenotype of EWS/FLI1 transformation. These cells retained their ability to transform murine 3T3 cells which could be grown as xenografts *in vivo* (103).

1.2.3.2. EWS/FLI1 target genes

Modulation of target genes by EWS/FLI1 has been shown to be critical for tumorigenesis. The fusion protein activates and represses a wide range of target genes leading to activation or inhibition of distinct pathways (reviewed in (104, 105). Attempts to identify a defined target gene signature started with the discovery of the fusion protein itself (106). Most of the assays were using RNA interference

(siEWS/FLI1 or shEWS/FLI1) or introduction of recombinant EWS/FLI1 into mouse progenitor cells or other cell lines. This led to the discovery of a variety of EWS/FLI1 activated genes including CAV-1 (107), Nkx2.2 (108), NR0B1 (109), IGF1 (110), SOX2 (111) and repressed genes as IGFBP3 (112) or PHLDA-1 (113). Further, not only protein coding genes are upregulated, but EWS/FLI1 also specifically influences long non-coding RNAs like EWSAT1 (114). Depletion of most of these direct or indirect target genes reduces cell growth and tumorigenesis. However, none of them was identified as a sole driver target gene responsible for Ewing sarcoma tumorigenesis. Until now, it is believed that a defined subset of target genes is responsible for the malignant phenotype rather than a single driver downstream gene. Further, several studies revealed that a much higher number of genes are repressed than activated by EWS/FLI1 which is mediated by interaction with the NuRD co-repressor complex (9, 105, 115). Despite the NuRD complex, it is not yet exactly clear by which other mechanism repression is controlled. Since, not only the DNA-binding domain of EWS/FLI1 is important for full oncogenic activity, also the C-terminus has been linked to support the transcriptional modulation of activated target genes (116).

Most importantly, EWS/FLI1 expression and its target gene pattern is context dependent. In most cell lines, EWS/FLI1 induction leads to growth inhibition or a senescence like phenotype in human or mouse fibroblasts (117, 118). In rhabdomyosarcoma cells, induction of EWS/FLI1 changes histology and gene expression (119). Only few cell lines are known to be permissive for oncogenic transformation, and so NIH 3T3 or human mesenchymal stem cells are most commonly used to model EWS/FLI1 transformation (116, 120, 121).

1.2.4. Cell cycle deregulation in Ewing sarcoma

Due to its low mutation rate, cell cycle deregulation in Ewing sarcoma tumors is a direct effect induced by the EWS/FLI1 protein rather than a result of mutational burden. It was shown that depletion of EWS/FLI1 results in G0/G1 arrest which is accompanied by repression of cyclin D or cyclin E and activation of p21, p27, p57 or pRb. Unbalanced expression of G1/S regulatory factors supports tumorigenesis (122-126). Further, EWS/FLI1 mediates evasion of senescence most likely via the Skp2-p27 axis (125, 127). Thus, oncogenic transformation of Ewing sarcoma is highly dependent on EWS/FLI1 cell cycle control. Similar effects were observed for full length FLI1 which inhibited cell differentiation by downregulation of cyclin D2 or D3 and other genes implicated in cell cycle or cell proliferation control in Friend virus-induced erythroleukemia (128).

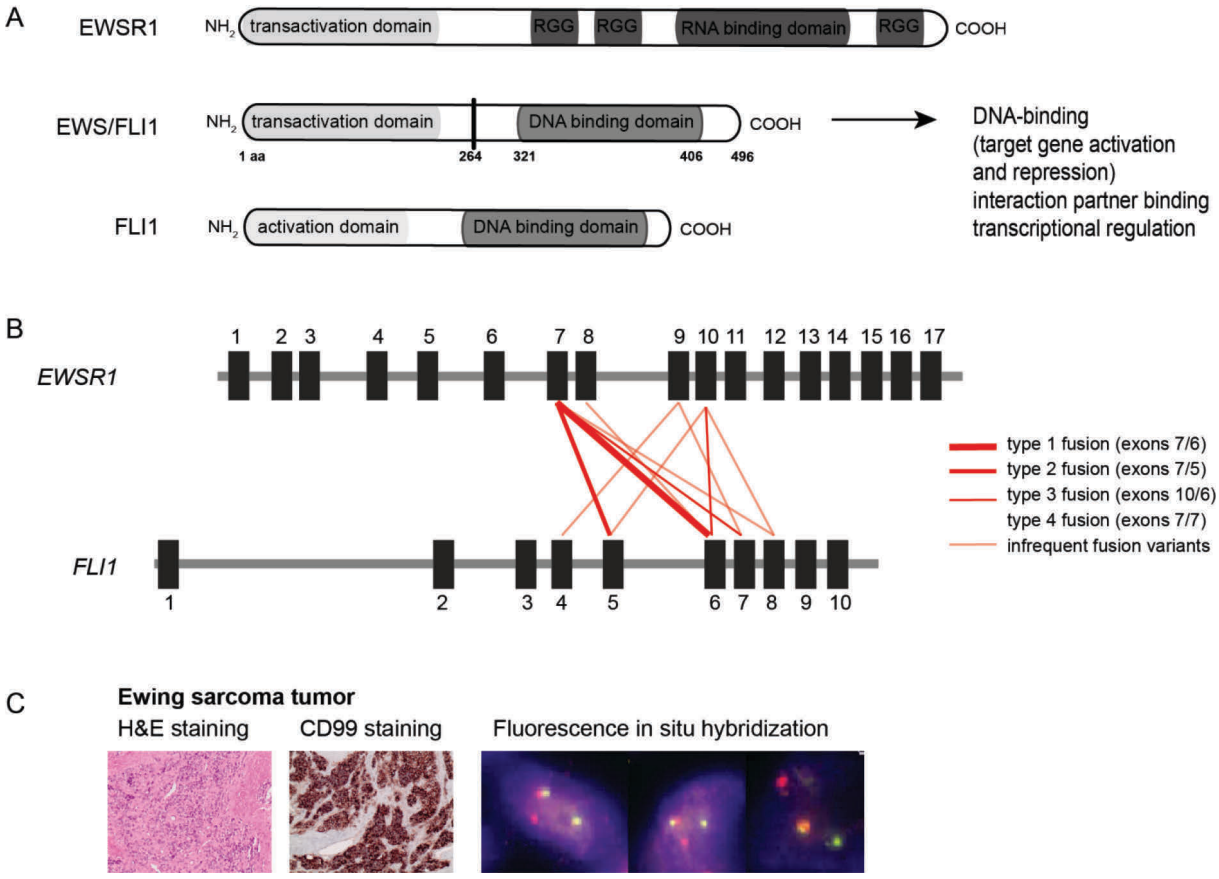

Fig. 6: The EWS/FLI1 fusion protein is solely characteristic for Ewing sarcoma tumor cells. (A) The EWS/FLI1 protein is a balanced translocation of EWSR1 and FLI1 gene rearrangement. It harbors a strong transactivation domain in the N-terminal part and the DNA-binding domain from FLI1. RGG= arginine-glycin-glycin repeats. (B) Several fusion types are described. Most common are type 1 fusion and type 2, many more infrequent variants are known (A and B modified after (75)). (C) EWSR1 translocations are detected diagnostically by FISH with probes for telomeric and centromeric EWSR1. The exact fusion partner is determined by additional methods (Images by P. Bode, University Hospital Zurich, Switzerland).

1.2.5. EWS/FLI1 interacting proteins

The fusion protein EWS/FLI1 is a chimera consisting of largely unstructured regions of the EWSR1 full length protein and a structured DNA-binding domain in its C-terminal FLI1 part. Consequently, the EWS/FLI1 interactome network is based on interactions originally arising from EWSR1 and FLI1 or is unique to the fusion protein in its cellular background. EWS/FLI1 is capable to self-associate and to interact with EWSR1 and FLI1 full length proteins (129, 130). Later, a phage display library screen revealed RNA helicase A (RHA) as an important interactor and transcriptional co-factor of EWS/FLI1, both binding to specific EWS/FLI1 target genes promoters. Functionally, both proteins together have a greater transforming capacity (131). Development of the small compound YK-4-279 resulted in the disruption of EWS/FLI1 and RHA interaction leading to apoptosis in Ewing cell lines and a reduction in tumor growth *in vivo* (132, 133). Despite this prominent example, EWS/FLI1 is highly involved in splicing processes by interacting with hsRBP7 RNA polymerase subunit (134) or small nuclear ribonucleoprotein U1 (135). However, EWS/FLI1 interferes and alters the splicing procedure by full length EWSR1 which is contributing to the malignant phenotype (136-138). Recent larger interactome

studies revealed that EWS/FLI1 interacts with a splicing network rather than with single components of the splicosome. EWS/FLI1 binds to several splicing factors and is alternatively splicing several genes implicated in oncogenesis (139).

1.2.6. The ETS family and cancer

E-26 transforming specific (ETS) family members are strong activators or repressors of transcription with a highly conserved ETS domain (140-143). The ETS transcription factors bind most commonly in complexes to a GGA core region in order to mediate gene expression (144, 145). Main biological functions include regulation of differentiation, lineage determination of the hematopoietic system and control of angiogenesis (146-148).

Most of the ETS family members have oncogenic potential. Truncated or overexpressed ETS proteins have been linked to several cancer entities (149-152). ERG or ETV1 are frequently fused to the TMPRSS2 promoter in prostate cancer, whereas ETV6 is fused to AML1 and implicated in acute lymphoblastic leukemia (153, 154). Further, ETV6 germline variants resulting from mutational events are associated with onset of leukemia (155).

1.2.7. The ETS member FLI1

The Friend leukemia virus-induced erythroleukemia-1 (FLI1) full length protein is a member of the ETS family (156, 157). An alternatively spliced variant has been reported for human FLI1 (FLI1-1b) with the same transcriptional activation properties (158). FLI1 is nuclear localized and is harboring two independent nuclear import signals (one at the N-terminus and one in the ETS DNA-binding domain) and one export signal which is partly CRM1 dependent (159). Posttranslationally, FLI1 is sumoylated by PIASxα at lysine 67 located in the N-terminal activation domain in order to repress its transcriptional activation (160). Further, FLI1 is phosphorylated at threonine 312 in the DNA binding domain by Protein Kinase C δ disruption its interaction to the p300/ CREB binding protein-associated factor (PCAF) (161, 162). Phosphorylation was independently reported in T-cells resulting in a relative short half life time of approximately 2h (163).

In a non-pathogenic context, FLI1 is preferentially expressed in hematopoetic or endothelial cells (164), and implicated in normal hematopoietic stem cell and megakaryocyte homeostasis (165). Further, it regulates megakaryocytic differentiation (159), erythropoiesis (166) and pre-thymic T-cell progenitors (167). However, deregulation of FLI1 leads to an imbalanced differentiation and proliferation with a tumorigenic potential (128, 168-170). Besides inducing the friend virus-induced erythroleukemia in mice (171), FLI1 is the major driver of several human erythroleukemia (157, 172) and involved in various gene fusions (74, 173). In diffuse large B-cell lymphoma, several clinical patient samples showed a higher expression of FLI1 which was associated with a gain of 11q24.3, the area where the *Fli1* gene is located (174).

1.2.8. EWSR1 full length protein

The EWSR1 full length protein belongs to the FET family of TATA-box binding and RNA-binding proteins (175). EWSR1, but also TLS and TAF15, harbor a strong activation domain, several RGG boxes, a RNA-binding domain and a Cys_2–Cys_2 zinc finger (176). EWSR1 also has an alternative splice variant, EWSR1-b both being ubiquitously expressed (177). Apart from Ewing sarcoma, gene fusions have been described such as the EWS/ATF1 fusion gene in clear cell sarcoma (178, 179).
EWSR1 itself is expressed in the nucleus and only in secretory cells cytoplasmic. However, EWSR1 seems to display a cell-specific expression patterns and is specifically targeted to stress granules when induced by heat shock and oxidative stress (180). While its N-terminal domain is intrinsically disordered, it has been reported that the aromatic side chains in the activation domain are critical for transcription and transforming activity of EWSR1 related fusions (181).
Posttranslationally, EWSR1 is methylated (182) and phosphorylated at threonine 79 and serine 266. While serine 266 phosphorylation regulates transcriptional activity, threonine 79 is phosphorylated upon mitogens or in response to DNA damage by ERK1 and ERK2 (183, 184).

Besides RNA-binding properties and being part of fusion proteins, the exact function of EWSR1 is not unraveled yet. Genetic depletion of EWSR1 was reported to affect mitosis and midzone formation during mitosis and accumulates at sites of DNA damage (185-187). Most importantly, several studies suggest the involvement of EWSR1 in mitochondrial homeostasis and energy metabolism. In EWSR1-/- mice, loss of brown pre-adipocytes during development was observed (188). Later, it has been confirmed that depletion of EWSR1 reduces the abundance and activity of mitochondria which subsequently leads to a decrease in brown fat tissue and skeletal muscles (189).

1.2.9. The Ewing sarcoma cell of origin and tumor models

The cell of origin of bone and soft tissue Ewing sarcoma is in the focus of various debates. Proposed cells are derived from a neural crest or mesenchymal origin. Attempts to investigate the cell of origin usually include the comparison of Ewing sarcoma tumors to reference tissue gene expression pattern, overexpression of EWS/FLI1 in a permissive cell type as well as EWS/FLI1 silencing approaches in Ewing cell lines for comparison of the resulting gene expression pattern to other tissues.
A very early study Ewing sarcoma cells were treated with cyclic AMP and TPA. It was observed that the morphology was similar to a neural differentiation pattern accompanied by an upregulation of neural markers (190). While EWS/FLI1 expression causes growth arrest in most primary cells and cannot transform most cell lines, induction of EWS/FLI1 in RD cells resulted in neuron-specific characteristics and neural crest development was abrogated upon direct transformation into neural crest cells (119, 191).
Other attempts to characterize the origin were based on the observation that primary bone marrow derived mesenchymal progenitors could be transformed by EWS/FLI1 alone (192). EWS/FLI1 silencing exhibited a gene expression pattern similar to that of mesenchymal stem cells (MSC). It was possible to differentiate Ewing cell lines along the adipogenic and osteogenic lineage upon inhibition of

EWS/FLI1 under appropriate conditions (193). Further, human MSCs seem to be permissive for stable EWS/FLI1 integration and maintenance. The resulting expression pattern was similar to that of Ewing cells (121). Several other groups found further evidence for a mesenchymal onset leading to changes in morphology and gene expression pattern (194-196).
The most recent study suggested embryonic osteochondrogenic progenitors as another possible origin. Injection of EWS/FLI1 transformed embryonic osteochondrogenic progenitors from the embryonic superficial zone of the long-bone induced a Ewing sarcoma like small round cell sarcoma (197).

Consequently, no genetically engineered mouse model exists up-to-date. Cell line or patient-derived mouse xenografts enable *in vivo* experiments. Attempts to use mice with conditional EWS/FLI1 expression in mesenchymal cells resulted in embryonic lethality. Even though mice were presenting with a number of developmental defects in the limbs, none of them developed tumors (198). Another cre-inducible EWS/FLI-1 expression based system resulted in the rapid onset of myeloid and erythroid leukemia (199). The only present alternative has been shown by an EWS/FLI1 zebrafish model (200).

1.2.10. Drug screenings to identify new therapeutic targets for Ewing sarcoma treatment

As described earlier, Ewing sarcoma treatment protocols and clinical outcomes have barely changed during the last decades. Even though the underlying molecular mechanism like the EWS/FLI1 fusion protein or the target gene signature are well characterized, little progress has been made towards a more targeted therapy approach.
One of the first screenings directed to Ewing sarcoma was performed with a small molecule library enriched for FDA approved drugs. Using a ligation mediated amplification assay to validate changes in EWS/FLI1 expression signature, cytosine arabinoside highly modulated expression profiles similar to a EWS/FLI1 depletion state as well as affected Ewing tumor growth *in vitro* and *in vivo* (201). However, when used in a phase II clinical trial, cytosine arabinoside (cytarabine) showed high toxicity with only minimal activity leading to termination of the clinical trial (202). Two other drug screenings also focused on the target gene signature as a read-out for Ewing sarcoma cell sensitivity. An NR0B1 promoter based luciferase screen revealed mithramycin as a potential candidate (203). Even though administered for few metastatic Ewing sarcoma patients decades ago (204, 205), it just entered Phase I/II trials for pediatric and adult solid tumors and especially Ewing sarcoma in 2012 in the US with yet unpublished results (Clinical trial identifier: NCT01610570). Another compound midostaurin has been identified in a screening using activated and repressed target genes as a read-out with a similar library (113). Midostaurin entered various phases of clinical trials for leukemia, but not sarcoma patients.

The search for new therapeutic strategies revealed Ewing sarcoma cells to be especially sensitive to PARP inhibitors. EWS/FLI1 complexes with PARP1 in order to activate PARP1 gene expression and induce a transcriptional positive feedback loop (206). The sensitivity to PARP1 inhibitors is highly dependent on ETS-based fusions (206, 207). However, Ewing sarcoma cells with the EWS/FLI1 fusion transcript are the most sensitive among a panel of several hundred cancer cell lines screened for

preclinical and clinical targeting agents (208). Several combinations with PARP inhibitors have been proposed revealing that combinations with DNA damaging agents like irinotecan or temozolomide even increased efficacy (209).

The most intensively studied pathway in Ewing sarcoma tumorigenesis involves the insulin-like growth factor (IGF) signaling cascade. First biological responses have been observed in Ewing sarcoma cells by addition of labeled recombinant IGF1 or inactivation of the IGF1 receptor (IGF1R) by receptor binding antibodies (210, 211). Implications for Ewing pathogenesis have first been shown by transformation of mouse fibroblasts with EWS/FLI1. Only wild type, but not IGF1R knockout fibroblasts were capable to form colonies in soft-agar (212). Inhibition of Ewing cell growth *in vitro* has been shown by treatment with monoclonal antibodies against IGF1R, antisense IGF1R and by expression of a dominant-negative mutant form (213-215). On target gene level, IGF1 has been characterized as an activated and IGFBP3 as a repressed target gene (110, 112). Several EWS/FLI1 repressed miRNAs are targets of the IGF signaling pathway (216).
Clinically IGF1R inhibition by monoclonal antibodies like Figitumumab, AMG479 or R1507 is well tolerated with only rare severe side effects. Phase I studies with small patient numbers demonstrated promising results(217-219). The hope for a new efficient treatment option rapidly decreased in Phase II trials as only a subset of patients had benefits while most of them showed only modest responses and quickly developed resistances towards IGF1R therapy (219-221).

It is still to be elucidated which biomarkers are predictive for response. While the ratio of IGF1 to IGFBP3 did not correlate with outcome data (222), it has been first suggested that patients with low free IGF1 levels do not benefit from anti-IGF1R therapy (223). However, two independent studies observed the opposite: A smaller Phase I/II study revealed that patients with high free IGF1 levels showed a lower overall survival rate. An immunohistochemical analysis of 290 patient samples showed that reduced activity of the IGF1 system correlated with a poor treatment response (224, 225).

1.2.11. Challenges and opportunities for novel treatment strategies

To summarize, outcome and survival rates of Ewing sarcoma patients are among the worst for all pediatric cancers and have not changed for the last two decade. Tumor metastasis and relapse are the two biggest challenges in Ewing sarcoma treatment. At the molecular level, research has focused on EWS/FLI1 induced target genes and their impact on tumorigenesis. Only in the last years, it became clear that other important mechanisms like splicing or epigenetic modulation are central characteristics in Ewing sarcoma tumorigenesis and of EWS/FLI1 function itself (139, 226, 227). One of the least studied regulations is EWS/FLI1 degradation and its impact in Ewing sarcoma pathogenesis. Drugs globally interfering with parts of the ubiquitin system like the proteasome inhibitor Bortezomib, the Nedd8-activating enzyme inhibitor MLN4914 or MDM2 inhibitor RG7112 have been tested in Ewing sarcoma cells and xenografts with differential results, but none of them are currently in Ewing sarcoma clinical trials (82, 228-232). Depletion of EWS/FLI1 protein itself by enhancing the turnover rate has not been in the focus of research.

1.2.12. Turnover in Ewing sarcoma pathogenesis

EWS/FLI1 regulation occurs over posttranslational modifications as glycosylation, phosphorylation and acetylation have been reported (233, 234). EWS/FLI proteasomal degradation has not been investigated so far even though a recent publication proposed that EWS/FLI1 degradation might be lysosomal as they have found the cation-independent mannose 6-phosphate receptor (CIMPR) as an interactor of EWS/FLI1 in HEK293T cells (235).

However, targeting the ubiquitin system could be of therapeutic benefit as it has been shown that the ubiquitin proteasome system was among the pathways which were differentially regulated in resistant Ewing tumors towards standard chemotherapy (236). So far, EWS/FLI1 proteasomal turnover presents a yet uncharacterized mechanism in Ewing sarcoma tumorigenesis which would have the potential to uncover novel therapeutic strategies for Ewing sarcoma therapy.

1.3. The ubiquitin proteasome system

1.3.1. A historical overview

Regulation of protein turnover is a crucial feature necessary for cell homeostasis, function and maintenance. Proteins are continuously synthesized and degraded by the ubiquitin proteasome system (UPS)- an efficient recycling machinery in eukaryotic cells. The proteasome is a ubiquitously expressed multisubunit protein complex responsible for destruction of the majority of all proteins. Although lysosomal proteolysis, discovered in the mid 1950s (237), was thought to be the only existing cellular degradation system, a pioneering article discovered ATP-dependent protein turnover in the late 1970s in a lysosomal-free reticulocyte lysate system (Fig. 7A) (238, 239).

Deservedly, the discovery made by Aaron Ciechanover, Avram Hershko and Irvine Rose (Fig. 7B) was jointly awarded with the Nobel Prize for Chemistry in 2004 for “the discovery of ubiquitin-mediated protein degradation" (press release at Nobelprize.org). Since then, many researchers contributed to unravel the puzzle of ubiquitination signaling and proteasomal turnover (historical timeline Fig. 7C).

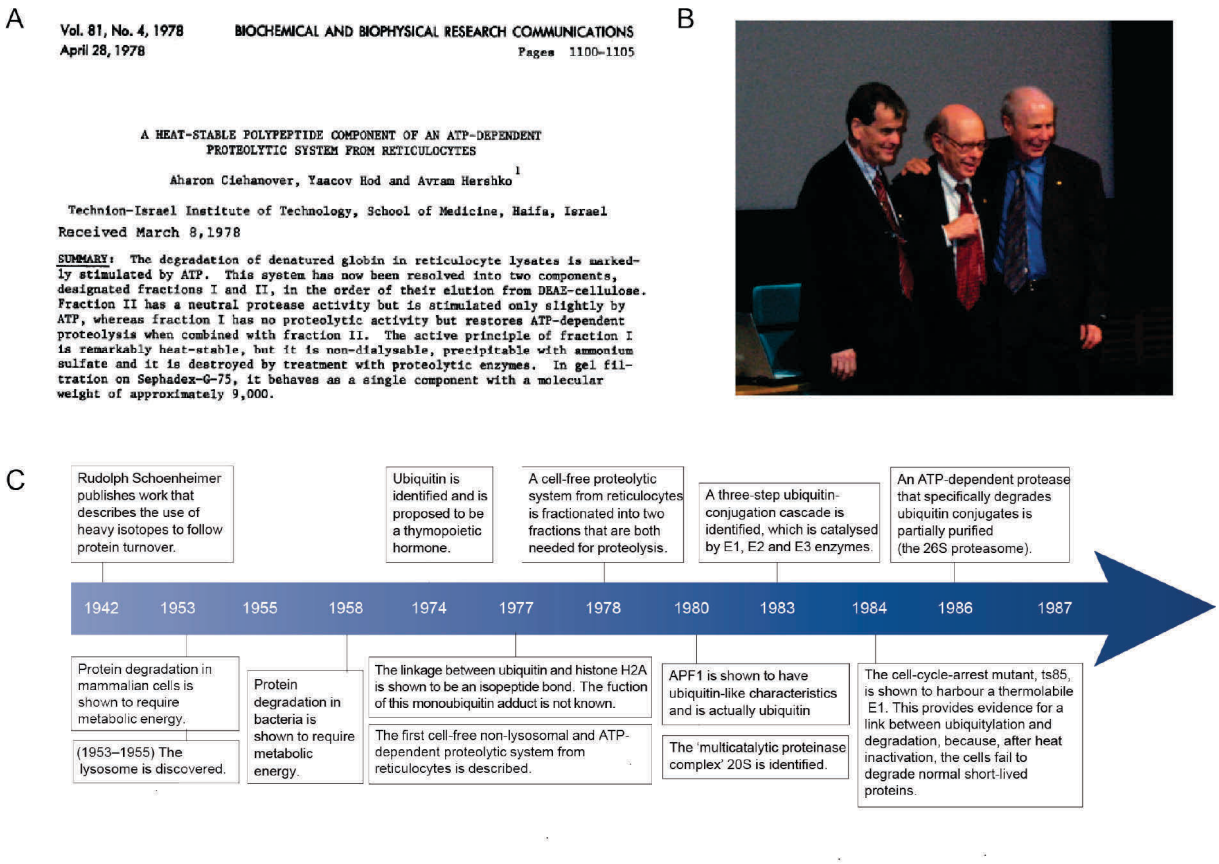

Fig. 7: Historical overview of UPS-mediated degradation. (A) Original article describing the initial discovery of a non-lysosomal and ATP-dependent proteolytic system (239). (B) The Nobel Prize for Chemistry was jointly awarded in 2004 for “the discovery of ubiquitin-mediated protein degradation" to Aaron Ciechanover, Avram Hershko and Irwin Rose (240). (C) Timeline of important discoveries and milestones in research on intracellular protein degradation (modified after (241)).

1.3.2. Mechanism of intracellular proteolysis

The regulation of protein stability is a highly conserved and multistep system most necessary to ensure cell homeostasis or to react to exogenous stimuli. It is a well balanced multi-complex system which not only triggers the destruction of proteins, but has many more functions (242-244). The 8kDa protein ubiquitin determines the fate of proteins upon its intrinsic lysine linkages and linkage to substrate lysines. Proteolysis can be mediated by proteasomal, lysosomal or autophagosomal degradation (241).

1.3.3. Proteasomal degradation

Ubiquitin-mediated proteolysis occurs primarily over the 26S proteasome, a large multisubunit complex for around 70% of all intracellular proteins (245). Assembly of this large construct occurs most commonly in the cytosol, but also nuclear proteasomal degradation has been observed (246-248).

First evidence for ubiquitin-mediated degradation of substrates via an ATP-dependent protease came from the observation that ubiquitin-conjugated lysozyme was much faster degraded in the presence of ATP (249-251). This high molecular weight protease consists of the multisubunit complexes 26S and 20S proteases which are highly conserved in size and shape and were later termed as the proteasome (252-254). The 20S subunit is the catalytic core of the complex and requires ATP for proteolysis. It is composed of seven different α-subunits and seven different β-subunits (255, 256). Later, the mammalian proteasome was found to consist of a barrel like structure, the 20S, and two 19S lids on each site with a rather flexible linker in between (Fig. 8B) (257, 258). The association of all multisubunit components to the full 26S proteasome is reversible (259-261). Substrate bound ubiquitin chains are recognized by proteasome receptors as S5a (262). Activation of the proteasome by ubiquitinated proteins occurs over the binding to USP14, an enzyme associated with the proteasome complex. This results in gate opening of the 20S subunit, providing an additional mechanism of substrate selectivity for degradation (263).

1.3.4. The process of protein ubiquitination

The process of ubiquitin attachment involves a sequential cascade of an E1 activating, E2 conjugating and E3 ligating enzyme. E1 mediates the initiation of the cascade by activating the C-terminal glycine residue of the ubiquitin in an ATP-dependent step. The E2 then accepts the activated ubiquitin, operating as a carrier which subsequently binds to the E3 ligase. The E3 ligase catalyzes the transfer of the E2-ubiquitin complex to the substrate. The dynamics of the E2-E3-substrate complex pairing determines substrate specificity (Fig. 8A). Subsequently, the ubiquitinated proteins are degraded by a proteolytic complex like the proteasome or trigger different signaling events. For the transfer of ubiquitin, two E1, approximately 40 E2 and more than 600 E3 ligases are possible components of the enzymatic cascade in eukaryotes (Fig. 8C) (242-244, 264-270).

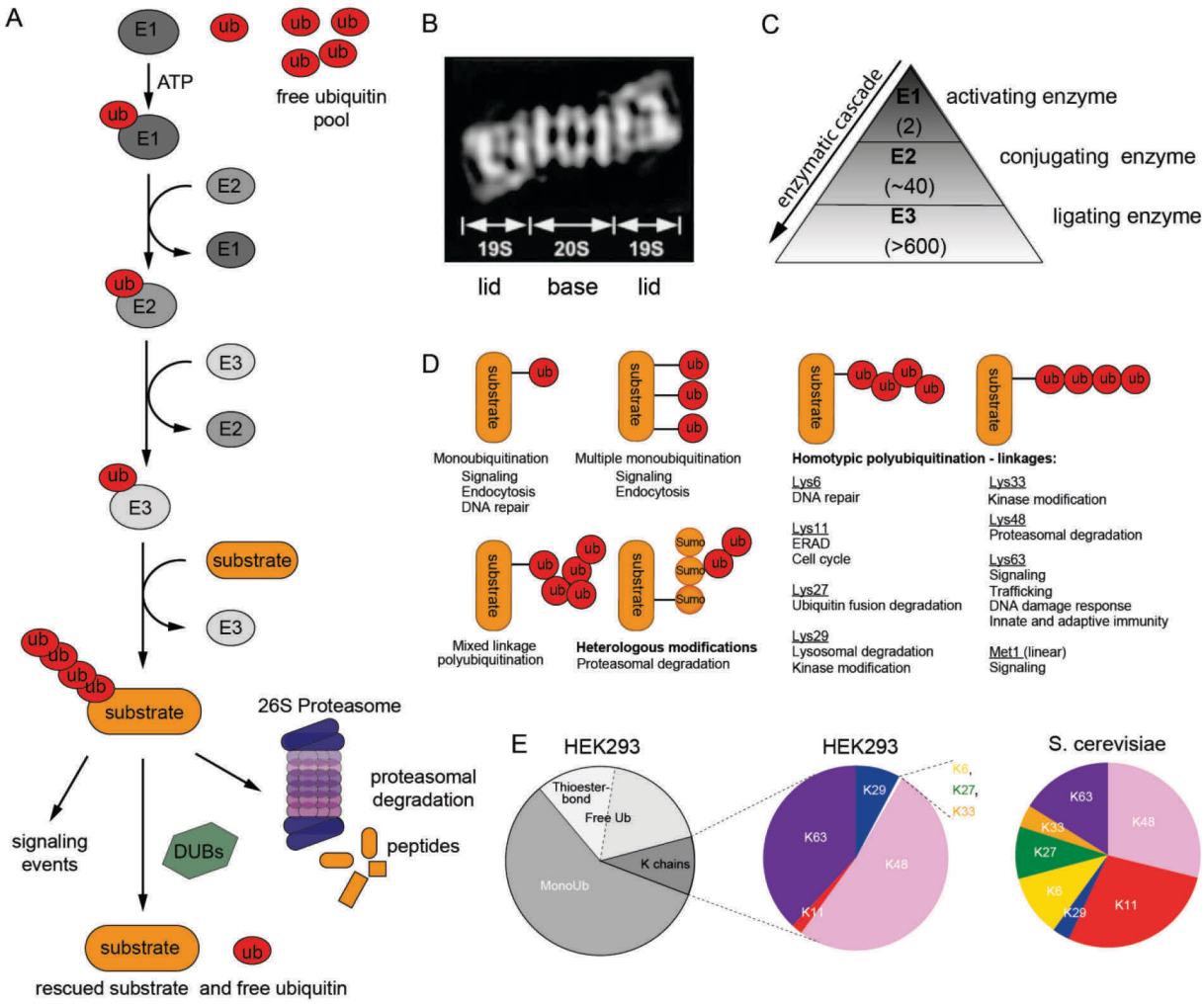

Fig. 8: The ubiquitin system. (A) An enzymatic cascade transfers an ubiquitin molecule from the E1 activating enzyme to the E2 conjugating enzyme to the E3 ligating enzyme to a substrate. The poly-ubiquitinated substrate can either be a trigger for a signaling event, rescued or modified by deubiquitination or subsequently degraded by the proteasome. (B) Three-dimensional structure of the 26S proteasome as displayed by electron microscopy (257). (C) The number of enzymes involved in the attachment of ubiquitin is organized in a hierarchical way with only two E1 enzymes to more than 600 existing E3 enzymes. (D) Possible ubiquitin linkages and their implication in cellular processes (modified after (271)). (E) Estimated ubiquitin pools in Hek293 cells (left circle). From ubiquitin linked chains, the prevalence of a particular lysine linked fraction was investigated in Hek293 cells (middle) or *Saccharomyces cerevisiae* (right) (272).

E3 ligases are subdivided into three main classes which are characterized according to their active domain: RING (really interesting new gene), HECT (homologous to the E6-AP carboxyl terminus) and U-box related domain (273-275). According to the sequential addition model, several rounds of ubiquitin transfer are resulting in a poly-ubiquitin chain of various length and linkage. The chain is initiated by a single ubiquitin molecule attached to a substrate lysine via an isopeptide bond (269, 276).

1.3.5. The ubiquitin code

Ubiquitin is encoded by four distinct genes. Single copies of the *UBA52* and *RPS27a* genes lead to ubiquitins fused to ribosomal subunits. Transcription of the *UBB* and *UBC* genes results in three, respectively nine, head-to-tail repeats of ubiquitins which are then cleaved into single units for the free ubiquitin pool (277, 278). A poly-ubiquitin chain is formed by the attachment of the C-terminal glycine 76 of one ubiquitin to one of the internal lysine residues of an adjacent ubiquitin (279). The internal lysines are situated along the ubiquitin molecule at residues K6, K11, K27, K29, K33, K48 and K63. Poly-ubiquitin chains can be formed by ubiquitins of the same linkage type or as a combination of different linkages (Fig. 8D). Poly-ubiquitin chains starting at the first methionine of the amino acid sequence are also possible and can mediate substrate degradation (280, 281). According to the ubiquitin chain conjugation, different outcomes are triggered, indicating a wide working spectrum of the ubiquitin code (269, 282).

K48-linked ubiquitins were the first linkage to be reported as a signal for proteasomal degradation (283, 284). They are the most prevalent linkage type among all chains (Fig. 8E). At least four ubiquitins were shown to be the minimum signal for efficient targeting by the proteasome (285). The process of K48-linked poly-ubiquitination is a two step process as shown for the E3 ligase complex of CDC4 and its substrate SIC1. Attachment of the first ubiquitin is rate-limiting and slow while the elongation process to K48-linked ubiquitin chain is fast (276). However, recent data suggest that multiple ubiquitinated lysine residues are more efficiently degraded by the proteasome than tetra-ubiquitin chains even with the same total number of conjugated ubiquitins as shown for APC/C E3 ligase substrates. Different studies showed that also mono-ubiquitin can be sufficient for proteasomal recognition as shown for the PAX3 protein (286). However, later it was investigated that only mono-ubiquitinated substrates with a size less than ~150 residues are efficiently degraded by the proteasome (287).

Regarding the specificity of directing proteins for proteasomal degradation, it was shown that K6- and K11-linked chains were also recognized by the proteasome (288, 289). K11-linked chains were preferentially found during mitosis and cell divisions (290, 291).
The linkages K29 and K63 have first been reported under stress-related conditions and as a response to DNA damage (292, 293). K63-linked chains have later been mapped to degradation of plasma membrane proteins in lysosomes (294). Especially EGF receptor degradation is targeted via this mechanism (295, 296).
The functions of atypical chains including Met1, K6, K27 or K29-linked ubiquitins have barely been uncovered (Fig. 8D). Most of them possibly contribute to non-proteolytic events and trigger signaling events (297). The prevalence of those linkages is only very small compared to the total pool of linkages (Figure 8E) (272, 298).

1.3.6. E3 ligases

1.3.6.1. Cullin-RING ligases

The superfamily of E3 cullin-RING ubiquitin ligases (CRLs) incorporates single subunit, multi-subunit and cullin-like complexes. The diversity of CRL-E3s is mainly achieved by multi-subunit complexes which also represent the largest class. In multisubunit CRLs, the human cullins CUL 1, 2, 3, 4A, 4B, 5, 7 and 9 serve as backbones with their distinct rigid architecture (299-302). The C-terminal region harbors the highly conserved sequence Cys-X_2-Cys-$X_{(9-39)}$-Cys-$X_{(1-3)}$-His-$X_{(2-3)}$-Cys-X_2-Cys-$X_{(4-48)}$-Cys-X_2-Cys necessary for a zinc binding RING-H2-domain protein (like Rbx1 or Roc1) serving as an E2-ubiquitin docking site (273). In close proximity, a conserved lysine residue is conjugated to NEDD8, a small and ubiquitin-like protein. For most CRLs, a variable region on the N-terminal domain of cullins allows binding of an adaptor protein to a substrate receptor (300). Both proteins, adaptor and substrate receptor, are specific for cullin scaffolds and determine substrate specificity (Fig. 9). For CRL1, the adaptor SKP1 binds CUL1 to the F-box protein substrate receptors whereas CUL3 binds its corresponding substrate receptor directly via BTB substrate receptors (broad complex, tramtrack, bric-a-brac) (303-306).

The ubiquitin transfer from the E2 to the substrate occurs over a conformational change of the complex. NEDD8 attachment results in the reduction of the 50Å gap between the ubiquitin and the substrate mediating the ubiquitin transfer (307, 308). Deneddylation (NEDD8 deconjugation) of cullin releases an ubiquitin tagged protein and disassembles the CRL complex. This process is regulated by the deneddylase activity of the COP9 signalosome (CSN), a major regulator of all CRLs. The CSN stabilizes CRL complex formation by serving as an assembly platform and mediates the various cycles of CRL assembly and disassembly leading to subsequent poly-ubiquitination of substrate proteins (309-314). In the non-complexed form, cullin backbones are bound by the inhibitory protein CAND1 (cullin-associated Nedd8-dissociated 1). Its interaction with CRL blocks both attachment sites and ensures availability of cullins for new complexes and substrate poly-ubiquitin chain elongation (315-319).

The best studied example of CRL formation is the SCF (SKP1-CUL1-F-box protein) complex which was originally discovered in *Saccharomyces cerevisiae* and later on in all other investigated species so far. All F-box proteins share a ~45 amino acid F-box domain and can additionally harbor WD40 repeats or leucine rich repeats (320-323). SCF function is crucially important for cell cycle progression (324, 325).

1.3.6.2. HECT E3 ligases

The class of HECT E3 ligases is characterized by a ~350 amino acid long region with a conserved cysteine residue within the last 32-34 C-terminal amino acids necessary for ubiquitin thioester formation (Fig. 9) (274). They are classified into the three main subgroups: HERC with RLD motifs

(RCC1-like domains), NEDD4/NEDD4-like with WW domains and a third diverse class without a consensus motif (reviewed in (326, 327)). Also HECT E3 ligases have been shown to transfer a variety of ubiquitin linkages (328).
In particular, NEDD4 family proteins with their conserved motif have been characterized in greater detail. Several different WW domains coexist within the members of the NEDD4 family to modulate protein-protein interaction between the E3 ligase and the substrate. The ten human WW domains recognize PPxY motifs, PPLP motifs, proline/arginine-containing (PR) sequences as well as phosphorylated serine/threonine-proline sites (pSP or pTP) (329-334) and serve as a platform for multi-protein networks (335). Like all HECT E3 ligases, NEDD4 members bind their substrate directly to mediate ubiquitin transfer.
The best characterized member is NEDD4 which was implicated in LATS1, SMAD4 or PTEN degradation and this seems to have a pro-oncogenic role (336-338). Further, other HECT E3 ligases are mediating degradation of oncogenic factors, but regulation can also be context or tissue dependent.

1.3.6.3. WWP1

WW-containing protein1 (WWP1) is a member of the NEDD4 subfamily containing a C2 domain, four WW domains and a HECT domain (339-341). High expression of WWP1 was found in heart and skeletal muscle tissue (342). The first identified WWP1 substrate was Krüppel-like factor 2 which is directly targeted for degradation by K48-linked ubiquitination (343, 344). Other substrates are TGFβ, p63, ERbB2/4, EGFR, HER4, and LATS1 whose degradation is mostly associated with a proliferative phenotype (345-350). Further, overexpressed WWP1 resulted in a delay of senescence in human fibroblasts by a $p27^{Kip1}$-mediated degradation (351). WWP1 was found to be overexpressed due to gene amplifications or point mutations in breast cancer, prostate cancer and hepatocellular carcinoma and to promote tumorigenesis (352-357).

1.3.6.4. U-box domain E3 ligases

The first identified U-box containing protein was UFD2 in yeast as an additional part of an E3-substrate complex (275). UFD2 and other proteins harbor a U-box core which was shown to display similarity to RING fingers by multiple alignments of their sequences (Fig. 9). However, the U-box E3 scaffold uses a system of salt-bridges and hydrogen bonds of conserved charged and polar residues to mediate ubiquitin transfer instead of a zinc-binding motif in RING E3 ligases (Aravind 2000).

Conserved amino acids are critical for U-box E3 function as deletion or mutation of the conserved region abolished the ubiquitination activity. UFD2a, UFD2b, CHIP, UIP5, CYC4 and PRP19 are predominantly poly-ubiquitinating lysine residues with linkages other than lysine 48 (358). All E3 U-box members can additionally harbor RING finger or WD40 repeats which are not required for the physical interaction with E2 conjugation enzymes (359).

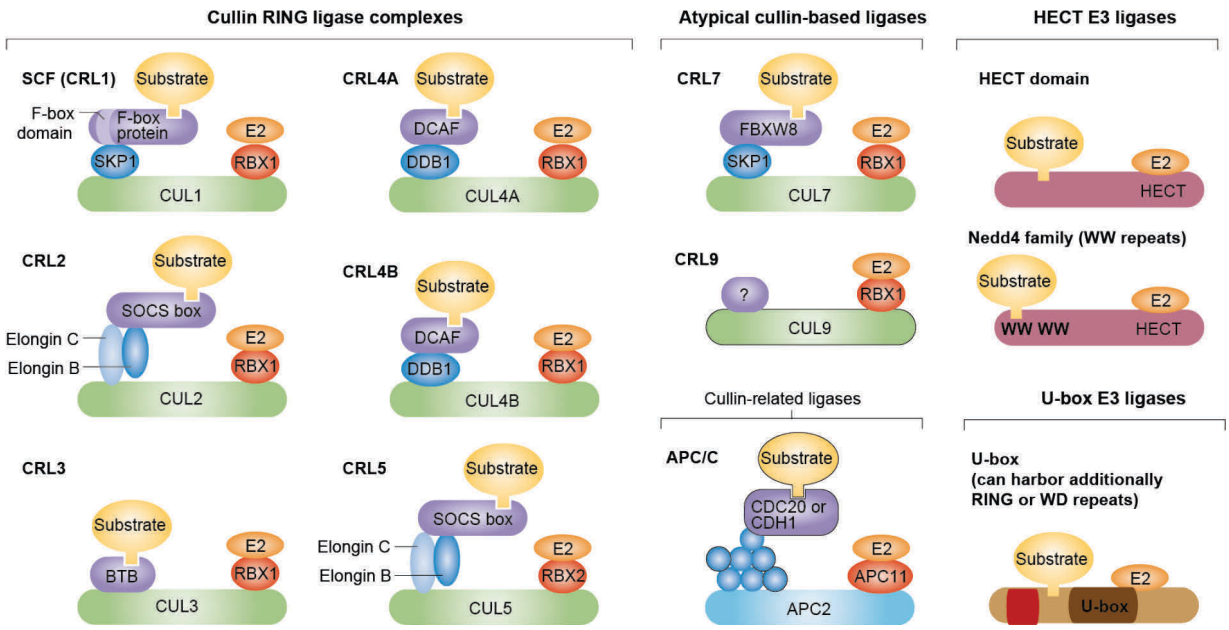

Fig. 9: E3 ligases present a diverse class of proteins. Cullin-RING ligases are multi-protein complexes with eight different cullins serving as scaffolds for complex assembly. They all harbor an E2 docking site and bind substrates via defined substrate receptors. HECT E3 ligases contain a backbone on which the ubiquitin transfer of the E2 enzyme to the substrate is mediated. U-box containing E3 ligases present a relatively small class of E3 ligases. The U-box is necessary for ubiquitin transfer to the substrate (modified after (360)).

Functionally, U-box proteins have been shown to facilitate the ubiquitination of chaperone substrates and thereby are involved in protein quality control and stress response. Most studied, CHIP combines with molecular chaperones to mediate ubiquitination of heat-shock protein substrates in a larger E3 complex (reviewed in (361, 362)).

1.3.7. Deubiquitinating enzymes

The family of deubiquitinating enzymes (DUBs) is comprised of around 100 family members classified into six subgroups according to their catalytical core domains USP, UCHs, OTU, MJD, JAMM and MCPIP with the USP family exhibiting more than half of all members (Fig. 10A) (363, 364). The USP family harbors a catalytic domain which consists of the two short and well conserved cysteine and histidine boxes which comprise the critical catalytic residue (365, 366). All DUBs are cysteine proteases except the JAMM subgroup as a metallo protease. Both groups primarily catalyze a non covalent intermediate with the substrate to release ubiquitins (363, 367).

DUBs are either substrate specific to an ubiquitin moiety or target specific to a protein or protein complex (363, 368, 369). Due to their ubiquitin specific capacity, DUBs are capable to discriminate between chain linkages, the site of the chain (end or intrinsic cleavage) and the length of poly-ubiquitin chains (Fig. 10B). Further, several DUBs like USP5 are responsible to recycle ubiquitin chains in order to maintain the free ubiquitin pool whereas others can edit existing poly-ubiquitin chains as shown for A20 in NF-κB signaling (370-372). DUBs are usually specific for a number of proteins, pathways or ubiquitin linkages. Identification of the overall DUB landscape using a mass spectrometry interactome

approach and platform for interaction proteomics (COMPASS) revealed that most DUBs are frequently associated with multi-protein complexes. Thereby, they regulate ubiquitination events to model complex activity (373). Several distinct processes are regulated by a variety of DUBs including protein stability, activation and interaction, chromatin structure remodeling or histone modification, DNA-damage response, immune response and many more (282, 374-376).

Few DUBs are proteasome associated as USP14, UCHL5, PSMD14 and PSMD7 which are cleaving ubiquitin and ubiquitin chains from degraded substrates to ensure availability of the free ubiquitin pool (377-379). USP14 is only activated upon association with the proteasome which results in ubiquitin binding to the catalytic cleft. This conformational change leads to an active state. The subsequent deubiquitination of the bound target enhances the catalytic activity of the proteasome (263, 380). However, most other USP members are highly activated when bound to the ubiquitin C-terminus (381). For another proteasome-associated DUB, UCHL5 is actively recruited to the proteasome by ADMR1 and incorporation of the complex to the 19S subunit allowing deubiquitination of substrate proteins (382-384).

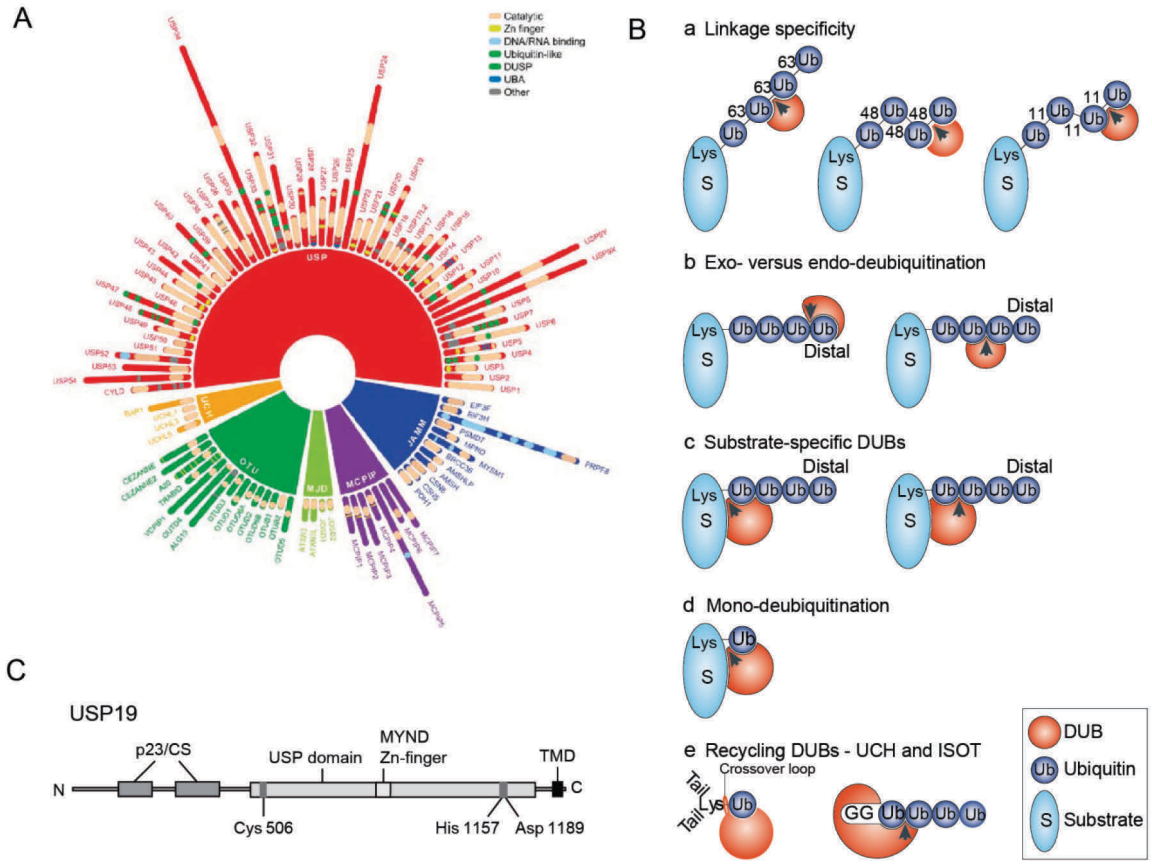

Fig. 10: Around 100 distinct human DUBs are described so far. (A) Human DUBs are classified into six main groups according to their catalytical core domain: USPs (red), UCHs (yellow), OTUs (dark green), MJDs (bright green), JAMMs (blue) and MCPIPs (purple) (364). (B) DUBs can modify the substrate ubiquitin chains in many different layers. They are capable to cleave at the start, middle or end of a poly-ubiquitin chain. Their activity can be substrate or linkage specific (modified after (370)). (C) Amino acid sequence of ubiquitin-specific protease 19 (USP19). TMD: transmembrane domain (385).

1.3.8. Ubiquitin specific protease 19 (USP19)

USP19 belongs to the USP family and has a size of 1318 amino acids. Several splice isoforms have been reported. At the N-terminus, USP19 harbors a CHORD and SGT1 (CS/p23) domain necessary for chaperone function. In the USP domain, a myeloid translocation protein 8, Nervy and Deaf1 (MYND) domain exists which mediates protein-protein interactions. At the C-terminal end, USP19 harbors a transmembrane domain (Fig. 10C) (385). USP19 cleaves K48- and K63-linked chains with a preference for the latter (386). Due to this transmembrane domain, USP19 function was mapped to substrate rescue of endoplasmic-reticulum-associated degradation (385). Further, stability of c-IAP1, cIAP2, HIF1α as well as the E3 ligases KPC1 and MARCH6 are regulated by USP19 (387-390). USP19 itself is regulated at the N-terminal site by the E3 ligases SIAH1 and SIAH2 as identified in a yeast-two hybrid screen (391). Most relevant, chaperone Hsp90 was characterized as an interaction partner of USP19 whereby binding promotes the deubiquitination activity (392).

The identification of the substrate KPC1, which itself regulates p27 stability, suggested that USP19 might also be implicated in cell cycle deregulation and subsequent cancer. Stabilized KPC1 resulted in enhanced proliferation whereas USP19 siRNA-mediated knockdown led to G1 arrest and delayed S-phase entry (388). Further, USP19 depletion was capable to inhibit proliferation of prostate cancer and breast epithelial cell lines suggesting USP19 to be oncogenic (393).
A second important function of USP19 is associated with muscle homeostasis. USP19 is highly expressed in muscle tissue of rats and myofibrillar muscle cells (394, 395). The presence of the endoplasmatic-reticulum localized form is critical for muscle cell differentiation and myogenesis (396, 397).

1.4. The role of the ubiquitin system in cancer

1.4.1. Deregulation of UPS components in cancer

Several cancer entities are associated with pathways of deregulated degradation. That usually accounts for activating mutation of E3 ligases or inhibition of DUBs which subsequently leads to the degradation of tumor suppressor genes or cell cycle inhibitory proteins. On the contrary, decreased degradation as a result of inhibited E3 ligase or increased DUB activity may contribute to stabilization of oncoproteins and therefore increased tumorigenesis (398, 399).

Several E3 ligases are known to be mutated or overexpressed in a variety of cancers (reviewed in (400)). Mutations of E3 ligases often occur in recognition motifs interfering with substrate or degradation complex binding. A prominent example is SKP2 as a member of the SCF. Its overexpression accelerates the degradation of p27 as the major substrate increasing cell cycle and proliferation. SKP2 is frequently overexpressed in prostate cancer, breast cancer and other epithelial tumor subtypes (401-403). The SCF substrate receptor FBW7 is characterized as a tumor suppressor. Mutation or loss of FBW7 leads to accumulation of the substrate CyclinE in most of the cases and was reported for breast, ovarian, gastric and endometrial cancer (404-408). While FBW7 mutations account usually for a small subset of cancer types, the mutation incidence can be up to 30% in endometrial cancer (405, 406).

Altered DUB activity often causes protein deregulation (364, 409). DUB mutations are well described for several members like BAP1 in metastasizing uveal melanoma, basal cell carcinomas or malignant mesothelioma. Inactive BAP1 increases proliferation due to its inability to stabilize substrates like the tumor suppressor BRCA1 (410-413). Further research focuses on the deubiquitinating role of DUBs on several substrates implicated in tumorigenesis. As Mdm2 targets p53 for degradation, USP7 induces a p53 dependent cell growth arrest and triggers apoptosis as direct deubiquitination rescues and stabilizes p53 (414). Further, oncogenic c-myc was shown to be stabilized by USP37 in lung cancer (415).
However, USP9X is a very prominent example on how DUBs can be context-dependent. One of the main USP9X substrates is MCL1 whose overexpression was reported in B- and mantle-cell lymphomas, chronic myeloid leukemia and multiple myeloma. Stabilization of MCL-1 by deubiquitinating activity of USP9X is tumorigenic (416). However, MCL-1 overexpression has also been observed in colon and lung cancer correlating with USP9X expression. USP9X inhibition sensitizes solid tumors to chemotherapeutic agents (417). In contrast, USP9X was found to be inactive or mutated in over 50% of pancreatic ductal adenocarcinoma. The respective low mRNA and protein levels correlated with an adverse outcome (418).

The UPS is not only pathogenic in cancer, deregulation is also highly implicated in several neurodegenerative diseases by aggregate accumulation of ubiquitin conjugates in neurofibrillary tangles in Alzheimer, in brainstem Lewy bodies in Parkinson or Bunina bodies in Amyotrophic Lateral

Sclerosis. Further, pathophysiological processes in the muscle can be affected leading to muscle atrophy and wasting (399, 419, 420). The complexity of disease-associated deregulation highlights UPS targeting to be a promising strategy for a variety of fields (421).

1.4.2. UPS associated targeting for cancer therapy

Targeting strategies of UPS associated pathways can be based on interference with differentially regulated levels of UPS components like mutated or overexpressed E3 ligases (422). However, cancers not associated with UPS deregulation are even though dependent on functional regulation networks which can also serve as specific targeting points for anti-neoplastic and pro-apoptotic effects (423-425).

Pharmacological inhibition of the proteasome uncovered many unique mechanisms of protein breakdown. Several different inhibitors targeting the catalytic proteasomal core (active subunits are β1, β2, and β5) are currently available with MG-132, Bortezomib or Lactacystein as the most widely used examples in research (426-431). Interestingly, proteasome inhibitors influence the degradation of not only abnormal and short-lived proteins and peptides, but also long-lived peptides in contrast to lysosomal inhibitors (427, 432). Even though the effects of proteasome inhibition cannot be pinpointed to a specific pathway, proteasome inhibitor induced apoptosis is likely to be most relevant for the sensitivity of a wide range of cancer cell lines or primary cells (reviewed in (433-436)). Next generation proteasome inhibitors like Carfizomib provide more specificity and less toxicity and might improve the clinical application beyond hematologic malignancies (437).

As described, transfer of an ubiquitin molecule to the substrate protein is dependent on an enzymatic cascade. The three enzymes E1, E2 and E3 can be inhibited by several compounds. While E1 inhibitor PYR-41 (438) inhibits formation of any further complexes, compounds targeting E2 conjugating enzymes like the CDC34 inhibitor CC0651 interfere with a subclass of degradation complexes (439). However, none of E1 or E2 inhibitors show high specificity or a potential for clinical trials yet.
Considering the hierarchical structure of the enzymatic cascade, E3 ligases provide most specificity with the greatest potential for targeted therapy. The millennium compound MLN4924 inhibits cullin neddylation, and subsequently activity, of all single and multisubunit cullin-RING ligases by interfering with the NEDD8-activating enzyme (440, 441). Quantitative proteomic analysis of MLN4924 treated melanoma cell lines not only revealed new cullin-RING ligase substrates, but also a defined subset of substrate proteins was shown to regulate MLN4924 cytotoxicity. Most of them were implicated in cell cycle regulation, DNA damage repair or ubiquitin transfer (442). Even more specific, several compounds have been developed which directly inhibit activity of very specific subclasses or even single ligases. Exemplarily, the small molecule SMER3 targets SCF-MET30 based cullin complexes and SCF-I2 interferes with the WD40 propeller from SCF-CDC34 ligases and other particular F-box proteins (443, 444).

However, most specificity would be achieved by directly targeting substrate binding sites of E3 ligases. Only few targeting compounds are developed which disrupt E3 substrate interaction. One of the best studied examples is the MDM2-p53 axis. The tumor suppressor protein p53 generally activates genes involved in cell cycle regulation and apoptosis. It accumulates upon DNA-damage or oncogene activation to ensure that cells do not become tumorigenic (reviewed in (445)). However, p53 is frequently mutated or absent in cancer cells (446, 447). The E3 ligase MDM2, which is frequently overexpressed in a variety of cancers, binds to the transactivation domain of p53 and thereby impairs its function (448, 449). The small molecule Nutlin-3 interferes with the binding of MDM2 to p53 by occupying the p53 binding pocket (450). Restored p53 activity induces cell cycle arrest and triggers apoptotic pathways in tumor cells. Like Nutlins, other MDM2-p53 disrupting compounds as MI-219 display similar effects (451, 452).

Selectivity in substrate targeting can also be achieved by DUB inhibition. USP7 is involved in p53 stabilization. Moreover, USP7 inhibitors like HBX41,108 and P5091 reveal anti-proliferative effects and cell cycle inhibition by p53 induction (453, 454). Further, P5091 demonstrated apoptotic effects and might be of therapeutic benefit for Bortezomib resistant patients (455). As described earlier, USP9X is highly implicated in several cancers. The small molecule WP1130 is mainly inhibiting USP9X, but also several other DUB members as USP5, USP14, and UCH37. Originally derived from a screen for Janus-activated kinase 2, it revealed pro-apoptotic function for several cancers (456-458). One of the most promising preclinical compounds is bAP-15, an inhibitor of USP14 and UCHL5 which are proteasome associated. *In vivo*, tumor progression was inhibited in solid tumors and multiple myeloma while organ filtration was decreased for acute lymphoblastic leukemia when bAP-15 was administered (459, 460).

Beyond targeting the main players in the UPS field (461), ubistatins block the binding of ubiquitinated substrates to the proteasome and therefore inhibit cell cycle progression. Mechanistically, ubistatins bind the ubiquitin-ubiquitin interface of selectively Lys48-linked chains (462).

Considering the variety and complexity of compounds targeting all parts of the UPS in a more or less specific way (Fig. 11), the UPS provides one of the most diverse fields for inhibitor development (463, 464). As proteasome inhibition already provided evidence for a successful treatment option, the combination of targeting E3 ligases or DUBs even exceeds the number of existing cancers. Most importantly, not only inhibition, but also E3 or DUB activation adds a second level of therapeutic possibilities. However, ongoing efforts are needed to develop new compounds or to characterize the effect of existing drugs on UPS components in order to provide better treatment strategies.

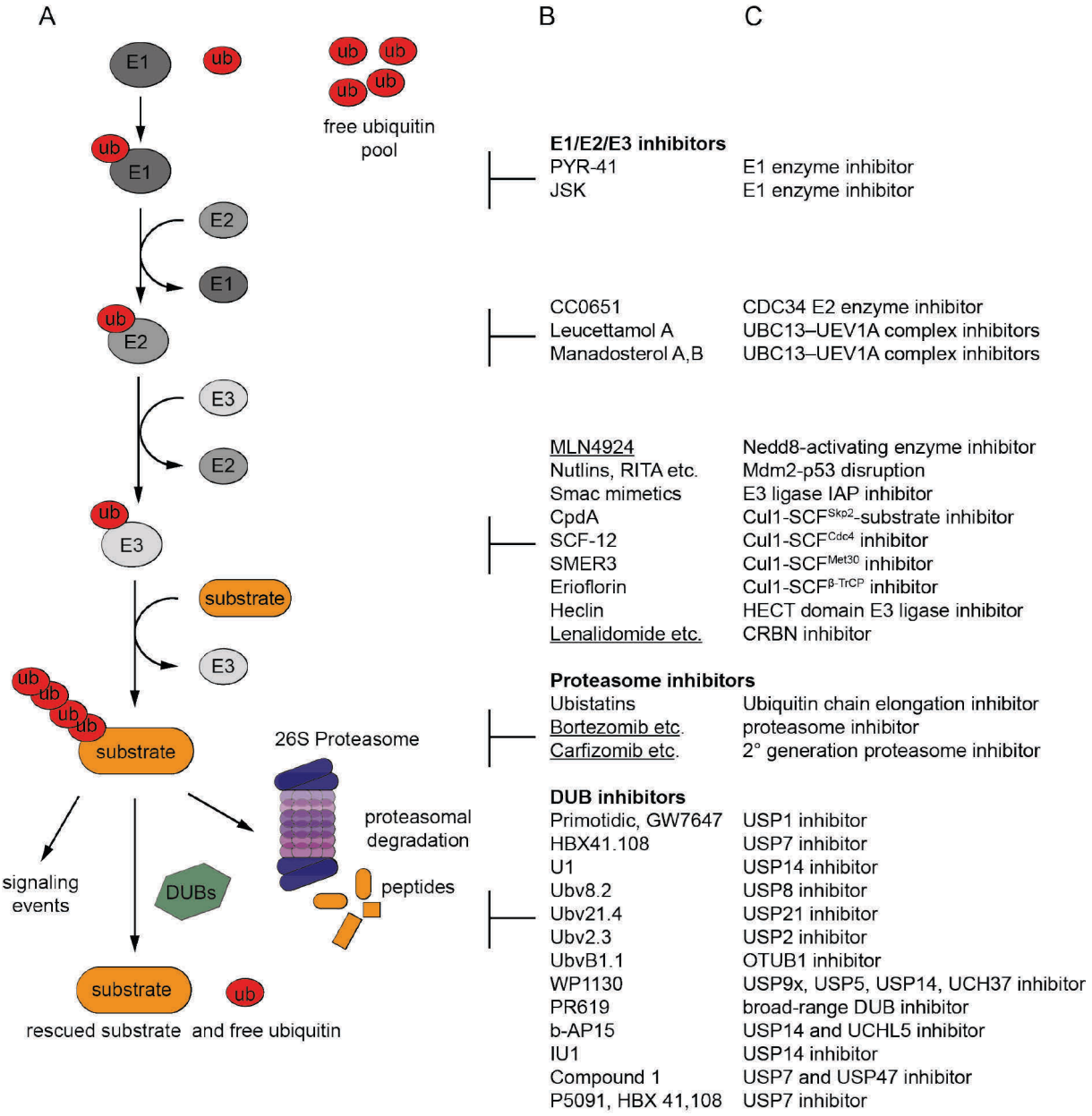

Fig. 11: UPS-based drugs. (A) The cascade of the ubiquitin proteasome system has a variety of target points. (B, C) List of drugs (name and target) capable to interfere with selected steps in the cascade. Underlined drugs are FDA approved and used in clinics (modified after (425, 465)).

1.4.3. Inhibitors of the ubiquitin system in clinics

Proteasome inhibitors have been shown to inhibit proliferation and induce apoptosis of human multiple myeloma cell lines and primary cells while sparing normal blood cells (466). Also several other cells have been shown to be susceptible like acute myeloid leukemia or B-cell malignancies (467, 468). Bortezomib was the first FDA approved proteasome inhibitor used in clinics, followed by Carfizomib (469-471). Bortezomib (Velcade®) is applied in relapsed and refractory multiple myeloma treatment. As a phase II study showed promising results, nearly 700 relapsed multiple myeloma patients were enrolled to compare dexamethasone to Bortezomib. An overall of 38% of patients revealed a combined complete and partial response rate (222, 472, 473). Later, Bortezomib was approved as a

first line treatment (471). Currently, proteasome inhibitors are included in clinical trials for multiple myeloma, hematologic malignancies and solid tumors (clinicaltrials.gov).
MLN4924 is the second UPS associated drug that entered clinical trials and is currently implicated in different phase studies for melanoma, solid tumors, hematologic malignancies and specifically multiple myeloma (clinicaltrials.gov).

1.4.4. Degradation of fusion proteins as a novel strategy in targeted therapy

Gene fusions present an attractive target as tumor cells are usually highly dependent on continuous expression of these proteins. Several target specific drugs are indirectly enhancing or modulating turnover of fusion proteins. The BCR/ABL fusion in chronic myelogenous leukemia is a tyrosine kinase which is specifically targeted with imatinib mesylate (Gleevec). Binding to the ATP-binding site of the ABL kinase domain inactivates BCR/ABL activity (474). However, imatinib mesylate treatment resistant CML remains sensitive to several other compounds like heat shock protein 90 inhibitors which are all implicated in final degradation of the BCR/ABL fusion and subsequently trigger apoptosis (475-477). For another fusion protein, our laboratory could recently show that PLK1 kinase inhibitors trigger regression of alveolar rhabdomyosarcoma. On a molecular level, PLK1 depletion increased PAX3/FOXO1 ubiquitination and subsequently reduced protein level and target gene activation (478).

Understanding and modulating turnover of fusion proteins presents a novel strategy for initial or resistant therapy. Thus, general inhibition of proteasomal processes with broad range inhibitors are leading to general cell collapse while more precise targeting of specific E3 ligases or DUBs may selectively induce apoptosis in cancer cells. However, two different mechanisms involving degradation-dependent targeting are well characterized for fusion proteins in prostate cancer and acute promyelocytic leukemia.

1.4.4.1. Degradation of ERG and ERG fusions in prostate cancer

The ETS family member ERG is also highly implicated in cancer development. Around 40% of prostate cancer patients are diagnosed with a truncated ERG version fused to the promoter of the TMPRSS2 gene (151). Most commonly, the 5'-untranslated region of TMPRSS2 is fused with exons 4 or 5 of ERG. Much less cases are reported to involve additionally TMPRSS2 exon 3 or already ERG exons 1 or 2 (479). However, also non-truncated ERG was reported to be frequently overexpressed in prostate cancer (152). Both, overexpressed ERG and TMPRSS2/ERG fusion genes, mediate cell invasion, migration and tumor progression (480, 481).

Most interestingly, proteasomal degradation of full length ERG proteins has recently been investigated. Protein turnover is regulated over CUL3 based complexes with the E3 ligase SPOP as the central substrate receptor (482, 483). SPOP is binding to a degron motif in the N-terminal region of ERG in order to ubiquitinate and subsequently degrade the protein which is suppressing prostate

cancer. In 4-15% of the prostate cancer patients, SPOP harbors mutations in the MATH domain necessary for substrate binding. Upon loss of proteasomal regulation, ERG is stabilized and is driving tumorigenesis (483). Further, the SPOP binding motif is located at amino acids 42-46 of full length ERG. The regulation is consequently lost in TMPRSS2/ERG Δ99 fusions, but also in TMPRSS2/ERG Δ39 fusions as SPOP requires the full N-terminal domain for binding. Hence, the truncated ERG protein is differentially degraded than its full length counterpart (482). Nevertheless, phosphorylation of ERG by CKI is a necessary modification to trigger SPOP mediated degradation. CKI-mediated phosphorylation partially triggers TMPRSS2/ERG Δ39 fusions for degradation. DNA-damaging agents, like topoisomerase inhibitors, are capable to activate CKI and enhance ERG degradation (483). Even though specificity of DNA damaging agents to selectively target ERG or TMPRSS2/ERG Δ39 fusions is questionable, it still represents a novel strategy of targeted therapy.
In contrast, DUB targeting presents another mechanism of ERG repression. USP9X was identified in an interactome study as an interacting protein and a deubiquitinase of ERG. The USP9X inhibitor WP1130 mediates ERG repression which subsequently reduces prostate cancer growth *in vivo.* It has not been reported if ERG fusions are regulated by USP9X (484).

Both described strategies, E3 ligase SPOP activation and DUB USP9X inhibition, highlight the pivotal role of ERG turnover in prostate cancer for targeted therapy approaches. Most interestingly, prostate cancer harboring SPOP mutations or TMPRSS2/ERG fusions are mutually exclusive indicating that these two distinct clinical subgroups might benefit from different targeted therapy approaches in closer future.

It is noteworthy to mention that the ETS member ETV1 has also been linked to proteasomal degradation. The E3 ligase COP1 binds at the N-terminal part of ETV1 and poly-ubiquitinates the protein. A truncated version fused to the TMPRSS2 promoter in prostate cancer exhibits this regulation and shows a prolonged half life similar to TMPRSS2/ERG (485). Speculatively, proteasomal turnover might be conserved among ETS proteins while E3 ligase binding differs.

1.4.4.2. Selective degradation of PML/RARα in acute promyelocytic leukemia therapy

Acute promyelocytic leukemia (APL) expressing the fusion proteins PML/RARα is sensitive to treatment with retinoic acid (RA) while APL patients with PLZF/RARα fusions respond poorly. However, nowadays APL treatment additionally implicates the combination of RA with arsenic trioxide (As_2O_3). It was shown that the combination treatment resulted in prolonged survival of leukemic mice harboring PML/RARα, but not PLZF/RARα fusions (486).

On a molecular level, RA treatment alone accelerates PML/RARα degradation resulting in cell differentiation and apoptosis. Treatment with RA and the proteasome inhibitor lactastatin rescued the degradation effect indicating a degradation-mediated targeted therapy (487). Even though RA treatment induces PLZF/RARα degradation, it did not result in cell differentiation (488). However, RA triggers proteasomal degradation of the RARα part in fusion proteins, respectively of the RARα full

length protein (489). Certainly, sensitivity to RA is based on an additional mechanism. Transgenic mice with PML/RARα fusions develop RA sensitive leukemia while PLZF/RARα fusions are indeed RA insensitive as shown in clinical settings. Interestingly, RA sensitivity has been shown to be regulated by different fusion associated co-repressor complexes (490). Later, it has been revealed that arsenic trioxide is involved in PML/RARα mediated degradation. PML/RARα was observed to be sumoylated at K160 residue by the sumo E3 ligase PIAS1 (491-493). Sumoylation at the K160 is critical for APL development. Transgenic mice with a PML/RARα mutation to K160R develop myeloproliferative syndromes, but not APL (493). PML sumoylation allows attachment of poly-ubiquitin chains by E3 ligase RNF4 in order to subsequently degrade PML/RARα (494, 495).
Even though the targeted effect of RA and arsenic trioxide on PML/RARα degradation was discovered *a posteriori*, it still represents an impressive example for UPS-mediated treatment of fusion-positive cancers. In APL combination therapy, the accelerated degradation of PML/RARα results in a cure rate of above 90% (496, 497).

1.4.5. Ewing sarcoma – therapeutic potential of UPS targeted therapy

As neither upstream nor downstream targets have brought the success of a targeted therapy approach in Ewing sarcoma, the EWS/FLI1 protein is now the main subject of investigation (reviewed in (33, 498). Considering the central role of the EWS/FLI1 protein, unraveling its underlying proteolytic and non-proteolytic mechanisms is a key for the development of novel therapeutic strategies. The rising number of developed inhibitors against many parts of the ubiquitin cascade promises a great potential to identify new agents for Ewing sarcoma treatment.

2. Aims

Treatment protocols for pediatric Ewing sarcoma are still based on “old” drug combinations including doxorubicin, ifosfamide and vincristine. These well known chemotherapeutics are very effective in a large variety of cancers; however, they display high toxicity and act in a non-specific manner. The problematic of refractory and relapsed tumors as well as secondary neoplasms and severe side effects in children demand a high need for less toxic and highly tumor-specific treatment strategies. In Ewing sarcoma, the aberrant transcription factor EWS/FLI1 is the only consistent genetic abnormality. The protein is crucially required for tumor formation, maintenance and progression. Depletion of the oncogenic fusion results in tumor loss. The EWS/FLI1 protein therefore serves as an ideal target. Transcription factors can be targeted indirectly by modulation of their downstream effector targets, by disruption of important protein-protein interactions or by altering posttranslational modifications of the protein. Over the last years, targeting components or pathways of the ubiquitin proteasome system have become an emerging field in cancer therapy. Due to their presence and regulatory ability in every cell, they present a variety of novel therapeutic targets.

In this thesis, we aim to develop novel strategies for Ewing sarcoma treatment based on targeting the turnover of the EWS/FLI1 fusion protein. First, we aim to elucidate how EWS/FLI1 stability and turnover is regulated on a molecular level. Using mass spectrometry, we will identify possible ubiquitin acceptor sites to better understand how regulation of stabilization is implicated in Ewing sarcoma pathogenesis (Fig. 12 part 1). In a second part, we aim to determine E3 ligase(s) responsible for EWS/FLI1 poly-ubiquitination and to characterize their interaction with the fusion protein. Speculatively, activation of E3 ligases would result in destabilization of the EWS/FLI1 fusion protein (Fig. 12 part 2). Finally, we will characterize a possible mechanism of stabilization by deubiquitination of EWS/FLI1. An siRNA-based screening approach will be used to identify DUBs that modulate EWS/FLI1 stability. A possible candidate will be characterized on the molecular and physiological level (Fig. 12 part 3).

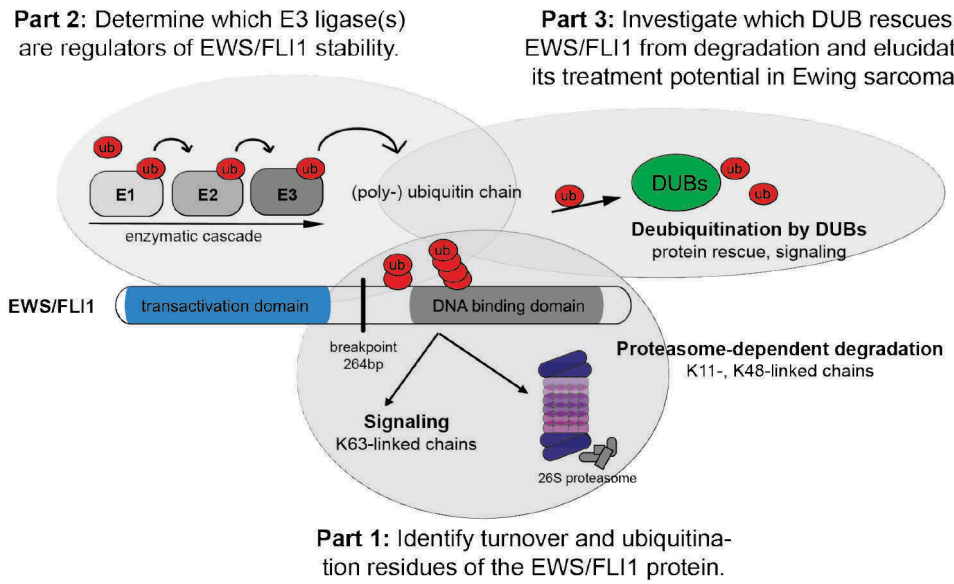

Fig. 12: Specific aims to unravel EWS/FLI1 protein turnover. In part 1, we aim to investigate ubiquitin acceptor lysine(s) mediating EWS/FLI1 protein degradation. Part 2 and 3 focus on the identification of the E3 ligases and deubiquitinating enzymes modulating EWS/FLI1 protein ubiquitination.

3. Results

4. Manuscript I

Proteasomal degradation of the EWS-FLI1 fusion protein is regulated by a single lysine residue

Maria E. Gierisch, Franziska Pfistner, Laura A. Lopez-Garcia, Lena Harder, Beat W. Schäfer*, Felix K. Niggli

From the Department of Oncology and Children's Research Center, University Children´s Hospital, Steinwiesstrasse 32, 8032 Zurich, Switzerland

*Corresponding author:

Beat Schäfer, Department of Oncology, Children´s Hospital Zurich, Steinwiesstrasse 32, 8032 Zurich, Switzerland, Tel. +41 44 2667553, Fax +41 44 6348859, Email beat.schaefer@kispi.uzh.ch

Running title: EWS-FLI1 degradation is mediated by one lysine residue

Keywords: Ewing sarcoma, EWS-FLI1, ETS transcription factors, protein turnover, ubiquitin, target genes

Manuscript published in Journal of Biological Chemistry

DOI: 10.1074/jbc.M116.752063

Contributions to the manuscript:

I performed and analyzed all experiments except the GPS approach and experiments were established and performed together with Franziska Pfistner. The mass spectrometry run and analysis were performed by Laura Lopez. Stable exchange cell lines have been sorted by Lena Harder. Microarray expression data have been analyzed by the Functional Genomics Center Zurich. Data interpretation, manuscript writing and formatting was done by me.

Abstract

E-26 transformation specific (ETS) proteins are transcription factors directing gene expression through their conserved DNA-binding domain. They are implicated as truncated forms or interchromosomal rearrangements in a variety of tumors including Ewing sarcoma, a pediatric tumor of the bone. Tumor cells express the chimeric oncoprotein EWS-FLI1 from a specific t(22;11)(q24;12) translocation. EWS-FLI1 harbors a strong transactivation domain from EWSR1 and the DNA-binding ETS domain of FLI1 in the C-terminal part of the protein. Even though Ewing cells are crucially dependent on continuous expression of EWS-FLI1, its regulation of turnover has not been characterized in detail.

Here, we identify the EWS-FLI1 protein as a substrate of the ubiquitin proteasome system with a characteristic poly-ubiquitination pattern. Using a Global Protein Stability approach, we determined the half life of EWS-FLI1 to lie between 2h-4h whereas full length EWSR1 and FLI1 were more stable. By mass spectrometry, we identified two ubiquitin acceptor lysine residues of which only mutation of K380 in the ETS domain of the FLI1 part abolished EWS-FLI1 ubiquitination and stabilized the protein posttranslationally. Expression of this highly stable mutant protein in Ewing cells, while simultaneously depleting the endogenous wild type protein, differentially modulates two subgroups of target genes to be either EWS-FLI1 protein dependent or turnover dependent. The majority of target genes is in an unaltered state and cannot be further activated.

Our study provides novel insights into EWS-FLI1 turnover, a critical pathway in Ewing sarcoma pathogenesis and lies new grounds to develop novel therapeutic strategies in Ewing sarcoma.

Introduction

E-26 transforming specific (ETS) family members are strong activators or repressors of transcription with a highly conserved ETS domain (1-3). ETS transcription factors (TFs) bind most commonly in complexes to a GGA core region in order to mediate gene expression (4,5). Their main biological functions include regulation of differentiation, lineage determination of the hematopoietic system and control of angiogenesis (6,7). Most of the ETS family members have oncogenic potential, since truncated or overexpressed ETS proteins have been linked to several cancer entities (8-11). ERG or ETV1 are frequently fused to the TMPRSS2 promoter in prostate cancer, whereas ETV1 and ETV6 are implicated in leukemia (12,13). Like other aberrant fusion proteins, they act as drivers of uncontrolled cell growth and survival (14,15). However, most TFs do not harbor an enzymatic pocket and are therefore difficult to target directly. Novel strategies which uncover vulnerable sites in TFs are urgently needed to develop novel targeted therapies (16).

Ewing sarcoma is a rare pediatric bone and soft tissue tumor with an aggressive behavior and prevalence to metastasize (17,18). Its main genetic abnormalities are EWS–ETS rearrangements, among them most commonly the EWS gene on chromosome 22 fused to FLI1 on chromosome 11 which results in expression of the chimeric transcription factor EWS-FLI1 (19-21). Continuous expression of the fusion protein is crucial for tumor formation, progression and maintenance (22,23) and its downregulation inhibits proliferation and reduces tumor cell growth (24-26). EWS-FLI1 is thought to function mainly as modulator to activate and repress a wide range of target genes, but also to regulate splicing processes or being a component of large interaction networks (27-31). However, inhibition of a single downstream target gene has not been proven effective yet for Ewing sarcoma therapy.

The turnover of most intracellular proteins is mediated via the ubiquitin proteasome system (UPS) which triggers protein degradation (32). Several ETS proteins can be poly-ubiquitinated by different E3 ligases and subsequently degraded by the proteasome (33-36). Considering their high conservation, proteasomal degradation is likely to be the main mechanism of turnover for most ETS family members. Most interestingly, truncated ERG and ETV1 are lacking the N-terminal E3 binding domain which results in a delayed turnover of aberrant ETS proteins (34, 36). Here, we focus specifically on the turnover of the fusion protein EWS-FLI1 which only harbors the ETS and the C-terminal domain from FLI1. The impact on the turnover of this domain fused to N-terminal region of EWSR1, has not been investigated yet. Hence, EWS-FLI1 proteasomal turnover represents a so far uncharacterized mechanism in Ewing sarcoma tumorigenesis, even though EWS-FLI1 degradation has already been linked

to the lysosomal pathway (37). Moreover, the exact lysine acceptor residues for poly-ubiquitination have not yet been identified for any wild type or truncated ETS protein.

In the present study, we demonstrate that EWS-FLI1 is predominantly a proteasomal substrate with an unexpectedly high turnover rate mediated by poly-ubiquitination at a single lysine residue. Surprisingly, expression of this highly stable mutant protein in Ewing cells specifically induced subgroups of high-level expressed or turnover sensitive target genes, while the majority of target genes are unaltered.

Hence, our study provides novel insights into EWS-FLI1 turnover suggesting that deflecting its stability could contribute to new therapeutic concepts in Ewing sarcoma.

Results

EWS-FLI1 turnover is proteasome dependent. Since EWS-FLI1 expression is crucial for tumor cell survival (24-26), we were interested to analyze degradation and turnover rate of the fusion protein. To address this, we first used a panel of six different inhibitors targeting proteasomal, lysosomal and autophagosomal protein degradation pathways. Incubation with 20μM of the various inhibitors resulted in a 2-fold upregulation of EWS-FLI1 protein levels only upon MG-132 and Bortezomib treatment, both inhibitors of the chymotrypsin-like proteasome activity (Fig. 1A). We next confirmed this result by selectively inhibiting the proteasomal and lysosomal degradation pathways with two compounds in three different Ewing sarcoma cell lines. Incubation with 20μM of the proteasome inhibitor MG-132 resulted in stabilization of endogenous EWS-FLI1 fusion protein by at least 2-fold while this was not the case for the lysosomal inhibitor chloroquine (Fig. 1B). P27 and LAMP1 were used as positive controls and showed upregulation after treatment as expected. In addition, stabilization of the fusion protein in Ewing cells by MG-132 increased over a 2h-8h treatment period in a time- dependent manner (Fig. 1C). Hence, degradation of EWS-FLI1 is primarily proteasome dependent under steady-state conditions. However, incubation with 20μM cycloheximide (CHX) had only limited reducing effect on the endogenous fusion protein in the Ewing cells over the same 8h time period (Fig. 1D).

Next, we investigated whether the fusion protein is ubiquitinated. To this end, 3xflag-EWS-FLI1 was co-expressed with HA-ubiquitin in HEK293T cells and immunoprecipitated after 48h using anti-flag antibody. Western blotting with an anti-HA antibody revealed at least four distinct ubiquitin bands for EWS-FLI1 which could not be increased by prior treatment with MG132 (Fig. 1E), suggesting a constant ubiquitination of the fusion protein. We next co-expressed 3xflag-EWS-FLI1 with wild type HA-ubiquitin or ubiquitin mutants which are deficient for K48- and K63- linked chains. Immunoprecipitation of the ubiquitinated 3xflag-EWS-FLI1 revealed mainly a decrease of the ubiquitination pattern using K48R HA-ubiquitin (Fig. 1F) indicating that this is the major, but not only, linked ubiquitin chains of the fusion protein

To further validate the fusion protein turnover and to overcome the limitations of classical CHX treatment to determine protein half lives, we next used the Global Protein Stability (GPS) approach (38) (Fig. 2A). Briefly, HEK293T cells were transduced with a reporter construct DsRed-IRES-EGFP in which EGFP is fused to EWS-FLI1. The ratio EGFP/DsRed was determined by FACS and represents a measure for protein stability. Known degron motifs with distinct half lives were used as internal standards and allowed to estimate the half life of EWS-FLI1 to be between 1h and 4h (Fig. 2B). Incubation with MG-132 shifted the ratio closer to 4h, confirming that EWS-FLI1 is a substrate of the proteasome system with a high turnover rate. Additionally, we treated cells with the nuclear export inhibitor leptomycin B (LMB) for 4h and 8h. Treatment with 50nM LMB stabilized EWS-FLI1 in a time-dependent manner (Fig. 2C) indicating that the proteasomal degradation mainly occurs in the cytosol. Similar results were obtained in transiently or stably transduced Ewing cells (Fig. 2D-E), suggesting that the high turnover of EWS-FLI1 is mostly independent of the cellular background. Interestingly, incubation with 20μM CHX again displayed a limited effect on the EGFP/DsRed ratio of EWS-FLI1 reporter construct (Fig. 2B,2E) indicating that classical CHX barely reflects the steady- state turnover rate of the EWS-FLI1 protein and possibly other proteins.

Taken together, our results indicate that EWS-FLI1 is a poly-ubiquitinated protein with an unexpectedly high turnover rate in Ewing sarcoma cells.

EWS-FLI1 turnover depends on one critical lysine residue. To better understand fusion protein turnover, we aimed to identify the lysine residue(s) that are important for degradation. To this, we purified large amounts of 3xflag-EWS-FLI1 or a dominant-negative R386N mutant (39,40) from HEK293T cells. The inactive mutant was included as the inability to bind DNA increases the possibility for ubiquitination. Both samples were then enzymatically digested and subjected to mass spectrometry to identify peptide shifts due to covalently attached ubiquitin. This identified two peptides with the characteristic glycine-glycine shift including residues K298 and K380 (Fig. 3A, supplementary S1A). To determine whether both sites are important for fusion protein turnover, we mutated them individually to arginine. After co-expressing the mutant EWS-FLI1 with HA-ubiquitin and immunoprecipitation from A673 Ewing cells, we found that the K298R mutant was still ubiquitinated comparable to the wild type, while the K380R lost this characteristic pattern (Fig. 3B). In addition, transient expression of the mutants in both A673 and SKNMC Ewing cells revealed that the K380R and the double mutant K298/380R were 2.5-fold, 3.5-fold respectively, more stable than wild type or the K298R mutant (Fig. 3C-D). As wild type EWS-FLI1, also the K380 mutant was still localized in the nucleus (Fig. 3E). We then investigated the role of both lysines in proteasomal turnover by GPS. The half life of the K298R was comparable to wild type EWS-FLI, while K380R shifted close to 24h (Fig. 3F). Wild type EWS-FLI1 and the K298R could be stabilized by an additional incubation with MG-132, however the EGFP/DsRed ratio of the K380R mutant did not change upon treatment (Fig. 3G). Hence, our findings suggest that K380 is the major site required to regulate EWS-FLI1 protein turnover by the proteasome.

EWS-FLI1 fusion protein and wild type FLI1 share a unique site for turnover. To investigate whether turnover by K380 is unique to the fusion protein, we subsequently compared stability and ubiquitination pattern to the full length proteins EWSR1 and FLI1. Surprisingly, both wild type proteins were more stable with half lives of >4h (FLI1) and close to 24h (EWSR1) (Fig. 4A). While FLI1 could be stabilized by incubation with MG-132 (or destabilized by CHX), EWSR1 did not change its already long half life by these treatments (Fig. 4B). As FLI1 was clearly poly-ubiquitinated similar to the fusion protein, EWSR1 showed strong mono- and di-ubiquitination (Fig 4C). Next, we mutated the previously identified lysine residue to arginine (FLI1: K334). By GPS, the K334R also increased its half life towards 24h (Fig. 4D). Additionally, mass spectrometry of purified 3xflag-FLI1 revealed glycine-glycine shifts for peptides containing lysines K172 and K252 (peptide spectra in supplementary S1B-C). Whereas K172 is located in the N-terminal part and therefore not present in the fusion protein, K252 corresponds to the EWS-FLI1 K298 residue. Single arginine mutants of both residues display EGFP/DsRed ratios comparable to wild type FLI1 (Fig. 4D, dotted lines) indicating that both fusion and full length protein turnover is regulated by one single lysine residue. Indeed, incubation of FLI1 and K334R with MG-132 only shifted the wild type, but not the K334R mutant ratio (data not shown). Interestingly, the K334/K380 residue is conserved within most ETS family members (Fig. 4E).

Together, our findings indicate that, despite differences in turnover, stability of both EWS-FLI1 and wild type FLI1 is regulated by the same critical conserved residue in the ETS domain.

EWS-FLI1 target genes expression is subdivided into three major groups. Modulation of EWS-FLI1 target gene signature is one of the best studied mechanisms in Ewing sarcoma. EWS-FLI1 is activating a wide range of target genes like NKX2.2, NR0B1 or IGF1 (30,31,41-43), but has also repressive functions as shown for IGFBP3, PHLDA1 and LOX (44-46). Consequently, this is thought to be critical for oncogenic properties as depletion of the fusion protein results in growth inhibition and cellular senescence (24,47). To better understand the effect of EWS-FLI1 stability on the target gene signature, we established inducible exchange cell lines which were capable to knock down the endogenous EWS-FLI1 while simultaneously expressing 3xflag-EWS-FLI1 or the K380R mutant. To this, we first sorted cells expressing these flag tagged overexpression constructs by flow cytometry for the same low EGFP expression (the selection marker of the pInducer21 vector) to obtain a homogeneously expressing population (Fig. 5A). We then subsequently transduced each of these clonal pools with two different shRNA constructs against the 3'UTR of EWS-FLI1 (Fig. 5B). Upon doxycyline induction for 48h, endogenous

EWS-FLI1 was exchanged with ectopic wild type or mutant 3xflag-EWS-FLI1versions (Fig. 5C). As observed before, the K380R mutant stabilized the protein posttranslationally by at least four-fold (Fig. 5C) while EWS-FLI1 mRNA levels were comparable as shown for shEF#2 (Fig. 5D, not shown for shEF#1 based cell lines). We then extracted total RNA for microarray expression profiling and analyzed the EWS-FLI1 target genes signature for their differential expression upon stabilized fusion protein (supplementary S2). A total of 497 probe sets were downregulated by at least 1.5-fold due to EWS-FLI1 depletion from which 250 could be rescued to at least normal levels by induction of EWS-FLI1 wild type (Fig. 6A-B). Only if the EWS-FLI1 target genes were modulated and recovered in the paired comparison of EWS-FLI1 induction and knockdown at each 24h and 48h, they were considered as rescued. This pattern was similar for repressed target genes as 333 probe sets were at least 1.5-fold upregulated from which 164 could be again repressed by ectopic EWS-FLI1 (Fig. 6A, 6C). However, we were most interested in the target genes which were further modulated with stabilized protein levels. Surprisingly, the large majority of these genes appeared to be unmodified and displayed no difference in target gene expression between wild type and mutant EWS-FLI1. However, two subgroups were modulated differentially by the mutated fusion protein. One subgroup seems to be protein sensitive as 15 individual genes displayed higher RNA levels by at least 1.5-fold upon expression of stabilized EWS-FLI1 protein. From the other subgroup, 29 rescued candidates were fusion protein turnover sensitive and could only partly be modulated by the mutant in comparison to wild type EWS-FLI1 (Fig. 6A-B, list supplementary S2). Among the protein sensitive candidates, IGF1 and long non-coding RNA EWSAT1 have been already characterized (41,48) while most other target genes have not been implicated in EWS-FLI1 oncogenesis. Selected target genes from the protein dependent and unmodified group were validated by quantitative RT-PCR level for two different shEWS-FLI1 sequences (Fig. 6D, shown for shEF#2). Even though the exact mechanism of EWS-FLI1 gene repression is not fully understood, the pattern of target gene modulation resembled that of activated target genes. The majority of repressed genes were unmodified, but also here two subgroups differentially modulated repression upon expression of stabilized protein levels (Fig. 6C, 6E, list supplementary S2).

Taken together, our results indicate that 82% of activated, and 93% of repressed target genes have unaltered levels and cannot be further increased by higher EWS-FLI1 protein levels. Only subsets of the target gene signature are differentially modulated implying that stability of EWS-FLI1 directs these important subgroup or primarily modulates other mechanisms.

Discussion

Here, we demonstrated that EWS-FLI1 is a polyubiquitinated substrate that is primarily degraded by the proteasome. The high turnover of the fusion protein is controlled by one critical lysine residue located in the conserved ETS domain. By exchanging the wild type EWS-FLI1 with its turnover deficient mutant, we could show that protein stabilization differentially modulates two subsets of target genes whose expression could either be enhanced (protein dependent) or only partially rescued (turnover dependent). However, the majority of target genes are in an unmodified state and independent of protein stabilization.

Attachment of ubiquitins to a substrate triggers a variety of outcomes including degradation and signaling depending on the ubiquitin acceptor site and ubiquitin chain linkage (32). Here, we identified the fusion protein EWS-FLI1 as a substrate of the proteasome system in a time and dose dependent manner. The previously suggested lysosomal degradation route (37) possibly contributes to turnover, but appears less relevant compared to the proteasomal pathway under steady state conditions.

During the last decades, a variety of different technologies have been developed to dissect and understand ubiquitin mediated processes (49). GPS profiling was initially established to identify novel proteasomal or cullin-RING ligase substrates (38,50,51). Thus, we applied this approach to analyze EWS-FLI1 turnover. Displaying the EGFP/DsRed ratio for the fusion protein and known standard reporter constructs, we confirmed EWS-FLI1 turnover as proteasome dependent and mapped the half life to be between 1h-4h. As most potent transcription factors, also EWS-FLI1 displays a fast turnover (52,53). Using Leptomycin B, we could show that EWS-FLI1 is indeed exported out of the nucleus for degradation suggesting

that the fusion protein tightly keeps balance of its cytosolic proteolysis. The apparent exclusive nuclear localization might therefore be due to its rapid cytosolic degradation.

However, incubation of cells with the translation synthesis inhibitor CHX barely reflected the high turnover observed in the GPS under steady-state conditions. Using this assay, others already suggested EWS-FLI1 as a stable protein (37). In contrast, by using antisense oligodeoxynucleotides (26) and RNAi approaches, it is known that the fusion protein can be efficiently downregulated within a short 24h time frame which would not be possible with a highly stable protein. The discrepancy between the GPS/RNAi data and CHX treatment therefore remains. However, complete inhibition of protein synthesis by CHX also affects other components of the ubiquitin system such as E2 conjugating enzymes or E3 ligases. Possibly, if a required E3 ligase is unstable and immediately depleted, EWS-FLI1 turnover might be prolonged as seen here with classical CHX treatment.

While EWS-FLI1 has been shown to be posttranslationally modified (54-56), ubiquitination remained unknown. Here, we demonstrated that the fusion protein is polyubiquitinated with a clear and distinct pattern which supports the concept of a constant turnover. To better understand how the ubiquitinated fusion protein is degraded, we used affinity purified EWS-FLI1 for mass spectrometry and searched for glycine-glycine modifications in the fragmented peptide sequence. From two possible ubiquitin acceptor sites, only mutation of the K380 clearly abolished ubiquitination and posttranslationally stabilized the protein. While focusing on EWS-FLI1 degradation, we do not exclude that this critical lysine may also trigger non-proteolytic signaling via alternative linked polyubiquitin chains. It is also worth to mention here that we have analyzed our mass spectrometry data for occurrence of glycine-glycine shifts of the ubiquitin moieties. We have identified peptide shifts mainly for K48-, but also K63-linked ubiquitins (data not shown) confirming our findings that K48-linked chains are highly abundant, but not the exclusive EWS-FLI1 ubiquitination pattern. Other ubiquitin linked chains or mixed chains might also be relevant.

Further, mutation of this residue may also inhibit other modifications such as sumoylation. Acetylation of this residue has not been detected in contrast to the K298 site (55).

The comparison of EWS-FLI1 with its full length proteins revealed that the polyubiquitin pattern is similar to FLI1. Indeed, mutation of the corresponding lysine residue in the ETS domain posttranslationally stabilizes both proteins. As the K380/K334 residue is highly conserved among most ETS family members, it might contribute to proteasomal degradation in other ETS proteins and their fusion proteins. Most interestingly, EWS-FLI1 displays a higher turnover compared to its full length proteins EWSR1 and FLI1. In contrast, the ETS proteins ERG or ETV1 which are fused to the TMPRSS2 promoter in prostate cancer stabilize the protein and confer a physiological advantage to cancer cells (33,34,36). The truncated protein versions display increased stability due to loss of the N-terminal E3 ligase motif. However, EWS-FLI1 is not a truncated version of FLI1, instead the N-terminal domain is dominated by EWSR1 with a stronger transactivation domain. If the turnover and subsequent E3 ligase binding of ETS members is conserved, EWS-FLI1 might possibly interact with E3 ligases via its EWSR1 domain giving rise to a new regulatory mechanism. However, the basic concept that truncated oncogenic TFs are more stable than their wild type counterparts (36) might not apply for fusion proteins consisting of two unrelated protein domains. Whether this is indeed a general paradigm or rather specific for EWSR1 related fusion proteins needs to be further elucidated.

We then deciphered the role of EWS-FLI1 turnover in transcriptional regulation of target genes. To investigate the influence of stabilized EWS-FLI1 on target gene expression, we established an inducible Ewing cell system allowing to deplete endogenous EWS-FLI1 protein while simultaneously expressing the wild type fusion protein or a turnover deficient mutant. This system largely circumvents interference with endogenous fusion protein, enabling us to study the dynamic behavior of posttranslationally stabilized EWS-FLI1 protein on transcriptional regulation. Surprisingly, around 85% of both activated and repressed target genes are in an unaltered state including well characterized target genes such as NR0B1 or STEAP1 (30,57).

Even though our EWS-FLI1 wild type overexpression constructs are around 2-fold above the endogenous EWS-FLI1 levels, it is possible that co-factors expressed at endogenous levels or interacting proteins are limiting further

modulation. The knowledge of the EWS-FLI1 interactome is continuously expanding (28,29), however, it still remains unsolved which co-factors or interacting proteins are most important or influence the fusion protein in a context dependent matter. Nevertheless, longer induction of wild type or mutated ectopic EWS-FLI1 up to 96h induced cell death irrespective of the construct (data not shown).

Besides the majority of unmodified target genes, two other subgroups display a different behavior. 15 activated target genes are higher expressed upon stabilized EWS-FLI1 protein levels. This group includes protein-coding genes such as IGF1 (41) or LEMD1 and RNA-coding genes such as EWSAT1 (48). Interestingly, EWSAT1 was also observed to be elevated upon higher EWS-FLI1 expression in a different experimental setting (48) suggesting that our approach reflects a global pattern. Further, 29 activated target genes are less expressed upon stabilized EWS-FLI1. None of these turnover sensitive target genes have yet been characterized even though few interesting candidates as ALK or TP63 appeared.

Most interestingly, the activity of TFs can be influenced by their own turnover as shown for estrogen receptor α or c-MYC (58,59). It was recently shown that the proteasomal turnover of c-myc is required for full activity. Lysine mutated c-MYC failed to induce tumorigenesis as inhibitory complexes could not be removed during target gene activation (58) while other TFs are independent of ongoing degradation for their transcriptional activity (60). Surprisingly, EWS-FLI1 induced distinct behavior in three subgroups of target genes. Speculatively, the two small subgroups of EWS-FLI1 protein sensitive and turnover sensitive target genes might be of greater importance and their dynamics might trigger different response pathways in Ewing sarcoma oncogenicity. Even though it is not yet clear how these subgroups are defined at their regulatory regions, possible driver target genes might be found in these two subgroups. Alternatively, since we see most target gene levels unaltered, oncogenic properties might depend also on additional mechanisms such as interacting proteins and/or influence on the splicing machinery.

Taken together, turnover regulation of the major oncogenic driver EWS-FLI1 represents an important regulatory mechanism in Ewing sarcoma pathogenesis. Interference with fusion protein degradation might not only be a novel therapeutic strategy in Ewing sarcoma treatment, but might also be applicable to other ETS based fusion proteins.

Experimental procedure

Cell lines and reagents- HEK293T cells were cultured in DMEM (Sigma Aldrich, Buchs, Switzerland) supplemented with 10% FBS (Sigma Aldrich), 2mmol/L glutamine (BioConcept, Allschwil, Switzerland) and 100U/ml penicillin/streptomycin (ThermoFisher Scientific AG, Reinach, Switzerland) at 37°C in 5% CO_2. Ewing sarcoma cell lines A673, SKNMC and TC71 were cultured in RPMI as described above. Additionally, dishes were pre-coated with 0.2% gelatine (Sigma Aldrich). All cell lines have been tested mycoplasma negative. The following reagents were used: Bortezomib (Selleckchem, Houston, TX, USA), Chloroquine, cycloheximide, DMSO, doxycycline, E64, leptomycin B (all Sigma Aldrich), LY294002, MG-132 (Millipore, Billerica, MA, USA) and 3-Methyladenine (ApexBio, Houston, TX, USA).

Plasmids and cloning- The coding sequence for human EWS-FLI1, FLI1 and EWS, were subcloned into the Not1 site of pCMV-3xflag vector (Sigma Aldrich). For Global Protein Stability, the coding sequences of DsRed-IRES-EGFP or d24-EGFP or d4-EGFP or d1-EGFP (addgene #41941, #41944, #41943, #41942) were cloned into the EcoR1 site of pR-EF1 (Cellecta Inc., Mountain View, CA, USA). All cDNAs (EWS-FLI1, FLI1, EWS and mutants) were inserted into the BSTB1 site at the 3' end of DsRed-IRES-EGFP.
3xflag-EWS-FLI1 cDNA was cloned into the Spe1-BamH1 sites of pInducer21 ORF (Addgene #46948). The pRSIT-U6Tet-shRNA-PGKTetRep-2A-GFP-2A-puro vector with shRNAs against EWS-FLI1 was purchased from Cellecta Inc. with the following target sequences: shEF#1 5' ATAGAGGTGGGAAGCTTATAA 3' (previously described in (31)) and shEF#2 5' CGTCATGTTCTGGTTTGAGAT 3' (designed against the C-terminal FLI1 part according to RefSeq# NM_002017.4).
Cloning was performed by In-Fusion cloning HD (Clontech Laboratories Inc., Mountain View, CA, USA) according to manufacturer's protocol. All mutations were introduced using site-directed mutagenesis. Detailed information

of plasmids, cloning and mutagenesis primers can be found in supplementary table ST1. All clonings were verified by sequencing.

Transient transfection- For HEK293T cells, DMEM complete medium was mixed with PolyethylenimineMax (Polyscience, Cham, Switzerland) and plasmids for 15min and added to the cells for 48h. For Ewing sarcoma cells, JetPrime (Polyplus Transfections, Illkirch, France) reagent was used according to manufacturer's instruction in antibiotics-free RPMI medium.

Viral production and transduction- HEK293T cells were transfected with cDNA vectors and pMDL, pREV, and pVSV with JetPrime according to manufacturer's instruction in antibiotics-free DMEM medium. Medium was replaced 24h after transfection and virus was harvested after additional 48h. Viral supernatant was cleared by centrifugation, filtered and concentrated if necessary (Amicon® Ultra 15 mL, Millipore). Ewing sarcoma cells were infected with the viral supernatant supplemented with 10µg/ml polybrene (Sigma Aldrich) for 16-18h.

Global Protein Stability Assay and flow cytometry- Lentivirus from HEK293T transfected with pR-EF1-DsRed-IRES-d1/d4/d24/EGFP-cDNA, pMDL, pREV and pVSV was used to transduce HEK293T or Ewing sarcoma cells as described to about 5-10% of DsRed positive cells. Cells were harvested 72h after transduction, incubated with cycloheximide, leptomycin B or MG-132 for 4-8h as indicated and analyzed by FACS. Cells were resuspended in PBS and filtered using a 40µm cell strainer (BD Becton, Dickinson and Company, Franklin Lakes, NJ, USA). FACS analysis was performed on a FACS Canto™ II Cytometry system (BD) and data were analyzed by FlowJo software (Treestar Inc., Ashland, OR, USA). At least 50000 cells were recorded for each experiment. Cell sorting was done with a FACS AriaTM III Cytometry system (BD).

Cell lysis, western blotting and antibodies- Cells were harvested and lysed in standard lysis buffer (50mM Tris/HCl, 150mM NaCl, 50mM NaF, 5mM $Na_4P_2O_7$, 1mM Na_3VO_4 and 10mM ß-glycerolphosphate, 1% TritonX with protease inhibitor cocktail, Complete Mini® (Sigma Aldrich)). Lysates were sonicated and cleared by centrifugation. Proteins were separated by 4%-12% or 10% BisTris NuPAGE pre-cast gels (ThermoFisher Scientific AG) and transferred to nitrocellulose membranes (GE Healthcare). Membranes were blocked with 5% milk powder in 0.2% PBS-Tween and primary antibodies were incubated over night at 4°C followed by 2h of HRP-linked secondary antibody at room temperature. Proteins were detected by chemiluminescence using Amersham ECL detection reagent (GE Healthcare, Glattbrugg, Switzerland) or SuperSignal™ Western blotting reagent (ThermoFisher Scientific AG). Quantification of blots was performed by using ImageJ (version 1.46r). The following commercial antibodies were used: anti-Actin (dilution 1:1000, Cell Signaling), anti-Flag (clone M2, 1:1000, Sigma Aldrich), anti-FLI1 (1:1000, MyBiosource LLC, San Diego, CA, USA), anti-GAPDH (1:1000, Cell Signaling), anti-HA (1:1000, Millipore), anti-LAMP1 (1:500, DSHB, Iowa City, Iowa, USA), anti-p27 (1:1000, Cell Signaling and 1:200 ThermoFisher Scientific AG) and anti-Tubulin (1:40000 Sigma Aldrich).

Immunoprecipitation of ubiquitinated proteins- Cells were transfected for 48h and treated with 10µM MG-132 prior to lysis in ubiquitin lysis buffer (2% SDS, 150mM NaCl, 10mM Tris/HCl, 2mM Na_3VO_4, 50mM NaF with Complete Mini Protease inhibitor cocktail), boiled for 10min and sonicated. Lysates were diluted 1:10 in dilution buffer (150mM NaCl, 10mM Tris/HCl, 2mM EDTA, 1% Triton X), incubated for 30min at 4°C and cleared by centrifugation for 30min at maximum speed. Immunoprecipitation was performed using anti-Flag antibody (Sigma Aldrich) coupled to Dynabeads ProteinG (ThermoFisher Scientific AG). Lysates were incubated for 1h at 4°C, washed three times, eluted at room temperature using 3xflag peptide (Sigma Aldrich) and prepared for western blot analysis. Extended description for detection of EWS-FLI1 ubiquitination sites by mass spectrometry can be found in supplementary S1.

Immunofluorescence and microscopy- A673 cells were seeded on cover slides for 24h and transiently transfected with flag tagged plasmids for additional 48h. After fixing with 4% PFA (Carl Roth, Arlesheim, Switzerland), cells were permeabilized and stained with anti-Flag antibody (1:300, Sigma Aldrich) in 4% horse serum (Sigma Aldrich) and 0.1% PBS-TritonX over night. Fluorescent secondary

antibody (Alexa-488 anti-mouse, Sigma Aldrich) in PBS with 4% horse serum was applied for 1h. Cover slides were fixed on objective glass with DAPI Vectashield® mounting medium (Vector laboratories Inc., Burlingame, CA, USA) and analyzed by an Axioskop 2 MOT Plus (Carl Zeiss Microscopy LLC, Thornwood, NY, USA).

Quantitative PCR and microarray analysis- Total RNA was extracted from Ewing sarcoma cells using Qiagen RNeasy Kit (Qiagen Instruments AG, Hombrechtikon, Switzerland). cDNA synthesis was carried out using High-Capacity Reverse Transcription Kit (Applied Biosystems by ThermoFisher Scientific AG). Quantitative PCR was performed using TaqMan gene expression master mix (ThermoFisher Scientific AG) and assays on demand (Applied Biosystems by ThermoFisher Scientific AG). A complete list can be found in supplementary table ST1. Replicate values were pooled and represented as geometric mean values with a 95% confidence interval. Microarray expression analysis with total RNA was performed using GeneChip® Human Gene 2.0 ST Array (Atlas Biolabs, Berlin, Germany). Data are accessible under GSE81018.

Microarray data analysis- The raw microarray data were processed and normalized using the RMA algorithm (61). Differential expression was computed using the Bioconductor package limma providing a moderated t-test that is adapted to low number of replicates (62). Differential expression results were filtered based on fold-change and p-values. All computations were done using R/Bioconductor. Extended description for target gene grouping can be found in supplementary S2.

FOOTNOTES

Funding sources: Swiss National Science Foundation 31003A-144177

Conflict of interest: The authors declare that they have no conflicts of interest with the contents of this article.

Author's contributions: MG, BS, FN designed the study and wrote the paper. MG and FP designed, performed and analyzed the experiments. LL performed and analyzed the mass spectrometry experiments. LH provided help with flow cytometry and sorted stable cell lines. All authors reviewed the results and approved the final version of the manuscript.

References

1. Hollenhorst, P. C., McIntosh, L. P., and Graves, B. J. (2011) Genomic and biochemical insights into the specificity of ETS transcription factors. *Annu Rev Biochem* **80**, 437-471
2. Laudet, V., Hanni, C., Stehelin, D., and Duterque-Coquillaud, M. (1999) Molecular phylogeny of the ETS gene family. *Oncogene* **18**, 1351-1359
3. Wasylyk, B., Hahn, S. L., and Giovane, A. (1993) The Ets family of transcription factors. *Eur J Biochem* **211**, 7-18
4. Li, R., Pei, H., and Watson, D. K. (2000) Regulation of Ets function by protein - protein interactions. *Oncogene* **19**, 6514-6523
5. Nye, J. A., Petersen, J. M., Gunther, C. V., Jonsen, M. D., and Graves, B. J. (1992) Interaction of murine ets-1 with GGA-binding sites establishes the ETS domain as a new DNA-binding motif. *Genes Dev* **6**, 975-990
6. Lelievre, E., Lionneton, F., Soncin, F., and Vandenbunder, B. (2001) The Ets family contains transcriptional activators and repressors involved in angiogenesis. *Int J Biochem Cell Biol* **33**, 391-407
7. Sharrocks, A. D. (2001) The ETS-domain transcription factor family. *Nat Rev Mol Cell Biol* **2**, 827-837
8. Davidson, B., Reich, R., Goldberg, I., Gotlieb, W. H., Kopolovic, J., Berner, A., Ben-Baruch, G., Bryne, M., and Nesland, J. M. (2001) Ets-1 messenger RNA expression is a novel marker of poor survival in ovarian carcinoma. *Clin Cancer Res* **7**, 551-557
9. Golub, T. R., Barker, G. F., Bohlander, S. K., Hiebert, S. W., Ward, D. C., Bray-Ward, P., Morgan, E., Raimondi, S. C., Rowley, J. D., and Gilliland, D. G. (1995) Fusion of the TEL gene on 12p13 to the AML1 gene on 21q22 in acute lymphoblastic leukemia. *Proc Natl Acad Sci U S A* **92**, 4917-4921
10. Petrovics, G., Liu, A., Shaheduzzaman, S., Furusato, B., Sun, C., Chen, Y., Nau, M., Ravindranath, L., Chen, Y., Dobi, A., Srikantan, V., Sesterhenn, I. A., McLeod, D. G., Vahey, M., Moul, J. W., and Srivastava, S. (2005) Frequent overexpression of ETS-related gene-1 (ERG1) in prostate cancer transcriptome. *Oncogene* **24**, 3847-3852
11. Tomlins, S. A., Rhodes, D. R., Perner, S., Dhanasekaran, S. M., Mehra, R., Sun, X. W., Varambally, S., Cao, X., Tchinda, J., Kuefer, R., Lee, C., Montie, J. E., Shah, R. B., Pienta, K. J., Rubin, M. A., and Chinnaiyan, A. M. (2005) Recurrent fusion of TMPRSS2 and ETS transcription factor genes in prostate cancer. *Science* **310**, 644-648
12. Kumar-Sinha, C., Tomlins, S. A., and Chinnaiyan, A. M. (2008) Recurrent gene fusions in prostate cancer. *Nat Rev Cancer* **8**, 497-511
13. Seth, A., and Watson, D. K. (2005) ETS transcription factors and their emerging roles in human cancer. *Eur J Cancer* **41**, 2462-2478
14. Mertens, F., Antonescu, C. R., Hohenberger, P., Ladanyi, M., Modena, P., D'Incalci, M., Casali, P. G., Aglietta, M., and Alvegard, T. (2009) Translocation-related sarcomas. *Semin Oncol* **36**, 312-323
15. Mitelman, F., Johansson, B., and Mertens, F. (2007) The impact of translocations and gene fusions on cancer causation. *Nat Rev Cancer* **7**, 233-245
16. Hagenbuchner, J., and Ausserlechner, M. J. (2015) Targeting transcription factors by small compounds-Current strategies and future implications. *Biochem Pharmacol*
17. Bernstein, M., Kovar, H., Paulussen, M., Randall, R. L., Schuck, A., Teot, L. A., and Juergens, H. (2006) Ewing's sarcoma family of tumors: Current management. *Oncologist* **11**, 503-519
18. Esiashvili, N., Goodman, M., and Marcus, R. B., Jr. (2008) Changes in incidence and survival of Ewing sarcoma patients over the past 3 decades: Surveillance Epidemiology and End Results data. *J Pediatr Hematol Oncol* **30**, 425-430
19. Delattre, O., Zucman, J., Plougastel, B., Desmaze, C., Melot, T., Peter, M., Kovar, H., Joubert, I., de Jong, P., Rouleau, G., and et al. (1992) Gene fusion with an ETS DNA-binding domain caused by chromosome translocation in human tumours. *Nature* **359**, 162-165

20. May, W. A., Gishizky, M. L., Lessnick, S. L., Lunsford, L. B., Lewis, B. C., Delattre, O., Zucman, J., Thomas, G., and Denny, C. T. (1993) Ewing sarcoma 11;22 translocation produces a chimeric transcription factor that requires the DNA-binding domain encoded by FLI1 for transformation. *Proc Natl Acad Sci U S A* **90**, 5752-5756
21. May, W. A., Lessnick, S. L., Braun, B. S., Klemsz, M., Lewis, B. C., Lunsford, L. B., Hromas, R., and Denny, C. T. (1993) The Ewing's sarcoma EWS/FLI-1 fusion gene encodes a more potent transcriptional activator and is a more powerful transforming gene than FLI-1. *Mol Cell Biol* **13**, 7393-7398
22. Bailly, R. A., Bosselut, R., Zucman, J., Cormier, F., Delattre, O., Roussel, M., Thomas, G., and Ghysdael, J. (1994) DNA-binding and transcriptional activation properties of the EWS-FLI-1 fusion protein resulting from the t(11;22) translocation in Ewing sarcoma. *Mol Cell Biol* **14**, 3230-3241
23. Braun, B. S., Frieden, R., Lessnick, S. L., May, W. A., and Denny, C. T. (1995) Identification of target genes for the Ewing's sarcoma EWS/FLI fusion protein by representational difference analysis. *Mol Cell Biol* **15**, 4623-4630
24. Kovar, H., Aryee, D. N., Jug, G., Henockl, C., Schemper, M., Delattre, O., Thomas, G., and Gadner, H. (1996) EWS/FLI-1 antagonists induce growth inhibition of Ewing tumor cells in vitro. *Cell Growth Differ* **7**, 429-437
25. Tanaka, K., Iwakuma, T., Harimaya, K., Sato, H., and Iwamoto, Y. (1997) EWS-Fli1 antisense oligodeoxynucleotide inhibits proliferation of human Ewing's sarcoma and primitive neuroectodermal tumor cells. *J Clin Invest* **99**, 239-247
26. Toretsky, J. A., Connell, Y., Neckers, L., and Bhat, N. K. (1997) Inhibition of EWS-FLI-1 fusion protein with antisense oligodeoxynucleotides. *J Neurooncol* **31**, 9-16
27. Petermann, R., Mossier, B. M., Aryee, D. N., Khazak, V., Golemis, E. A., and Kovar, H. (1998) Oncogenic EWS-Fli1 interacts with hsRPB7, a subunit of human RNA polymerase II. *Oncogene* **17**, 603-610
28. Selvanathan, S. P., Graham, G. T., Erkizan, H. V., Dirksen, U., Natarajan, T. G., Dakic, A., Yu, S., Liu, X., Paulsen, M. T., Ljungman, M. E., Wu, C. H., Lawlor, E. R., Uren, A., and Toretsky, J. A. (2015) Oncogenic fusion protein EWS-FLI1 is a network hub that regulates alternative splicing. *Proc Natl Acad Sci U S A* **112**, E1307-1316
29. Toretsky, J. A., Erkizan, V., Levenson, A., Abaan, O. D., Parvin, J. D., Cripe, T. P., Rice, A. M., Lee, S. B., and Uren, A. (2006) Oncoprotein EWS-FLI1 activity is enhanced by RNA helicase A. *Cancer Res* **66**, 5574-5581
30. Kinsey, M., Smith, R., and Lessnick, S. L. (2006) NR0B1 is required for the oncogenic phenotype mediated by EWS/FLI in Ewing's sarcoma. *Mol Cancer Res* **4**, 851-859
31. Smith, R., Owen, L. A., Trem, D. J., Wong, J. S., Whangbo, J. S., Golub, T. R., and Lessnick, S. L. (2006) Expression profiling of EWS/FLI identifies NKX2.2 as a critical target gene in Ewing's sarcoma. *Cancer Cell* **9**, 405-416
32. Hershko, A., and Ciechanover, A. (1998) The ubiquitin system. *Annu Rev Biochem* **67**, 425-479
33. An, J., Ren, S., Murphy, S. J., Dalangood, S., Chang, C., Pang, X., Cui, Y., Wang, L., Pan, Y., Zhang, X., Zhu, Y., Wang, C., Halling, G. C., Cheng, L., Sukov, W. R., Karnes, R. J., Vasmatzis, G., Zhang, Q., Zhang, J., Cheville, J. C., Yan, J., Sun, Y., and Huang, H. (2015) Truncated ERG Oncoproteins from TMPRSS2-ERG Fusions Are Resistant to SPOP-Mediated Proteasome Degradation. *Mol Cell* **59**, 904-916
34. Gan, W., Dai, X., Lunardi, A., Li, Z., Inuzuka, H., Liu, P., Varmeh, S., Zhang, J., Cheng, L., Sun, Y., Asara, J. M., Beck, A. H., Huang, J., Pandolfi, P. P., and Wei, W. (2015) SPOP Promotes Ubiquitination and Degradation of the ERG Oncoprotein to Suppress Prostate Cancer Progression. *Mol Cell* **59**, 917-930
35. Ji, Z., Degerny, C., Vintonenko, N., Deheuninck, J., Foveau, B., Leroy, C., Coll, J., Tulasne, D., Baert, J. L., and Fafeur, V. (2007) Regulation of the Ets-1 transcription factor by sumoylation and ubiquitinylation. *Oncogene* **26**, 395-406
36. Vitari, A. C., Leong, K. G., Newton, K., Yee, C., O'Rourke, K., Liu, J., Phu, L., Vij, R., Ferrando, R., Couto, S. S., Mohan, S., Pandita, A., Hongo, J. A., Arnott, D., Wertz, I. E., Gao, W. Q., French,

D. M., and Dixit, V. M. (2011) COP1 is a tumour suppressor that causes degradation of ETS transcription factors. *Nature* **474**, 403-406
37. Elzi, D. J., Song, M., Hakala, K., Weintraub, S. T., and Shiio, Y. (2014) Proteomic Analysis of the EWS-Fli-1 Interactome Reveals the Role of the Lysosome in EWS-Fli-1 Turnover. *J Proteome Res* **13**, 3783-3791
38. Yen, H. C., Xu, Q., Chou, D. M., Zhao, Z., and Elledge, S. J. (2008) Global protein stability profiling in mammalian cells. *Science* **322**, 918-923
39. Liang, H., Mao, X., Olejniczak, E. T., Nettesheim, D. G., Yu, L., Meadows, R. P., Thompson, C. B., and Fesik, S. W. (1994) Solution structure of the ets domain of Fli-1 when bound to DNA. *Nat Struct Biol* **1**, 871-875
40. Welford, S. M., Hebert, S. P., Deneen, B., Arvand, A., and Denny, C. T. (2001) DNA binding domain-independent pathways are involved in EWS/FLI1-mediated oncogenesis. *J Biol Chem* **276**, 41977-41984
41. Riggi, N., Suva, M. L., Suva, D., Cironi, L., Provero, P., Tercier, S., Joseph, J. M., Stehle, J. C., Baumer, K., Kindler, V., and Stamenkovic, I. (2008) EWS-FLI-1 expression triggers a Ewing's sarcoma initiation program in primary human mesenchymal stem cells. *Cancer Res* **68**, 2176-2185
42. Kinsey, M., Smith, R., Iyer, A. K., McCabe, E. R., and Lessnick, S. L. (2009) EWS/FLI and its downstream target NR0B1 interact directly to modulate transcription and oncogenesis in Ewing's sarcoma. *Cancer Res* **69**, 9047-9055
43. Tirado, O. M., Mateo-Lozano, S., Villar, J., Dettin, L. E., Llort, A., Gallego, S., Ban, J., Kovar, H., and Notario, V. (2006) Caveolin-1 (CAV1) is a target of EWS/FLI-1 and a key determinant of the oncogenic phenotype and tumorigenicity of Ewing's sarcoma cells. *Cancer Res* **66**, 9937-9947
44. Boro, A., Pretre, K., Rechfeld, F., Thalhammer, V., Oesch, S., Wachtel, M., Schafer, B. W., and Niggli, F. K. (2012) Small-molecule screen identifies modulators of EWS/FLI1 target gene expression and cell survival in Ewing's sarcoma. *Int J Cancer* **131**, 2153-2164
45. Prieur, A., Tirode, F., Cohen, P., and Delattre, O. (2004) EWS/FLI-1 silencing and gene profiling of Ewing cells reveal downstream oncogenic pathways and a crucial role for repression of insulin-like growth factor binding protein 3. *Mol Cell Biol* **24**, 7275-7283
46. Sankar, S., Bell, R., Stephens, B., Zhuo, R., Sharma, S., Bearss, D. J., and Lessnick, S. L. (2013) Mechanism and relevance of EWS/FLI-mediated transcriptional repression in Ewing sarcoma. *Oncogene* **32**, 5089-5100
47. Matsunobu, T., Tanaka, K., Nakamura, T., Nakatani, F., Sakimura, R., Hanada, M., Li, X., Okada, T., Oda, Y., Tsuneyoshi, M., and Iwamoto, Y. (2006) The possible role of EWS-Fli1 in evasion of senescence in Ewing family tumors. *Cancer Res* **66**, 803-811
48. Marques Howarth, M., Simpson, D., Ngok, S. P., Nieves, B., Chen, R., Siprashvili, Z., Vaka, D., Breese, M. R., Crompton, B. D., Alexe, G., Hawkins, D. S., Jacobson, D., Brunner, A. L., West, R., Mora, J., Stegmaier, K., Khavari, P., and Sweet-Cordero, E. A. (2014) Long noncoding RNA EWSAT1-mediated gene repression facilitates Ewing sarcoma oncogenesis. *J Clin Invest* **124**, 5275-5290
49. Williamson, A., Werner, A., and Rape, M. (2013) The Colossus of ubiquitylation: decrypting a cellular code. *Mol Cell* **49**, 591-600
50. Emanuele, M. J., Elia, A. E., Xu, Q., Thoma, C. R., Izhar, L., Leng, Y., Guo, A., Chen, Y. N., Rush, J., Hsu, P. W., Yen, H. C., and Elledge, S. J. (2011) Global identification of modular cullin-RING ligase substrates. *Cell* **147**, 459-474
51. Yen, H. C., and Elledge, S. J. (2008) Identification of SCF ubiquitin ligase substrates by global protein stability profiling. *Science* **322**, 923-929
52. Kodadek, T., Sikder, D., and Nalley, K. (2006) Keeping transcriptional activators under control. *Cell* **127**, 261-264
53. Muratani, M., and Tansey, W. P. (2003) How the ubiquitin-proteasome system controls transcription. *Nat Rev Mol Cell Biol* **4**, 192-201

54. Bachmaier, R., Aryee, D. N., Jug, G., Kauer, M., Kreppel, M., Lee, K. A., and Kovar, H. (2009) O-GlcNAcylation is involved in the transcriptional activity of EWS-FLI1 in Ewing's sarcoma. *Oncogene* **28**, 1280-1284
55. Schlottmann, S., Erkizan, H. V., Barber-Rotenberg, J. S., Knights, C., Cheema, A., Uren, A., Avantaggiati, M. L., and Toretsky, J. A. (2012) Acetylation Increases EWS-FLI1 DNA Binding and Transcriptional Activity. *Front Oncol* **2**, 107
56. Klevernic, I. V., Morton, S., Davis, R. J., and Cohen, P. (2009) Phosphorylation of Ewing's sarcoma protein (EWS) and EWS-Fli1 in response to DNA damage. *Biochem J* **418**, 625-634
57. Grunewald, T. G., Diebold, I., Esposito, I., Plehm, S., Hauer, K., Thiel, U., da Silva-Buttkus, P., Neff, F., Unland, R., Muller-Tidow, C., Zobywalski, C., Lohrig, K., Lewandrowski, U., Sickmann, A., Prazeres da Costa, O., Gorlach, A., Cossarizza, A., Butt, E., Richter, G. H., and Burdach, S. (2012) STEAP1 is associated with the invasive and oxidative stress phenotype of Ewing tumors. *Mol Cancer Res* **10**, 52-65
58. Jaenicke, L. A., von Eyss, B., Carstensen, A., Wolf, E., Xu, W., Greifenberg, A. K., Geyer, M., Eilers, M., and Popov, N. (2016) Ubiquitin-Dependent Turnover of MYC Antagonizes MYC/PAF1C Complex Accumulation to Drive Transcriptional Elongation. *Mol Cell* **61**, 54-67
59. Reid, G., Hubner, M. R., Metivier, R., Brand, H., Denger, S., Manu, D., Beaudouin, J., Ellenberg, J., and Gannon, F. (2003) Cyclic, proteasome-mediated turnover of unliganded and liganded ERalpha on responsive promoters is an integral feature of estrogen signaling. *Mol Cell* **11**, 695-707
60. Yao, J., Munson, K. M., Webb, W. W., and Lis, J. T. (2006) Dynamics of heat shock factor association with native gene loci in living cells. *Nature* **442**, 1050-1053
61. Irizarry, R. A., Hobbs, B., Collin, F., Beazer-Barclay, Y. D., Antonellis, K. J., Scherf, U., and Speed, T. P. (2003) Exploration, normalization, and summaries of high density oligonucleotide array probe level data. *Biostatistics* **4**, 249-264
62. Gentleman, R. (2005) *Bioinformatics and computational biology solutions using R and Bioconductor*, Springer Science+Business Media, New York

Figure Legends

Figure 1: EWS-FLI1 protein turnover is proteasome dependent. (A) Western blot analysis of EWS-FLI1 protein levels. A673 cells were treated with 20µM of indicated compounds for 8h, EWS-FLI1 protein levels were detected with anti-FLI1 antibody. Quantification represents ratio of FLI1 over GAPDH compared to DMSO control. (B) EWS-FLI1 turnover in various Ewing sarcoma cell lines. A673, SKNMC and TC71 cells were treated with 20µM MG-132 or chloroquine (CQ) for 10h (A673), 8h (SKNMC) and 9h (TC71), and immunoblotted with anti-FLI1 antibody. Quantification represents ratio of FLI1 over tubulin compared to DMSO control. (C) EWS-FLI1 stabilizes in a time-dependent manner. Western blot of A673 cells treated with 10µM MG-132 for indicated time points. Three independent experiments were quantified and are represented in the scatter blot with n=3 (2h-8h) or n=5 (DMSO), error bars as SD. (D) Half-life of endogenous EWS-FLI1 protein. Western blot of A673 cells treated with 20µg/ml CHX for indicated hours. Quantification of three independent experiments with n=3 (2h-8h) or n=5 (DMSO), error bars as SD. (E) EWS-FLI1 is ubiquitinated. 3xflag-EWS-FLI1 and HA-ubiquitin were co-expressed for 48h in HEK293T cells and incubated with 10µM MG-132 for indicated hours. After immunoprecipitation of EWS-FLI1 with anti-Flag, ubiquitination was visualized by anti-HA antibody. (F) EWS-FLI1 ubiquitination consists of K48-linked ubiquitin chains. 3xflag-EWS-FLI1 and wild-type or mutant HA-ubiquitins were co-expressed for 48h in HEK293T cells, immunoprecipitated and ubiquitination was visualized by anti-HA antibody.

Figure 2: The EWS-FLI1 protein displays a high turnover. (A) Scheme illustrating GPS approach in which a reporter construct of DsRed-IRES-EGFP is fused at the C-terminus of EGFP to a protein of interest. The EGFP/DsRed ratio is determined by FACS and represents a measure for protein stability. (B) EWS-FLI1 turnover measured by GPS. HEK293T were transduced for 72h with a reporter construct fused to EWS-FLI1 or degron (d) motifs with half lives of 1h (d1h), 4h (d4h) and 24h (d24h) and analyzed by FACS. The reporter construct fused to EWS-FLI1 was additionally incubated with 20µM MG-132 or 20µg/ml CHX for 8h or (C) with 50nM Leptomycin B (LMB) for 4h and 8h (dotted line). (D) EWS-FLI1 stability in Ewing cell line A673. GPS analysis of reporter constructs fused to EWS-FLI1 or standard degron motifs 72h after transduction. (E) A673 cells stably transfected with reporter-EWS-FLI1 construct were sorted and incubated with DMSO, 20µM MG-132 or 20µg/ml CHX for 8h.

Figure 3: Mass spectrometry identifies K380 residue as the main ubiquitination site. (A) Two lysine residues were identified to be ubiquitinated by mass spectrometry. Peptide spectra with glycine-glycine shift for residue K380 (peptide spectra for the K298 site in supplementary S1A). (B) Mutation of lysine residue K380 prevents EWS-FLI1 ubiquitination. 3xflag-EWS-FLI1, K298R and K380R mutants were co-expressed with HA-ubiquitin for 48h in A673 cells, purified ubiquitinated EWS-FLI1 was analyzed using anti-HA antibody by western blotting. (C) Mutated K380 residue stabilizes EWS-FLI1 protein. 3xflag-EWS-FLI1, single and double mutants were transiently overexpressed for 48h in A673 and SKNMC cells and analyzed with an anti-Flag antibody by western blot. (D) Scatter blot for quantification for n=3 independent experiments, error bars as SD. (E) EWS-FLI1 mutant show nuclear localization. 3xflag-EWS-FLI1 and K380R single mutant were transiently expressed for 48h in A673 cells. Cells were fixed, stained with anti-Flag antibody and used for immunofluorescence (40x magnification). (F) Mutation of K380 stabilizes EWS-FLI1 posttranslationally. HEK293T cells were transduced for 72h with reporter constructs of EWS-FLI1, mutants K298R and K380R and standards. EGFP/DsRed ratios were analyzed by FACS, (G) after additional incubation with DMSO or 20µM MG-132 for 8h.

Figure 4: Regulation of proteasomal turnover is conserved between EWS-FLI1 and FLI1. (A) EWS-FLI1 displays fastest turnover. GPS analysis of EWS-FLI1, EWSR1 and FLI1 reporter constructs and standards transduced into HEK293T cells and analyzed after 72h by FACS. (B) Full length proteins EWSR1 and FLI1 were additionally treated with 20µM MG-132 or 20µg/ml

CHX for 8h. (C) Immunoprecipitation of EWS-FLI1, EWSR1 and FLI1 proteins. 3xflag tagged versions were co-expressed with HA-ubiquitin for 48h and stabilized for additional 5h with 20µM MG-132. After immunoprecipitation of tag proteins, ubiquitin pattern was analyzed by anti-HA antibody. (D) Mutation of conserved residue K334R stabilizes FLI1 in GPS analysis. HEK293T cells were transduced for 72h with reporter constructs of FLI1, mutants K172R, K252R, K334R and standards. EGFP/DsRed ratio was analyzed by FACS. (E) Turnover dependent lysine residue is conserved within most ETS family members. ClustalW alignment of conserved ETS domain sequence, K334/K380 residue is marked in red.

Figure 5: Generation of exchange Ewing cell lines. (A) EGFP (selection marker) sorting of pInducer21 vector transduced cells. A673 cells with 3xflag, 3xflag-EWS-FLI1 or 3xflag-K380R mutant were sorted for same low EGFP expression. After sorting, all cell pools were analyzed by FACS for EGFP and plotted for corresponding mean fluorescent intensity (MFI). (B) ShEF sequences shRNA against the 3' UTR of EWS-FLI1 are sufficient to downregulate EWS-FLI1 protein. Western blot of A673 cells with shEF constructs #1 and #2 after incubation with 0.1ng/µl doxycycline for 48h. (C) Inducible EWS-FLI1 exchange cell lines. Double transduced A673 cells were incubated with 0.1ng/µl doxycycline for 48h. Endogenous and exogenous EWS-FLI1 protein levels were analyzed by western blotting using anti-FLI1 antibody, (D) and mRNA levels were analyzed by quantitative RT-PCR, with n=4 and error bars represent 95% confidence intervals.

Figure 6: Differential regulation of target gene expression by EWS-FLI1 protein levels. (A) Analysis of microarray expression data of A673 exchange cell lines reveals three subgroups of target gene regulation. Pie chart distribution for EWS-FLI1 activated (upper) and repressed (lower) target genes and their differential modulation of stabilized over wild type EWS-FLI1. (B-C) Heat map of activated-rescued (B) and repressed-rescued (C) target gene signature. The comparison of stabilized over wild type EWS-FLI1 target genes resembled in three distinct groups. (D-E) Validation of selected activated (D) or repressed (E) target genes by quantitative RT-PCR based on RNA extracted from shEF#2 exchange cell lines, with n=4 and error bars represent 95% confidence intervals.

Figures

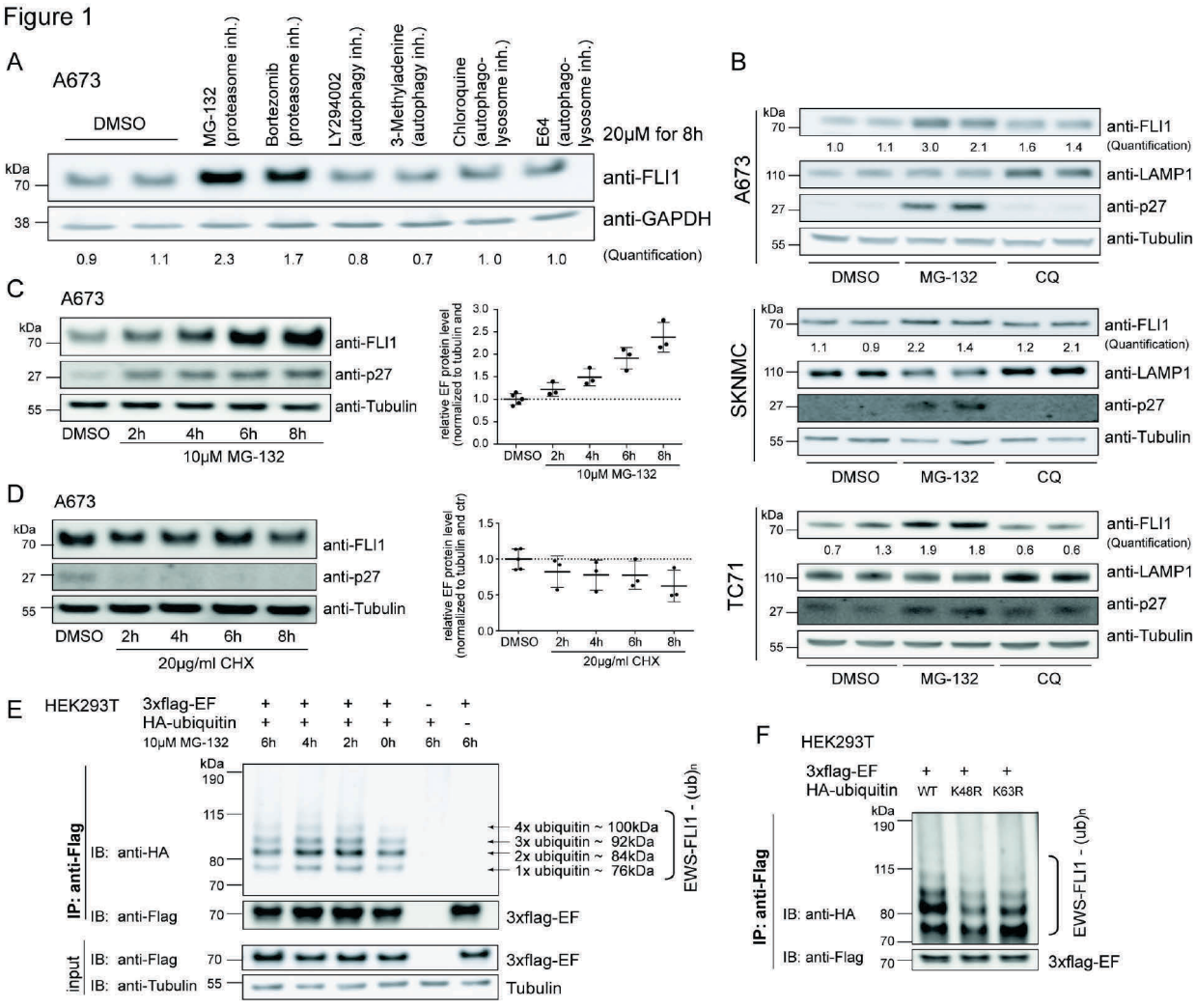
Figure 1
A
A673
DMSO
MG-132 (proteasome inh.)
Bortezomib (proteasome inh.)
LY294002 (autophagy inh.)
3-Methyladenine (autophagy inh.)
Chloroquine (autophago-lysosome inh.)
E64 (autophago-lysosome inh.)
20µM for 8h
kDa
70
anti-FLI1
38
anti-GAPDH
0.9 1.1 2.3 1.7 0.8 0.7 1. 0 1.0
(Quantification)
B
A673
kDa
70
anti-FLI1
1.0 1.1 3.0 2.1 1.6 1.4
(Quantification)
110
anti-LAMP1
27
anti-p27
55
anti-Tubulin
DMSO MG-132 CQ
SKNMC
70
anti-FLI1
1.1 0.9 2.2 1.4 1.2 2.1
(Quantification)
110
anti-LAMP1
27
anti-p27
55
anti-Tubulin
DMSO MG-132 CQ
TC71
70
anti-FLI1
0.7 1.3 1.9 1.8 0.6 0.6
(Quantification)
110
anti-LAMP1
27
anti-p27
55
anti-Tubulin
DMSO MG-132 CQ
C
A673
kDa
70
anti-FLI1
27
anti-p27
55
anti-Tubulin
DMSO 2h 4h 6h 8h
10µM MG-132
relative EF protein level (normalized to tubulin and
3.0
2.5
2.0
1.5
1.0
0.5
0.0
DMSO 2h 4h 6h 8h
10µM MG-132
D
A673
kDa
70
anti-FLI1
27
anti-p27
55
anti-Tubulin
DMSO 2h 4h 6h 8h
20µg/ml CHX
relative EF protein level (normalized to tubulin and ctr)
1.5
1.0
0.5
0.0
DMSO 2h 4h 6h 8h
20µg/ml CHX
E
HEK293T
3xflag-EF + + + + - +
HA-ubiquitin + + + + + -
10µM MG-132 6h 4h 2h 0h 6h 6h
kDa
190
115
80
70
IP: anti-Flag
IB: anti-HA
4x ubiquitin ~ 100kDa
3x ubiquitin ~ 92kDa
2x ubiquitin ~ 84kDa
1x ubiquitin ~ 76kDa
EWS-FLI1 - (ub)n
IB: anti-Flag
70
3xflag-EF
input
IB: anti-Flag
70
3xflag-EF
IB: anti-Tubulin
55
Tubulin
F
HEK293T
3xflag-EF + + +
HA-ubiquitin WT K48R K63R
kDa
190
115
80
70
IP: anti-Flag
IB: anti-HA
EWS-FLI1 - (ub)n
IB: anti-Flag
70
3xflag-EF

Figure 2

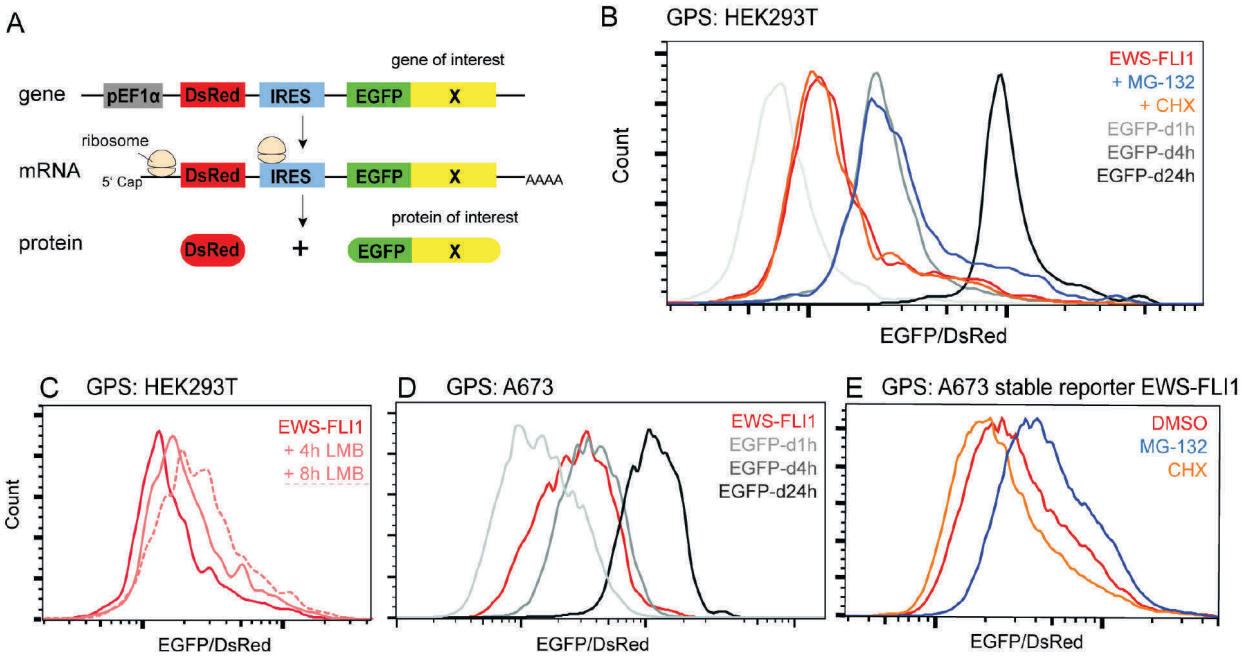
A
gene of interest
gene
pEF1α
DsRed
IRES
EGFP
X
ribosome
mRNA
5' Cap
AAAA
protein
protein of interest
B
GPS: HEK293T
EWS-FLI1
+ MG-132
+ CHX
EGFP-d1h
EGFP-d4h
EGFP-d24h
Count
EGFP/DsRed
C
GPS: HEK293T
EWS-FLI1
+ 4h LMB
+ 8h LMB
D
GPS: A673
E
GPS: A673 stable reporter EWS-FLI1
DMSO

Figure 3

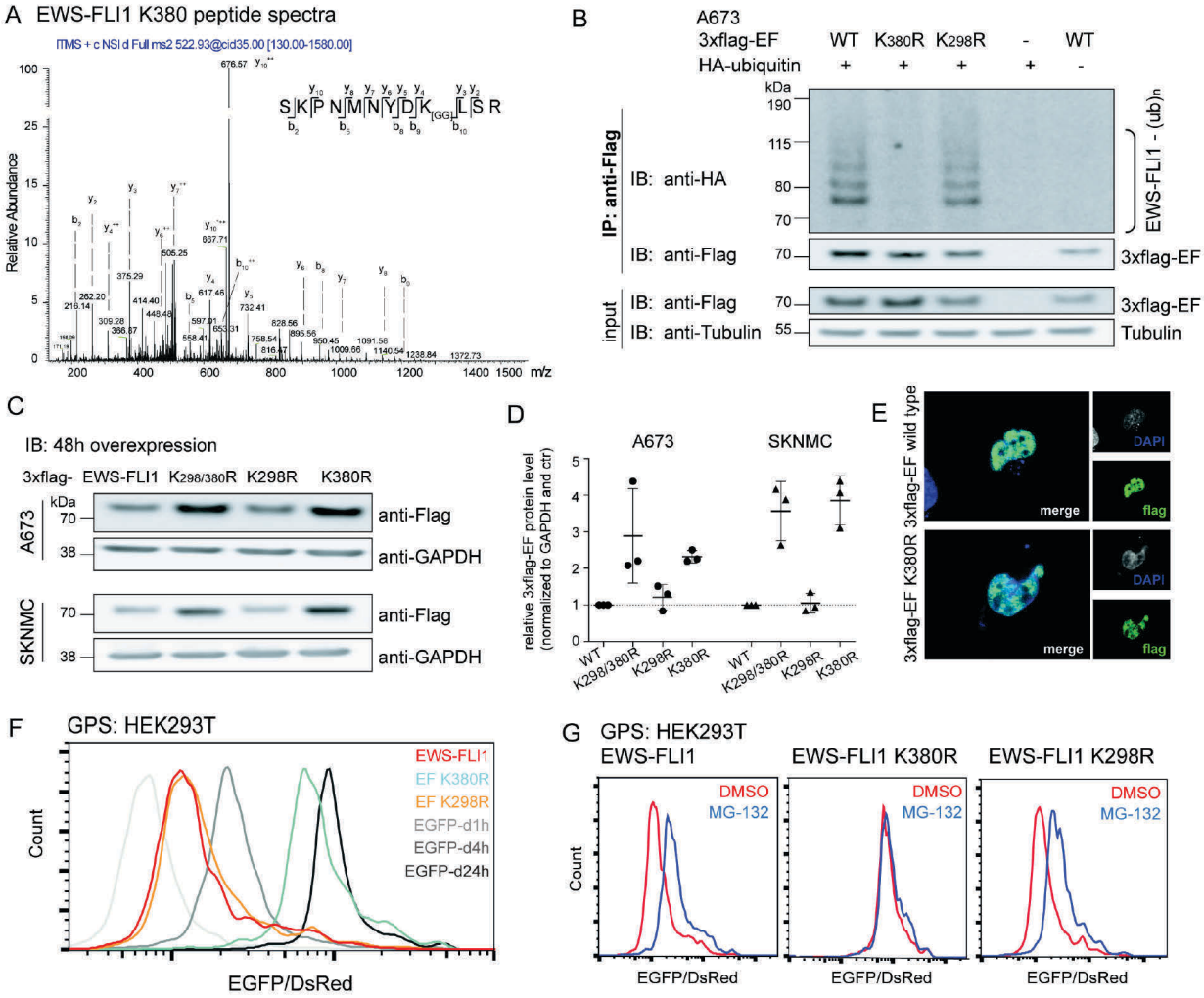
A EWS-FLI1 K380 peptide spectra
B
A673
3xflag-EF WT K380R K298R - WT
HA-ubiquitin + + + + -
IP: anti-Flag
IB: anti-HA
IB: anti-Flag
EWS-FLI1 - (ub)n
3xflag-EF
input
IB: anti-Flag
IB: anti-Tubulin
Tubulin
C
IB: 48h overexpression
3xflag- EWS-FLI1 K298/380R K298R K380R
A673
SKNMC
anti-Flag
anti-GAPDH
D
A673
SKNMC
relative 3xflag-EF protein level (normalized to GAPDH and ctr)
WT
K298/380R
K298R
K380R
E
3xflag-EF wild type
3xflag-EF K380R
DAPI
flag
merge
F
GPS: HEK293T
EWS-FLI1
EF K380R
EF K298R
EGFP-d1h
EGFP-d4h
EGFP-d24h
Count
EGFP/DsRed
G
GPS: HEK293T
EWS-FLI1
EWS-FLI1 K380R
EWS-FLI1 K298R
DMSO
MG-132
Count
EGFP/DsRed

Figure 4

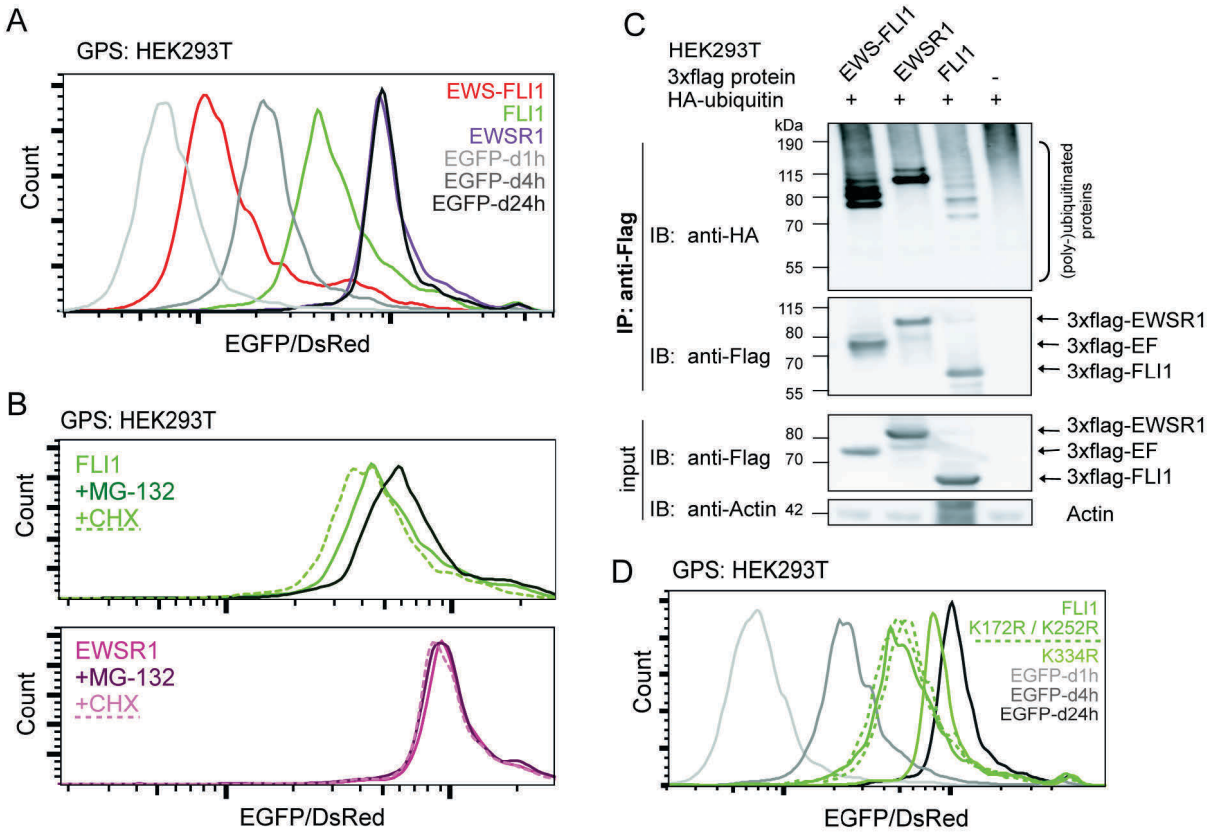

E

```
Fli1        -------GS--GQ-IQLWQFLLELL-SDSANASCITW-EGTNGEFKMTDPDEVARRWGERKSKPNMNYDKLSRALRYYYDKNIMTKVHGKRYAYKFDFHGIAQALQ
ERG         -------GS--GQ-IQLWQFLLELL-SDSSNSSCITW-EGTNGEFKMTDPDEVARRWGERKSKPNMNYDKLSRALRYYYDKNIMTKVHGKRYAYKFDFHGIAQALQ
FEV         -------GS--GQ-IQLWQFLLELL-ADRANAGCIAW-EGGHGEFKLTDPDEVARRWGERKSKPNMNYDKLSRALRYYYDKNIMSKVHGKRYAYRFDFQGLAQACQ
ETV5        --------R--GS-LQLWQFLVTLL-DDPANAHFIAW-TGRGMEFKLIEPEEVARRWGIQKNRPAMNYDKLSRSLRYYYEKGIMQKVAGERYVYKF-------VCD
ETV4        -------YQRRGA-LQLWQFLVALL-DDPTNAHFIAW-TGRGMEFKLIEPEEVARLWGIQKNRPAMNYDKLSRSLRYYYEKGIMQKVAGERYVYKF-------VCE
ETV2        -----------GP-IQLWQFLLELL-HDGARSSCIRW-TGNSREFQLCDPKEVARLWGERKRKPGMNYEKLSRGLRYYYRRDIVRKSGGRKYTYRFG---------
ETV1        --------R--GS-LQLWQFLVALL-DDPSNSHFIAW-TGRGMEFKLIEPEEVARRWGIQKNRPAMNYDKLSRSLRYYYEKGIMQKVAGERYVYKF-------VCD
POINTED     -------CS--GQPIHLWQFLKELLLKPHSYGRFIRWLNKEKGIFKIEDSAQVARLWGIRKNRPAMNYDKLSRSIRQYYKKGIIRK--------------------
ETS1        -------GS--GP-IQLRQFLLELL-TDKSCQSFISW-TGDGWEFKLSDPDEVARRWGKRKNKPKMNYEKLSRGLRYYYDKNIIHKTAGKRYVYRF----------
ETS2        AVLAGFTGS--GP-IQLWQFLLELL-SDKSCQSFISW-TGDGWEFKLADPDEVARRWGKRKNKPKMNYEKLSRGLRYYYDKNIIHKTSGKRYVYRF----------
GABPa       --------N--GQ-IQLWQFLLELL-TDKDARDCISW-VGDEGEFKLNQPELVAQKWGQRKNKPTMNYEKLSRALRYYYDGDMICKVQGKRFVYKF----------
Clustal W              *    * ***  **         * *       *       **  **  *  * *** *****  * **      *
```

Figure 5

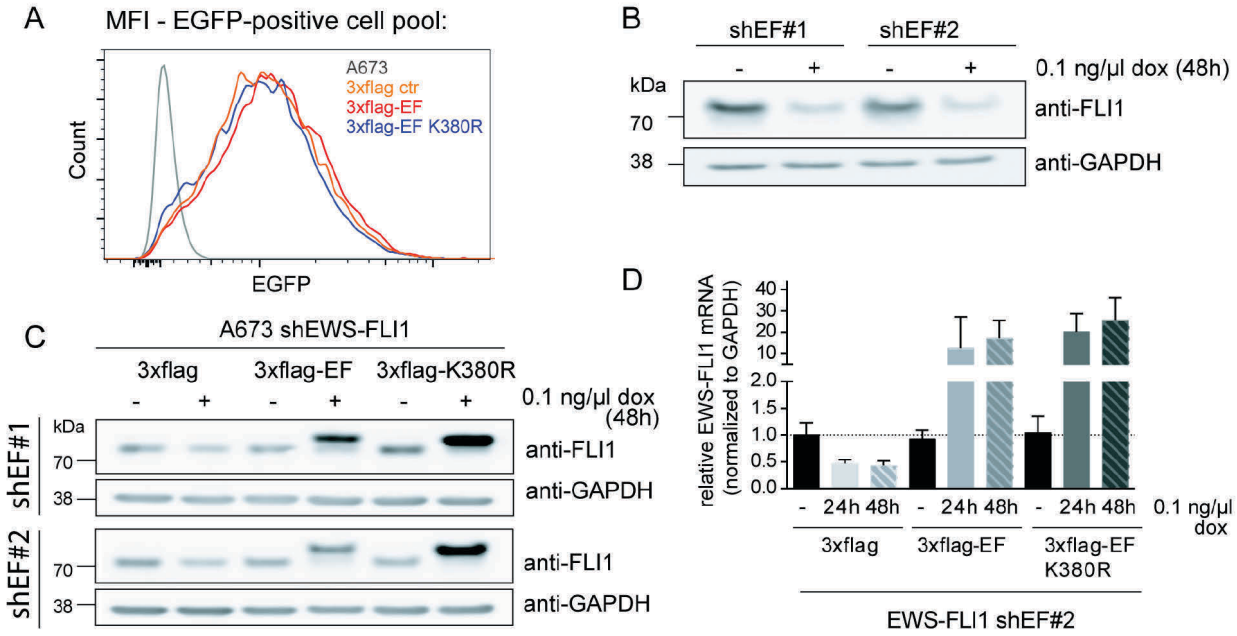
A
MFI - EGFP-positive cell pool:
A673
3xflag ctr
3xflag-EF
3xflag-EF K380R
Count
EGFP
B
shEF#1
shEF#2
- + - +
0.1 ng/µl dox (48h)
kDa
70
38
anti-FLI1
anti-GAPDH
C
A673 shEWS-FLI1
3xflag
3xflag-EF
3xflag-K380R
- + - + - +
0.1 ng/µl dox (48h)
shEF#1
shEF#2
kDa
70
38
anti-FLI1
anti-GAPDH
D
relative EWS-FLI1 mRNA (normalized to GAPDH)
40
30
20
10
2.0
1.5
1.0
0.5
0.0
- 24h 48h - 24h 48h - 24h 48h
0.1 ng/µl dox
3xflag
3xflag-EF
3xflag-EF K380R
EWS-FLI1 shEF#2

Figure 6

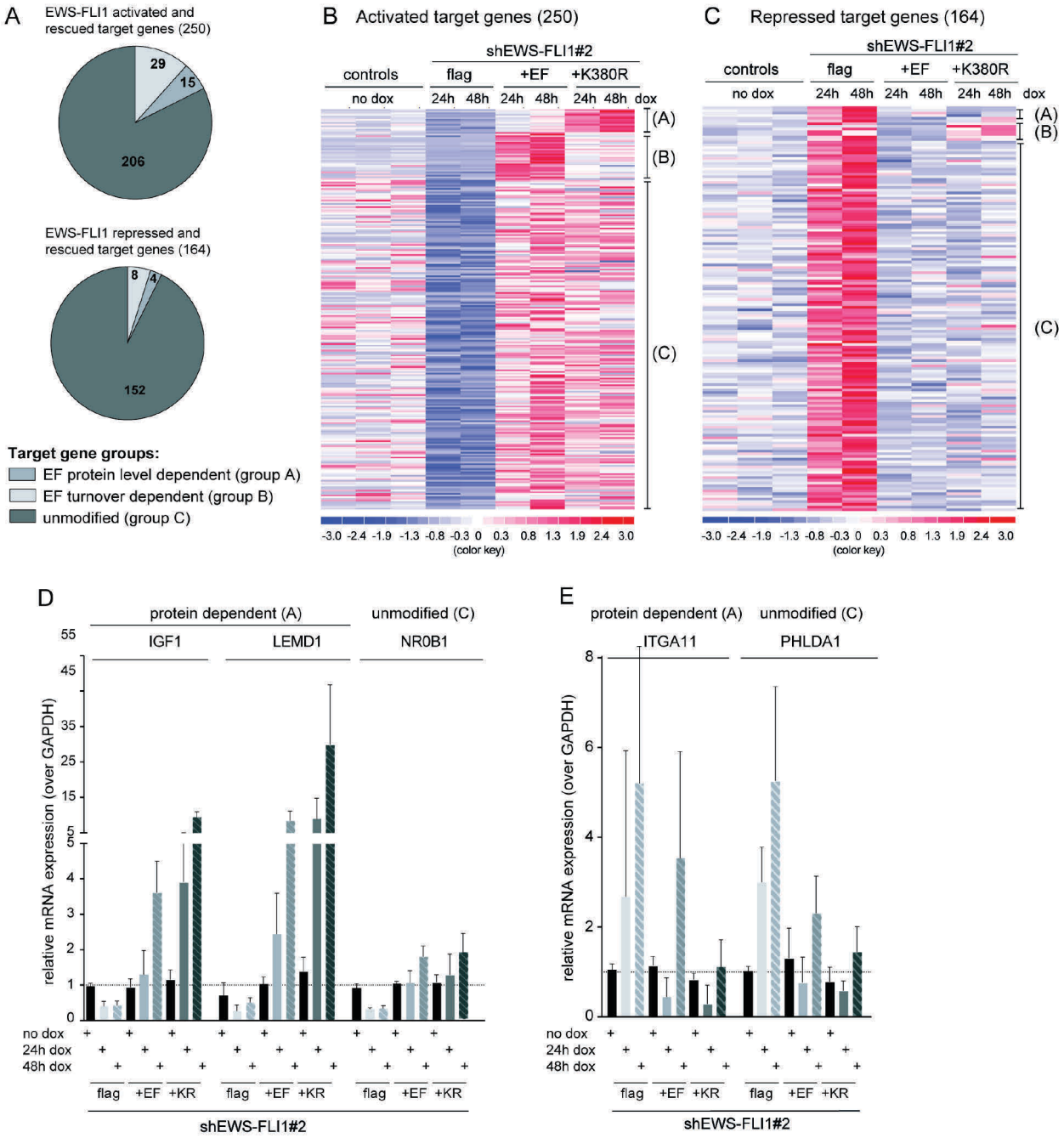
A
EWS-FLI1 activated and rescued target genes (250)
29
15
206
EWS-FLI1 repressed and rescued target genes (164)
8
4
152
Target gene groups:
EF protein level dependent (group A)
EF turnover dependent (group B)
unmodified (group C)
B Activated target genes (250)
shEWS-FLI1#2
controls
flag
+EF
+K380R
no dox
24h 48h 24h 48h 24h 48h dox
(A)
(B)
(C)
-3.0 -2.4 -1.9 -1.3 -0.8 -0.3 0 0.3 0.8 1.3 1.9 2.4 3.0
(color key)
C Repressed target genes (164)
shEWS-FLI1#2
controls
flag
+EF
+K380R
no dox
24h 48h 24h 48h 24h 48h dox
(A)
(B)
(C)
-3.0 -2.4 -1.9 -1.3 -0.8 -0.3 0 0.3 0.8 1.3 1.9 2.4 3.0
(color key)
D
protein dependent (A)
unmodified (C)
IGF1
LEMD1
NR0B1
relative mRNA expression (over GAPDH)
no dox
24h dox
48h dox
flag +EF +KR flag +EF +KR flag +EF +KR
shEWS-FLI1#2
E
protein dependent (A)
unmodified (C)
ITGA11
PHLDA1
relative mRNA expression (over GAPDH)
no dox
24h dox
48h dox
flag +EF +KR flag +EF +KR
shEWS-FLI1#2

Supplementary information

Proteasomal degradation of the EWS-FLI1 fusion protein is regulated by a single lysine residue

Maria E. Gierisch, Franziska Pfistner, Laura A. Lopez-Garcia, Lena Harder, Beat W. Schäfer*, Felix K. Niggli

From the Department of Oncology and Children's Research Center, University Children´s Hospital, Steinwiesstrasse 32, 8032 Zurich, Switzerland

*Corresponding author:

Beat Schäfer, Department of Oncology, Children´s Hospital Zurich, Steinwiesstrasse 32, 8032 Zurich, Switzerland, Tel. +41 44 2667553, Fax +41 44 6348859, Email beat.schaefer@kispi.uzh.ch

Running title: EWS-FLI1 degradation is mediated by one lysine residue

Keywords: Ewing sarcoma, EWS-FLI1, ETS transcription factors, protein turnover, ubiquitin, target genes

S1- supplementary information mass spectrometry

- Mass spectrometry peptide spectra for EWS-FLI1 K298, FLI1 K172 and K252
- Table with predicted and observed peptide mass
- Extended description of mass spectrometry sample preparation and analysis

S2 - supplementary information microarray expression

- Extended description of microarray expression data analysis
- Lists of protein and turnover dependent target genes

ST1 - supplementary information of plasmids, cloning primers and list of assays

on demand

Supplementary S1 - Mass spectrometry

A EWS-FLI1 K298 peptide spectra

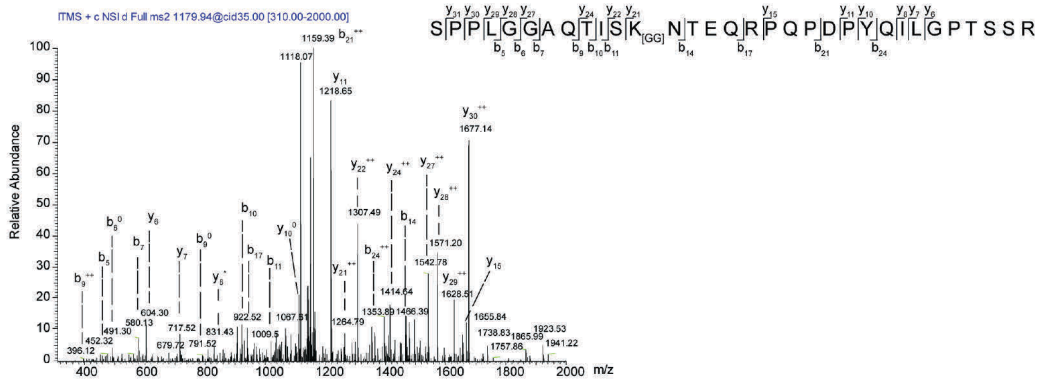

B FLI1 K172 peptide spectra

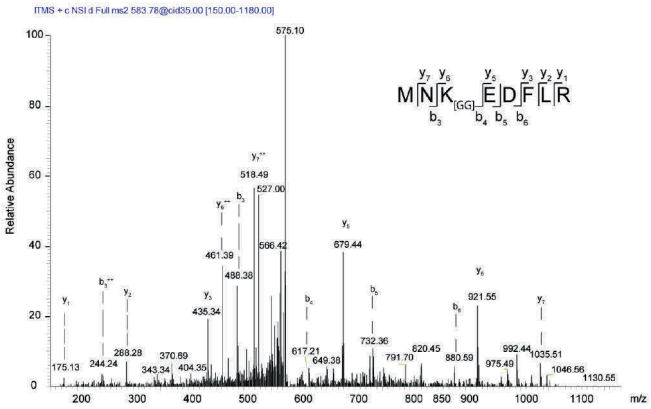

C FLI1 K252 peptide spectra

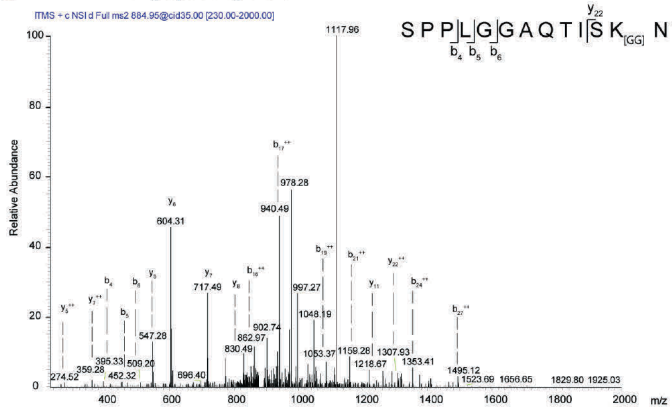

Figure:	Sample	Lysine residue	Residue number	Peptide sequence	Predicted mass	Observed mass
S1A:	EWS-FLI1	K298	287-318	SPPLGGAQTIS**K**NTEQRPQPDPYQILGPTSSR	3533.79	3533.78
F3A:	EWS-FLI1 R386N	K380	372-383	SKPNMNYD**K**LSR	1565.76	1565.75
S1B:	FLI1 wild type	K172	170-177	MN**K**EDFLR	1165.56	1165.55
S1C:	FLI1 wild type	K252	241-272	SPPLGGAQTIS**K**NTEQRPQPDPYQILGPTSSR	3533.79	3533.76

Mass spectrometry (MS) – extended description for sample preparation and analysis

Purification and sample preparation for MS.

Proteins were purified from HEK293T cells under denaturing conditions and separated by gel electrophoresis as described. The gel was stained with coomassie (Instant blue, Expedeon, Harston, UK) for 20min followed by washing with water for each 30min twice. Bands corresponding to the molecular weight of ubiquitinated EWS-FLI1 were excised from the gel and dried by speed vacuum for 10min. Digestion was performed with 50ng Trypsin (Promega, V511C) overnight at 37°C and stopped by addition of 0.2µl formic acid (FA). Peptides were extracted from the gel by adding twice 50% acetonitrile (ACN)- 5% trifluoroacetic acid (TFA).

After drying by speed vacuum for 1h, peptides were cleaned with ZIP-TIP C18 tips (ThermoFisher Scientific AG) by resuspending in 3% ACN- 0.1% TFA and eluted with 60% ACN- 0.1% TFA twice. Final resuspension was in 3% ACN- 0.2% FA with 10mM citric acid before injection into an LTQ-OrbitrapVelos mass spectrometer (ThermoFisher Scientific AG) coupled to an EksigentNanoLC-Ultra 1D plus (Eksigent Technologies, Dublin, CA, USA). Solvent composition at the two channels was 0.1% FA for channel A and 0.1% FA, 99.9% ACN for channel B. Peptides were loaded on a self-made frit column (75µm × 150mm) packed with reverse phase C18 material (ReproSil-Pur 120 C18-AQ, 1.9µm, Dr. Maisch GmbH, Ammerbuch, Germany) and eluted at a flow rate of 250nl per min by a gradient from 3 to 30% of B in 56min. Full-scan MS spectra (300−1700 m/z) were acquired in profile mode at a resolution of 30'000 at 400 m/z, an accumulation gain control (AGC) of $1x10^6$ and a maximum injection time of 200ms. Collision induced dissociation (CID) MS/MS spectra were recorded in data dependent manner in the ion trap from the twenty most intense signals above a threshold of 1000, using a normalized collision energy of 35% and an activation time of 10ms. The AGC value for MS/MS analysis was set to $1x10^4$ (ion trap detection, 100ms injection time) and the isolation width was set to 2amu. Charge state screening was enabled and singly charge states were rejected. Precursor masses already selected for MS/MS were excluded for further selection for 45s and the exclusion window was set to 10ppm. The size of the exclusion list was set to a maximum of 500 entries. The samples were acquired using internal lock mass calibration on m/z 429.088735 and 445.120025.

Data analysis.

The raw-files from the mass spectrometer were converted into Mascot generic files (mgf) with Mascot Distiller software 2.4.3.3 (Matrix Science Ltd.,London, UK). The peak lists were searched using Mascot Server 2.3.02 against the forward UniProtKB/Swiss-Prot database for human, concatenated to a reversed decoyed FASTA database consisting of a total of 135,183 proteins with accessions in Gene Ontology compatible format and 260 common protein contaminants (NCBI taxonomy ID 9606, release date 2012-04-12). The protein sequence of EWS-FLI1 (B1PRL2_HUMAN) was included in the database.

The parameters for precursor tolerance and fragment ion tolerance were set to ± 5ppm and ± 0.8Da, respectively. Gly-Gly and oxidation (M) were set as variable modifications. Enzyme specificity was set to trypsin, allowing up to 1 missed cleavage. Peptides having an expectation value higher of 0.05 and/or a Mascot score lower of 20 were excluded. Only peptides with internal lysine modified by glycine-glycine were considered. For the localization of glycine-glycine modification, the results of Mascot Site Analysis were used. All the spectra of ubiquitinated peptides were manually validated.

Supplementary S2 - microarray expression analysis

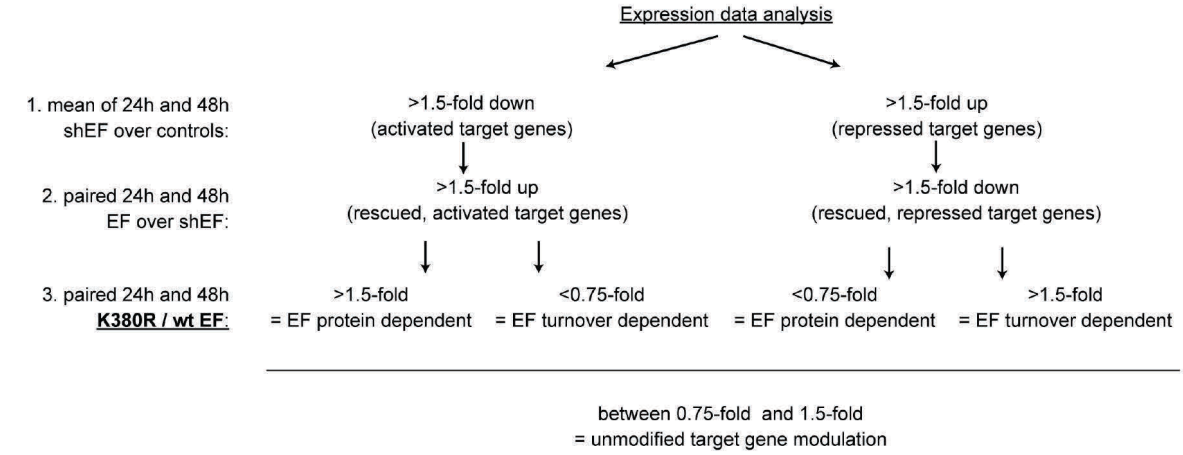

S2 supplementary table: List of activated target genes which expression is either EWS-FLI1 protein sensitive or turnover sensitive

EWS-FLI1 protein level sensitive

	Identifier	Gene Symbol	mRNA Accession	mRna - Description	Fold change (K380R / wild type EF)		Citation
1	17121292	SORD	ENST00000267814	ensembl_havana_transcript:known chromosome:GRCh38:15:45023104:45077185:1 ge	1,99	protein-coding	
2	16748814	LOC102724196	XR_432795	PREDICTED: Homo sapiens uncharacterized LOC102724196 (LOC102724196), ncRNA	2,23	non-coding RNA	
3	16802461	LINC00277	NR_026949	Homo sapiens long intergenic non-protein coding RNA 277 (LINC00277), long non-codi	2,06	non-coding RNA	**Howarth et al. 2012**
	17121206	LINC00277	NR_026949	Homo sapiens long intergenic non-protein coding RNA 277 (LINC00277), long non-codi	1,79	non-coding RNA	
4	16784564	---	NONHSAT037063	Non-coding transcript identified by NONCODE: Linc	1,86	non-coding RNA	
5	16769250	IGF1	NM_000618	Homo sapiens insulin-like growth factor 1 (somatomedin C) (IGF1), transcript variant 4,	2,81	protein-coding	**Cironi et al. 2008**
6	16712944	KIAA1462	NM_020848	Homo sapiens KIAA1462 (KIAA1462), mRNA.	1,66	protein-coding	
7	16967875	PARM1	NM_015393	Homo sapiens prostate androgen-regulated mucin-like protein 1 (PARM1), mRNA.	1,56	protein-coding	
8	16754269	TRHDE	NM_013381	Homo sapiens thyrotropin-releasing hormone degrading enzyme (TRHDE), mRNA.	1,52	protein-coding	
9	16833184	LOC102724731	XR_424812	PREDICTED: Homo sapiens uncharacterized LOC102724731 (LOC102724731), transcr	1,94	non-coding RNA	
10	17126082	---	---	non-annotated	1,57	unknown	
11	17126124	---	---	non-annotated	1,57	unkonwn	
12	16690739	KCNA2	NM_001204269	Homo sapiens potassium voltage-gated channel, shaker-related subfamily, member 2 (I	1,72	protein-coding	
13	16939479	ENTPD3	NM_001248	Homo sapiens ectonucleoside triphosphate diphosphohydrolase 3 (ENTPD3), transcript	1,83	protein-coding	
14	16698489	LEMD1	NM_001001552	Homo sapiens LEM domain containing 1 (LEMD1), transcript variant 3, mRNA.	3,96	protein-coding	
15	16837348	MAP2K6	NM_002758	Homo sapiens mitogen-activated protein kinase kinase 6 (MAP2K6), mRNA.	2,04	protein-coding	

EWS-FLI1 turnover sensitive

	Identifier	Gene Symbol	mRNA Accession	mRna - Description	Fold change (K380R / wild type EF)	
1	16972108	APELA	ENST00000507152	havana:novel chromosome:GRCh38:4:164877004:164897523:1 gene:ENSG000002483	0,56	protein-coding
2	16949537	TP63	NM_001114978	Homo sapiens tumor protein p63 (TP63), transcript variant 2, mRNA.	0,57	protein-coding
3	16894044	LINC01249	NR_034134	Homo sapiens long intergenic non-protein coding RNA 1249 (LINC01249), long non-coc	0,56	non-coding RNA
4	16679349	KMO	NM_003679	Homo sapiens kynurenine 3-monooxygenase (kynurenine 3-hydroxylase) (KMO), mRNA	0,58	protein-coding
5	16777544	LINC00463	NR_120428	Homo sapiens long intergenic non-protein coding RNA 463 (LINC00463), long non-codi	0,57	non-coding RNA
6	17010005	BAI3	NM_001704	Homo sapiens brain-specific angiogenesis inhibitor 3 (BAI3), mRNA.	0,45	protein-coding
7	16909277	SPHKAP	NM_001142644	Homo sapiens SPHK1 interactor, AKAP domain containing (SPHKAP), transcript varian	0,38	protein-coding
8	16947022	RP11-454C18.1	OTTHUMT00000357	cdna:all chromosome:VEGA56:3:151637174:151657966:1 Gene:OTTHUMG000001598	0,51	unknown
9	16670185	LOC284561	AK023809	Homo sapiens cDNA FLJ13747 fis, clone PLACE3000276.	0,37	non-coding RNA
10	16674965	---	NONHSAT008377	Non-coding transcript identified by NONCODE: Linc	0,53	non-coding RNA
11	16896049	ALK	NM_004304	Homo sapiens anaplastic lymphoma receptor tyrosine kinase (ALK), mRNA.	0,62	protein-coding
12	16816962	SCNN1G	NM_001039	Homo sapiens sodium channel, non-voltage-gated 1, gamma subunit (SCNN1G), mRN	0,64	protein-coding
13	16851801	RNF125	NM_017831	Homo sapiens ring finger protein 125, E3 ubiquitin protein ligase (RNF125), mRNA.	0,50	protein-coding
14	17120752	C12orf55	ENST00000524981	havana:putative chromosome:GRCh38:12:96489587:96875555:1 gene:ENSG00000188	0,42	protein-coding
15	16780133	SLITRK6	NM_032229	Homo sapiens SLIT and NTRK-like family, member 6 (SLITRK6), mRNA.	0,36	protein-coding
16	16982264	MTNR1A	NM_005958	Homo sapiens melatonin receptor 1A (MTNR1A), mRNA.	0,43	protein-coding
17	17004536	LOC101928047	XR_249939	PREDICTED: Homo sapiens uncharacterized LOC101928047 (LOC101928047), ncRNA	0,52	non-coding RNA
18	17016390	HIST1H2BG	NM_003518	Homo sapiens histone cluster 1, H2bg (HIST1H2BG), mRNA.	0,65	protein-coding
19	17125422	CD99P1	NR_033381	Homo sapiens CD99 molecule pseudogene 1 (CD99P1), transcript variant 2, non-coding	0,48	non-coding RNA
20	16975642	GABRA4	NM_000809	Homo sapiens gamma-aminobutyric acid (GABA) A receptor, alpha 4 (GABRA4), transc	0,34	protein-coding
21	17063507	KDM7A	NM_030647	Homo sapiens lysine (K)-specific demethylase 7A (KDM7A), mRNA.	0,53	protein-coding
22	16733038	RNU6-321P	ENST00000410912	ncrna:known chromosome:GRCh38:11:125277552:125277657:1 gene:ENSG00000222	0,20	non-coding RNA
23	16666055	CTH	ENST00000346806	ensembl_havana_transcript:known chromosome:GRCh38:1:70411383:70439204:1 gen	0,61	protein-coding
24	16685593	---	NONHSAT002513	Non-coding transcript identified by NONCODE: Linc	0,27	non-coding RNA
25	17005072	RNU6-522P	ENST00000364497	ncrna:known chromosome:GRCh38:6:15314920:15315026:1 gene:ENSG00000201367	0,39	non-coding RNA
26	16669278	FAM46C	NM_017709	Homo sapiens family with sequence similarity 46, member C (FAM46C), mRNA.	0,62	protein-coding
27	17115913	---	NONHSAT139285	Non-coding transcript identified by NONCODE: Linc	0,64	non-coding RNA
28	16669105	MAB21L3	NM_152367	Homo sapiens mab-21-like 3 (C. elegans) (MAB21L3), mRNA.	0,45	protein-coding
29	17013657	ULBP1	NM_025218	Homo sapiens UL16 binding protein 1 (ULBP1), mRNA.	0,31	protein-coding

S2 supplementary table: List of repressed target genes which repression is either EWS-FLI1 protein sensitive or turnover sensitive

EWS-FLI1 protein level sensitive

	Identifier	Gene Symbol	mRNA Accession	mRna - Description	Fold change (K380R / wild type EF)	
1	17077502	TOX	NM_014729	Homo sapiens thymocyte selection-associated high mobility group box (TOX), mRNA.	0,60	protein-coding
2	16888270	ITGA4	NM_000885	Homo sapiens integrin, alpha 4 (antigen CD49D, alpha 4 subunit of VLA-4 receptor) (IT	0,58	protein-coding
3	16778241	POSTN	NM_001135934	Homo sapiens periostin, osteoblast specific factor (POSTN), transcript variant 2, mRNA	0,52	protein-coding
4	16811085	ITGA11	NM_001004439	Homo sapiens integrin, alpha 11 (ITGA11), mRNA.	0,63	protein-coding

EWS-FLI1 turnover sensitive

	Identifier	Gene Symbol	mRNA Accession	mRna - Description	Fold change (K380R / wild type EF)	
1	16878731	EHD3	NM_014600	Homo sapiens EH-domain containing 3 (EHD3), mRNA.	1,69	protein-coding
2	16821377	CDH13	NM_001220488	Homo sapiens cadherin 13 (CDH13), transcript variant 2, mRNA.	1,55	protein-coding
3	16671457	IL6R	NM_000565	Homo sapiens interleukin 6 receptor (IL6R), transcript variant 1, mRNA.	1,56	protein-coding
4	17117110	CD24	BC064619	Homo sapiens CD24 molecule, mRNA (cDNA clone MGC:75043 IMAGE:5591617), cor	10,97	protein-coding
5	17020258	BMP5	NM_021073	Homo sapiens bone morphogenetic protein 5 (BMP5), mRNA.	2,01	protein-coding
6	16805287	MIR3175	NR_036136	Homo sapiens microRNA 3175 (MIR3175), microRNA.	1,96	non-coding RNA
	17118970	MIR3175	NR_036136	Homo sapiens microRNA 3175 (MIR3175), microRNA.	1,96	non-coding RNA
7	16979613	---	NONHSAT098206	Non-coding transcript identified by NONCODE: Linc	1,67	non-coding RNA
8	17044046	RPL23P8	NR_026673	Homo sapiens ribosomal protein L23 pseudogene 8 (RPL23P8), non-coding RNA.	1,65	non-coding RNA

Supplementary table ST1: List of plasmids and primers used for cloning and mutagensis + list of assay on demand for qRT-PCR

General plasmids:

pCMV-3xflag	Sigma Aldrich
EWS-FLI1	H. Kovar, Children's Cancer Research Institute, Vienna, Austria
EWSR1	H. Gehring, University of Zurich, Switzerland
FLI1	J. Ghysdael, Institute Curie, France (Bailly et al. 1994 MolCellBiol)

Primer name	**Primer sequence 5'-3'**	**Cloning strategy**
pCMV-3xflag-EWS FW	GACAAGCTTGCGGCCGCGCGTCCACGGATTACAGTACC	EWS-FLI1, EWS into pCMV-3xflag
pCMV-3xflagFLI1 FW	GACAAGCTTGCGGCCGCAAACCCTTCTTATGACTCAGTCAGAAG	FLI1 into pCMV-3xflag
pCMV-3xflag-FLI1 RS	GATGAATTCGCGGCCGCTCACTAGTAGTAGCTGCCTAAGTGTGA	EWS-FLI1, FLI1 into pCMV-3xflag
pCMV-3xflag-EWS RS	GATGAATTCGCGGCCGCTCACTAGTAGGGCCGATCTCTG	EWS into pCMV-3xflag

Global Protein Stability - plasmids:

pR-EF1-cDNA	Cellecta Inc.
MSCV-CMV-DsRed-IRES-EGFP-DEST	Addgene #41941
MSCV-CMV-DsRed-IRES-d1EGFP	Addgene #41942
MSCV-CMV-DsRed-IRES-d4EGFP	Addgene #41943
MSCV-CMV-DsRed-IRES-d24EGFP	Addgene #41944

Primer name	**Primer sequence 5'-3'**	**Cloning strategy**
RIG FW	TAG AGC TAG CGA ATT CAT GGC CTC CTC CGA GGA C	#41941/2/3/4 into pR-EF1
RIG RS	ATT TAA ATT CGA ATT CTT GGC CAG ATC TGA GTC C	#41941 into pR-EF1
d1/4 EGFP RS	ATT TAA ATT CGA ATT CCT ACA CAT TGA TCC TAG CAG	#41942/3 into pR-EF1
d24 EGFP RS	ATT TAA ATT CGA ATT CTT ACT TGT ACA GCT CGT CCA TG	#41944 into pR-EF1
RIG EF FW	TCT GGC CAG AAA TTC GAA ATG CGT CCA CGG ATT ACA GTA CC	EWS/FLI1, EWS in pR-EF1-RIG
RIG EF RS	TCC GAT TTA AAT TCG AAT TAC TAG TAG TAG CTG CCT AAG TGT G	EWS/FLI1, FLI1 in pR-EF1-RIG
RIG EWS RS	TCC GAT TTA AAT TCG AAT TAC TAG TAG GGC CGA TCT CTG C	EWS in pR-EF1-RIG
RIG FLI RS	TCT GGC CAG AAA TTC GAA ATG ACG GGA CTA TTA AGG AGG C	FLI1 in pR-EF1-RIG

Exchange cell lines - plasmids:

Cellecta shEF#1	Target sequence 5' ATAGAGGTGGGAAGCTTATAA 3'
Cellecta shEF#2	Target sequence 5' CGTCATGTTCTGGTTTGAGAT 3'
pINDUCER21 (ORF-EG)	Addgene #46948

Primer name	**Primer sequence 5'-3'**	**Cloning strategy**
pInd 3xf EF FW	GCG GCC CCG AAC TAG TAT GGA CTA CAA AGA CCA TGA C	3xflag-EWS-FLI1, 3xflag into pInducer21
pInd 3xf EF RS	TCG TAT GGG TAT TCG AAC TAC TAG TAG TAG CTG CCT AAG	3xflag-EWS-FLI1 into pInducer21
pInd 3xflag RS	GTA TGG GTA TTC GAA CTA CTA TGC GGC CGC AAG CTT GTC	3xflag into pInducer21

Primer for site directed mutagenesis

Primer name	**Primer sequence 5'-3'**	**Mutagenesis**
EF K298R FW	GGG GCA CAA ACG ATC AGT AGG AAT ACA GAG CAA CGG CCC	EWS-FLI1 and FLI1 in K298/252>R
EF K298R RS	GGG CCG TTG CTC TGT ATT CCT ACT GAT CGT TTG TGC CCC	EWS-FLI1 and FLI1 in K298/252>R
EF K380R FW	AAG CCC AAC ATG AAT TAC GAC AGG CTG AGC CGG GCC CTC	EWS-FLI1 and FLI1 in K380/334>R
EF K380R RS	GAG GGC CCG GCT CAG CCT GTC GTA ATT CAT GTT GGG CTT	EWS-FLI1 and FLI1 in K380/334>R
FLI1 K172R FW	GGA TGG CAA GGA ACT GTG TAA AAT GAA CAG GGA GGA C	FLI1 in K172>R
FLI1 K172 RS	GTC CTC CCT GTT CAT TTT ACA CAG TTC CTT GCC ATC C	FLI1 in K172>R
EF R386N FW	CTGAGCCGGGCCCTCAATTATTACTATG	EWS-FLI1 in R386>N
EF R386N RS	CATAGTAATAATTGAGGGCCCGGCTCAG	EWS-FLI1 in R386>N
Ub K48R FW	AGG CTC ATC TTT GCA GGC AGG CAG CTG GAA GAT GGC CG	HA-ubiquitin K48>R
Ub K48R RS	CGG CCA TCT TCC AGC TGC CTG CCT GCA AAG ATG AGC CT	HA-ubiquitin K48>R
Ub K63R FW	TCT GAC TAC AAC ATC CAG AGG GAG TCG ACC CTG CAC CT	HA-ubiquitin K63>R
Ub K63R RS	AGG TGC AGG GTC GAC TCC CTC TGG ATG TTG TAG TCA GA	HA-ubiquitin K63>R

List of commercially available assay on demand for qRT-PCR

Gene:	**Applied Biosystems assays on demand:**
EWS-FLI1	Hs03024807_ft
GAPDH	Hs04420697_g1
IGF1	Hs01547656_m1
LEMD1	Hs01077215_m1
NR0B1	Hs00230864_m1
ITGA11	Hs00201927_m1
PHLDA1	Hs00378285_g1

5. Manuscript II

The E3 ubiquitin ligase WWP1 regulates EWS-FLI1 stability in Ewing sarcoma

Franziska Pfistner, Maria E. Gierisch, Felix Niggli, Beat W. Schäfer

Department of Oncology and Children's Research Center, University Children´s Hospital, Steinwiesstrasse 32, 8032 Zurich, Switzerland

Corresponding author: Beat Schäfer, Department of Oncology, Children's Hospital Zurich, Steinwiesstrasse 32, 8032 Zurich, Switzerland, beat.schaefer@kispi.uzh.ch, +41442667553

Manuscript prepared for submission

Contributions to the manuscript:

Experiments, data interpretation and manuscript writing have been performed by Franziska Pfistner under my direct supervision during her time as a Master student in the lab. I contributed by providing help and supervision with experimental planning and layout, conduction of experiments at first times and data interpretation.

Abstract

Ewing sarcoma is the second most common bone tumor in children and adolescents and is characterized by a chromosomal translocation leading to expression of the unique oncogenic fusion protein EWS-FLI1. Although the fusion protein represents an attractive target for treatment, only little is known about enzymes regulating EWS-FLI1 stability and turnover. In this study, we found that EWS/FLI1 ubiquitination and stability is regulated by its PPxY motif, which is a known recognition and binding motif for NEDD4 family E3 ligases. Mutation of this motif decreased ubiquitination and hence increased stability of the fusion protein. Furthermore, a functional screen of NEDD4 family members identified WWP1 to negatively regulate EWS/FLI1 stability by direct binding to the PPxY motif of the fusion protein. Physiologically, WWP1 overexpression reduced Ewing sarcoma cell growth and colony formation, thereby suggesting that this E3 ligase has a tumor suppressive function in Ewing sarcoma cells. Taken together, these results lead to a better understanding of the molecular biology underlying Ewing sarcoma and offers novel treatment options by modulating the turnover of the oncogenic fusion protein EWS-FLI1.

Keywords

WWP1, EWS-FLI1, protein turnover,

Introduction

Ewing sarcoma is a rare and aggressive cancer of bone and soft tissues, which mostly presents in the second decade of life (1). 20-30% of patients already exhibit metastasis at diagnosis, which reduces 10-year survival from about 70% in patients with non-metastatic disease to less than 30% (2). Therefore, novel therapeutic strategies improving overall survival are urgently needed.

At the molecular level, 85% of all Ewing sarcoma tumors are characterized by the chromosomal translocation t(11;22)(q24;q12) which fuses the 5' end of the *EWSR1* gene with the 3' end of the *FLI1* gene (3,4). This leads to expression of the diagnostically characteristic oncogenic fusion protein EWS-FLI1, which acts as an aberrant transcription factor by activating and repressing various target genes (5,6). Importantly, EWS-FLI1 is the main driver of oncogenesis in Ewing sarcoma and essential for tumor cell survival (7,8). Even though EWS-FLI1 is a potential target for treatment, direct pharmacologic interference with transcription factor activity remains therapeutically challenging. Thus, alternative strategies to indirectly interfere with the expression and stability of the fusion protein need to be developed.

The turnover of most proteins is controlled by the ubiquitin-proteasome system (UPS) which involves the covalent attachment of ubiquitin chains to substrate proteins for subsequent proteasomal degradation. Substrate specificity of ubiquitination is mainly determined by E3 ligases, which transfer ubiquitin to substrate proteins in the last step of the ubiquitination cascade. Targeting the UPS, especially the highly specific E3 ligases, has become an emerging field for anti-cancer therapy over the past years (9,10). As example, targeting fusion proteins such as BCR/ABL and PML/RARA for degradation has been shown to be a promising therapeutic approach in leukemia (11,12). We could recently demonstrate that the turnover of EWS-FLI1 is controlled by ubiquitination at its lysine residue K380 leading to proteasomal degradation of the fusion protein (Gierisch et al. 2016a submitted). Furthermore, reduction of EWS-FLI1 protein levels by inhibition of its deubiquitinating enzyme USP19 resulted in cell growth inhibition *in vitro* and *in vivo* (Gierisch et al. 2016b submitted). However, it is not yet known which E3 ligase is involved in regulating turnover and stability of the fusion protein.

The WW domain containing E3 ubiquitin protein ligase 1 (WWP1) belongs to the NEDD4 family of E3 ligases within the homologous to E6 carboxy-terminus (HECT) E3 ligases main class (13,14). Members of the NEDD4 family are characterized by a C-terminal HECT domain and an N-terminal substrate recognition domain (15). WW domains within the substrate recognition domain are known to recognize and bind proline-rich sequences such as PPxY motifs of substrate proteins (16,17). WWP1 is involved in essential cellular processes and ubiquitinates various substrate proteins including the TGF-β type 1 receptor (18), SMAD4 (19), TRAF6 (20), HER4 (21) as well as p53 (22) and p63 (23). WWP1 has been shown to be overexpressed in various cancers such as prostate and breast cancer (24-26) and plays an oncogenic role in osteosarcoma (27). However, whether WWP1 is involved in Ewing sarcoma pathogenesis by regulating EWS-FLI1 turnover has not yet been explored.

In this study we found that ubiquitination and stability of EWS-FLI1 is regulated by its PPxY motif located in the EWS domain. Furthermore, we observed that the E3 ligase WWP1 negatively regulates EWS-FLI1 protein levels and has a tumor suppressive function in Ewing sarcoma cells.

Materials and Methods

Cell lines

A673, SKNMC and HEK293T cells were obtained from the American Type Culture Collection ATCC (Manassas, USA). A673 and SKNMC cells were cultured in RPMI medium (Sigma-Aldrich, Buchs, Switzerland), HEK293T cells were cultured in DMEM medium (Sigma-Aldrich, Buchs, Switzerland) supplemented with 10% FBS (Sigma-Aldrich, Buchs, Switzerland), 1% (2mM) L-glutamine (Bioconcept AG, Allschwil, Switzerland) and 1% (100U/ml) penicillin/streptomycin (Thermo Fisher Scientific AG, Reinach, Switzerland) at 37°C and 5% CO_2.

Transfection and transduction

A673 and HEK293T cells were transiently transfected using jetPRIME transfection (Polyplus transfection, Illkirch, France) according to the manufacturer's instructions. For co-immunoprecipitation and ubiquitination assays, HEK293T cells were transfected with PolyethylenimineMax (Polyscience, Cham, Switzerland). For virus production, HEK293T cells were transfected with the plasmid of interest, together with pVSV, pMDL and pREV plasmids and viral particles were collected 72h after transfection. Cells were transduced overnight with viral particles supplemented with 10µg/ml of polybrene (Sigma-Aldrich, Buchs, Switzerland).

Plasmids

pCMV-3xFlag-EWS-FLI1, pCDNA3-HA-ubiquitin and pCDNA3-HA-EWS-FLI1 plasmids were generated as described before (Gierisch et al 2016a submitted). Plasmids expressing HA- or 3xFlag-EWS-FLI1 PPxY mutated and 3xFlag-WWP1-C890A were generated by site-directed mutagenesis using AccuPrime polymerase and Dpn1 (both Thermo Fisher Scientific AG, Reinach, Switzerland) digest of parental DNA template. 3xFlag-tagged E3 ligases from the NEDD4 family were generated by PCR of cDNA clones (see Supplementary Table S1) purchased from Dharmacon (Thermo Fisher Scientific Biosciences GmbH, St. Leon-Rot, Germany) and subcloning into pCMV-3xFlag vector. DsRed-IRES-EGFP construct was amplified from retroviral vector (Addgene, No. 41941) and subcloned into pR-EF1 lentiviral vector (Cellecta Inc., Mountain View, CA, USA). For functional assays, 3xFlag-WWP1 was cloned into pBABE retroviral vector (Addgene, No. 33336). 3xMyc-WWP1 was generated by subcloning of WWP1 into pCDNA3-3xMyc vector. All subcloning was performed by In-Fusion Cloning technology (Clontech Laboratories Inc., Mountain View, CA, USA). See Supplementary Table S2 for all primers used for cloning and site-directed mutagenesis.

Cell harvesting and western blotting

Cells were harvested and proteins of cell lysates were separated by 4-12% NuPAGE® Bis-Tris Gels (Thermo Fisher Scientific AG, Reinach, Switzerland) and transferred to nitrocellulose membranes (GE Healthcare, Glattbrugg, Switzerland) which were blocked in 5% milk and incubated with the primary antibody overnight. After washing with 1xTBS/ 0.1% Tween, HPR-linked secondary antibody was added and proteins were analyzed with ECL detection reagent (GE Healthcare, Glattbrugg, Switzerland).

Co-immunoprecipitation and ubiquitination assay

For co-immunoprecipitation, HEK293T cells were lysed 48h after transfection and incubated for 30min-1h at 4°C with anti-flag antibody (Sigma-Aldrich, Buchs, Switzerland) coupled Dynabeads Protein G (Thermo Fisher Scientific AG, Reinach, Switzerland). Thereafter, beads were washed and proteins were eluted with 3xFlag-Peptide (Sigma-Aldrich, Buchs, Switzerland) diluted 1:24 in 50mM Tris/ 150mM NaCl. Proteins were analyzed by Western blotting. For ubiquitination assay, HEK293T cells were lysed 48h after transfection with SDS containing lysis buffer, boiled and sonicated. Samples were diluted ten times in a dilution buffer and incubated for 30 min at 4°C. Immunoprecipitation was performed using anti-flag antibody as described above.

Stability analysis by FACS

Stability analysis was performed as described before (28). HEK293T and A673 cells were transduced with lentiviral particles containing the reporter construct DsRed-IRES-EGFP-EWS/FLI1 wt or PPxY mutated at a low multiplicity of infection in order to obtain ~5% (HEK293T) and ~10% (A673) double-positive cells. 72h after transduction, cells were harvested and prepared for FACS analysis in PBS suspension, and fluorescence was measured by in a FACSCanto^{TM} II (BD Becton, Dickinson and Company, Franklin Lakes, NJ, USA). Data were further analyzed using FlowJo software (Tree Star Inc., Ashland, OR, USA).

Fluorescence immunohistology and microscopy

A673 cells were grown on round cover slides, transfected with 3xFlag-EWS/FLI1 wt or PPxY mutated and prepared for microscopy 48h after transfection. Cells were fixed with 4% PFA, permeabilized with PBS/0.1% Triton X and incubated overnight with anti-Flag antibody diluted in horse serum followed by incubation with anti-mouse antibody labeled with Alexa-488 (Sigma-Aldrich, Buchs, Switzerland). Cells were washed and fixed with mounting media containing DAPI (Vector laboratories Inc., Burlingame, CA, USA). Immunofluorescence was analyzed by an Axioskop 2 MOT Plus microscope (Carl Zeiss Microscopy LLC, Thornwood, NY, USA).

Functional assays

SKNMC cells stably expressing 3xFlag-WWP1 or the control construct were generated by infection with retroviral particles and sorting for EGFP positive cells using a FACSAria^{TM} III (BD Becton, Dickinson and Company, Franklin Lakes, NJ, USA). To determine cell number over time, cells were plated in a 6-well plate and counted after four and eight days. 3xFlag-WWP1 overexpression was

confirmed by western blot analysis. For colony formation assays, 100 to 200 cells were plated in a 6-well plate. 14 days after plating, cells were fixed with 4% PFA, stained with crystal violet and colonies were counted.

Antibodies

The following antibodies were used: FLAG (clone M2; Sigma-Aldrich, Buchs, Switzerland), HA (clone 6E2; Cell Signalling Technology, Berverly, MA, USA; and clone 05-904; Millipore, Billerica, MA, USA), Fli1 (MBS 300723; MyBioSource LLC, San Diego, CA, USA), Myc (clone 9B11; Cell Signalling Technology, Berverly, MA, USA), WWP1 (H00011059-M01; Abnova, Taipei City, Taiwan), tubulin (clone DM 1A; Sigma-Aldrich, Buchs, Switzerland). All antibodies are used in a dilution 1:1000.

qRT-PCR

Cells were lysed in RLT lysis buffer and total RNA was extracted using RNeasy Mini kit (Qiagen Instruments AG, Hombrechtikon, Switzerland). cDNA was synthesized using High-Capacity cDNA Reverse Transcription kit (Thermo Fisher Scientific AG, Reinach, Switzerland). qRT-PCR was performed for WWP1 and GAPDH (Hs00366931_g1, Hs04420697_g1, Applied Biosystems by Thermo Fisher Scientific AG, Reinach, Switzerland) using TaqMan gene expression master mix (Thermo Fisher Scientific AG, Reinach, Switzerland) on a 7900HT Fast Real-Time PCR System (Thermo Fisher Scientific AG, Reinach, Switzerland). Data was analyzed using SDS software (Thermo Fisher Scientific AG, Reinach, Switzerland) and the ΔΔCt method and Ct values were normalized to GAPDH.

Results

EWS-FLI1 ubiquitination and stability is regulated by its PPxY motif

E3 ubiquitin ligases from the NEDD4 family are known to interact with PPxY motifs of substrate proteins (16,29). Since EWS-FLI1 contains a PPxY motif in the EWS domain of the fusion protein, we used site-directed mutagenesis to investigate whether this motif might play a role in EWS-FLI1 turnover (Fig. 1A). To examine first whether the mutation affects EWS-FLI1 cellular localization, we used fluorescence immunohistology of wild type (wt) or PPxY motif mutated 3xFlag-EWS-FLI1 in A673 Ewing sarcoma cells. We observed that the nuclear localization of the fusion protein was not altered upon PPxY mutation (Fig. 1B).

We could recently show that EWS-FLI1 is a substrate of the ubiquitin-proteasome system and its turnover is controlled by polyubiquitination (Gierisch et al. 2016a submitted). Since we hypothesize here that mutation of the PPxY motif influences EWS-FLI1 ubiquitination and stability, we next directly investigated EWS-FLI1 polyubiquitination. We observed clearly reduced ubiquitination of the fusion protein in A673 Ewing sarcoma cells upon PPxY mutation (Fig. 1C). Hence, EWS-FLI1 ubiquitination seems to be regulated at least in part by its PPxY motif, which might be the binding site for NEDD4

family E3 ligases. To assess whether decreased EWS-FLI1 ubiquitination also leads to increased stability of the fusion protein, we next used a FACS-based approach which has been used previously to investigate global protein stability (GPS) (28). GPS analysis is based on a reporter construct containing DsRed, an internal ribosome entry site (IRES) and EGFP fused to EWS-FLI1, which leads to the expression of the two florescent proteins DsRed and EGFP from the same mRNA transcript. Thus, DsRed serves as an internal control, whereby the EGFP/DsRed ratio measures EWS-FLI1 stability. We generated HEK293T and A673 cell lines stably expressing DsRed-IRES-EGFP fused to either EWS-FLI1 wt or EWS-FLI1 PPxY mutated and analyzed fluorescence by FACS. Mutation of the PPxY motif led to increased EGFP/DsRed ratios compared to the wt protein in both cell lines, thereby indicating stabilization of the fusion protein (Fig. 1D). These results suggest that the PPxY motif of EWS/FLI1 plays an essential role in the regulation of EWS-FLI1 ubiquitination and stability, which likely involves the binding of E3 ubiquitin ligases from the NEDD4 family to the PPxY motif of the fusion protein.

E3 ligases from the NEDD4 family regulate EWS-FLI1 protein levels

To investigate which members of the NEDD4 family are involved in EWS-FLI1 degradation, we performed gain-of-function experiments. To this end, we cloned all NEDD4 family members (except HECW1) with a 3xflag tag and transiently overexpressed HA-EWS-FLI1 together with two different concentrations of flag-tagged E3 ligases in HEK293T cells. EWS-FLI1 protein levels were analyzed by western blotting after 48h. We observed both stabilization as well as destabilization of the fusion protein upon E3 ligase overexpression. NEDD4L, WWP2, HECW2 and ITCH all increased EWS-FLI1 protein levels, whereas NEDD4, SMURF1, SMURF2 and WWP1 clearly reduced EWS-FLI1 protein levels (Fig. 2A). Importantly, overexpression of both NEDD4 and WWP1 reduced EWS-FLI1 protein levels by almost 50% (Fig. 2B). These findings indicate that NEDD4, SMURF1, SMURF2 and WWP1 are candidate E3 ligases that might be involved in the degradation of the fusion protein EWS-FLI1.

WWP1 negatively regulates endogenous EWS-FLI1 protein levels in Ewing sarcoma cells

Since cellular context plays an important role in EWS-FLI1 biology, we further examined the effect of the candidate E3 ligases NEDD4, SMURF1, SMURF2 and WWP1 on endogenous EWS-FLI1 protein levels in Ewing sarcoma cells. Thus, A673 cells were transiently transfected with two concentrations of the four candidates and endogenous EWS-FLI1 protein levels were analyzed by western blotting. We found that WWP1 was the only E3 ligase which significantly reduced endogenous EWS-FLI1 protein levels, whereas the other candidates had inconsistent effects (Fig. 3A). Overexpression of WWP1 reduced EWS-FLI1 protein levels by 30-40% (Fig. 3B). Taken together, the E3 ligase WWP1 from the NEDD4 family seems to play an important role in the degradation of the fusion protein EWS-FLI1.

WWP1 regulates EWS-FLI1 protein levels by interaction via the PPxY motif of the fusion protein

The HECT domain of NEDD4 family E3 ligases is highly conserved and contains the active site cysteine, which is essential to accept and transfer ubiquitin (13). In order to investigate the activity of the E3 ligase WWP1 for EWS-FLI1 degradation, we co-expressed HA-EWS-FLI1 together with wt WWP1 or the catalytic inactive WWP1 C890A mutant in HEK293T cells and analyzed EWS-FLI1 protein levels by western blotting. We found that exogenous EWS-FLI1 protein levels were reduced by almost 50% upon overexpression of wt WWP1, whereas this effect was clearly diminished when overexpressing the catalytic inactive WWP1 C890A mutant (Fig. 4A). However, EWS-FLI1 degradation was not completely blocked by the mutant, which might be due to remaining WWP1 activity or an indirect effect of WWP1 on EWS-FLI1 protein levels. Since we found that the PPxY motif plays an essential role in EWS-FLI1 stability, we examined whether the PPxY motif is important for WWP1-mediated degradation. Thus, we co-expressed HA-EWS-FLI1 PPxY mutated together with 3xFlag-WWP1 wt in HEK293T cells and analyzed protein levels by western blotting. Overexpression of WWP1 led to a diminished reduction of PPxY mutated EWS-FLI1 protein levels compared to wt, even though degradation could not be completely prevented (Fig. 4B). Since these findings suggest alternative binding sites for WWP1 within the fusion protein, we directly investigated interaction of WWP1 with the PPxY motif of EWS-FLI1 by co-immunoprecipitation experiments. To this end, HEK293T cells were transiently transfected with 3xFlag-EWS-FLI1 or control together with 3xMyc-WWP1 and cell lysates were immunoprecipitated using anti-flag antibody. Western blot analysis revealed specific interaction of WWP1 with EWS-FLI1 since WWP1 did not interact with the control vector (Fig. 4C). Importantly, this interaction was clearly reduced when mutating the PPxY motif of the fusion protein, thereby indicating that WWP1 indeed binds to the PPxY motif of EWS-FLI1. However, interaction of WWP1 with PPxY mutated EWS-FLI1 was not completely abolished suggesting that alternative binding sites within the fusion protein might be present. Furthermore, this residual binding might be sufficient to induce low level EWS-FLI1 degradation as observed before. In summary, these data suggest that WWP1 is a negative regulator of EWS-FLI1 protein levels by binding to the PPxY motif as well as to other binding sites in the fusion protein.

WWP1 has a tumor suppressive function in Ewing sarcoma cells

To further explore the physiological function of WWP1 in Ewing sarcoma, we analyzed its protein levels in different Ewing sarcoma cell lines (A673, SKNMC, TC71, SKES, RDES) as well as in a peripheral neuroectodermal tumor cell line (SKPNDW), which belongs to the Ewing sarcoma tumor family (30). QRT-PCR and western blot analysis revealed that WWP1 mRNA and protein are expressed at different levels in the various cell lines (Fig. 5A, B). To analyze the cellular localization of WWP1 in Ewing sarcoma cells, we transfected A673 cells with 3xFlag-WWP1. Fluorescence immunostaining indicated that WWP1 is localized both in the nucleus as well as in the cytoplasm (Fig. 5C), thereby suggesting a broad function in Ewing sarcoma cells.

Continuous expression of EWS-FLI1 is essential for Ewing sarcoma cell survival and proliferation (7,8). Since we found that WWP1 is a negative regulator of EWS-FLI1 expression, we hypothesized that WWP1 overexpression also reduces Ewing sarcoma cell growth. To address this hypothesis, we generated SKNMC cell lines stably expressing 3xflag-WWP1 or control and used them to investigate proliferation as well as anchorage independent cell growth. Overexpression of WWP1 led to reduced cell proliferation after four as well as after eight days (Figure 5D). To investigate anchorage independent growth, cells were plated at reduced density and number of colonies was determined after 14 days. We observed less colonies upon WWP1 overexpression compared to the control cells (Fig. 5E). These results suggest that WWP1 might have a tumor suppressive function in Ewing sarcoma cells.

Discussion

Here, we identify the first E3 ubiquitin ligase that is involved in EWS-FLI1 turnover and stability. The results reveal an important role of the PPxY motif in the regulation of EWS-FLI1 ubiquitination which is modulated by the E3 ubiquitin ligase WWP1 and which also shows a tumor suppressive function in Ewing sarcoma cells.

Even though proteomic approaches have been applied earlier to identify substrate proteins for certain E3 ubiquitin ligases such as cullin RING ligases (31,32), the identification of E3 ligases regulating the degradation of a specific protein of interest remains challenging. Degradation of several ETS family members is known to be regulated by the E3 ligase COP1 binding to the N-terminal part of these ETS proteins (33,34). Since the fusion protein EWS-FLI1 lacks the N-terminal part of the ETS family member FLI1, other binding sites for E3 ligases might be important. Indeed, we identified the PPxY motif, which is present in the EWS part of the fusion protein, as a potential recognition site for NEDD4 family E3 ligases since mutation of the PPxY motif led to reduced ubiquitination and increased stability of EWS-FLI1. Our hypothesis that E3 ligases from the NEDD4 family bind to the PPxY motif of EWS-FLI1 is supported by a study showing that EWS full length protein interacts with WW domains of NEDD4 family members (35). It is important to note that the change in ubiquitination might also affect signaling pathways other than proteasomal degradation. Furthermore, we observed only slight EWS-FLI1 stabilization upon PPxY mutation by GPS analysis suggesting alternative binding sites for NEDD4 family E3 ligases. This is consistent with earlier reports demonstrating that E3 ligases from the NEDD4 family can also bind substrate proteins lacking a PPxY motif (35).

To identify the specific NEDD4 family E3 ligase which negatively regulates EWS-FLI1 protein levels, we overexpressed all family members in HEK293T cells. We found that NEDD4, SMURF1, SMURF2 as well as WWP1 reduced EWS-FLI1 protein level upon overexpression. Thus, the regulation of EWS-FLI1 protein levels might involve several E3 ligases presumably also from the same E3 ligase family. This notion is supported by our attempts to knockdown WWP1 in Ewing cells, which did not lead to EWS-FLI1 stabilization (data not shown), thereby indicating compensatory mechanisms. Similarly, involvement of several E3 ligases from the same family in protein turnover has been observed for

LATS1, whose degradation is regulated by several NEDD4 family members including NEDD4 (36), WWP1 (37) and ITCH (38). Nevertheless, WWP1 was the only candidate having a consistent effect on endogenous EWS-FLI1 protein levels in Ewing sarcoma cells, thereby indicating a predominant role of WWP1 for EWS-FLI1 degradation.

Further validation of WWP1 as a regulator of EWS-FLI1 turnover revealed that WWP1 interacts with the PPxY motif of the fusion protein. Interaction of WWP1 with PPxY or proline-rich domains of substrate proteins has been reported before (22,23). However, we observed that overexpression of WWP1 still reduced EWS-FLI1 protein levels upon PPxY mutation. This might be due to alternative binding sites within the fusion protein, as also observed by co-immunoprecipitation, which might be sufficient to induce EWS-FLI1 degradation. Furthermore, overexpression of the catalytic inactive WWP1 protein still slightly decreased EWS-FLI1 protein levels, thereby suggesting degradation mechanisms additionally to the active site cysteine of WWP1 or indirect effects. Importantly, regulation of EWS-FLI1 stability might involve not only WWP1 but also other E3 ligases such as RING E3 ligases since redundancy within the ubiquitin-proteasome system (39) or collaboration between different E3 ligases (40) has been reported before. Interestingly, EWS-FLI1 has been shown to interact with the RING domain of BARD1, which is part of a E3 ligase complex (41). Furthermore, the conserved ETS domain of FLI1 has been shown to interact with the SUMO E3 ligase PIAS (42), which might be another candidate to regulated EWS-FLI1 turnover.

Physiologically, we observed that WWP1 has a tumor suppressive function in Ewing sarcoma cells since overexpression of WWP1 led to reduced cell growth and colony formation. WWP1 has been shown to have various cellular functions including modulation of EGF and TGFß signaling as well as apoptosis (43). Interestingly, WWP1 is overexpressed and has oncogenic properties in various cancers (25,27,44). However, a tumor suppressive function of WWP1 in cancer cells was less characterized until now. Whether the inhibitory effect of WWP1 on Ewing sarcoma cell growth is due to its direct role in EWS-FLI1 degradation or other molecular mechanisms remains to be further investigated. Other additional properties of WWP1 are likely to contribute to its rather small inhibitory effect on Ewing sarcoma proliferation.

The importance of regulating the turnover of transcription factors has been highlighted by the tumor suppressor p53, whose stability is controlled by several E3 ligases (45). Furthermore, E3 ligases have become an attractive target for cancer therapy over the past years since they are often aberrantly expressed in cancers (9,10). Here, we found that the E3 ubiquitin ligase WWP1 is an important regulator of EWS/FLI1 turnover. Since the fusion protein is the main driver of tumorigenesis in Ewing sarcoma, we suggest that interference with EWS-FLI1 turnover might be a novel strategy to induce tumor growth inhibition.

Acknowledgments

The authors thank Lena Harder for their support with cell sorting and FACS analysis.

References

1. Cotterill SJ, Ahrens S, Paulussen M, Jürgens HF, Voûte PA, Gadner H, et al. Prognostic factors in Ewing's tumor of bone: analysis of 975 patients from the European Intergroup Cooperative Ewing's Sarcoma Study Group. J Clin Oncol. 2000;18:3108–14.
2. Duchman KR, Gao Y, Miller BJ. Cancer Epidemiology. Cancer Epidemiology. Elsevier Ltd; 2015;39:189–95.
3. Turc-Carel C, Philip I, Berger MP, Philip T, Lenoir G. [Chromosomal translocation (11; 22) in cell lines of Ewing's sarcoma]. C R Seances Acad Sci III. 1983;296:1101–3.
4. Turc-Carel C, Aurias A, Mugneret F, Lizard S, Sidaner I, Volk C, et al. Chromosomes in Ewing's sarcoma. I. An evaluation of 85 cases of remarkable consistency of t(11;22)(q24;q12). Cancer Genet Cytogenet. 1988;32:229–38.
5. Siligan C, Ban J, Bachmaier R, Spahn L, Kreppel M, Schaefer K-L, et al. EWS-FLI1 target genes recovered from Ewing's sarcoma chromatin. Oncogene. 2005;24:2512–24.
6. Sankar S, Bell R, Stephens B, Zhuo R, Sharma S, Bearss DJ, et al. Mechanism and relevance of EWS/FLI-mediated transcriptional repression in Ewing sarcoma. Nature Publishing Group; 2012;32:5089–100.
7. Hu-Lieskovan S. Sequence-Specific Knockdown of EWS-FLI1 by Targeted, Nonviral Delivery of Small Interfering RNA Inhibits Tumor Growth in a Murine Model of Metastatic Ewing's Sarcoma. Cancer Research. 2005;65:8984–92.
8. Crompton BD, Stewart C, Taylor-Weiner A, Alexe G, Kurek KC, Calicchio ML, et al. The Genomic Landscape of Pediatric Ewing Sarcoma. Cancer Discovery. 2014;4:1326–41.
9. Nalepa G, Rolfe M, Harper JW. Drug discovery in the ubiquitin–proteasome system. Nat Rev Drug Discov. 2006;5:596–613.
10. Skaar JR, Pagan JK, Pagano M. SCF ubiquitin ligase-targeted therapies. Nature Publishing Group. Nature Publishing Group; 2014;13:889–903.
11. Gorre ME. BCR-ABL point mutants isolated from patients with imatinib mesylate-resistant chronic myeloid leukemia remain sensitive to inhibitors of the BCR-ABL chaperone heat shock protein 90. Blood. 2002;100:3041–4.
12. de Thé H, Chen Z. Acute promyelocytic leukaemia: novel insights into the mechanisms of cure. Nature Publishing Group; 2010;:1–9.
13. Huibregtse JM, Scheffner M, Beaudenon S, Howley PM. A family of proteins structurally and functionally related to the E6-AP ubiquitin-protein ligase. Proc Natl Acad Sci USA. 1995;92:2563–7.
14. Rotin D, Kumar S. Physiological functions of the HECT family of ubiquitin ligases. Nat Rev Mol Cell Biol. 2009;10:398–409.
15. Berndsen CE, Wolberger C. New insights into ubiquitin E3 ligase mechanism. Nature Publishing Group. Nature Publishing Group; 2014;21:301–7.
16. Chen HI, Sudol M. The WW domain of Yes-associated protein binds a proline-rich ligand that differs from the consensus established for Src homology 3-binding modules. Proc Natl Acad Sci USA. 1995;92:7819–23.
17. Ingham RJ, Gish G, Pawson T. The Nedd4 family of E3 ubiquitin ligases: functional diversity within a common modular architecture. Oncogene. 2004;23:1972–84.
18. Komuro A, Imamura T, Saitoh M, Yoshida Y, Yamori T, Miyazono K, et al. Negative regulation of transforming growth factor-β (TGF-β) signaling by WW domain-containing protein 1 (WWP1). Oncogene. 2004;23:6914–23.
19. Moren A, Imamura T, Miyazono K, Heldin CH, Moustakas A. Degradation of the Tumor Suppressor Smad4 by WW and HECT Domain Ubiquitin Ligases. Journal of Biological Chemistry. 2005;280:22115–23.
20. Lin X-W, Xu W-C, Luo J-G, Guo X-J, Sun T, Zhao X-L, et al. WW domain containing E3 ubiquitin protein ligase 1 (WWP1) negatively regulates TLR4-mediated TNF-α and IL-6 production by proteasomal degradation of TNF receptor associated factor 6 (TRAF6). PLoS ONE. 2013;8:e67633.
21. Feng SM, Muraoka-Cook RS, Hunter D, Sandahl MA, Caskey LS, Miyazawa K, et al. The E3 Ubiquitin Ligase WWP1 Selectively Targets HER4 and Its Proteolytically Derived Signaling Isoforms for Degradation. Mol Cell Biol. 2009;29:892–906.
22. Laine A, Ronai Z. Regulation of p53 localization and transcription by the HECT domain E3 ligase WWP1. Oncogene. 2007;26:1477–83.

23. Li Y, Zhou Z, Chen C. WW domain-containing E3 ubiquitin protein ligase 1 targets p63 transcription factor for ubiquitin-mediated proteasomal degradation and regulates apoptosis. Cell Death and Differentiation. 2008;15:1941–51.

24. Zhi X, Chen C. WWP1: a versatile ubiquitin E3 ligase in signaling and diseases. Cell Mol Life Sci. 2011;69:1425–34.

25. Chen C, Zhou Z, Ross JS, Zhou W, Dong J-T. The amplified WWP1 gene is a potential molecular target in breast cancer. Int J Cancer. 2007;121:80–7.

26. Chen C, Sun X, Guo P, Dong X-Y, Sethi P, Zhou W, et al. Ubiquitin E3 ligase WWP1 as an oncogenic factor in human prostate cancer. Oncogene. 2007;26:2386–94.

27. Wu Z, Zan P, Li S, Liu J, Wang J, Chen D, et al. Knockdown of WWP1 inhibits growth and invasion, but induces apoptosis of osteosarcoma cells. Int J Clin Exp Pathol. 2015;8:7869–77.

28. Yen H-CS, Xu Q, Chou DM, Zhao Z, Elledge SJ. Global protein stability profiling in mammalian cells. Science. 2008;322:918–23.

29. Staub O, Dho S, Henry P, Correa J, Ishikawa T, McGlade J, et al. WW domains of Nedd4 bind to the proline-rich PY motifs in the epithelial Na+ channel deleted in Liddle's syndrome. EMBO J. 1996;15:2371–80.

30. Tsokos M, Alaggio RD, Dehner LP, Dickman PS. Ewing Sarcoma/Peripheral Primitive Neuroectodermal Tumor and Related Tumors. Pediatric and Developmental Pathology. 2012;15:108–26.

31. Yen H-CS, Elledge SJ. Identification of SCF ubiquitin ligase substrates by global protein stability profiling. Science. 2008;322:923–9.

32. Emanuele MJ, Elia AEH, Xu Q, Thoma CR, Izhar L, Leng Y, et al. Global Identification of Modular Cullin-RING Ligase Substrates. Cell. Elsevier Inc; 2011;147:459–74.

33. Vitari AC, Leong KG, Newton K, Yee C, O'Rourke K, Liu J, et al. COP1 is a tumour suppressor that causes degradationof ETS transcription factors. National Cancer Institute. Nature Publishing Group; 2012;474:403–6.

34. Baert J-L, Monte D, Verreman K, Degerny C, Coutte L, de Launoit Y. The E3 ubiquitin ligase complex component COP1 regulates PEA3 group member stability and transcriptional activity. Oncogene. Nature Publishing Group; 2010;29:1810–20.

35. Ingham RJ, Colwill K, Howard C, Dettwiler S, Lim CSH, Yu J, et al. WW Domains Provide a Platform for the Assembly of Multiprotein Networks. Mol Cell Biol. 2005;25:7092–106.

36. Salah Z, Cohen S, Itzhaki E, Aqeilan R. NEDD4 E3 ligase inhibits the activity of the Hippo pathway by targeting LATS1 for degradation. Cell Cycle. 2014;12:3817–23.

37. Yeung B, Ho K-C, Yang X. WWP1 E3 Ligase Targets LATS1 for Ubiquitin-Mediated Degradation in Breast Cancer Cells. Viglietto G, editor. PLoS ONE. 2013;8:e61027.

38. Ho K-C, Zhou Z, She Y-M, Chun A, Cyr TD, Yang X. Itch E3 ubiquitin ligase regulates large tumor suppressor 1 stability [corrected]. Proc Natl Acad Sci USA. 2011;108:4870–5.

39. Rubenstein EM, Hochstrasser M. Redundancy and variation in the ubiquitin-mediated proteolytic targeting of a transcription factor. Cell Cycle. 2010;9:4282–5.

40. Poulsen EG, Steinhauer C, Lees M, Lauridsen A-M, Ellgaard L, Hartmann-Petersen R. HUWE1 and TRIP12 collaborate in degradation of ubiquitin-fusion proteins and misframed ubiquitin. PLoS ONE. 2012;7:e50548.

41. Spahn L, Petermann R, Siligan C, Schmid JA, Aryee DNT, Kovar H. Interaction of the EWS NH2 terminus with BARD1 links the Ewing's sarcoma gene to a common tumor suppressor pathway. Cancer Research. 2002;62:4583–7.

42. van den Akker E, Ano S, Shih H-M, Wang L-C, Pironin M, Palvimo JJ, et al. FLI-1 functionally interacts with PIASxalpha, a member of the PIAS E3 SUMO ligase family. J Biol Chem. 2005;280:38035–46.

43. Zhi X, Chen C. WWP1: a versatile ubiquitin E3 ligase in signaling and diseases. Cell Mol Life Sci. 2011;69:1425–34.

44. Cheng Q, Cao X, Yuan F, Li G, Tong T. Knockdown of WWP1 inhibits growth and induces apoptosis in hepatoma carcinoma cells through the activation of caspase3 and p53. Biochemical and Biophysical Research Communications. 2014;448:248–54.

45. Chao CC-K. Mechanisms of p53 degradation. Clin Chim Acta. 2015;438:139–47.

Figures

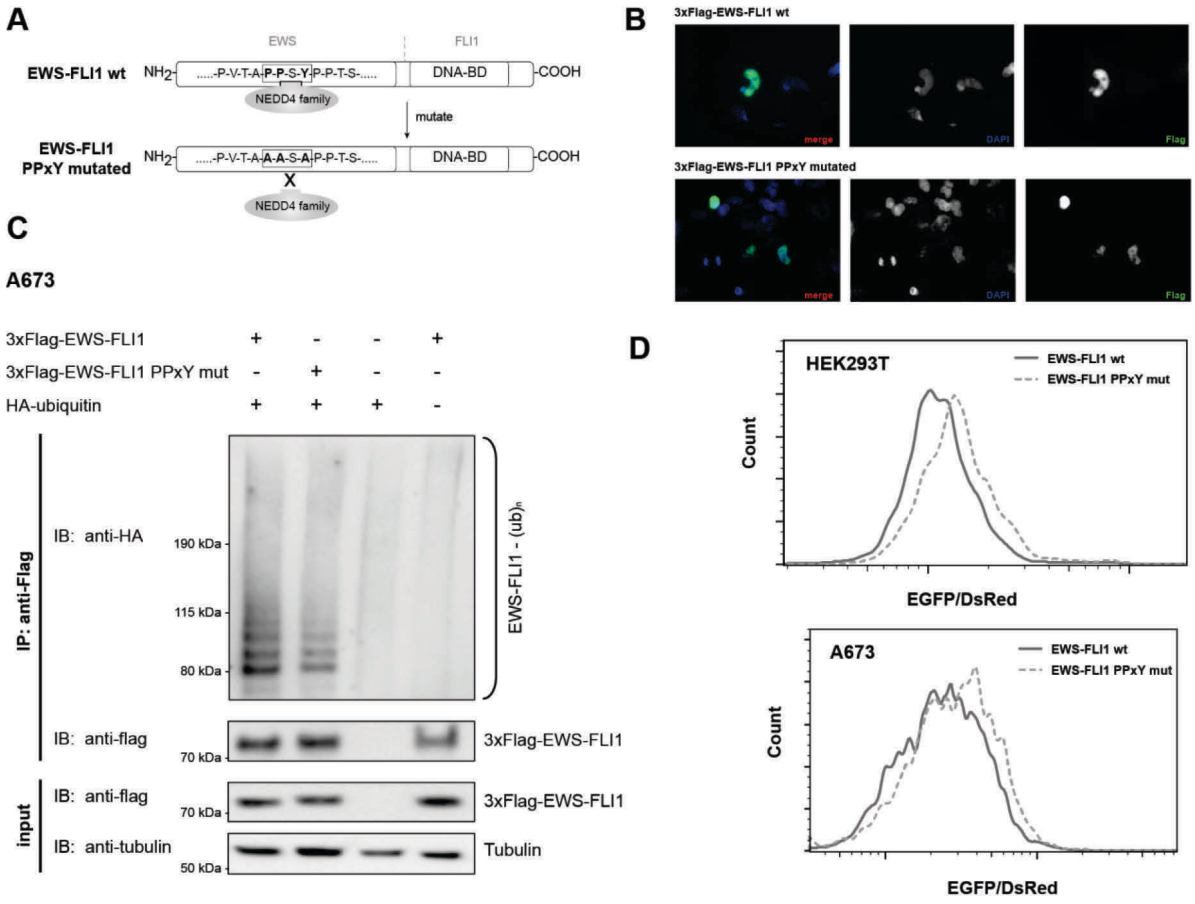

Fig. 1: EWS-FLI1 ubiquitination and stability is regulated by its PPxY motif. (A) The PPxY motif of EWS-FLI1 was mutated by site-directed mutagenesis in order to prevent binding of NEDD4 family E3 ligases. (B) A673 cells were transfected with pCMV-3xFlag-EWS-FLI1 wt or pCMV-3xFlag-EWS-FLI1 PPxY mutated. After 48h, cells were fixed and immunostained by Alexa-488 linked antibody and DAPI. EWS-FLI1 localization and cell nucleus were analyzed by fluorescence microscopy using 63x magnification. (C) A673 cells were transfected with pCMV-3xFlag-EWS-FLI1 wt or PPxY mutated together with HA-ubiquitin as indicated. 48h after transfection, cell lysates were immunoprecipitated under denaturing conditions using anti-flag antibody. Polyubiquitinated EWS-FLI1 was analyzed by western blotting using anti-HA and anti-flag antibodies. Representative western blot is shown. (D) HEK293T and A673 cells were transduced with lentiviral particles containing the reporter construct DsRed-IRES-EGFP fused to EWS/FLI1 wt or PPxY mutated. 72h after transduction, fluorescence was measured by FACS and data were further analyzed using FlowJo software. Representative histograms show EGFP/DsRed ratios of double-positive cells.

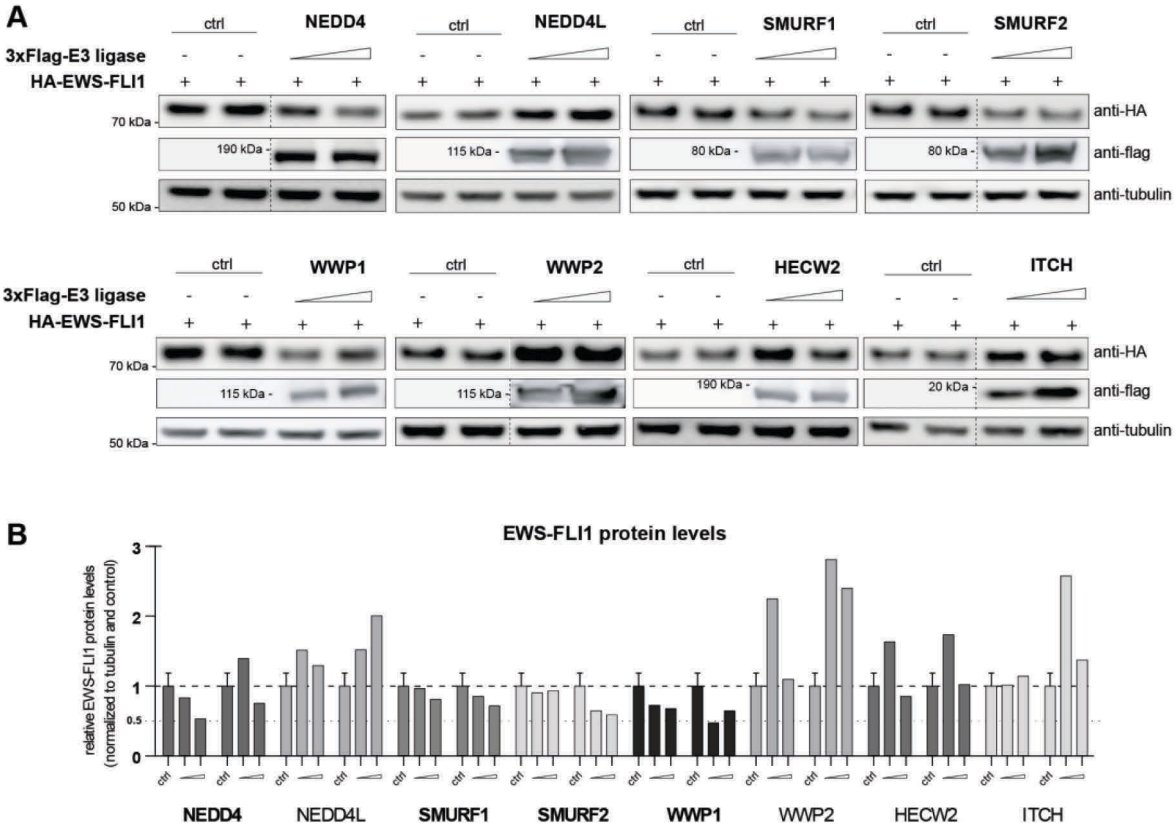

Fig. 2: E3 ligases from the NEDD4 family regulate EWS-FLI1 protein levels. (A) HEK293T cells were transfected with pCDNA3-HA-EWS-FLI1 and two increasing concentrations of pCMV-3xFlag-E3 ligases as indicated. 48h after transfection, cell lysates were analyzed by western blotting using anti-FLI1 and anti-flag antibodies. Representative western blots are shown. Samples separated by dotted lines were on the same blot. (B) Quantification of two independent experiments as shown in (A) using ImageJ software. Controls are represented as mean of 35 replicates ± SD.

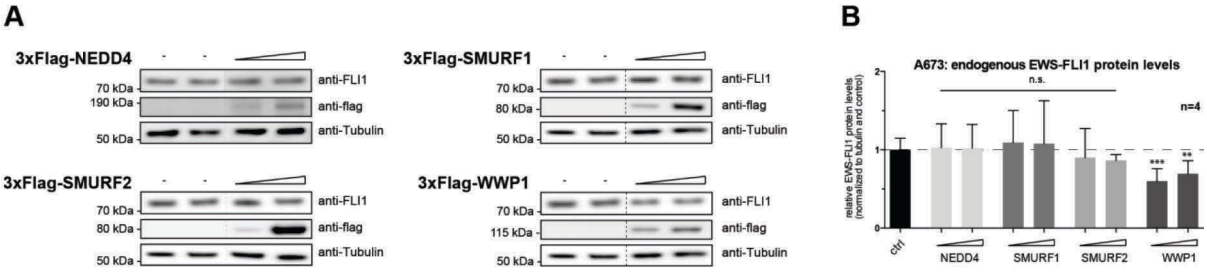

Fig. 3: WWP1 negatively regulates endogenous EWS-FLI1 protein levels in Ewing sarcoma cells. (A) A673 cells were transfected with two increasing concentrations of pCMV-3xFlag-E3 ligases as indicated. 48h after transfection, cell lysates were prepared for western blot analysis using anti-FLI1 and anti-flag antibodies. Representative western blot is shown. Samples separated by dotted lines were on the same blot. (B) Quantification of endogenous EWS/FLI1 protein levels shown in (A) of 4 independent replicates ± SD using ImageJ software. **p<0.01, *** p<0.001, n.s.=not significant by two-tailed Student‘s t test.

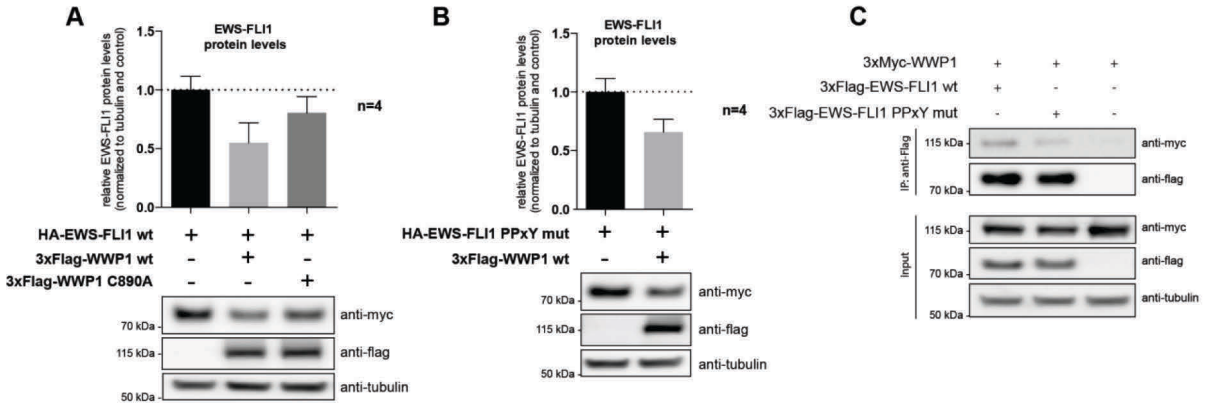

Fig. 4: WWP1 regulates EWS-FLI1 protein levels by interaction via the PPxY motif of the fusion protein. (A) HEK293T cells were transfected with pCDNA3-HA-EWS-FLI1 and pCMV-3xFlag-WWP1 wt or C890A as indicated. 48h after transfection, cell lysates were prepared for western blotting using anti-HA and anti-flag antibodies. Data were quantified using ImageJ software and represented as mean ± SD. Representative western blot is shown. (B) HEK293T were transfected with pCDNA3-HA-EWS-FLI1 wt or PPxY mutated and pCMV-3xFlag-WWP1 as indicated. Protein levels were analyzed and shown as in (A). (C) HEK293T cells were transfected with pCMV-3xFlag-EWS-FLI1 wt or PPxY mutated together with pCDNA3-3xMyc-WWP1 as indicated. After 48h, EWS-FLI1 was immunoprecipitated using anti-flag antibody and interaction was analyzed by western blotting using anti-myc and anti-flag antibodies. Representative western blot is shown.

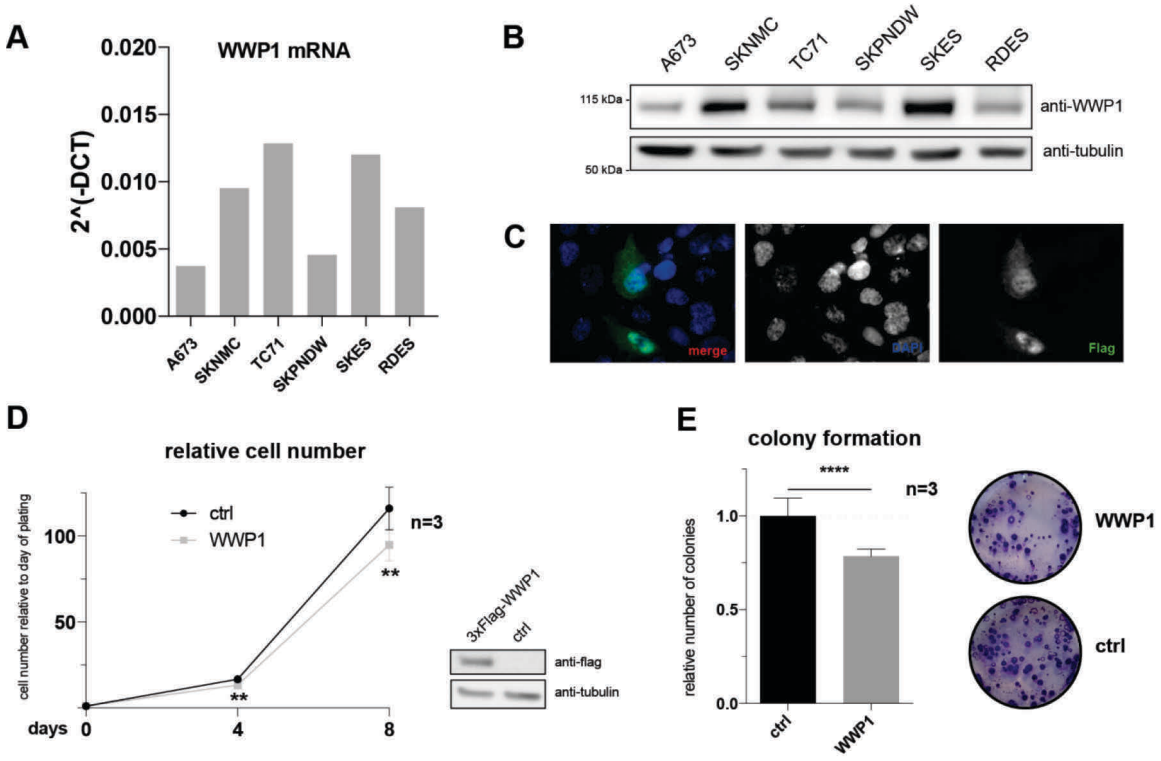

Fig. 5: WWP1 has a tumor suppressive function in Ewing sarcoma cells. (A, B) Cell lysates of different Ewing sarcoma (A673, SKNMC, TC71, SKES, RDES) and peripheral neuroectodermal tumor (SKPNDW) cell lines were prepared for qRT-PCR analysis (A) and western blot analysis using anti-WWP1 antibody (B). (C) A673 cells were transfected with pCMV-3xFlag-WWP1, fixed and immunostained with anti-Flag and secondary Alexa-488 labeled antibody. DAPI was used for nuclear staining. Cells were analyzed by fluorescence microscopy at 63x magnification. (D) SKNMC cells were transduced with retroviral titer containing 3xFlag-WWP1 or a control vector together with a GFP selection marker. GFP-positive cells were sorted by FACS and WWP1 overexpression was analyzed by western blotting. Cells were plated in a 6-well and counted after 4 and 8 days. Data are represented as mean ±SD, **p<0.01 by two-tailed Student‘s t test. (E) SKNMC cells stably expressing WWP1 were plated for colony formation assay. Colonies were stained with crystal violet after 14 days and counted. Data are represented as mean ±SD, ****p<0.0001 by two-tailed Student‘s t test.

Supplementary tables

Supplementary table S1: Clone IDs ordered from Dharmacon Inc. (Buckinghamshire, UK).

Gene	Clone ID
NEDD4	9020595
NEDD4L	5528964
ITCH (only partial sequence was available)	3451168
SMURF1	9052935
SMURF2	7939721
WWP1	5296005
WWP2	3453212
HECW2	40125745

Supplementary table S2: Primers used for In-Fusion Cloning.

3xFlag-/3xMyc-E3 ligases in mammalian expression vector	
3xFlag-NEDD4	FW GACAAGCTTGCGGCCGCAGCACAAAGCTTACGATTG RS GATGAATTCGCGGCCGCCTACTAATCAACTCCATC
3xFlag-NEDD4L	FW GACAAGCTTGCGGCCGCAGCGACCGGGCTCGGGG RS GATGAATTCGCGGCCGCCTATTAATCCACCCCTTC
3xFlag-SMURF1	FW GACAAGCTTGCGGCCGCATCGAACCCCGGGACACG RS GATGAATTCGCGGCCGCCTATCACTCCACAGCAAACCC
3xFlag-SMURF2	FW GACAAGCTTGCGGCCGCATCTAACCCCGGAGGC RS GATGAATTCGCGGCCGCCTATCATTCCACAGCAAATCC
3xFlag-HECW2	FW GACAAGCTTGCGGCCGCAGCTAGTTCAGCCCG RS GATGAATTCGCGGCCGCCTATCACTCAAGTCCAAAAG
3xFlag-WWP1	FW GACAAGCTTGCGGCCGCAGCCACTGCTTCACCAAGG RS GATGAATTCGCGGCCGCCTATCATTCTTGTCCAAATC
3xFlag-WWP2	FW GACAAGCTTGCGGCCGCAGCATCTGCCAGCTC RS GATGAATTCGCGGCCGCCTATTACTCCTGTCCAAAGCC
3xFlag-ITCH	FW GACAAGCTTGCGGCCGCACAAGAGATTGATTTG RS GATGAATTCGCGGCCGCCTATTACTCTTGTCCAAATC
3xMyc-WWP1	FW CTGGAATTCAGGATCCAATCTGGCGGGGCCAGTGC RS GCGGATATCAGGATCCCTATCATTCTTGTCCAAATC
WWP1 in retroviral vector	
3xFlag-WWP1	FW GAATTCAGATCTCGAGATGGACTACAAAGACCATGACG RS ATTGATCCCGCTCGAGCTATCATTCTTGTCCAAATC
Site-directed mutagenesis	
EWS/FLI1-AAxA	FW TCACTGCAGCTGCATCCGCCCCTCCTACCAGCTATTCC RS GGTAGGAGGGGCGGATGCAGCTGCAGTGACTGGCTGCAT
WWP1 C890A	FW 5' CCAAGAAGCCATACAGCTTTTAATCGCTTGGATCTACC 3' RS 5' GGTAGATCCAAGCGATTAAAAGCTGTATGGCTTCTTGG 3'

6. Manuscript III

EWS-FLI1 protein is stabilized by the deubiquitinating enzyme USP19 that constitutes a novel therapeutic target for Ewing sarcoma

Maria E. Gierisch, Gloria Pedot, Franziska Pfistner, Laura A. Lopez-Garcia, Patricia Jaaks, Beat W. Schäfer, Felix K. Niggli

Department of Oncology and Children's Research Center, University Children´s Hospital, Steinwiesstrasse 32, 8032 Zurich, Switzerland

Running title: Regulation of EWS-FLI1 stability by USP19

Keywords: Ewing sarcoma, EWS-FLI1, USP19, stability, fusion protein

Additional information:

Financial support: Swiss National Science Foundation 31003A-144177

Corresponding author: Beat Schäfer, Department of Oncology, Children´s Hospital Zurich, Steinwiesstrasse 32, 8032 Zurich, Switzerland, beat.schaefer@kispi.uzh.ch, +41442667553

Conflict of interest: The authors declare no conflict of interest.

Word count: abstract 208 words, manuscript 4576 words (without references and figure legends)

Number of figures: 6 main figures

Supplementary information: 5 supplementary figures and figure legends, 2 supplementary tables

References: 47

Manuscript submitted in Cancer Research

Contributions to the manuscript:

I performed and analyzed all experiments, formatted and wrote the manuscript. Franziska Pfistner established the siRNA-based ubiquitination assay (Fig. 3C). Laura Lopez provided help with all transfection experiments. Patricia Jaaks provided help by establishing the mouse experiment. Mouse tissue stainings have been performed by Sophistolab AG.

Abstract

Ewing sarcoma is the second most common pediatric bone and soft tissue tumor with an aggressive behavior and prevalence to metastasize. The diagnostic translocation t(22;11)(q24;12) leads to expression of the chimeric oncoprotein EWS-FLI1 harboring a strong transactivation and a DNA-binding domain. The EWS-FLI1 protein is uniquely expressed in all tumor cells and maintains their survival. Constant EWS-FLI1 protein turnover is precisely regulated by the ubiquitin proteasome system. Here, we identified ubiquitin specific protease 19 (USP19) as a regulator of EWS-FLI1 stability. Depletion of USP19 resulted in diminished EWS-FLI1 protein levels and, vice versa, upregulation of active USP19 stabilized EWS-FLI1 in a dose-dependent manner. Importantly, stabilization appears to be specific for the fusion protein as it could not be observed neither for EWSR1 and nor FLI1 wild type proteins. Mechanistically, we show USP19 to directly interact with the N-terminal EWS part to induce deubiquitination at a specific acceptor lysine in the FLI1 domain. Further, stable shRNA expression to deplete USP19 resulted in decreased cell growth and diminished colony forming capacity *in vitro*, and significantly delayed tumor growth *in vivo*. Hence, our findings not only provide novel insights into the regulation of EWS-FLI1 protein stability, but also identify USP19 as a novel therapeutic target for the treatment of Ewing sarcoma.

Introduction

Ewing sarcoma is a rare bone and soft tissue tumor which is highly distinct from other sarcoma subtypes due to its histology, molecular characteristics and prevalence to metastasize (1). It most commonly arises in children and adolescents with an age dependent distribution. Histologically, it presents as an undifferentiated and blue small round cell tumor. The 5-year survival rate for localized disease is around 70% whereas it is less than 40% for patients with metastasis at initial diagnosis (1,2). Current treatment includes surgery and chemotherapy with long known standard agents like doxorubicin and vincristine (3). High chemotherapeutic toxicity, relapsed tumors and an unfavorable prognosis of patients with metastasis are demanding for novel therapeutic strategies.

In contrast to adult cancers harboring an accumulation of multiple driver mutations, pediatric lesions display a high frequency of chromosomal rearrangements and a comparably low mutational burden (4-6). Indeed, recent sequencing efforts revealed that, besides a recurrent translocation, the genomic landscape of Ewing sarcoma is characterized by only very few additional mutational events such as STAG2 and TP53 point mutations in a subset of patients (7,8). The main genetic event therefore is the balanced translocation between chromosomes 11 and 22 leading to expression of the chimeric transcription factor EWS-FLI1, in the majority of the cases (9). This aberrant fusion protein is indispensable for tumor formation and progression as its depletion induces tumor growth inhibition (10-12). EWS-FLI1 triggers a defined program of target gene activation and repression and is further implicated in remodeling a wide network of protein-protein interactions (13-17). Given the fact that Ewing sarcoma cells are highly dependent on continuous expression of the fusion protein, reduction of EWS-FLI1 levels represents an attractive therapeutic avenue.

Regulation of protein stability is a highly conserved system ensuring maintenance of cell homeostasis and/or response to exogenous stimuli. Most intracellular proteins are degraded by the ubiquitin proteasome system. Ubiquitin tagged proteins are either subjected for destruction or induce signaling cascades (18,19). The process of ubiquitin chain attachment and elongation is regulated by an enzymatic cascade whereby E3 ligases mediate the ubiquitin transfer (20). The poly-ubiquitin chains can be removed or modified by deubiquitinating enzymes (DUBs) whose family is comprised of around 100 members classified into six subgroups according to their catalytical core domains (21).

Ubiquitin specific protease 19 (USP19) is a USP family member with several splice isoforms. The N-terminus is responsible for chaperone function whereas the USP domain mediates protein-protein interactions. At the C-terminal end, USP19 harbors a transmembrane domain which mapped its function initially to substrate rescue of endoplasmic-reticulum-associated degradation (22,23). USP19 is known to play a critical role in cellular homeostasis by supporting protein quality control and clearing misfolded proteins (24). Also muscle homeostasis is maintained by USP19, its inactivation protects against muscle wasting (25-27). However, the identification of the substrate KPC1, a regulator of p27 stability, suggested that USP19 might also be implicated in cell cycle deregulation. Finally, USP19 knockdown inhibited proliferation of prostate cancer and breast epithelial cell lines suggesting USP19 to be oncogenic (28,29).

We have recently identified EWS-FLI1 as a substrate of the proteasome system with a distinct turnover (30). In the present study, we utilized a siRNA-based screening approach to identify the deubiquitinating enzyme USP19 as a specific stabilizer of the EWS-FLI1 fusion protein. Depletion of USP19 increased EWS-FLI1 ubiquitination and enhanced its degradation. USP19 inhibition subsequently resulted in decreased tumor cell growth *in vitro* and *in vivo*. Our data suggest selective EWS-FLI1 destabilization by means of DUB inhibition to be an entirely new class of targeting mechanism for Ewing sarcoma treatment.

Material and methods

Cell lines

HEK293T and HEK293 cells were cultured in DMEM (Sigma Aldrich, Buchs, Switzerland) with 10% FBS (Sigma Aldrich), 2mmol/L glutamine (BioConcept, Allschwil, Switzerland) and 100U/ml penicillin/streptomycin (ThermoFisher Scientific AG, Reinach, Switzerland) at 37°C in 5% CO_2. All Ewing sarcoma cell lines and primary cells were cultured in RPMI medium with the same supplements. A673, RDES and primary cells were plated on 0.2% gelatine (Sigma Aldrich) pre-coated dishes. G418 selection of A673 and RDES clonal cell lines was carried out with 1.5mg/ml G418 for one week, and kept in 0.2mg/ml G418 for further culturing. Puromycin selection was performed with 1.5µg/ml, whereas 0.5µg/ml was used for maintenance. All cell lines have been tested mycoplasma negative. Ewing cell lines were authenticated by cell line typing analysis (STR profiling) 2016/05. Primary Ewing cell lines were characterized by karyotyping at the diagnostic laboratory of the Children´s Hospital Zurich, Switzerland and described before (31).

Reagents and antibodies

The following reagents were used: DMSO, doxycycline (both Sigma Aldrich), G418 (Promega, Duebendorf, Switzerland), puromycin (ThermoFisher Scientific AG). The following commercial antibodies were used: anti-Flag (clone M2, dilution 1:1000, Sigma Aldrich), anti-FLI1 (1:1000, MBS300723 MyBioSource LLC, San Diego, CA, USA), anti-GAPDH (1:1000, D16H11 Cell Signaling Technology, Beverly, MA, USA), anti-HA (both 1:1000, clone 6E2 Cell Signaling Technology and 05-904 Millipore), anti-Myc (1:1000, clone 9B11 Cell Signaling Technology) anti-p27 (1:200, clone DCS-72.F6 ThermoFisher Scientific AG), anti-Tubulin (1:1000, clone DM1A Sigma Aldrich) and anti-USP19 (1:1000, WB: A301-587A Bethyl Laboratories, Montgomery, TX, USA and 1:200, IHC or 1:1000 WB: ab93159 Abcam, Cambridge, UK).

Plasmids and cloning

The pRSIT-U6Tet-shRNA-PGK-TetRep-2A-GFP-2A-puro vector with shRNA sequences against USP19 or a negative control construct were purchased from Cellecta Inc. (Mountain View, CA, USA) with the following target sequences: shControl 5'-TTGGTGCTCTTCATCTTGTTG-3', shUSP19#1 5'-GTGAAACAGAAGGTGCACTGC-3' and shUSP19#2 5'-AAGTGATGGAGACCTTGGCAC-3'. USP19 cDNA (Addgene #36306) was introduced into pCMV-3xflag or pCDNA-3xmyc vectors (tag N-terminal

of USP19) by In-Fusion cloning HD (Clontech Laboratories Inc., Mountain View, CA, USA) according to manufacturer's protocol. USP19 C506A was mutated by site-directed mutagenesis using the forward primer 5'-CAATTAGGCAACACCGCCTTCATGAACAGCGTC-3' and reverse primer 5'-GACGCTGTTCATGAAGGCGGTGTTGCCTAAATTG-3'. pCMV-3xflag-EWS-FLI1, pCMV-3xflag-EWSR1 and pCMV-3xflag-FLI1 have been described previously (30). All clonings have been verified by sequencing.

***In silico* candidate selection and screening method**

Twelve publicly available microarray data sets of Ewing cell lines and tumors were used to select DUB candidates (Supplementary Table ST1). Genes were ranked according to the total number of present calls from all data sets and their expression values. For the screen, cells were reversely seeded with single siRNAs in a 96-well plate. After 48h, cells were lysed in standard lysis buffer (50mM Tris/HCl, 150mM NaCl, 50mM NaF, 5mM $Na_4P_2O_7$, 1mM Na_3VO_4 and 10mM ß-glycerolphosphate, 1% Triton X-100 with protease inhibitor cocktail, Complete Mini®, Sigma Aldrich) and cleared by centrifugation. For each well, 1/10 of the lysate was used to determine protein concentration by Pierce BCA Protein Assay Kit (ThermoFisher Scientific AG) and 9/10 were transferred to an anti-flag® high sensitivity M2 coated 96-well plate (Sigma Aldrich) and incubated for 2h at room temperature while shaking. Wells were then incubated with anti-FLI1 antibody followed by HRP-linked anti-rabbit antibody, each for 2h. To detect protein levels, wells were incubated with ready-to-use peroxidase substrate containing 3,3',5,5'-tetramethylbenzidine (Sigma Aldrich). Absorbance was measured by ELISA reader at 640nm. Each well was normalized to its corresponding protein concentration.

Transient transfection, virus production and cell transduction with viral supernatant

For siRNA silencing, RNAiMAX transfection reagent was mixed with siRNAs (both ThermoFisher Scientific AG) according to the manufacturer's protocol and reversely seeded with cells in antibiotics-free medium. For screening, three different siRNAs per gene were used (Silencer®Select, ThermoFisher Scientific AG, Supplementary Table ST2). For transient plasmid transfections, JetPrime (Polyplus Transfections, Illkirch, France) reagent was mixed with plasmids according to manufacturer's instruction in antibiotics-free medium and added to cells for 48h. For the production of lentiviral particles, HEK293T cells were transiently transfected with pMDL, pREV, pVSV and shRNA plasmids using JetPrime according to manufacturer's instruction in antibiotics-free DMEM medium. After 24h, medium was replaced and virus supernatant was harvested after a total of 72h. Viral supernatant was cleared by centrifugation, filtered and concentrated (Amicon Ultra 15 mL Centrifugal Filters, Millipore). Cells were transduced with the viral supernatant supplemented with 10µg/ml polybrene (Sigma Aldrich) by centrifugation for 1h at 32°C.

Cell lysis and western blotting

Cells were lysed in standard lysis buffer, sonicated and cleared by centrifugation. Protein separation was performed with 4-12% BisTris NuPAGE pre-cast gels (ThermoFisher Scientific AG) and transferred to nitrocellulose membranes (GE Healthcare, Glattbrugg, Switzerland). After 1h of blocking in 5% milk powder in 0.2% PBS-Tween, membranes were incubated with primary antibodies over

night at 4°C and 2h of HRP-linked secondary antibody at room temperature. Protein detection was carried out by chemiluminescence using Amersham ECL detection reagent (GE Healthcare) or SuperSignal™ Western blotting reagent (ThermoFisher Scientific AG). Quantification of blots was performed using ImageJ (version 1.46r).

Co-immunoprecipitation and immunoprecipitation of ubiquitinated proteins

HEK293T cells were lysed in interactor lysis buffer 1 (50mM Tris/HCl, 150mM NaCl, 1mM EDTA, 0.5% Triton X-100 with protease inhibitor cocktail) and HEK293 cells in interactor lysis buffer 2 (50mM Tris/HCl, 50mM NaCl, 1.5mM MgCl2, 25mM NaF, 10mM β-glycerolphosphate, 5mM $Na_4P_2O_7$, 2mM Na_3VO_4, 10% glycerol 0.3% NP40 with protease inhibitor cocktail). Lysates were cleared by centrifugation and incubated with anti-Flag antibody coupled to Dynabeads ProteinG (ThermoFisher Scientific AG) for 30min at 4°C. After three washing steps, the protein was eluted from the beads with 3xFlag-Peptide (Sigma Aldrich) at room temperature and prepared for western blot analysis.

To detect ubiquitinated proteins, cells were lysed in ubiquitin lysis buffer (2% SDS, 150mM NaCl, 10mM Tris/HCl, 2mM Na_3VO_4, 50mM NaF with protease inhibitor cocktail), boiled for 10min and sonicated. Lysates were rotating for 30min at 4°C after dilution in nine volumes of dilution buffer (150mM NaCl, 10mM Tris/HCl, 2mM EDTA, 1% Triton X-100) and cleared by centrifugation for 30 min at maximum speed. After immunoprecipitation, ubiquitinated proteins were analyzed by western blotting.

RNA extraction and quantitative RT-PCR

Total RNA was extracted from Ewing cells using RNeasy (Qiagen, Hombrechtikon, Switzerland) according to manufacturer's instruction. Complementary DNA synthesis was carried out using a High-Capacity Reverse Transcription Kit (ThermoFisher Scientific AG). Quantitative RT-PCR was performed using TaqMan gene expression master mix (ThermoFisher Scientific AG) and assays on demand (Applied Biosystems by ThermoFisher Scientific AG) with the following numbers: USP19 (Hs00324123_m1, Hs01103464_g1), EWS-FLI1 (Hs03024807_ft), GAPDH (Hs04420697_g1), HMBS (Hs00609296_g1), ITGA11 (Hs00201927_m1), LEMD1 (Hs01077215_m1), LOX (Hs00942481_m1), MAP2K6 (Hs00992389_m1), NGFR (Hs00609976_m1), NKX2.2 (Hs00159616_m1), NR0B1 (Hs00230864_m1), PHLDA1 (Hs00378285_g1). Relative expression values were calculated by the $\Delta\Delta C_t$ method. Replicate values were pooled and represented as the geometric mean with a 95% confidence interval as error bars.

Immunofluorescence and immunohistochemistry

For immunofluorescence, cells were seeded on cover slides and transiently transfected for 48h. Cells were fixed with 4% PFA (Carl Roth, Arlesheim, Switzerland) and permeabilized. After overnight staining with anti-Flag antibody (1:300) in 4% horse serum (Sigma Aldrich) 0.1% PBS Triton X-100, secondary antibody Alexa-488 (anti-mouse, Sigma Aldrich) in 4% horse serum PBS was applied for 1h. Slides were fixed on objective glass with DAPI Vectashield® mounting medium (Vector laboratories Inc., Burlingame, CA, USA). Cells were analyzed by an Axioskop 2 MOT Plus fluorescence microscope (Carl Zeiss Microscopy LLC, Thornwood, NY, USA). For

immunohistochemistry, tumors were fixed, embedded in paraffin and stained by Sophistolab AG (Muttenz, Switzerland).

Functional assays

A673 and SKNMC cells were seeded in 96 well plates. After indicated times, the following assays were carried out: For cell viability assays, cells were incubated with WST1 reagent (1:10 in medium, Sigma Aldrich) at 37°C and absorbance was measured at 440nm and 640nm. For BrdU incorporation, the Cell Proliferation ELISA Brdu chemiluminescent kit (Sigma Aldrich) was used according to the manufacturer's instructions. For cell number assay, cells were fixed with 4% PFA (Carl Roth) for 10min and stained with 0.05% crystal violet solution (Sigma Aldrich) for 20min. After a washing step in water, the dried staining was dissolved in methanol and absorbance was measured at 540nm. For colony formation, 100 (SKNMC) or 500 (A673) cells were seeded in a 6-well plate and stained with 0.05% crystal violet solution after 12-14 days. Colonies were manually counted.

Xenograft studies

SKNMC cells ($4x10^6$ cells) were engrafted subcutaneously in the left flank of NOD/Scid il2rg-/- mice (all female). Mice with a tumor volume of 50-100mm^3 were intraperitoneally injected with 53.3mg/kg doxycycline or corresponding PBS for the first two days. Mice were fed with doxycycline (625mg/kg) or PBS supplemented food (Provimi Kliba SA, Kaiseraugust, Switzerland). Tumor sizes were measured by caliper for two diameters at right angles. Tumor volume was calculated by $V=4/3*pi*((d_1+d_2)/4)^3$. Termination point was reached by a tumor volume of 1000mm^3.

Results

SiRNA-based screening to identify regulators of EWS-FLI1 stability. We have previously demonstrated that EWS-FLI1 protein has a high turnover mediated via the ubiquitin-proteasome system (30). As EWS-FLI1 protein expression is crucial for tumor cell survival (10,12), we aimed to destabilize the fusion protein by depleting EWS-FLI1 partner protein(s) of the ubiquitin system. Most relevantly, DUBs can rescue substrates from degradation and thereby directly modulate protein expression. To identify relevant candidates, we selected 21 DUBs of the ubiquitin-specific protease family *in silico* based on high gene expression in publicly available gene expression profiles of Ewing sarcoma cell lines and tumors (Fig. 1A, Supplementary Table ST1). Next, we established a screening strategy to directly measure EWS-FLI1 protein levels as a read-out by monitoring the amount of flag-tagged EWS-FLI1 protein in an ELISA-type assay upon transient transfection with individual siRNAs (Fig. 1B, Supplementary Table ST2). As positive control, a siRNA directed against the fusion protein was used which is capable to downregulate both exogenous and endogenous EWS-FLI1 protein levels with similar efficiency as shown by western blotting (Fig. S1A). Using three different siRNAs for each of the 21 candidates, we identified USP19 as the most potent modulator of EWS-FLI1 protein levels 48h after transfection. At least two siRNAs against USP19 decreased EWS-FLI1 protein levels by more than 25% in each of three screening rounds (Fig. 1C), values which were compensated by total protein levels for each individual well to ensure that diminished EWS-FLI1 protein levels are not

simply a result of decreased cell numbers (Fig. S1B). To validate that USP19 depletion could be relevant in Ewing sarcoma cells, we analyzed protein and mRNA expression of USP19 across six different Ewing sarcoma cell lines and three primary cell samples (Fig. 1D-E). USP19 protein presents with various isoforms of different sizes in Ewing sarcoma cell lines and primary cells whereby the highest band matches the size of overexpressed USP19. The amount of mRNA correlated well with protein expression in all the cell lines, with SKNMC and TC71 displaying highest levels. Overexpression of 3xflag-USP19 showed that the protein is predominantly localized in the cytoplasm of Ewing cell lines (Fig S1C). Hence, out of a pre-selected subset of candidates we identified USP19 as a potential modulator of EWS/FLI1 stability.

USP19 specifically modulates EWS-FLI1 protein level. To validate USP19 as modulator of EWS-FLI1 stability, we first investigated the effect of USP19 depletion on endogenous EWS-FLI1 protein across two different cell lines with two different siRNAs. Similar to the observations made in the initial screening, USP19 knockdown resulted in an efficient reduction of USP19 protein levels and a subsequent decrease of EWS-FLI1 protein of around 40% after 72h in both A673 and SKNMC cells (Fig. 2A-B). P27 protein levels slightly increased after depletion as already described before, and possibly mediated by inhibition of the E3 ligase KPC1 (28,29). As expected, transient USP19 knockdown also affected a subset of both activated and repressed EWS-FLI1 target genes in SKNMC cells. NKX2.2, NGFR, LEMD1, LOX and ITAG11 displayed modulated expression levels, while NR0B1 or PHLDA1 were not affected (Fig. S2A). Next, we transiently co-expressed flag-tagged EWS-FLI1 with two increasing concentrations of 3xmyc-tagged USP19 in HEK293T cells. EWS-FLI1 levels were stabilized more than 2-fold in a dose-dependent manner by active USP19, but to a much lesser extend with the catalytically inactive C506A mutant (22), indicating that indeed the deubiquitinating activity of USP19 is responsible for modulation of fusion protein levels (Fig. 2C-D). Interestingly, the stabilization of EWS-FLI1 by USP19 might be specific for the fusion protein as the protein levels of full length wild type EWSR1 or FLI1 remained constant upon co-expression with 3xmyc-USP19 (Fig. 2E). Therefore, we next assessed if EWS-FLI1 and USP19 could interact directly. For this, tagged versions of USP19 and EWS-FLI1 were co-expressed and immunoprecipitated from HEK293T cells. We observed a consistent pull-down of UPS19 with tagged EWS-FLI1 and vice versa (Fig. 2E, S2B), suggesting that the two proteins interact directly. Strikingly, when USP19 was co-expressed with the full length proteins EWS and FLI1, only full length EWS, but not wild type FLI1 could be immunoprecipitated indicating that USP19 binds to the N-terminal domain of both proteins (Fig. 2F). Taken together, our results indicate that USP19 is indeed a specific regulator of EWS-FLI1 protein stability and activity.

USP19 destabilizes EWS-FLI1 by direct deubiquitination. It was previously shown that USP19 directly deubiquitinates and rescues a variety of substrates from proteasomal degradation (32-34). We therefore aimed next to investigate whether USP19 could also deubiquitinate and subsequently stabilize the fusion protein. First, we depleted USP19 with three different siRNAs prior to immunoprecipitation of tagged ubiquitinated EWS-FLI1 in A673 cells. This resulted in increased EWS-FLI1 ubiquitination compared to control treated cells (Fig 3A). To further underscore this notion, we co-expressed 3xflag-EWS-FLI1 and HA-ubiquitin together with either active or mutant 3xmyc-USP19 in

A673 cells. Immunoprecipitation of ubiquitinated EWS-FLI1 revealed a reduction of the ubiquitination pattern and higher fusion protein levels when co-expressed with active USP19 compared to its catalytically inactive form (Fig. 3B).
Taken together, our findings identify EWS-FLI1 as a novel substrate of USP19 which directly reduces ubiquitination levels of the fusion protein by its enzymatic activity.

Depletion of USP19 affects Ewing sarcoma cell growth. To validate USP19 as a possible therapeutic target for Ewing sarcoma, we next assessed if USP19 knockdown affects the physiology of Ewing cells. To this end, we established SKNMC and A673 cells using two inducible shUSP19 constructs which allows to deplete USP19 by addition of doxycycline. Indeed, treatment of this cell populations resulted in reduction of both mRNA and protein levels with the specific, but not with the control shRNA sequence (Fig. 4A-B, S3A-B). To investigate the effect on tumor cell growth, we plated cells with and without doxycycline induction and determined cell numbers after four and eight days. Upon specific depletion of USP19, cell numbers are greatly reduced by 50% after four days and between 70-85% after eight days compared to non-induced and control cells for both Ewing cell lines (Fig. 4C, S3C). Analysis of the corresponding protein levels in SKNMC cells after eight days by western blotting revealed that depletion of USP19 is accompanied by a decrease in EWS-FLI1 protein levels by 40%, but no significant changes in EWS-FLI1 mRNA levels (Fig. 4D-F). USP19 depletion further decreased metabolic viability as shown by WST1 assay and proliferation by reduced BrdU incorporation (Fig. 4G-H, S3D). To assess long-term consequences, we analyzed the ability of Ewing cells to form colonies after 14 (SKNMC) and 12 days (A673), respectively. Upon USP19 depletion, colony forming capacity was reduced to less than 20% compared to non-induced and control cells which showed similar numbers of total colonies (Fig. 4I-J, S3E-F). In contrast, transient overexpression of ectopic myc-USP19 for only 48h already increased cell growth, viability and proliferation in both A673 and SKNMC cells which was not observed when a catalytically inactive mutant was expressed (Fig. S4A-G). Interestingly, USP19 depletion in non-tumorigenic cells such as MRC5 fibroblasts or HEK293T cells did not or only slightly affect cell viability as shown by WST1 measurements (Fig S3G-J). Similar growth rates of USP19-/- HEK293T cells have been described previously (24), suggesting that the oncogenic effect of USP19 is specific for Ewing sarcoma cells, despite a slight off-target effect observed for shUSP19#2. Hence, our data suggest that USP19 depletion is a relevant mechanism for Ewing cell growth inhibition *in vitro* which is mediated, at least in part, by EWS-FLI1 protein destabilization.

Loss of USP19 delays tumor growth in xenografts. Finally, we investigated whether USP19 depletion would affect tumor growth in mouse xenografts. To this end, we subcutaneously injected inducible shControl or shUSP19#1 SKNMC cells and allowed tumors to grow up to a volume of at least 50mm^3 (Fig. 5A). Then, we fed the animals with either control or doxycycline supplemented food to induce USP19 knockdown. Efficient reduction of USP19 protein levels could already be seen after five days of doxycycline administration compared to control cells, as shown by both western blotting and immunohistochemistry (Fig. 5B, S3A). While all tumors from control mice reached the final volume of 1000mm^3 after around ten days, tumors from doxycycline treated shUSP19 xenograft mice showed

a clear delay in tumor growth. While two mice reached the maximum tumor volume only after more than double of the time period, tumors of three other mice were stable at a volume of around 200mm^3 over the entire observation period (Fig.5C-D). Analysis of USP19 mRNA and protein from all tumors confirmed an efficient and selective downregulation of USP19 only upon doxycycline administration, even after a longer time period (Fig. 5E, S3B-C). Taken together, we could show that USP19 depletion significantly delays tumor cell growth also *in vivo* which corroborates our *in vitro* findings. Selective inhibition of DUBs, as shown here for USP19, therefore represents a novel strategy to inhibit Ewing sarcoma tumor growth.

Discussion

In this study, we investigated EWS-FLI1 protein destabilization by deubiquitinating enzymes as a novel therapeutic strategy in Ewing sarcoma. In particular, we identified USP19 as a specific modulator of EWS-FLI1 protein stability mediated by increased fusion protein deubiquitination. The enhanced turnover of EWS-FLI1 protein abrogated long term cell growth and delayed tumor growth in mouse xenograft experiments.

The majority of screening efforts in Ewing sarcoma utilized either single or subgroups of target genes as well as cell viability as read-outs for specificity and efficacy (35-38). As we have recently identified EWS-FLI1 turnover as an important regulatory pathway in Ewing sarcoma (30), we aimed at identifying potential stabilizers of the fusion protein, and utilize their inhibition which consequently would result in EWS-FLI1 degradation and tumor depletion. Therefore, we chose to screen for DUBs as they display a limited number of family members, harbor enzymatic activity and are currently an emerging field in drug development (39,40). Focusing on the 21 USP family members highly expressed in Ewing sarcoma cell lines and tumor samples allowed us to perform an unbiased screen for their ability to modulate EWS-FLI1 protein levels as a read-out in two different Ewing cell lines. We chose a short 48h incubation time to minimize secondary events due to general inhibition of cell growth. This led to the identification of USP19 as a novel regulator of EWS-FLI1 protein levels. However, it is very likely that other DUBs potentially regulate EWS-FLI1 turnover in a proteolytic or non-proteolytic manner as we could not observe more than 40% reduction in fusion protein levels.

Nevertheless, we clearly confirmed USP19 as a stabilizer of endogenous EWS-FLI1 by analyzing fusion protein levels upon USP19 knockdown. We also observed an increase of p27 protein which has been reported previously for USP19 and therefore further confirms specificity of our knockdown (28,29). On the other hand, co-expression of active USP19 with EWS-FLI1 stabilized the fusion protein whereas full length EWS and FLI1 protein levels remained unchanged. This suggests that inhibition of USP19 might be particularly attractive for Ewing sarcoma therapy since it would not affect ubiquitously expressed EWS or FLI1 wild type proteins thereby potentially decreasing therapy related side-effects. Indeed, our data suggest the following mechanistic model (Fig. 6): USP 19 can bind to the EWS domain of the fusion protein, as demonstrated here by co-immunoprecipitation experiments,

and reduces ubiquitination which occurs at a single acceptor lysine site (K380) in the FLI1 domain (30), thereby explaining its specificity for the fusion protein.

Other fusion proteins were shown to be targets of a variety of DUBs. For example, USP37 modulates PLZF-RARA fusion protein levels in acute promyelocytic leukemia (41). It was found to regulate only stability of PLZF-RARA, but not the closely related PML-RARA suggesting that the N-terminal domain may be relevant for DUB binding. Therefore, the mechanisms identified here might apply to additional products of chromosomal translocations.

Interestingly, USP9X was identified as a DUB for ERG, an ETS family member closely related to FLI1 (42,43). Similar to our results, it could be demonstrated that depletion of USP9X increased ERG ubiquitination and subsequently suppressed prostate tumor growth. As about 10% of Ewing sarcoma tumors carry an alternative EWS-ERG fusion, inhibition of this DUB as a therapeutic strategy might also be effective in this subgroup of tumors. Further, USP9X regulation was also suggested to modulate wild type FLI1 stability even though only binding was shown (42). In our screening approach, USP9X knockdown resulted in a decrease of EWS-FLI1 stability of around 12% which did not reach our defined threshold to be considered as candidate. Whether USP9X might further affect EWS-FLI1 levels in combination with USP19, remains to be investigated.

To better understand if the decrease in EWS-FLI1 level is due to enhanced ubiquitination and degradation, we performed *in vivo* DUB assays by depleting endogenous USP19 or overexpressing an ectopic version. Both assays revealed a modulation of EWS-FLI1 ubiquitination pattern suggesting that this is indeed the main regulatory mechanism. USP19 was initially identified as an ER-resident DUB able to rescue degradation of ERAD substrates (22), but has now predominantly been localized to the cytosol in association with heat shock protein 90 (Hsp90) and other chaperones as a main substrate (23). It is therefore likely that EWS-FLI1 interacts with USP19 in the cytosol as the fusion protein displays a high turnover and is constantly shuffling in and out of the nucleus (30).

Finally, we investigated the physiological consequences of USP19 depletion on Ewing sarcoma cell growth. For this, we used a doxycycline inducible model to deplete endogenous USP19 to ensure that no cell subpopulations were selected over time. In these studies, we observed selective diminished cell growth, proliferation and colony formation in Ewing sarcoma cell lines upon specific USP19 depletion. However, it cannot be excluded that also secondary effects may contribute to the phenotype as USP19 likely has other substrates such as the cell cycle regulator p27, regulators of apoptosis cIAPs or the E3 ligase MARCH6 (28,29,32,34). Even though only few USP19 substrates have been identified so far, without a common ontology, USP19 expression clearly seems to be oncogenic in the context of Ewing sarcoma as USP19 depletion did not influence cell viability of control cell lines of non-tumorigenic origin.

Most importantly, we also observed a significant growth delay upon USP19 knockdown in an in vivo xenograft model. Combining USP19 inhibition with other treatment strategies such as classical

chemotherapeutics, PARP inhibitors (5,44), DNA-damaging agents (45), inhibition of signaling pathways such as the PI3K pathway (46), or antagonists of the Wnt pathway (47) might further enhance its growth inhibitory properties. A recent study suggested that inhibition of EWS-FLI1 function results in de-repression of metastasis-associated gene programs, as a minority of ES tumors showed increased β-catenin pathway activation (47). Whether this might also be the case here, remains to be further investigated. Nevertheless, in macroscopic examinations, we did not observe any obvious formation of metastasis in mice carrying USP19 depleted tumors.

In summary, our study identifies a novel therapeutic approach, namely selective targeting of EWS-FLI1 turnover. Even though USP19 may not be the only DUB regulating fusion protein degradation, it seems to have a major impact and represents a novel potential target for Ewing sarcoma therapy.

Acknowledgment

We thank Prof. Roman Muff and Dr. Sander Botter (from the Laboratory for Orthopedic Research, Balgrist University Hospital Zurich, Switzerland) for the primary Ewing sarcoma cell lines. Further, we thank the team from Sophistolab AG (Muttenz, Switzerland) for stainings of the xenograft sections and Dr. Peter Bode (from the Pathology, University Hospital Zurich, Switzerland) for help with analyzing the USP19 xenograft stainings.

References:

1. Esiashvili N, Goodman M, Marcus RB, Jr. Changes in incidence and survival of Ewing sarcoma patients over the past 3 decades: Surveillance Epidemiology and End Results data. J Pediatr Hematol Oncol **2008**;30:425-30
2. Gorlick R, Janeway K, Lessnick S, Randall RL, Marina N. Children's Oncology Group's 2013 blueprint for research: bone tumors. Pediatric blood & cancer **2013**;60:1009-15
3. Bernstein M, Kovar H, Paulussen M, Randall RL, Schuck A, Teot LA*, et al.* Ewing's sarcoma family of tumors: Current management. Oncologist **2006**;11:503-19
4. Downing JR, Wilson RK, Zhang J, Mardis ER, Pui CH, Ding L*, et al.* The Pediatric Cancer Genome Project. Nature genetics **2012**;44:619-22
5. Lawrence MS, Stojanov P, Polak P, Kryukov GV, Cibulskis K, Sivachenko A*, et al.* Mutational heterogeneity in cancer and the search for new cancer-associated genes. Nature **2013**;499:214-8
6. Mitelman F, Johansson B, Mertens F. The impact of translocations and gene fusions on cancer causation. Nat Rev Cancer **2007**;7:233-45
7. Crompton BD, Stewart C, Taylor-Weiner A, Alexe G, Kurek KC, Calicchio ML*, et al.* The Genomic Landscape of Pediatric Ewing Sarcoma. Cancer Discov **2014**;4:1326-41
8. Tirode F, Surdez D, Ma X, Parker M, Le Deley MC, Bahrami A*, et al.* Genomic landscape of Ewing sarcoma defines an aggressive subtype with co-association of STAG2 and TP53 mutations. Cancer Discov **2014**;4:1342-53
9. Delattre O, Zucman J, Plougastel B, Desmaze C, Melot T, Peter M*, et al.* Gene fusion with an ETS DNA-binding domain caused by chromosome translocation in human tumours. Nature **1992**;359:162-5
10. Kovar H, Aryee DN, Jug G, Henockl C, Schemper M, Delattre O*, et al.* EWS/FLI-1 antagonists induce growth inhibition of Ewing tumor cells in vitro. Cell Growth Differ **1996**;7:429-37
11. Tanaka K, Iwakuma T, Harimaya K, Sato H, Iwamoto Y. EWS-Fli1 antisense oligodeoxynucleotide inhibits proliferation of human Ewing's sarcoma and primitive neuroectodermal tumor cells. J Clin Invest **1997**;99:239-47
12. Toretsky JA, Connell Y, Neckers L, Bhat NK. Inhibition of EWS-FLI-1 fusion protein with antisense oligodeoxynucleotides. J Neurooncol **1997**;31:9-16
13. Kinsey M, Smith R, Lessnick SL. NR0B1 is required for the oncogenic phenotype mediated by EWS/FLI in Ewing's sarcoma. Mol Cancer Res **2006**;4:851-9
14. Sankar S, Bell R, Stephens B, Zhuo R, Sharma S, Bearss DJ*, et al.* Mechanism and relevance of EWS/FLI-mediated transcriptional repression in Ewing sarcoma. Oncogene **2013**;32:5089-100
15. Selvanathan SP, Graham GT, Erkizan HV, Dirksen U, Natarajan TG, Dakic A*, et al.* Oncogenic fusion protein EWS-FLI1 is a network hub that regulates alternative splicing. Proc Natl Acad Sci U S A **2015**;112:E1307-16
16. Smith R, Owen LA, Trem DJ, Wong JS, Whangbo JS, Golub TR*, et al.* Expression profiling of EWS/FLI identifies NKX2.2 as a critical target gene in Ewing's sarcoma. Cancer Cell **2006**;9:405-16
17. Toretsky JA, Erkizan V, Levenson A, Abaan OD, Parvin JD, Cripe TP*, et al.* Oncoprotein EWS-FLI1 activity is enhanced by RNA helicase A. Cancer Res **2006**;66:5574-81
18. Glickman MH, Ciechanover A. The ubiquitin-proteasome proteolytic pathway: destruction for the sake of construction. Physiological reviews **2002**;82:373-428
19. Hershko A, Ciechanover A. The ubiquitin system. Annu Rev Biochem **1998**;67:425-79
20. Jentsch S. The ubiquitin-conjugation system. Annual review of genetics **1992**;26:179-207
21. Nijman SM, Luna-Vargas MP, Velds A, Brummelkamp TR, Dirac AM, Sixma TK*, et al.* A genomic and functional inventory of deubiquitinating enzymes. Cell **2005**;123:773-86
22. Hassink GC, Zhao B, Sompallae R, Altun M, Gastaldello S, Zinin NV*, et al.* The ER-resident ubiquitin-specific protease 19 participates in the UPR and rescues ERAD substrates. EMBO reports **2009**;10:755-61
23. Lee JG, Kim W, Gygi S, Ye Y. Characterization of the deubiquitinating activity of USP19 and its role in endoplasmic reticulum-associated degradation. The Journal of biological chemistry **2014**;289:3510-7
24. Lee JG, Takahama S, Zhang G, Tomarev SI, Ye Y. Unconventional secretion of misfolded proteins promotes adaptation to proteasome dysfunction in mammalian cells. Nature cell biology **2016**;18:765-76

25. Combaret L, Adegoke OA, Bedard N, Baracos V, Attaix D, Wing SS. USP19 is a ubiquitin-specific protease regulated in rat skeletal muscle during catabolic states. American journal of physiology **2005**;288:E693-700
26. Sundaram P, Pang Z, Miao M, Yu L, Wing SS. USP19-deubiquitinating enzyme regulates levels of major myofibrillar proteins in L6 muscle cells. American journal of physiology **2009**;297:E1283-90
27. Bedard N, Jammoul S, Moore T, Wykes L, Hallauer PL, Hastings KE*, et al.* Inactivation of the ubiquitin-specific protease 19 deubiquitinating enzyme protects against muscle wasting. FASEB J **2015**;29:3889-98
28. Lu Y, Adegoke OA, Nepveu A, Nakayama KI, Bedard N, Cheng D*, et al.* USP19 deubiquitinating enzyme supports cell proliferation by stabilizing KPC1, a ubiquitin ligase for p27Kip1. Mol Cell Biol **2009**;29:547-58
29. Lu Y, Bedard N, Chevalier S, Wing SS. Identification of distinctive patterns of USP19-mediated growth regulation in normal and malignant cells. PLoS One **2010**;6:e15936
30. Gierisch ME, Pfistner F, Lopez-Garcia LA, Harder L, Schafer BW, Niggli FK. Proteasomal degradation of the EWS-FLI1 fusion protein is regulated by a single lysine residue. The Journal of biological chemistry **2016**
31. Muff R, Botter SM, Husmann K, Tchinda J, Selvam P, Seeli-Maduz F*, et al.* Explant culture of sarcoma patients' tissue. Laboratory investigation; a journal of technical methods and pathology **2016**;96:752-62
32. Mei Y, Hahn AA, Hu S, Yang X. The USP19 deubiquitinase regulates the stability of c-IAP1 and c-IAP2. The Journal of biological chemistry **2011**;286:35380-7
33. Lim KH, Choi JH, Park JH, Cho HJ, Park JJ, Lee EJ*, et al.* Ubiquitin specific protease 19 involved in transcriptional repression of retinoic acid receptor by stabilizing CORO2A. Oncotarget **2016**;7:34759-72
34. Nakamura N, Harada K, Kato M, Hirose S. Ubiquitin-specific protease 19 regulates the stability of the E3 ubiquitin ligase MARCH6. Exp Cell Res **2014**;328:207-16
35. Boro A, Pretre K, Rechfeld F, Thalhammer V, Oesch S, Wachtel M*, et al.* Small-molecule screen identifies modulators of EWS/FLI1 target gene expression and cell survival in Ewing's sarcoma. Int J Cancer **2012**;131:2153-64
36. Garnett MJ, Edelman EJ, Heidorn SJ, Greenman CD, Dastur A, Lau KW*, et al.* Systematic identification of genomic markers of drug sensitivity in cancer cells. Nature **2012**;483:570-5
37. Grohar PJ, Woldemichael GM, Griffin LB, Mendoza A, Chen QR, Yeung C*, et al.* Identification of an inhibitor of the EWS-FLI1 oncogenic transcription factor by high-throughput screening. J Natl Cancer Inst **2011**;103:962-78
38. Stegmaier K, Wong JS, Ross KN, Chow KT, Peck D, Wright RD*, et al.* Signature-based small molecule screening identifies cytosine arabinoside as an EWS/FLI modulator in Ewing sarcoma. PLoS Med **2007**;4:e122
39. Ndubaku C, Tsui V. Inhibiting the deubiquitinating enzymes (DUBs). J Med Chem **2015**;58:1581-95
40. Pal A, Young MA, Donato NJ. Emerging potential of therapeutic targeting of ubiquitin-specific proteases in the treatment of cancer. Cancer Res **2014**;74:4955-66
41. Yang WC, Shih HM. The deubiquitinating enzyme USP37 regulates the oncogenic fusion protein PLZF/RARA stability. Oncogene **2013**;32:5167-75
42. Wang S, Kollipara RK, Srivastava N, Li R, Ravindranathan P, Hernandez E*, et al.* Ablation of the oncogenic transcription factor ERG by deubiquitinase inhibition in prostate cancer. Proc Natl Acad Sci U S A **2014**;111:4251-6
43. Wasylyk B, Hahn SL, Giovane A. The Ets family of transcription factors. Eur J Biochem **1993**;211:7-18
44. Brenner JC, Feng FY, Han S, Patel S, Goyal SV, Bou-Maroun LM*, et al.* PARP-1 inhibition as a targeted strategy to treat Ewing's sarcoma. Cancer Res **2012**;72:1608-13
45. Stewart E, Goshorn R, Bradley C, Griffiths LM, Benavente C, Twarog NR*, et al.* Targeting the DNA repair pathway in Ewing sarcoma. Cell Rep **2014**;9:829-41
46. Giorgi C, Boro A, Rechfeld F, Lopez-Garcia LA, Gierisch ME, Schafer BW*, et al.* PI3K/AKT signaling modulates transcriptional expression of EWS/FLI1 through specificity protein 1. Oncotarget **2015**;6:28895-910
47. Pedersen EA, Menon R, Bailey KM, Thomas DG, Van Noord RA, Tran J*, et al.* Activation of Wnt/beta-Catenin in Ewing Sarcoma Cells Antagonizes EWS/ETS Function and Promotes Phenotypic Transition to More Metastatic Cell States. Cancer Res **2016**;76:5040-53

Figures and Figure Legends

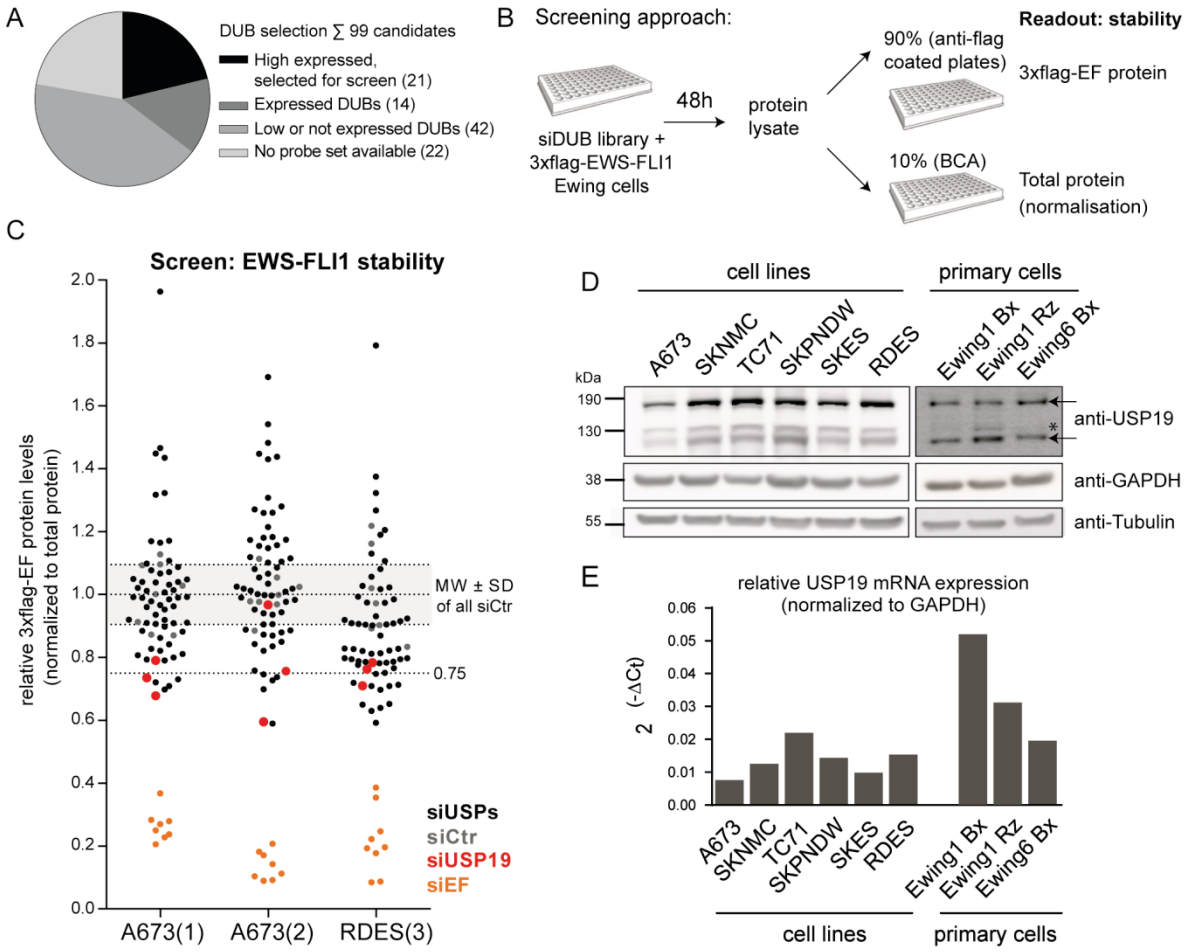

Fig. 1: SiRNA screen identifies USP19 as a modulator of EWS-FLI1 stability. (A) *In-silico* selection of candidates. 21 deubiquitinating enzymes were selected based on their expression levels from publicly available microarray data sets of Ewing cell lines and tumors. (B) Screening setup. A673 and RDES cells stably expressing flag-tagged EWS-FLI1 were reverse transfected with an siRNA library. After 48h, lysates were incubated in anti-flag coated plates to determine EWS-FLI1 protein normalized to total protein. (C) EWS-FLI1 protein levels upon candidate knockdown. Each dot represents 3xflag-EWS-FLI1 protein and is normalized to its total protein for each single well. 3xflag-EWS-FLI1 levels upon USP19 knockdown are indicated with larger red dots and for EWS-FLI1 knockdown in orange. (D) Expression levels of USP19 in indicated cell lines and primary samples were analyzed by western blot. The arrows indicate specific USP19 isoforms, asterix marks unspecific band. (E) mRNA expression of USP19 was determined by quantitative RT-PCR from same cells and normalized to GAPDH.

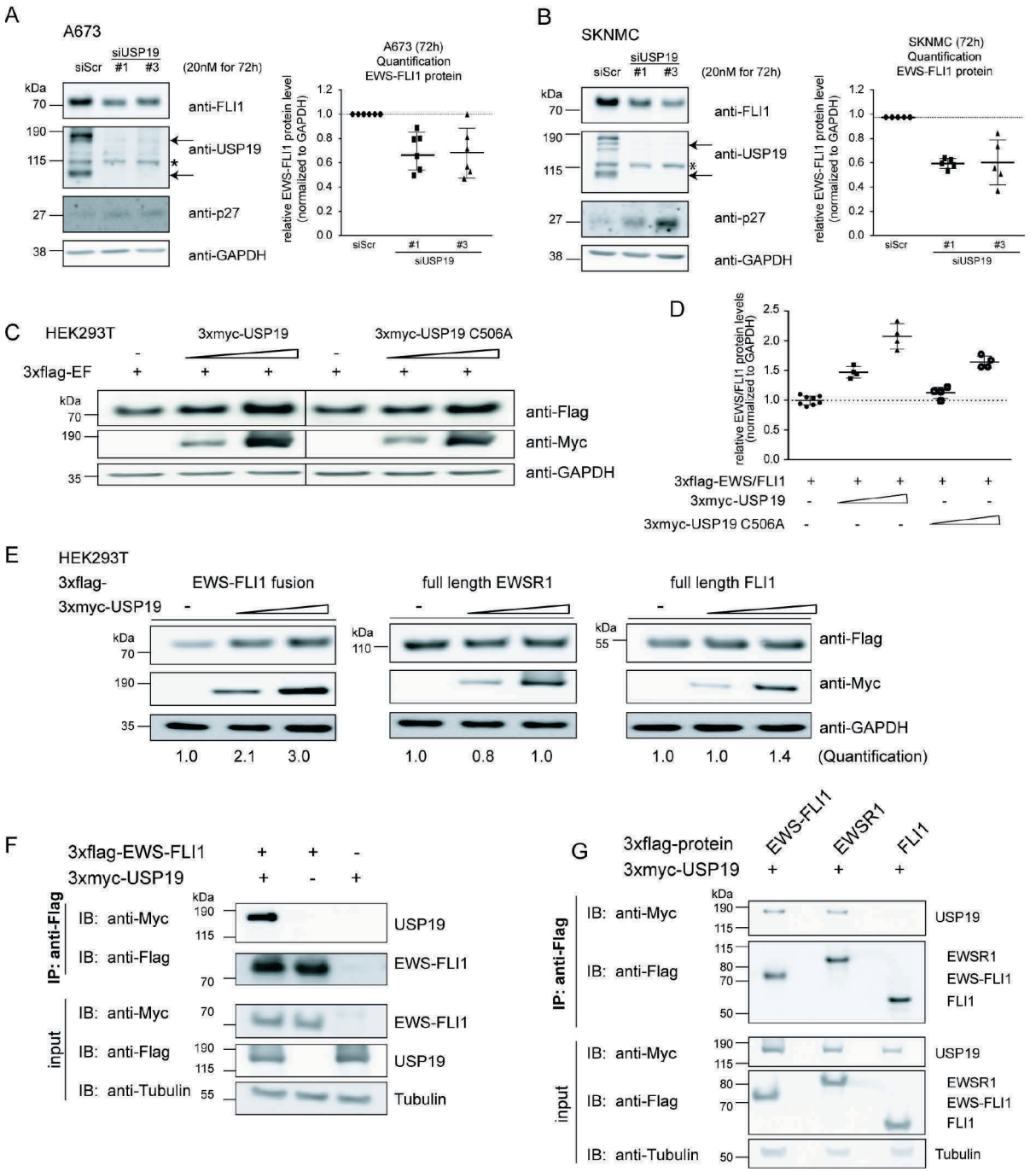

Fig. 2: USP19 specifically modulates EWS-FLI1 protein levels and activity. (A,B) Immunoblot analysis (IB) of USP19 depleted cells. (A,B) A673 and SKNMC cells were transiently transfected with 20nM siRNAs for 72h as indicated. Lysates were subjected to western blot analysis and analyzed by anti-FLI1 and anti-USP19 antibodies. Arrows indicate specific USP19 isoforms, asterix marks an unspecific band. Besides, quantification of EWS-FLI1 proteins levels (n=5-6, error bars as SD). (C) Active USP19 stabilizes EWS-FLI1 protein. 3xflag-EWS-FLI1 was transiently co-expressed with a control vector or increasing levels (ratios 3xflag-EWS-FLI1 to 3xmyc-USP19 1:2 and 1:4) of wild-type or catalytically inactive 3xmyc-USP19 for 48h in HEK293T cells. Lysates were analyzed by western blotting using anti-flag and anti-myc antibodies. (D) Quantification of 3xflag-EWS-FLI1 protein levels of

(C) with n=8 for control and n=4 for others, error bars as SD. (E) USP19 overexpression stabilizes specifically EWS-FLI1. 3xflag-EWS-FLI1, 3xflag-EWSR1 and 3xflag-FLI1 were transiently co-expressed with increasing concentrations (ratios 3xflag-protein to 3xmyc-USP19 1:2 and 1:4) of active 3xmyc-USP19 for 48h in HEK293T cells. Lysates were analyzed by western blotting using anti-flag and anti-myc antibodies. Numbers below represent densitometrically quantified flag tagged protein over loading control GAPDH of a representative experiment. (F) EWS-FLI1 interacts with USP19. 3xflag-EWS-FLI1 and 3xmyc-USP19 were co-expressed in HEK293T cells for 48h. After co-immunoprecipitation, lysates were analyzed by western blotting as indicated. (G) EWSR1 also interacts with USP19. 3xflag-EWS-FLI1, 3xflag-EWSR1 or 3xflag-FLI1 were co-expressed with 3xmyc-USP19 in HEK293 cells for 48h. After co-immunoprecipitation, lysates were analyzed by western blotting as indicated.

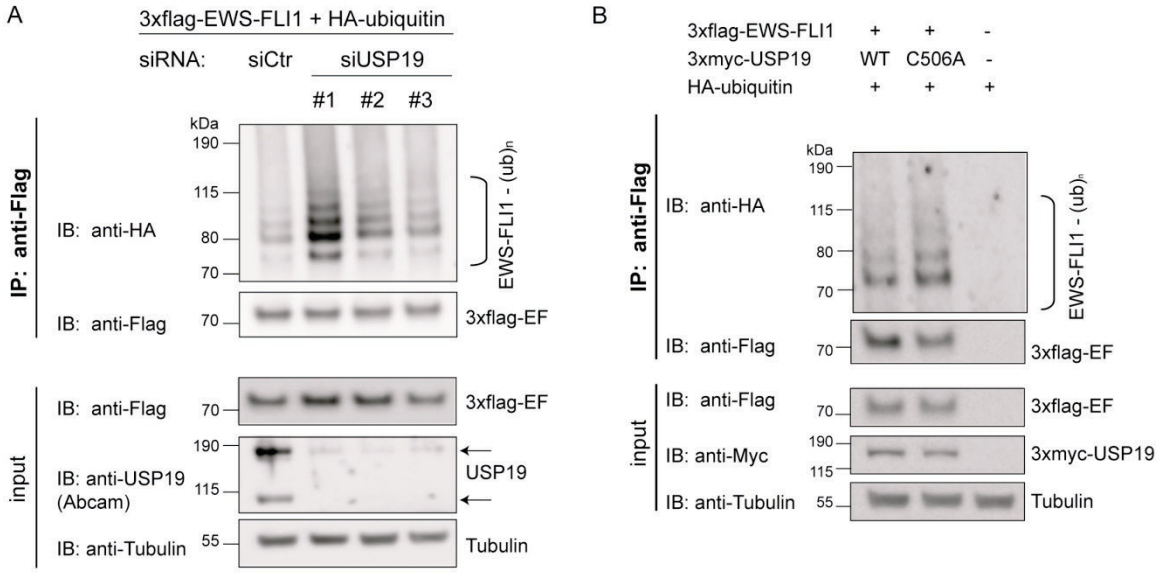

Fig. 3: EWS-FLI1 ubiquitination is modulated by USP19. (A) USP19 depletion increases EWS-FLI1 ubiquitination. A673 cells were transiently incubated with three different siRNAs against USP19 or a control siRNA for 24h followed by co-expression of 3xflag-EWS-FLI1 and HA-ubiquitin for 48h. Ubiquitination of EWS-FLI1 was analyzed by western blot analysis using anti-HA antibody. (B) EWS-FLI1 ubiquitination is decreased upon active USP19 expression. 3xflag-EWS-FLI1 and HA-ubiquitin were co-expressed with either wild type or a catalytically inactive USP19 for 48h in A673 cells. After immunoprecipitation of 3xflag-EWS-FLI1, ubiquitination was determined by anti-HA antibody.

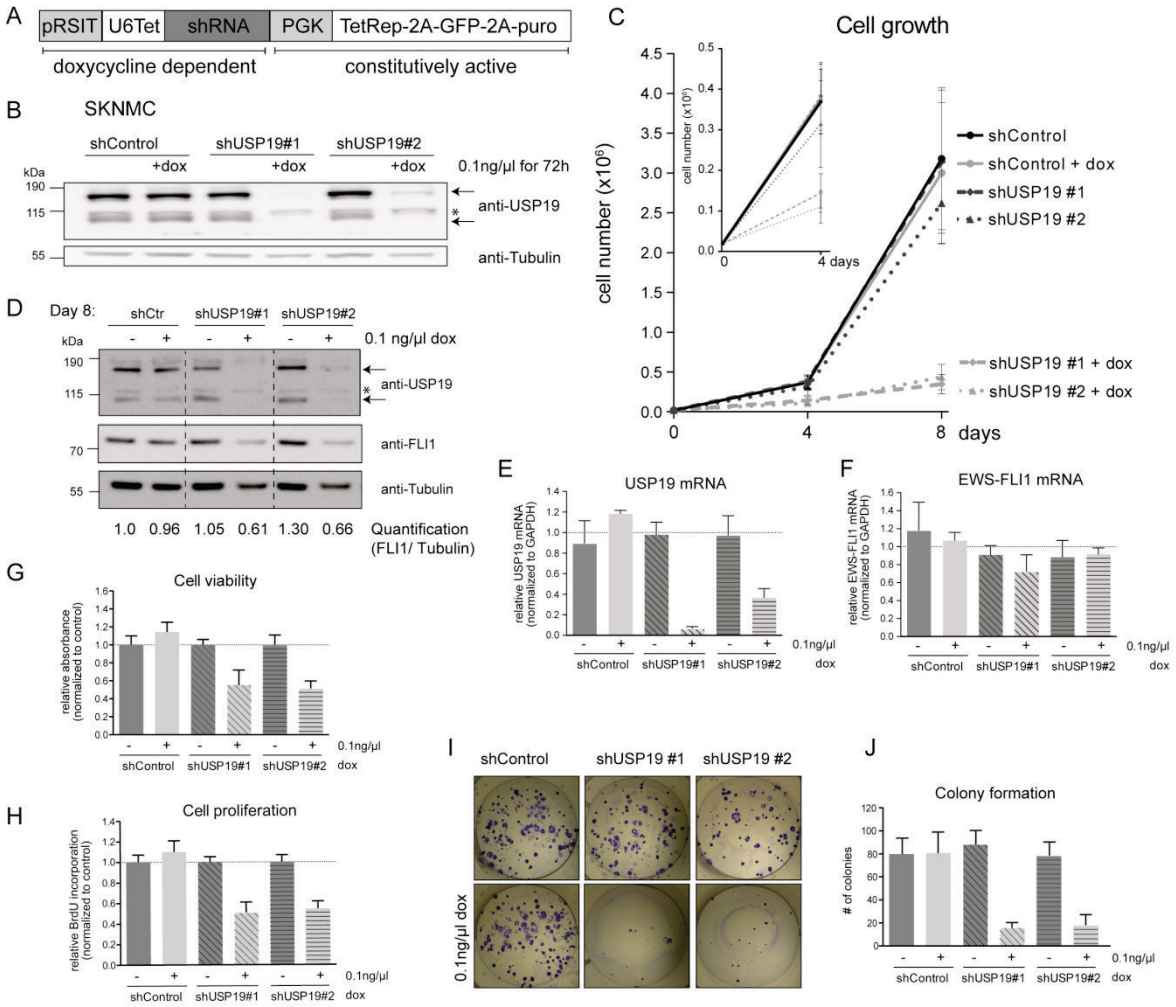

Fig. 4: Depletion of USP19 affects Ewing sarcoma cell growth *in vitro*. (A) Schematic illustrating shRNA vector for stable transduction. The constitutively active part includes selection marker and a tetracycline repressive element. The doxycycline dependent part includes a tetracycline dependent promoter and the shRNA sequence. (B) SKNMC cells were stably transduced with two different shRNA sequences targeting USP19 and a control sequence. After incubation with 0.1ng/µl doxycycline for 72h, USP19 protein levels were analyzed by western blotting using anti-USP19 antibody. Arrows indicate specific bands, asterix marks unspecific band. (C) USP19 depletion affects cell growth. Knockdown of USP19 was induced in $2x10^4$ SKNMC cells as indicated and cells were counted after 4 (smaller graph) and 8 days (larger graph). Total cell numbers were plotted from three independent experiments, error bars as SD. (D) USP19 depletion reduces EWS-FLI1 protein levels. 8 day lysates from one independent experiment of (C) were subjected to western blotting and analyzed by anti-FLI1 and anti-USP19 antibodies. Numbers represent densitometrically quantified bands of EWS-FLI1 over loading control tubulin. (E-F) USP19 depletion reduces USP19 mRNA, but only marginally affect EWS-FLI1 mRNA. All three samples of (C) at 8 days were analyzed by quantitative RT-PCR for USP19 and EWS-FLI1 mRNA expression. Numbers were normalized to GAPDH and related to shControl without doxycycline treatment. (G-J) Depletion of USP19 affects Ewing cell metabolic activity, proliferation and long-term cell survival. Doxycyline induced and non-induced

SKNMC cells were incubated with WST1 reagent after 96h (G), assessed for incorporation of BrdU after 96h (H), and colony formation after 14 days (I). Values are shown relative to untreated shControl cells (n=3, error bars as SD). (J) Quantification of colonies from (I).

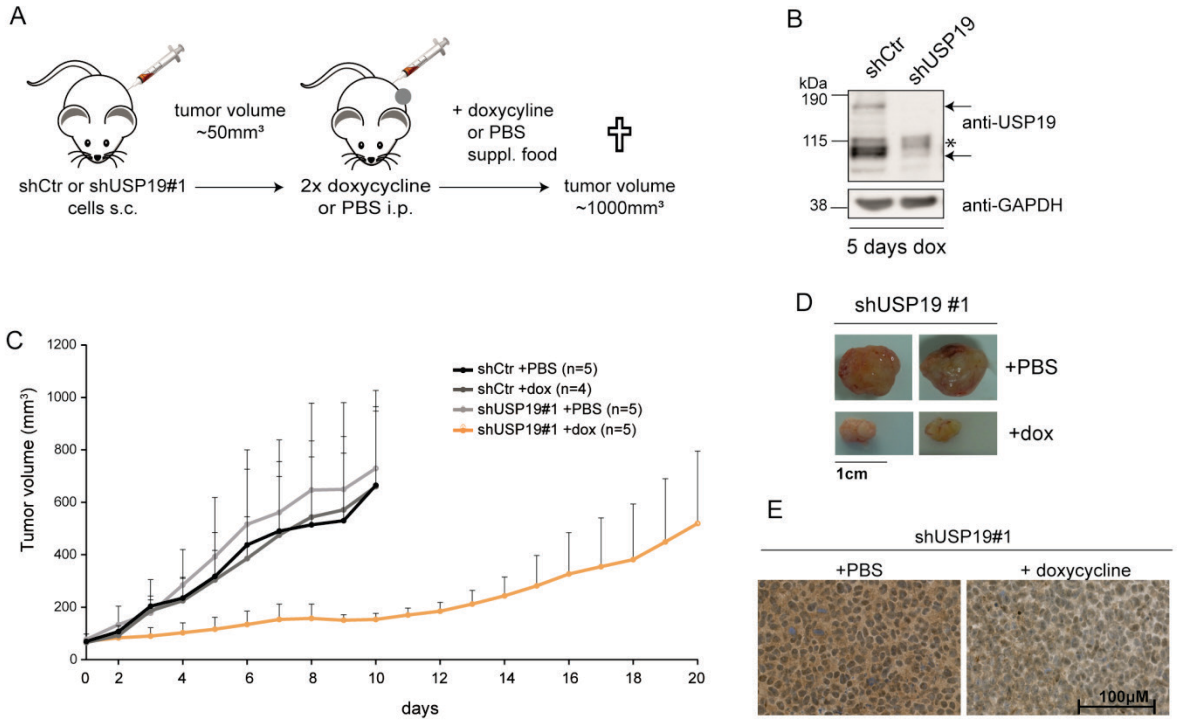

Fig. 5: Depletion of USP19 delays tumor growth *in vivo*. (A) Scheme of xenograft experiments using SKNMC inducible cell lines. (B) Doxycyline induces USP19 knockdown *in vivo*. Two mice with engrafted tumors of ~200mm^3 (shCtr and shUSP19#1) were treated for five days with doxycyline. Tumor lysates were analyzed by western blotting with anit-USP19. (C) Tumor growth rate of indicated cell lines and treatment of subcutaneously injected SKNMC cells, error bars as SD. (D) Tumors of two representative mice transplanted with SKNMC shUSP19#1 cells and treated with doxycyline or PBS. (E) Immunohistochemistry analysis of sections from tumor with SKNMC shUSP19#1 cells and treated with doxycyline or PBS using an USP19 antibody.

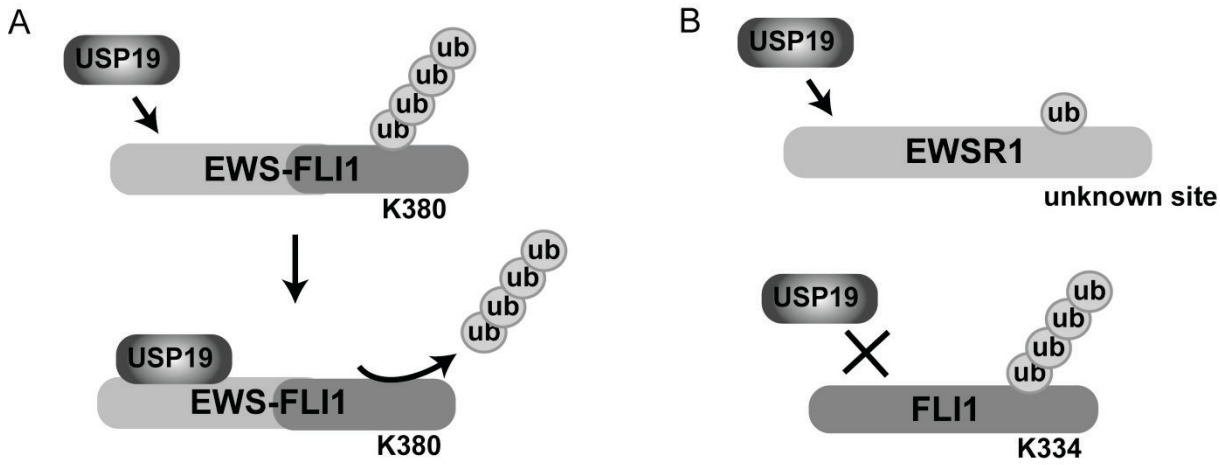

Fig. 6: USP19 selectively stabilizes EWS-FLI1. (A) USP19 binds to the EWS-FLI1 fusion protein which is further deubiquitinated most possibly at the K380 lysine residue in the C-terminal part. (B) USP19 also binds to the stable EWSR1 full length protein at an unknown site resulting in deubiquitination of non-proteolytic ubiquitin(s) rather than in destabilization. As USP19 does not bind to full length FLI1, its polyubiquitination remains.

Supplementary figures

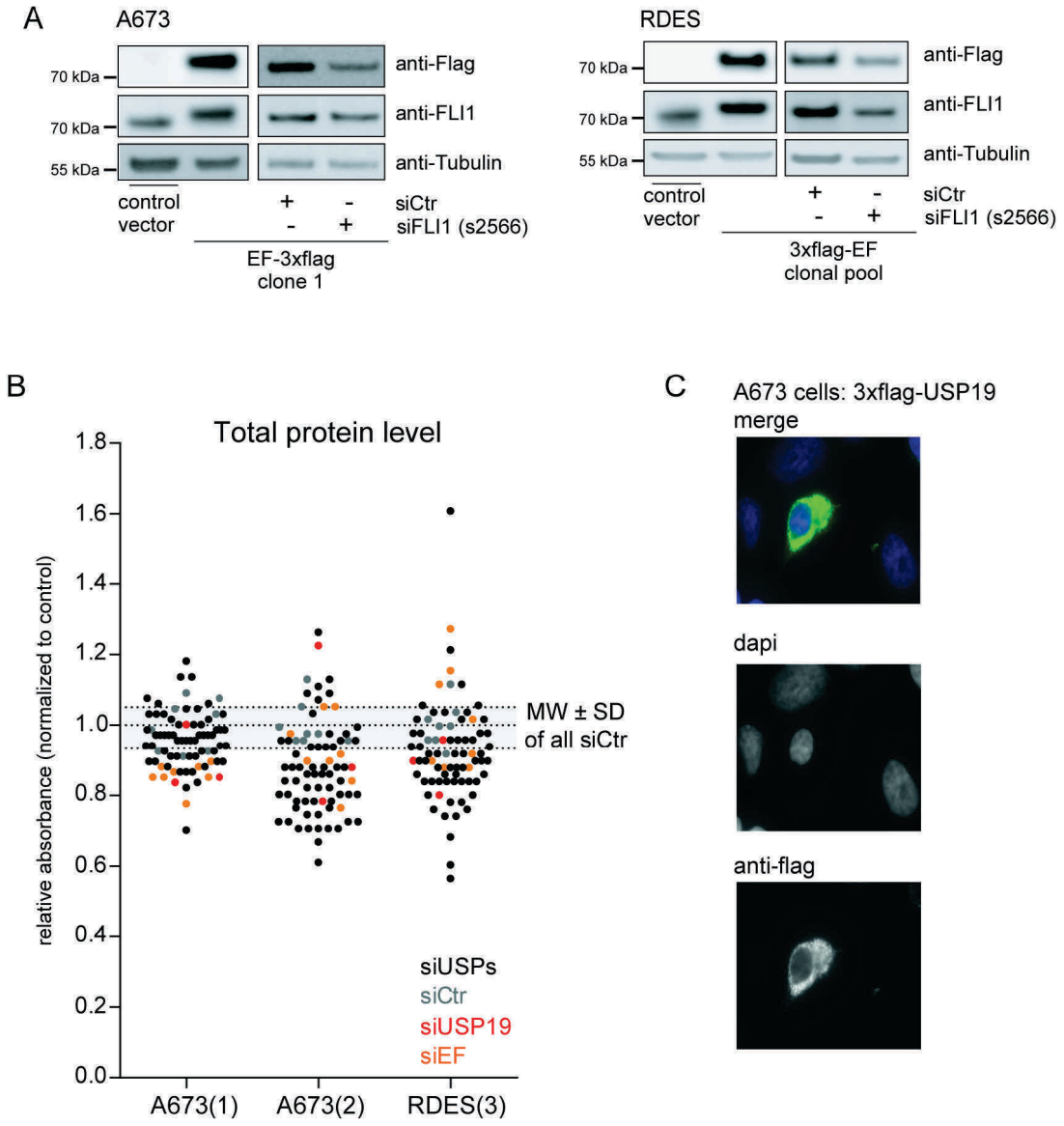

Supplementary Fig. 1: (A) Western blot analysis of lysates from A673 and RDES cell lines stably expressing 3xflag-EWS-FLI1 with anti-FLI1 and anti-Flag antibodies. Both clonal cell lines were transiently transfected with control siRNA or siRNA targeting the FLI1 part in the fusion protein. (B) Total protein levels upon candidate knockdown. Each dot represents total protein level for normalization of Fig. 1C. Protein levels upon USP19 knockdown are indicated with red dots and for EWS-FLI1 knockdown in orange. (C) USP19 is localized in the cytosol. 3xflag-USP19 was transiently expressed for 48h in A673 cells. Cells were fixed, stained with anti-Flag antibody and analyzed by fluorescence microscopy (63x magnification).

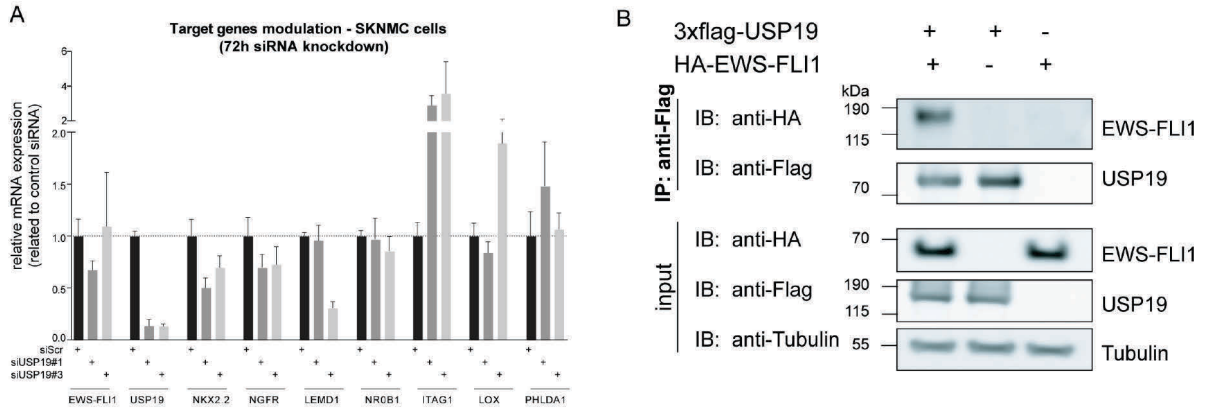

Supplementary Fig. 2: (A) USP19 knockdown modulates a subset of EWS-FLI1 target genes. SKNMC cells were transiently transfected with 20nM siRNAs for 72h as indicated and expression of indicated target genes was analyzed by quantitative RT-PCR and related to control siRNA for each gene (n=6, geometric mean, error bars as 95% confidence interval). (B) USP19 interacts with EWS-FLI1. 3xflag-USP19 and HA-EWS-FLI1 were co-expressed in HEK293T cells for 48h. After co-immunoprecipitation, lysates were analyzed by western blotting as indicated.

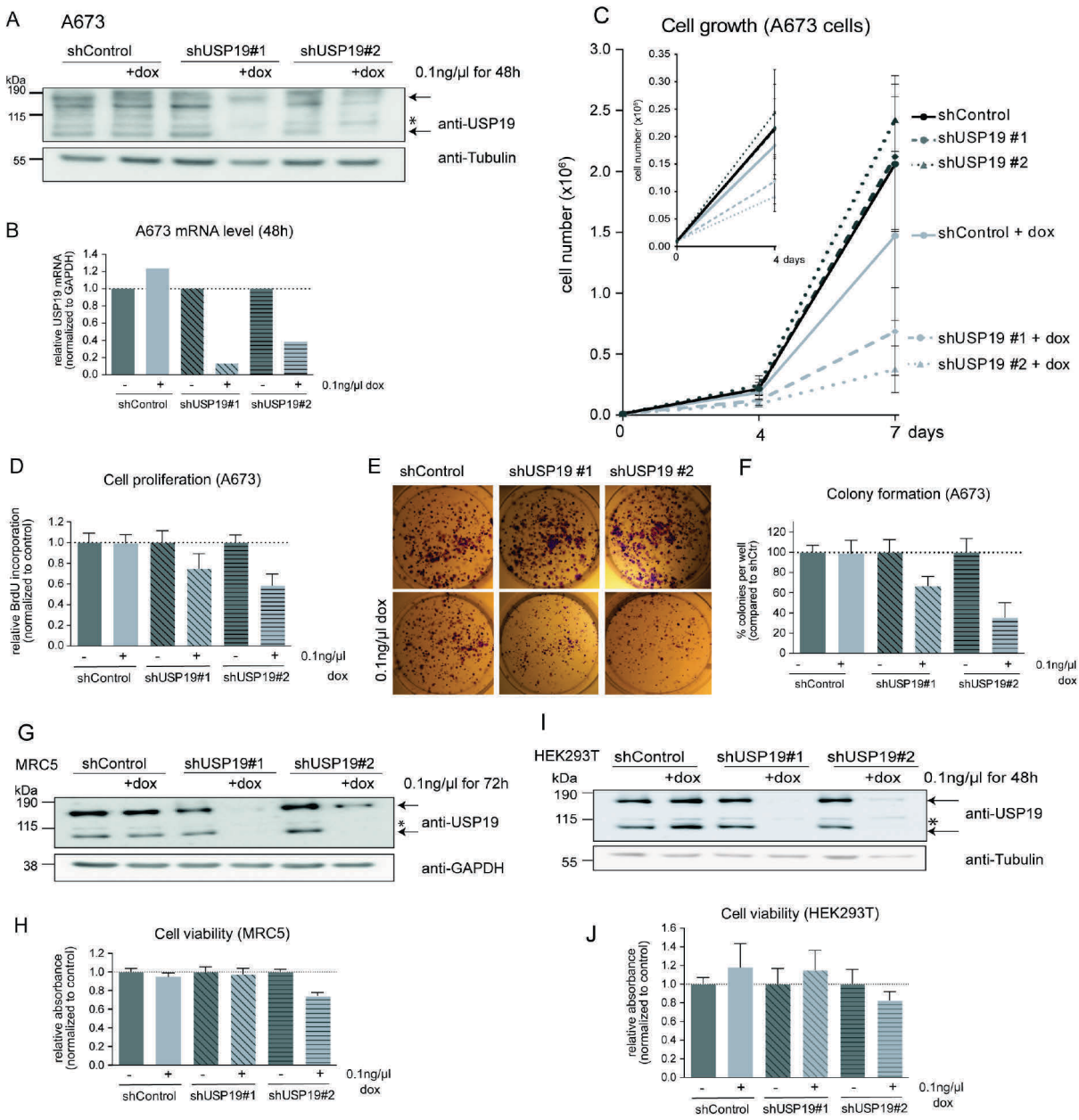

Supplementary Fig. 3: (A,B) A673 cells were stably transduced with two different shRNA sequences targeting USP19 and a control sequence. After incubation with 0.1ng/µl doxycycline for 72h, (A) USP19 protein levels were analyzed by western blotting using anti-USP19 antibody, arrows indicate specific bands, asterix marks unspecific band. (B) mRNA levels were analyzed by quantitative RT-PCR and represented as induced over not-induced ratios for individual each cell line. (C) USP19 depletion affects cell growth. Knockdown of USP19 was induced in $1x10^4$ A673 cells as indicated and cells were counted after 4 (smaller graph) and 7 days (larger graph). Total cell numbers were plotted from three independent experiments, error bars as SD. (D-F) Depletion of USP19 affects Ewing cell proliferation and long-term cell survival. Doxycyline induced and non-induced A673 cells were assessed for incorporation of BrdU after 96h (D) and colony formation after 12 days (E-F). Values are represented as induced over not-induced ratios for each cell line (n=3, error bars as SD). (G-J) USP19 depletion has limited to no effect in unrelated non-tumorigenic cell lines. (G) MRC5 or (I) HEK293T

cells were transduced with two different shRNA sequences targeting USP19 and a control sequence and incubated with 0.1ng/µl doxycycline for 72h. USP19 protein levels were assessed by western blotting using anti-USP19 antibody, arrows indicate specific bands, asterix marks unspecific band. Doxycyline induced and non-induced (H) MRC5 or (J) HEK293T cells were assessed for cell viability by WST1 after 96h (MCR5 cells n=3 with 6 biological replicates each and for HEK293T cells two independent experiments with n=6 biological replicates each).

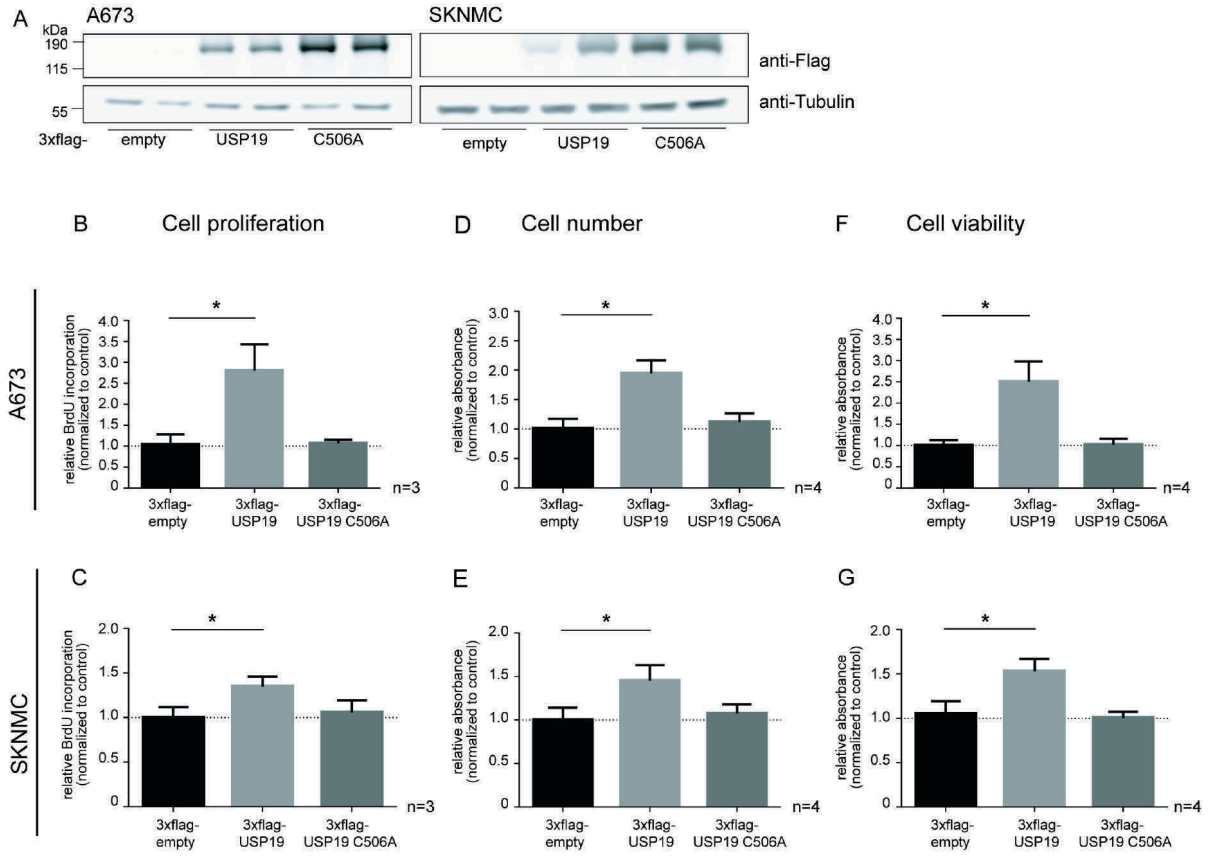

Supplementary Fig. 4: (A) A673 and SKNMC were transiently transfected with control, 3xflag-USP19 or 3xflag-USP19 C506A mutant. Protein expression was analyzed by western blotting using anti-Flag antibody. Cells were analyzed for cell proliferation by BrdU incorporation (B-C), for cell number by crystal violet staining (D-E) and for cell viability by WST1 incubation (F-G) with n=3 or 4 independent experiments, error bars as SD.

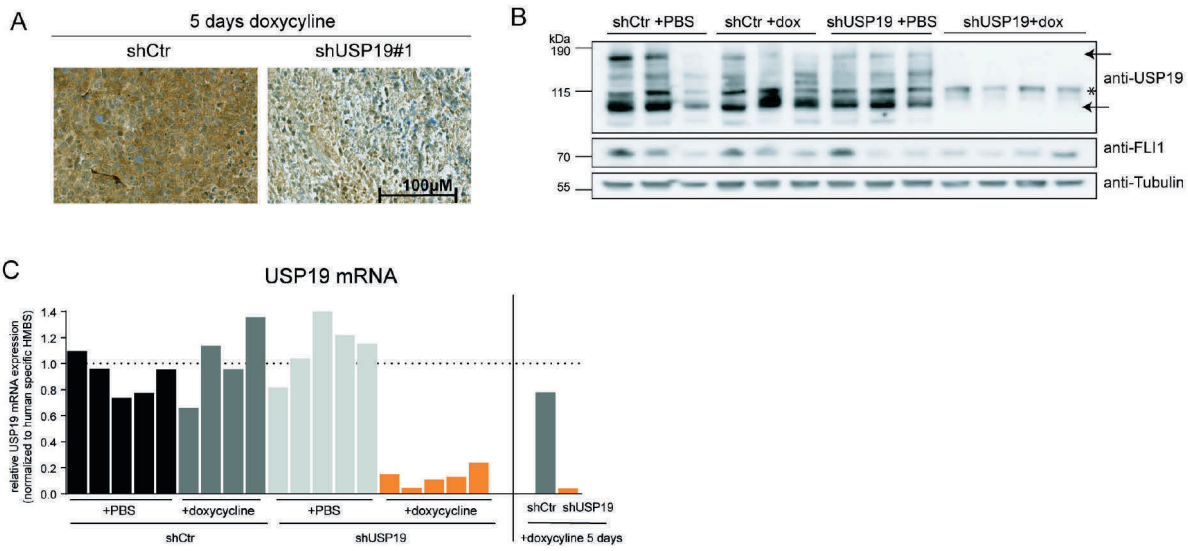

Supplementary Fig. 5: Depletion of USP19 delays tumor growth *in vivo*. (A) Immunohistochemistry analysis of section from tumor in Fig. 5B using an USP19 antibody. (B-C) Tumors lysates were analyzed by (B) western blotting with anti-USP19, anti-FLI1, and anti-p27 antibodies, arrows indicate specific bands, asterix marks unspecific band. (C) mRNA expression was determined by quantitative RT-PCR normalized to HMBS.

Supplementary tables

Supplementary table 1: Publicly available gene expression data sets

Sample	# of files	Affymetrix chip	GEO accession	Authors
Cell lines:				
SKNMC cells	1	Hg-U133A	GSE1824	Staege et al. 2004
A673 cells (siRNA control)	2	Hg-U133A	GSE7007	Prieur et al. 2004
A673 cells (luciferase knockdown controls)	4	Hg-U133A	GSE4565	Smith et al. 2006
A673 cells (DMSO controls)	17	Hg-U133A	GSE6930	Stegmaier et al. 2007
EW24, SKNMC cells (shRNA control)	4	Hg-U133A	GSE7007	Tirode et al. 2007
A673, RD ES cells	6	Hg-U133p2	https://cabig.nci.nih.gov/caArray_GSKdata/	Greshock et al. 2010
Different Ewing cell lines	10	Hg-U133p2	GSE17679	Savola et al. 2011
Different Ewing cell lines	5	Hg-U133p2	GSE36139	Barretina et al. 2012
Tumor samples:				
Tumor samples	5	Hg-U133A	GSE1825	Staege et al. 2004
Tumor samples	27	Hg-U133A	GSE7007	Tirode et al. 2007
Tumor samples	35	Hg-U133p2	GSE12102	Scotlandi et al. 2009
Tumor samples	90	Hg-U133p2	GSE17679	Savola et al. 2011

Supplementary table 2: SiRNA library for screening

		Silencer® Select siRNA:		
No.	**Gene name**	**#1**	**#2**	**#3**
1	USP1: ubiquitin specific peptidase 1	s14724	s14725	s14723
2	USP10: ubiquitin specific peptidase 10	s17367	s17368	s17369
3	USP11: ubiquitin specific peptidase 11	s15741	s15739	s15740
4	USP12: ubiquitin specific peptidase 12	s47597	s47595	s47596
5	USP13: ubiquitin specific peptidase 13	s17130	s17131	s17129
6	USP14: ubiquitin specific peptidase 14	s17358	s17359	s17360
7	USP15: ubiquitin specific peptidase 15	s19338	s19339	s19340
8	USP16: ubiquitin specific peptidase 16	s20808	s20810	s20809
9	USP19: ubiquitin specific peptidase 19	s21339	s21340	s21341
10	USP20: ubiquitin specific peptidase 20	s21336	s21337	s21338
11	USP21: ubiquitin specific peptidase 21	s25689	s25690	s223719
12	USP22: ubiquitin specific peptidase 22	s23566	s23568	s230744
13	USP3: ubiquitin specific peptidase 3	s19343	s19341	s19342
14	USP33: ubiquitin specific peptidase 33	s22873	s22874	s22872
15	USP4: ubiquitin specific peptidase 4	s14681	s14683	s14682
16	USP46: ubiquitin specific peptidase 46	s35034	s35035	s35036
17	USP5: ubiquitin specific peptidase 5	s15595	s15596	s15597
18	USP6: ubiquitin specific peptidase 6	s17363	s17361	s17362
19	USP7: ubiquitin specific peptidase 7	s15439	s15440	s15441
20	USP8: Ubiquitin specific peptidase 8	s17372	s17370	s17371
21	USP9X: ubiquitin specific peptidase 9, X-linked	s15743	s15742	s15744
pos. control	EWS (siRNAs only for region exons 1-7)	s4887	s4888	
pos. control	EWS/Fli1	s5266	s5268	
pos. control	EWS/FLI1 breakpoint specific siRNA (Prieur et al. 2004)	5′ GGC AGC AGA ACC CUU CUU A-dCdG 3'		
neg. control	Silencer® Select Negative Control No. 1 siRNA			
neg. control	Silencer® Select Negative Control No. 2 siRNA			
neg. control	Silencer® Negative Control No. 3 siRNA			
neg. control	Silencer® Negative Control No. 4 siRNA			
transf. Control	Silencer® KIF11 (Eg5) siRNA (Human, Mouse, Rat)			

7. Discussion

7.1. Targeting the ubiquitin system – current state and future opportunities

Targeting the ubiquitin system for cancer therapy has a variety of advantages over other regulatory pathways: It is a highly conserved system which is present in every cell of the human body including cancer cells whether they are proliferative or in a quiescent state. Further, drugs specifically targeting components of the ubiquitin system have the potential to not only inhibit the activity of certain oncogenic regulatory proteins, but they can also activate protein function by manipulating their turnover as shown for lenalidomide and derivatives (499, 500). Currently, our understanding of the UPS's critical regulation in human diseases including cancer has generated high interest for the development of small molecules targeting critical steps of the pathway including ubiquitin attachment and removal. As drug developing is at the start of its future potential, tumor resistances have barely been observed in contrast to kinase inhibitors providing a whole new branch of possible targeting points (reviewed in (461)).

After the success of Bortezomib in multiple myeloma, next generation proteasome inhibitors are in the pipeline promising higher efficacy and less toxicity (437, 470, 501). The ubiquitin activation inhibitor MLN4924 demonstrated that also E3 subclasses can be inhibited efficiently and entered clinical trials promising even more specificity upon targeting yet smaller subclasses (440, 441, 502). Besides these two examples, which other strategies have the potential as first line cancer treatment, in which tumor types would they be most relevant for treatment and which approach could be of significance for Ewing sarcoma?

7.1.1. The developing field of ubiquitin drug targets

Inhibition of the activity of oncogenic proteins has long been in the center of cancer research. Kinase inhibitors are one of the most clinically relevant classes of compounds which target protein phosphorylation. Consequently, their effect is mediated by blockage of protein activity and subsequent disruption of signaling cascades. Kinase inhibitors most commonly target the ATP binding or small hydrophobic pocket of proteins or induce conformational changes due to allosteric inhibition (reviewed in (503)). The most prominent example is again the tyrosine kinase inhibitor imatinib mesylate (Gleevec) used in BCR/ABL fusion positive chronic myelogenous leukemia (474). Around 16 kinase inhibitors are approved for treatment while more than 150 compounds are in the pipeline in clinical trials of various phases (503). Like phosphorylation, the process of ubiquitination is implicated in nearly all cellular aspects. Currently, clinically relevant compounds are limited to the use of Bortezomib and MLN4924 and only few additional inhibitors which specifically target ubiquitin based pathways entered clinical trials. The process of ubiquitination is more complex than phosphorylation as it involves different ubiquitin linked chains and a high complexity of components as well as similarly structured ubiquitin-like modifiers. Attempts to identify relevant compounds from chemical libraries mostly focus on modulating E3 ligase or DUB activity as they are the most specific target points (464,

503). Inhibition of E3 ligase activity or disruption of their ubiquitin transfer capacity is rather challenging and no general chemical screening approach has yet been established. Therefore, most E3 ligase modulators are ligase antagonists which disrupt substrate binding and induce conformational changes (464). The most relevant example presents the disruption of MDM2 and p53 by the small molecule Nutlin-3 (450).

The selective degradation of especially TFs represents the most specific way to eliminate oncogenic proteins which are themselves considered “undruggable”. *A posteriori* identified, this strategy is adopted by thalidomide and its derivatives. This well known compound displays high efficacy in multiple myeloma and other B cell neoplasms. Thalidomide is binding to CRBN which is a substrate receptor of CUL4A-DDB1 complexes (504). In multiple myeloma, thalidomide occupies the substrate binding site of CRBN leading to recruitment of IKZF1 and IKZF3. Both essential IKAROS TFs are ubiquitinated and subsequently degraded explaining the response pathway in multiple myeloma patients (500, 505). However, it was also suggested that thalidomide has dual activity as it blocks MEIS2 binding to CRL4-CRBN complexes and instead promotes IKZF1 and IKZF3 recruitment (505). Most interestingly, the drug showed high efficiency in other diseases such as the myelodysplastic syndrome where it operates through recruitment of CK1α to CRL4-CRBN to induce TF degradation (499).

Both DUB inhibitors and antagonists are currently in the research focus. Few compounds have been developed and tested for efficiency *in vitro* and *in vivo* as the USP1 inhibitor SJB2-043 in acute myelogenous leukemia (506), the USP7 inhibitor HBX 19,818 in multiple myeloma (455) or the USP14 inhibitor b-AP15 in various solid tumors and leukemia (459). As DUBs harbor enzymatic activity and provide therefore a direct targeting point, the number of inhibitory compounds most probably will increase considerably. Unlike most E3 ligases, DUBs do not build protein complexes and provide with about 100 family members are rather overseeable group of targets.

7.1.2. Chemical inducers of protein degradation

A variety of other chemical approaches have been developed over the years to investigate and dissect protein turnover. Targeting protein levels instead of protein activity is a very recent approach for all proteins which are considered “undruggable” due to their lack of enzymatic activity (507).

The hydrophobic tagging technology for Halo-tag constructs was developed to precisely study effects of protein stabilization and destabilization. For this assay, the Halo-tag with an additional hydrophobic linker was fused to the protein of interest and expressed in target cells. Ligand mediated degradation was achieved using the small molecule HyT13 which was directly binding to the hydrophobic area of the Halo-tag and induced degradation. Destabilization was shown for a variety of proteins both *in vitro* and *in vivo*. Halo-tagged HRAS with an activating mutation highly induced tumor growth in mouse xenografts, whereas treatment with HyT13 significantly reduced the tumor volume (508). In contrast, Halo tagged proteins could also be stabilized by the small molecule HALTS1. It inhibits the interaction

of the Halo-tag to Hsp70 and thereby hinders ubiquitination and degradation (509). This technique provides a great platform to investigate specific protein turnover without affecting other proteins or using unspecific compounds (Fig. 13A). Therefore, Halo-tag fusions would allow depleting EWS/FLI1 and other oncogenic TFs faster than applying RNAi. Using the CRISPR technology to introduce the Halo-tag at the endogenous EWS/FLI1 levels enables selective manipulation of fusion protein levels. This approach would allow more accurate investigation of stabilized EWS/FLI1 protein levels than the fusion protein exchange system we have used in this work.

Another very interesting approach of small chemical inducers represents proteolysis targeting chimeras (Protacs). Mechanistically, one domain contains a peptide which is recognized by substrate receptors of SCF complexes or other E3 ligases due to being abundant, constitutively active and harboring a characterized binding site. The initial strategy used the SCF-βTRCP E3 ligases for targeted degradation (Fig. 13B).The other domain contains a sequence to which the target protein is known to bind. To this end, non-SCF substrates can now be ubiquitinated and degraded via this pathway (510). An important challenge to modify Protacs was based on the fact that they were not cell penetrating *in vivo.* To prove that the principle is working, Protacs have been introduced to cells via microinjection. Visualization by GFP tagged estrogen receptors revealed that more than 70% of cells had a minimal, partial, or complete disappearance of the protein by target specific Protacs after 1h, an effect which was abrogated upon proteasome inhibition (511). Later, soluble Protacs with the degron motif of the hypoxia inducible factor-1α (HIF1α) were used to degrade androgen and estrogen receptors. This subsequently resulted in reduced proliferation by G1 arrest *in vitro* indicating that it might be a possible application *in vivo* to eliminate disease promoting proteins such as EWS/FLI1 (512, 513). Successful targeting of the fusion BCR/ABL has been reported. The small molecule Protacs were consisting of the E3 ligases cereblon (CRBN) or Van-Hippel-Lindau factor (VHL) and were linked to different target tyrosine kinase inhibitor ligands. Combinations induced BCR/ABL degradation to different extents (514). The best Protac molecule induced a selective decrease in viability in the BCR-ABL driven cell line K562. This strategy should also be applicable to EWS/FLI1. However, it may be more challenging to identify appropriate binding ligands as EWS/FLI1 displays no enzymatic activity. Nevertheless, the Protac technology is fast developing in terms of specificity, cell permeability and efficacy towards clinical approaches (515).

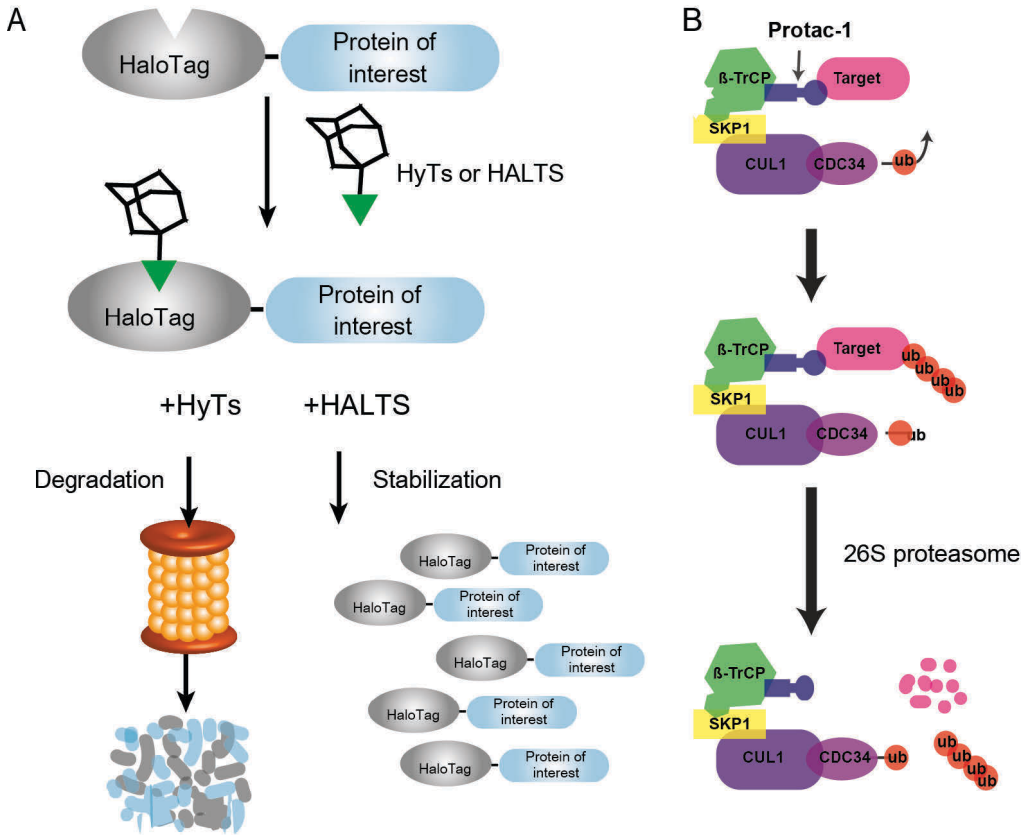

Fig. 13: Strategies to chemically induce protein degradation. (A) Turnover can be studied by fusions between substrates and a Halo-tag. Incubation with HyT or HALTS small molecule compounds results in binding and either degradation or stabilization of the tag and subsequently the protein of interest (modified after (508, 509)). (B) Protacs are small linker molecules to mediate interaction between a known E3 ligase complex and the target substrate. Upon binding, ubiquitins are transferred to the target and degradation is induced (modified after (510)).

7.1.3. Therapy induced targeting – PML/RARα as a model for EWS/FLI1

Most cancer subtypes are driven by a deregulated cancer genome with various genetic backgrounds which can be altered within tumor growth and relapse due to the existence and outgrowth of multiple subclones (14, 19). Instead, self-renewal and survival capacities of tumors with fusion proteins most commonly show continuous dependency on the chromosomal rearrangements (516). As an example, the combination treatment of retinoic acid and arsenic trioxide in fusion positive APL has an astonishing cure rate of 90% (497). PML/RARα degradation is mediated by two independent mechanisms: arsenic trioxide targets the PML moiety in nuclear bodies for sumoylation which leads to RNF4 dependent ubiquitination and degradation by the proteasome (Fig. 14A). Moreover, retinoic acid triggers a conformational change, phosphorylation of the RARα part and recruitment of the proteasome (Fig. 14A). Both events allow therapy induced degradation of the fusion protein (reviewed by (516)).

In comparison, kinase inhibition is used in the treatment of chronic myelogenous leukemia. Imatinib mesylate blocks the ATP binding site of the ABL kinase and therefore inhibits its activity but retains the fusion protein (474). Induced blockage of fusion protein activity instead of protein degradation requires

continuous drug administration and can only be discontinued if minimal residual disease detection is negative for a longer time period (517). The treatments in APL and CML pursue two different strategies: inhibition of protein activity and selected protein degradation.

However, both leukemia display treatment related resistances and relapse. Resistance to arsenic trioxide and/or retinoic acid of APL patients is most commonly associated with mutations in the PML/RARα fusion protein. Two mutation hotspots have been identified in the B2 domain of the PML part and in the LBD domain of RARα (518-520). If the fusion protein is mutated in the PML B2 domain, protein sumoylation is abrogated and subsequently arsenic acid induced degradation fails (519, 520). At least *in vitro*, higher doses of arsenic trioxide have been shown to partly overcome this resistance (519). Mutations in the RARα domain resulted in APL relapse, but a secondary remission using the standard combination can be achieved. In contrast, this is not possible for patients harboring mutations in each of the hotspots simultaneously (520). To overcome resistance, various compound screens are ongoing. It has been recently shown that the small molecule LG362B inhibited proliferation and induced apoptosis *in vitro* and *in vivo* which effect was driven by PML/RARα degradation (521).

It is to be hoped that a similar degradation can be developed to treat Ewing sarcoma in the future. According to our studies, EWS/FLI1 protein depletion should be favored. As a first step, we characterized in this thesis the mechanism regulating EWS/FLI1 turnover.

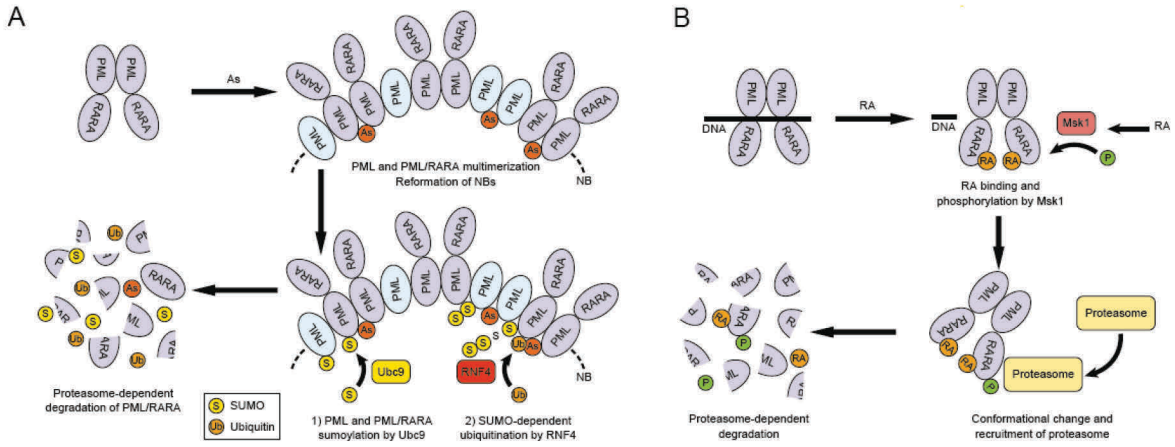

Fig. 14: Therapy induced degradation of PML/RARα fusion protein (516). (A) Arsenic trioxide targets the PML moiety of PML/RARα which is subsequently sumoylated by the Ubc9 conjugation enzyme and then polyubiquitinated by the SUMO-dependent E3 ligase RNF4 resulting in PML/RARα degradation. (B) Retinoic acid docks to the ligand-binding domain of the RARα moiety and triggers a conformational change. This allows recruitment of the proteasome and degradation.

7.2. EWS/FLI1 stability and turnover

Attachment of ubiquitin(s) to a substrate protein triggers a variety of outcomes including degradation which are dependent on the attachment site, ubiquitin chain length and linkage to each other. Over the years, several different technologies have been developed to decipher and understand ubiquitin mediated processes (reviewed by (522)). Research has focused on identifying ubiquitination enzymes of substrates and on discovering novel substrates regulated by the proteolytic machinery. This was mainly achieved by affinity purification combined with mass spectrometry or protein stability profiling. Several of these methods have been adapted here to study the process of EWS/FLI1 ubiquitination and turnover.

In order to better understand EWS/FLI1 fusion protein turnover, we first analyzed the half life and proteasomal regulation. In contrast to previous suggestions (235), we observed that proteasomal degradation of EWS/FLI1 is clearly favored over the lysosomal pathway under steady state conditions. As most potent transcriptions factors, EWS/FLI1 has a fast turnover which is mediated by one single lysine residue in the DNA-binding domain.

7.2.1. Global Protein Stability profiling to dissect proteolytic turnover

The Global Protein Stability approach (GPS) was initially established to identify novel proteasomal substrates (523, 524). In brief, a vector encoding for one transcript of a DsRed-IRES-EGFP is transiently expressed in target cells and allows analyzing protein turnover by flow cytometry. Integration of open reading frame (ORF) libraries C-terminal of the EGFP tag enables high throughput screenings for stability. In the first screening, cells with a stable integrated ORF library were incubated with or without the proteasomal inhibitor MG-132 and fractionated by flow cytometry according to their EGFP/DsRed ratio. Sequencing of all separate fractions allowed the identification of proteins with a shift in their turnover. This most elegant approach was later used to identify substrates of the different cullins by treating GPS cells with the NEDD8-activating enzyme inhibitor MLN4924 (325). In terms of high throughput screenings, GPS alone or in combination with drug treatments represents a strong method to evaluate substrate regulation.

As shown here, this method could also be used to investigate the turnover of a single protein and identify substrate modulators. We cloned the EWS/FLI1 cDNA C-terminal of the DsRed-IRES-EGFP tag and were able to identify EWS/FLI1 as a substrate of proteasomal regulation both in HEK293T and Ewing sarcoma cells. As fluorescence measurements by flow cytometry are determined in intact cells, incomplete protein lysis and detections with unspecific antibodies are not interfering with the results. By using standard reporter constructs with known half lives (EGFP fusions to degron motifs of wild type and mutants of the ornithine decarboxylase), the EWS/FLI1 turnover could be determined in between 1-4h indicating that the TF is constantly targeted for degradation.

It would now be interesting to identify regulators or regulatory complexes of EWS/FLI1 stability. Therefore, the established GPS assay could be combined with an siRNA, shRNA or CRISPR

knockout screen. After knockdown or knockout of candidate sub-libraries, cell pools would be sorted for fractions which display shifts in their EGFP/DsRed ratio indicating either stabilization or destabilization of the fusion protein. This effort would allow discovering a variety of novel co-regulators and cellular pathways associated with EWS/FLI1 turnover.

7.2.2. Proteasomal degradation of EWS/FLI1 – common for other ETS members?

To better understand the degradation process, we identified the main site responsible for EWS/FLI1 turnover and were able to show that mutation of this residue posttranslationally stabilizes the protein and abolishes ubiquitination. EWS/FLI1 ubiquitination is dependent on its C-terminus as full length FLI1 displays a similar ubiquitination pattern with distinct localized polyubiquitin bands and harbors the same ubiquitin acceptor site.

To identify EWS/FLI1 ubiquitin sites, we applied mass spectrometry of purified 3xflag-EWS/FLI1 under denaturing conditions. The protein was digested into peptides using the proteolytic enzyme trypsin (bottom-up approach) followed by identification using a tandem mass spectrometry approach. In addition, stable isotopic labeling of amino acids in cell culture (SILAC) would have allowed quantifying the relative abundance of protein ubiquitination, but has not been done yet. Further, so called K-GG specific antibodies would improve sensitivity and provide the basis of whole ubiquitome profiling in *e.g.* Ewing sarcoma cells (reviewed in (464)).
Several other members of the ETS family including their truncated versions or fusions have been shown to be substrates of the proteasome system indicating that this is a common feature (482, 483, 485). We observed in the first study that not only EWS/FLI1, but also FLI1 can be stabilized by proteasomal inhibition. Mutation of the K380/K334 residue in the ETS domain posttranslationally stabilizes both proteins in the GPS approach. As the K380/K334 site is highly conserved in most of the ETS members, it may, at least partly, contribute to proteasomal degradation of other ETS proteins as well.

At this point, we are not excluding that ubiquitination of the K380 residue triggers signaling events besides degradation. Mutation of this side may also cause disturbances in other pathways which we have not dissected. Further, we have also not yet investigated if the K380 lysine residue serves as a potential sumoylation site. However, a yeast two-hybrid screen identified the SUMO E3 ligase PIASxα as an interactor of full length FLI1. A binding somewhere near the DNA-binding domain resulted in sumoylation of the K67 residue (160). Sumoylation itself has not been investigated in our laboratory as identification by mass spectrometry is challenging. The covalently attached peptide sequence displays high absence of a basic residue and therefore results in an at least 27 amino acid long peptide sequence (525). Moreover, lysines can be acetylated to modulate gene expression and protein-protein interaction (526). An *in vitro* mass spectrometry approach characterized acetylation of the C-terminal FLI1 domain which was also present in the fusion protein. Most interestingly, the K380 residue was not found acetylated, whereas the K298 site displayed acetylation (234). Mutation of the latter site did not abolish ubiquitination and was not used for further investigation as the ubiquitin mark may have

"jumped" to another lysine. However, our own mass spectrometry analysis did not detect any acetylation mark (our own data, unpublished). Even though other modifications may play a role in Ewing sarcoma pathogenesis, we focused our effort on the regulation of proteasomal degradation by ubiquitination of the K380 residue in the ETS domain of EWS/FLI1.

7.2.3. Control of TFs by the proteasome system

Around ~1'700-1'900 protein coding TFs with distinct DNA binding domains are present in the human genome necessary for a variety of processes such as transcriptional control, co-factor regulation as well as histone and chromatin remodeling. They can be tissue specific and differ in their expression level (527).
Strikingly, EWS/FLI1 displays a higher turnover rate than full length FLI1. In contrast, it is known for a variety of oncogenes that stabilized protein versions are driving oncogenicity and confer a physiological advantage to cancer cells. In prostate cancer, a truncated ERG protein (Δ39) displays increased stability due to the loss of the N-terminal E3 ligase binding site for SPOP. Higher truncated versions as ERGΔ99 are even more resistant to proteasomal degradation and continuously drive tumorigenesis (482, 483). A similar regulation was observed for truncated ETV1 proteins where COP1 binding deficiency resulted in a stabilization of the tumor driving ETV1 (485). In Burkitt's lymphoma, c-MYC mediates cell proliferation and tumor growth. At a genomic level MYC can be elevated due to gene amplifications or rearrangements, but also to mutations primarily in the n-terminal transactivation domain that intrinsically stabilize protein levels (528-530). For both proteins, the N-terminal domain is crucial to drive turnover of the protein and its depletion results in protein stabilization.

However, EWS/FLI1 is not a truncated version of full length FLI1 and a large fraction of the N-terminal domain is exchanged by EWSR1 harboring a stronger transactivation domain. If turnover and subsequent E3 ligase binding of ETS members is conserved, EWS/FLI1 may possibly complex with E3 ligases via its EWSR1 part which therefore directs degradation properties. Most interestingly, we identified EWSR1 as a very stable protein being only mono- and diubiquitinated. Speculatively, the transactivation domain of EWSR1 might be responsible for a variety of E3 ligase interactions which would normally mediate specific processes like the DNA damage response in terms of the full length monoubiquitinated EWSR1 (186). The generalized idea that truncated oncogenic TFs are always more stable than their wild type domains (485) might not be correct for fusion proteins consisting of two independent protein parts. We suggest that fusion TFs are more unstable when harboring an exchange for a stronger activation domain. Hypothetically, due to their stronger capacity of transcriptional modulation, they might need less time to initiate and stimulate transcription in order to regulate the same set of target genes as their wild type proteins and therefore only need to be present at a low level. If this is indeed a general paradigm or rather specific for the EWSR1 related fusion protein needs to be further elucidated.

Generally, the ubiquitin system influences transcription at three major levels by controlling protein localizations, co-factors levels and TF abundance at promoters (reviewed by (531)). TFs display an

especially diverse dynamic behavior upon binding to promoter regions. Some TFs such as estrogen receptor α (ERα) require continuous turnover for high level activation and periodically cycle at promoters (532). For c-MYC, it was recently shown that proteasomal turnover is required for full activity. Turnover deficient MYC fails to induce tumorigenesis as inhibitory MYC/PAF1C complexes cannot be removed during transcriptional target gene activation (533). Disassembly of transcriptional complexes for ERα and MYC at promoters seems to be a prerequisite for target gene activation, whereas the activity of the heat-shock factor (HSF) is triggered upon proteasomal inhibition and does not require ongoing degradation (534). Further, several models reveal monoubiquitination as a licensing event for initiation of transcription. After elongation to a polyubiquitin chain, the TFs are removed from the promoter to either provide space for other TFs or to reinduce activity by another round of active monoubiquitinated TFs (reviewed by (535)).

In Ewing sarcoma, around 80% of both activated and repressed target genes are in a saturated state whereas 10% increase with higher protein levels and another 10% are less expressed upon turnover deficiency. Hence, EWS/FLI1 target genes reflect not only one type of promoter behavior, but instead are divided into these subgroups. Surprisingly, the majority of target genes are in a saturated state and they cannot be higher expressed with increasing EWS/FLI1 protein levels as shown for the Ewing sarcoma exchange cell lines with EWS/FLI1 K380R. Speculatively, the other two subgroups of EWS/FLI1 protein sensitive and turnover sensitive target genes might be of greater importance and their dynamics may trigger two different response pathways in Ewing sarcoma oncogenicity. Even though it is not yet clear what defines the subgroups, characterization of target genes from the saturated group might be of less therapeutic relevance.

7.3. Identification of relevant Ewing sarcoma targets for ubiquitin-based drug treatments

To better understand the physiological relevance of EWS/FLI1 turnover, we investigated which E3 ligase and DUBs are capable to interact and destabilize the fusion protein on a molecular level. Indirect targeting of these regulators may affect the degradation rate of EWS/FLI1 and subsequently tumor growth. We focused our attempts on understanding ubiquitin related degradation most possibly over K11- and K48-linked chains even though there is a general relevance in ubiquitin mediated signaling and DNA damage response by mainly K27- and K63-linked polyubiquitin chains.

7.3.1. EWS/FLI1 regulation by E3 ligases and their potential for therapy

The identification of E3 ligases for distinct substrates is challenging. Two approaches are most commonly applied which include identification of the proteome by mass spectrometry or degron motif profiling of substrates. To characterize the ubiquitination process of EWS/FLI1, we aimed to identify which E3 ligase(s) might be a potential interaction partner. For that, we purified flag tagged EWS/FLI1 from Ewing cell lines and subjected them to mass spectrometry. Here, we decided to not co-express tagged ubiquitin as this might lead to artifacts as shown for neddylated proteins (536). Instead, we stabilized the transient E3 ligase- substrate interactions by short term incubation with the proteasome inhibitor MG-132. However, we found very few E3 ligases and none of them seemed to induce EWS/FLI1 degradation by overexpression (our own data, unpublished). It is possible that we have not co-purified the turnover mediating E3 ligases due to the transient nature of the interaction with substrates (522).

We then identified an N-terminal PPxY motif to bind HECT E3 ligases (333). This directed us to the identification of WWP1 as a possible E3 ligase responsible for fusion protein degradation. As the observed degradation is only limited, it may not be the only E3 ligase to regulate EWS/FLI1 turnover. Interestingly, the binding motif of the E3 ligase is in the EWSR1 part which we have characterized as a very stable protein. Speculatively, this motif allows binding of a variety of HECT E3 ligases from the NEDD4 family and favors the ones mediating turnover in case of EWS/FLI1 while others might induce signaling events in case of EWSR1. This demonstrates again that EWS/FLI1 protein is more than just truncated versions of two proteins.

7.3.2. Destabilization of proteins – DUB inhibition as a promising approach?

We also hypothesized that the turnover of EWS/FLI1 is critically regulated by a continuous interplay between ubiquitination and deubiquitination. Inhibition of DUBs which are involved in EWS/FLI1 stabilization may serve as a potential therapeutic target. In an siRNA based screening, we identified USP19 as a stabilizer of EWS/FLI1 protein levels. Inhibition of USP19 increased the ubiquitination of the fusion protein and posttranslationally stabilized the protein. Phenotypically, USP19 depletion resulted in a clear delay of tumor cell growth and proliferation *in vitro* and *in vivo*. Our data clearly

suggest that DUB inhibition might be a valid novel therapeutic strategy for Ewing sarcoma therapy. However, no specific USP19 inhibitor is yet available.

EWS/FLI1 regulation by USP19 presented a quite unexpected top candidate in the screening. Later, we were able to show that neither full length EWSR1 nor FLI1 protein levels were influenced by USP19. This could be explained by the fact that USP19 might possibly bind to the EWSR1 part and is originally a regulator of the full length EWSR1. As EWSR1 is only a mono- and diubiquitinated protein with a half life of around 24h, cleavage of these chains may cause changes in other pathways. When USP19 modifies EWS/FLI1 protein, total polyubiquitin chains are removed subsequently leading to a rescue from degradation. This would support again the idea that the N-terminal domain is necessary for binding of stability regulators and the C-terminal part carries the polyubiquitin signal as shown for the K380 site.

Deubiquitination studies of ETS family proteins have only been conducted for full length ERG. Here, a mass spectrometry based interactome was used to identify USP9X as a regulator of ERG protein levels. Depletion of ERG resulted in growth arrest of prostate tumor growth in genetic assays as well as upon treatment with WP1130, an USP9X inhibitor with lower specificity to a few other DUBs. Most interestingly, the binding of ERG and USP9X was mapped to the ETS domain and was also demonstrated for full length FLI1 (484). Whether this might also be true for EWS/FLI1 needs to be further elucidated. In this case, EWS/FLI1 turnover might be co-regulated through both the EWSR1 and the FLI1 part.

Even though the regulation may be different, depletion of interacting DUBs represents an attractive strategy to target tumor growth for both EWS/FLI1 and ERG dependent cancers. This has been also shown for USP37 which was independently identified as a regulator of c-MYC in lung cancer and PLZF/RARα positive APL (415, 537). The latter confirms again that these interactions are specific and depend on one part of fusion proteins. USP37 modulates stability over the PLZF part and has therefore no impact on PML/RARα. Depletion of USP37 is inducing proteasomal degradation of the fusion protein in this subtype of leukemia which is characterized by resistance to arsenic trioxide and retinoic acid treatments (537).

7.4. A novel therapeutic strategy: degradation of EWS/FLI1 protein

To this end, we have identified EWS/FLI1 protein turnover as a critical mechanism in Ewing sarcoma pathogenesis. In the proposed model, our work identified members of the HECT E3 ligase family, most possibly WWP1, as regulators of ubiquitin attachment which is mediated over a conserved motif in the N-terminal EWSR1 part. Ubiquitin attachment at the K380 residue in the conserved ETS domain results in proteasomal degradation of the fusion protein. Due to the continuous transcriptional activity, EWS/FLI1 protein displays a high turnover. Even though target gene activation is controlled by EWS/FLI1 protein, the majority seems to be in a saturated state. The ubiquitin signal can be removed by USP19, rescuing EWS/FLI1 from degradation. USP19 depletion was identified as the strongest target for therapeutic interventions as inhibition decreased tumor growth *in vitro* and prolonged survival *in vivo* (Fig. 15). Our data provide a strong understanding of the proteolytic regulation of the EWS/FLI1 protein and led us to the identification of novel target strategies.

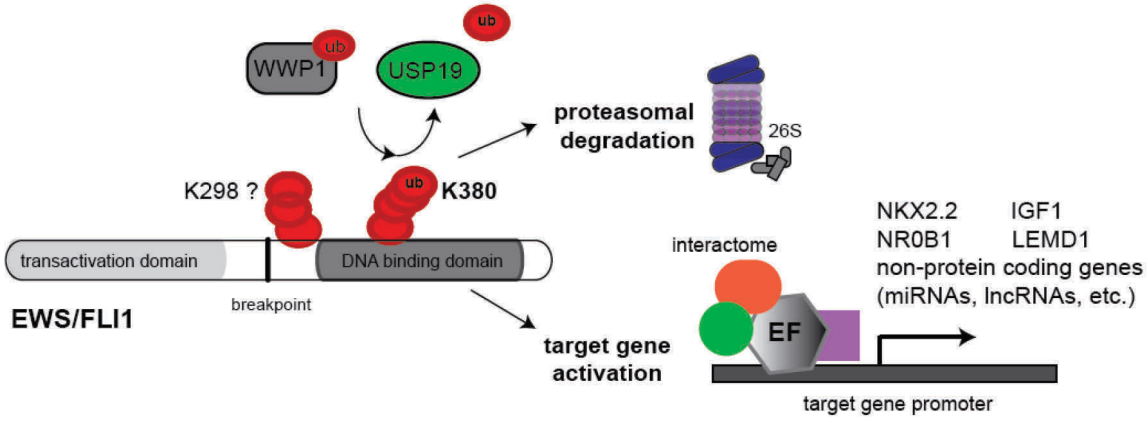

Fig. 15: Regulation of EWS/FLI1 turnover and its consequences. EWS/FLI1 was found to be ubiquitinated at two sites by mass spectrometry analysis. Ubiquitin is attached by E3 ligases including WWP1 and removed by the deubiquitinating enzyme USP19. Attachment of polyubiquitin at the K380 residue mediates proteasomal degradation. Unmodified EWS/FLI1 acts as a strong modulator of target genes from which only a subset is protein level dependent. The fast turnover of EWS/FLI1 protein ensures constant protein levels in the cell and continuous exchange at relevant promoter regions.

8. References

1. Siegel RL, Miller KD, & Jemal A (2015) Cancer statistics, 2015. *CA Cancer J Clin* 65(1):5-29.
2. FSO (2011) Cancer in Switzerland - Situation and development from 1983 to 2007. *Federal Statistical Office*.
3. DeSantis CE*, et al.* (2014) Cancer treatment and survivorship statistics, 2014. *CA Cancer J Clin* 64(4):252-271.
4. SCCR (2014) Swiss Childhood Cancer Registry - Annual Report 2013/2014. *Swiss Childhood Cancer Registry*.
5. Ward E, DeSantis C, Robbins A, Kohler B, & Jemal A (2014) Childhood and adolescent cancer statistics, 2014. *CA Cancer J Clin* 64(2):83-103.
6. Downing JR*, et al.* (2012) The Pediatric Cancer Genome Project. *Nature genetics* 44(6):619-622.
7. Bleyer A*, et al.* (2008) The distinctive biology of cancer in adolescents and young adults. *Nat Rev Cancer* 8(4):288-298.
8. Pui CH, Gajjar AJ, Kane JR, Qaddoumi IA, & Pappo AS (2011) Challenging issues in pediatric oncology. *Nat Rev Clin Oncol* 8(9):540-549.
9. Smith MA*, et al.* (2010) Outcomes for children and adolescents with cancer: challenges for the twenty-first century. *J Clin Oncol* 28(15):2625-2634.
10. Meadows AT*, et al.* (2009) Second neoplasms in survivors of childhood cancer: findings from the Childhood Cancer Survivor Study cohort. *J Clin Oncol* 27(14):2356-2362.
11. Hudson MM*, et al.* (2013) Clinical ascertainment of health outcomes among adults treated for childhood cancer. *JAMA* 309(22):2371-2381.
12. Hanahan D & Weinberg RA (2000) The hallmarks of cancer. *Cell* 100(1):57-70.
13. Hanahan D & Weinberg RA (2011) Hallmarks of cancer: the next generation. *Cell* 144(5):646-674.
14. Stratton MR, Campbell PJ, & Futreal PA (2009) The cancer genome. *Nature* 458(7239):719-724.
15. Vogelstein B*, et al.* (1988) Genetic alterations during colorectal-tumor development. *N Engl J Med* 319(9):525-532.
16. Vogelstein B*, et al.* (2013) Cancer genome landscapes. *Science* 339(6127):1546-1558.
17. Wood LD*, et al.* (2007) The genomic landscapes of human breast and colorectal cancers. *Science* 318(5853):1108-1113.
18. Greenman C*, et al.* (2007) Patterns of somatic mutation in human cancer genomes. *Nature* 446(7132):153-158.
19. Lawrence MS*, et al.* (2013) Mutational heterogeneity in cancer and the search for new cancer-associated genes. *Nature* 499(7457):214-218.
20. Hungerford DA*, et al.* (1970) Chromosome structure and function in man. 3. Pachytene analysis and indentification of the supernumerary chromosome in a case of Down's syndrome (mongolism). *Proc Natl Acad Sci U S A* 67(1):221-224.
21. Nowell PC (2007) Discovery of the Philadelphia chromosome: a personal perspective. *J Clin Invest* 117(8):2033-2035.
22. Rowley JD (1973) Identificaton of a translocation with quinacrine fluorescence in a patient with acute leukemia. *Ann Genet* 16(2):109-112.
23. Mitelman F, Johansson B, & Mertens F (2007) The impact of translocations and gene fusions on cancer causation. *Nat Rev Cancer* 7(4):233-245.
24. Mertens F*, et al.* (2009) Translocation-related sarcomas. *Semin Oncol* 36(4):312-323.
25. Sandberg AA (2002) Cytogenetics and molecular genetics of bone and soft-tissue tumors. *Am J Med Genet* 115(3):189-193.
26. Rabbitts TH (2009) Commonality but diversity in cancer gene fusions. *Cell* 137(3):391-395.
27. Andersson A*, et al.* (2005) Molecular signatures in childhood acute leukemia and their correlations to expression patterns in normal hematopoietic subpopulations. *Proc Natl Acad Sci U S A* 102(52):19069-19074.

28. Davicioni E*, et al.* (2006) Identification of a PAX-FKHR gene expression signature that defines molecular classes and determines the prognosis of alveolar rhabdomyosarcomas. *Cancer Res* 66(14):6936-6946.
29. Ford AM*, et al.* (1993) In utero rearrangements in the trithorax-related oncogene in infant leukaemias. *Nature* 363(6427):358-360.
30. Greaves MF & Wiemels J (2003) Origins of chromosome translocations in childhood leukaemia. *Nat Rev Cancer* 3(9):639-649.
31. Greaves MF, Maia AT, Wiemels JL, & Ford AM (2003) Leukemia in twins: lessons in natural history. *Blood* 102(7):2321-2333.
32. WHO (2002) Pathology and Genetics of Tumours of Soft Tissue and Bone. *WHO*.
33. Helman LJ & Meltzer P (2003) Mechanisms of sarcoma development. *Nat Rev Cancer* 3(9):685-694.
34. Thacker MM (2013) Benign soft tissue tumors in children. *Orthop Clin North Am* 44(3):433-444, xi.
35. HaDuong JH, Martin AA, Skapek SX, & Mascarenhas L (2015) Sarcomas. *Pediatr Clin North Am* 62(1):179-200.
36. ESMO (2014) Soft tissue and visceral sarcomas: ESMO Clinical Practice Guidelines for diagnosis, treatment and follow-up. *Ann Oncol* 25 Suppl 3:iii102-112.
37. Thacker MM (2013) Malignant soft tissue tumors in children. *Orthop Clin North Am* 44(4):657-667.
38. Meyer WH & Spunt SL (2004) Soft tissue sarcomas of childhood. *Cancer Treat Rev* 30(3):269-280.
39. Merchant MS & Mackall CL (2009) Current approach to pediatric soft tissue sarcomas. *Oncologist* 14(11):1139-1153.
40. Chugh R & Baker LH (2009) Pharmacotherapy of sarcoma. *Expert Opin Pharmacother* 10(12):1953-1963.
41. ESMO (2014) Bone sarcomas: ESMO Clinical Practice Guidelines for diagnosis, treatment and follow-up. *Ann Oncol* 25 Suppl 3:iii113-123.
42. Kaste SC (2011) Imaging pediatric bone sarcomas. *Radiol Clin North Am* 49(4):749-765, vi-vii.
43. Gorlick R, Janeway K, Lessnick S, Randall RL, & Marina N (2013) Children's Oncology Group's 2013 blueprint for research: bone tumors. *Pediatric blood & cancer* 60(6):1009-1015.
44. Forscher C, Mita M, & Figlin R (2014) Targeted therapy for sarcomas. *Biologics* 8:91-105.
45. Linch M, Miah AB, Thway K, Judson IR, & Benson C (2014) Systemic treatment of soft-tissue sarcoma-gold standard and novel therapies. *Nat Rev Clin Oncol* 11(4):187-202.
46. Harwood JL, Alexander JH, Mayerson JL, & Scharschmidt TJ (2015) Targeted Chemotherapy in Bone and Soft-Tissue Sarcoma. *Orthop Clin North Am* 46(4):587-608.
47. Wachtel M & Schafer BW (2010) Targets for cancer therapy in childhood sarcomas. *Cancer Treat Rev* 36(4):318-327.
48. Ewing J (1921) Classics in oncology. Diffuse endothelioma of bone. James Ewing. Proceedings of the New York Pathological Society, 1921. *CA Cancer J Clin* 22(2):95-98.
49. Cripe TP (2011) Ewing sarcoma: an eponym window to history. *Sarcoma* 2011:457532.
50. Esiashvili N, Goodman M, & Marcus RB, Jr. (2008) Changes in incidence and survival of Ewing sarcoma patients over the past 3 decades: Surveillance Epidemiology and End Results data. *J Pediatr Hematol Oncol* 30(6):425-430.
51. Ozaki T (2015) Diagnosis and treatment of Ewing sarcoma of the bone: a review article. *J Orthop Sci* 20(2):250-263.
52. Jawad MU*, et al.* (2009) Ewing sarcoma demonstrates racial disparities in incidence-related and sex-related differences in outcome: an analysis of 1631 cases from the SEER database, 1973-2005. *Cancer* 115(15):3526-3536.
53. Worch J*, et al.* (2011) Racial differences in the incidence of mesenchymal tumors associated with EWSR1 translocation. *Cancer Epidemiol Biomarkers Prev* 20(3):449-453.

54. Bacci G*, et al.* (2003) Therapy and survival after recurrence of Ewing's tumors: the Rizzoli experience in 195 patients treated with adjuvant and neoadjuvant chemotherapy from 1979 to 1997. *Ann Oncol* 14(11):1654-1659.
55. Schiffman JD & Wright J (2011) Ewing's Sarcoma and Second Malignancies. *Sarcoma* 2011:736841.
56. Bernstein M*, et al.* (2006) Ewing's sarcoma family of tumors: Current management. *Oncologist* 11(5):503-519.
57. Wagner LM*, et al.* (2007) Temozolomide and intravenous irinotecan for treatment of advanced Ewing sarcoma. *Pediatric blood & cancer* 48(2):132-139.
58. Ferrari S*, et al.* (2009) Response to high-dose ifosfamide in patients with advanced/recurrent Ewing sarcoma. *Pediatric blood & cancer* 52(5):581-584.
59. Hartman KR, Triche TJ, Kinsella TJ, & Miser JS (1991) Prognostic value of histopathology in Ewing's sarcoma. Long-term follow-up of distal extremity primary tumors. *Cancer* 67(1):163-171.
60. van Maldegem AM, Hogendoorn PC, & Hassan AB (2012) The clinical use of biomarkers as prognostic factors in Ewing sarcoma. *Clin Sarcoma Res* 2(1):7.
61. Cotterill SJ*, et al.* (2000) Prognostic factors in Ewing's tumor of bone: analysis of 975 patients from the European Intergroup Cooperative Ewing's Sarcoma Study Group. *J Clin Oncol* 18(17):3108-3114.
62. Karski EE, Matthay KK, Neuhaus JM, Goldsby RE, & Dubois SG (2013) Characteristics and outcomes of patients with Ewing sarcoma over 40 years of age at diagnosis. *Cancer Epidemiol* 37(1):29-33.
63. Karski EE*, et al.* (2016) Identification of Discrete Prognostic Groups in Ewing Sarcoma. *Pediatric blood & cancer* 63(1):47-53.
64. Nesbit ME, Jr.*, et al.* (1990) Multimodal therapy for the management of primary, nonmetastatic Ewing's sarcoma of bone: a long-term follow-up of the First Intergroup study. *J Clin Oncol* 8(10):1664-1674.
65. Burgert EO, Jr.*, et al.* (1990) Multimodal therapy for the management of nonpelvic, localized Ewing's sarcoma of bone: intergroup study IESS-II. *J Clin Oncol* 8(9):1514-1524.
66. Evans RG*, et al.* (1991) Multimodal therapy for the management of localized Ewing's sarcoma of pelvic and sacral bones: a report from the second intergroup study. *J Clin Oncol* 9(7):1173-1180.
67. Grier HE*, et al.* (2003) Addition of ifosfamide and etoposide to standard chemotherapy for Ewing's sarcoma and primitive neuroectodermal tumor of bone. *N Engl J Med* 348(8):694-701.
68. Miser JS*, et al.* (2004) Treatment of metastatic Ewing's sarcoma or primitive neuroectodermal tumor of bone: evaluation of combination ifosfamide and etoposide--a Children's Cancer Group and Pediatric Oncology Group study. *J Clin Oncol* 22(14):2873-2876.
69. Miser JS*, et al.* (2007) Treatment of metastatic Ewing sarcoma/primitive neuroectodermal tumor of bone: evaluation of increasing the dose intensity of chemotherapy--a report from the Children's Oncology Group. *Pediatric blood & cancer* 49(7):894-900.
70. DuBois SG & Grier HE (2009) Chemotherapy: The role of ifosfamide and etoposide in Ewing sarcoma. *Nat Rev Clin Oncol* 6(5):251-253.
71. Paulussen M*, et al.* (2008) Results of the EICESS-92 Study: two randomized trials of Ewing's sarcoma treatment--cyclophosphamide compared with ifosfamide in standard-risk patients and assessment of benefit of etoposide added to standard treatment in high-risk patients. *J Clin Oncol* 26(27):4385-4393.
72. Magnan H*, et al.* (2015) Ifosfamide dose-intensification for patients with metastatic Ewing sarcoma. *Pediatric blood & cancer* 62(4):594-597.
73. EWING2008 (2008) EWING 2008 trial protocol, EudraCT number: 2008-003658-13.
74. Delattre O*, et al.* (1992) Gene fusion with an ETS DNA-binding domain caused by chromosome translocation in human tumours. *Nature* 359(6391):162-165.

75. Sankar S & Lessnick SL (2011) Promiscuous partnerships in Ewing's sarcoma. *Cancer Genet* 204(7):351-365.
76. Sorensen PH*, et al.* (1994) A second Ewing's sarcoma translocation, t(21;22), fuses the EWS gene to another ETS-family transcription factor, ERG. *Nature genetics* 6(2):146-151.
77. Janknecht R (2005) EWS-ETS oncoproteins: the linchpins of Ewing tumors. *Gene* 363:1-14.
78. Crompton BD*, et al.* (2014) The Genomic Landscape of Pediatric Ewing Sarcoma. *Cancer Discov* 4(11):1326-1341.
79. Armengol G*, et al.* (1997) Recurrent gains of 1q, 8 and 12 in the Ewing family of tumours by comparative genomic hybridization. *Br J Cancer* 75(10):1403-1409.
80. Hattinger CM*, et al.* (2002) Prognostic impact of chromosomal aberrations in Ewing tumours. *Br J Cancer* 86(11):1763-1769.
81. Lynn M*, et al.* (2013) High-resolution genome-wide copy-number analyses identify localized copy-number alterations in Ewing sarcoma. *Diagn Mol Pathol* 22(2):76-84.
82. Mackintosh C*, et al.* (2012) 1q gain and CDT2 overexpression underlie an aggressive and highly proliferative form of Ewing sarcoma. *Oncogene* 31(10):1287-1298.
83. Tirode F*, et al.* (2014) Genomic landscape of Ewing sarcoma defines an aggressive subtype with co-association of STAG2 and TP53 mutations. *Cancer Discov* 4(11):1342-1353.
84. Brohl AS*, et al.* (2014) The genomic landscape of the Ewing Sarcoma family of tumors reveals recurrent STAG2 mutation. *PLoS Genet* 10(7):e1004475.
85. Abudu A*, et al.* (1999) Overexpression of p53 protein in primary Ewing's sarcoma of bone: relationship to tumour stage, response and prognosis. *Br J Cancer* 79(7-8):1185-1189.
86. de Alava E*, et al.* (2000) Prognostic impact of P53 status in Ewing sarcoma. *Cancer* 89(4):783-792.
87. Amir G*, et al.* (2002) Expression of p53 gene product and cell proliferation marker Ki-67 in Ewing's sarcoma: correlation with clinical outcome. *Hum Pathol* 33(2):170-174.
88. Lerman DM*, et al.* (2015) Tumoral TP53 and/or CDKN2A alterations are not reliable prognostic biomarkers in patients with localized Ewing sarcoma: a report from the Children's Oncology Group. *Pediatric blood & cancer* 62(5):759-765.
89. Zucman J*, et al.* (1993) Combinatorial generation of variable fusion proteins in the Ewing family of tumours. *EMBO J* 12(12):4481-4487.
90. Zoubek A*, et al.* (1996) Does expression of different EWS chimeric transcripts define clinically distinct risk groups of Ewing tumor patients? *J Clin Oncol* 14(4):1245-1251.
91. Le Deley MC*, et al.* (2010) Impact of EWS-ETS fusion type on disease progression in Ewing's sarcoma/peripheral primitive neuroectodermal tumor: prospective results from the cooperative Euro-E.W.I.N.G. 99 trial. *J Clin Oncol* 28(12):1982-1988.
92. van Doorninck JA*, et al.* (2010) Current treatment protocols have eliminated the prognostic advantage of type 1 fusions in Ewing sarcoma: a report from the Children's Oncology Group. *J Clin Oncol* 28(12):1989-1994.
93. Kovar H*, et al.* (1996) EWS/FLI-1 antagonists induce growth inhibition of Ewing tumor cells in vitro. *Cell Growth Differ* 7(4):429-437.
94. Tanaka K, Iwakuma T, Harimaya K, Sato H, & Iwamoto Y (1997) EWS-Fli1 antisense oligodeoxynucleotide inhibits proliferation of human Ewing's sarcoma and primitive neuroectodermal tumor cells. *J Clin Invest* 99(2):239-247.
95. Toretsky JA, Connell Y, Neckers L, & Bhat NK (1997) Inhibition of EWS-FLI-1 fusion protein with antisense oligodeoxynucleotides. *J Neurooncol* 31(1-2):9-16.
96. May WA*, et al.* (1993) Ewing sarcoma 11;22 translocation produces a chimeric transcription factor that requires the DNA-binding domain encoded by FLI1 for transformation. *Proc Natl Acad Sci U S A* 90(12):5752-5756.
97. Ohno T, Rao VN, & Reddy ES (1993) EWS/Fli-1 chimeric protein is a transcriptional activator. *Cancer Res* 53(24):5859-5863.
98. May WA*, et al.* (1993) The Ewing's sarcoma EWS/FLI-1 fusion gene encodes a more potent transcriptional activator and is a more powerful transforming gene than FLI-1. *Mol Cell Biol* 13(12):7393-7398.

99. Bailly RA*, et al.* (1994) DNA-binding and transcriptional activation properties of the EWS-FLI-1 fusion protein resulting from the t(11;22) translocation in Ewing sarcoma. *Mol Cell Biol* 14(5):3230-3241.
100. Wei GH*, et al.* (2010) Genome-wide analysis of ETS-family DNA-binding in vitro and in vivo. *EMBO J* 29(13):2147-2160.
101. Liang H*, et al.* (1994) The secondary structure of the ets domain of human Fli-1 resembles that of the helix-turn-helix DNA-binding motif of the Escherichia coli catabolite gene activator protein. *Proc Natl Acad Sci U S A* 91(24):11655-11659.
102. Pio F*, et al.* (1996) New insights on DNA recognition by ets proteins from the crystal structure of the PU.1 ETS domain-DNA complex. *The Journal of biological chemistry* 271(38):23329-23337.
103. Welford SM, Hebert SP, Deneen B, Arvand A, & Denny CT (2001) DNA binding domain-independent pathways are involved in EWS/FLI1-mediated oncogenesis. *The Journal of biological chemistry* 276(45):41977-41984.
104. Herrero-Martin D*, et al.* (2011) Factors Affecting EWS-FLI1 Activity in Ewing's Sarcoma. *Sarcoma* 2011:352580.
105. Owen LA & Lessnick SL (2006) Identification of target genes in their native cellular context: an analysis of EWS/FLI in Ewing's sarcoma. *Cell Cycle* 5(18):2049-2053.
106. Braun BS, Frieden R, Lessnick SL, May WA, & Denny CT (1995) Identification of target genes for the Ewing's sarcoma EWS/FLI fusion protein by representational difference analysis. *Mol Cell Biol* 15(8):4623-4630.
107. Tirado OM*, et al.* (2006) Caveolin-1 (CAV1) is a target of EWS/FLI-1 and a key determinant of the oncogenic phenotype and tumorigenicity of Ewing's sarcoma cells. *Cancer Res* 66(20):9937-9947.
108. Smith R*, et al.* (2006) Expression profiling of EWS/FLI identifies NKX2.2 as a critical target gene in Ewing's sarcoma. *Cancer Cell* 9(5):405-416.
109. Kinsey M, Smith R, & Lessnick SL (2006) NR0B1 is required for the oncogenic phenotype mediated by EWS/FLI in Ewing's sarcoma. *Mol Cancer Res* 4(11):851-859.
110. Cironi L*, et al.* (2008) IGF1 is a common target gene of Ewing's sarcoma fusion proteins in mesenchymal progenitor cells. *PLoS One* 3(7):e2634.
111. Riggi N*, et al.* (2010) EWS-FLI-1 modulates miRNA145 and SOX2 expression to initiate mesenchymal stem cell reprogramming toward Ewing sarcoma cancer stem cells. *Genes Dev* 24(9):916-932.
112. Prieur A, Tirode F, Cohen P, & Delattre O (2004) EWS/FLI-1 silencing and gene profiling of Ewing cells reveal downstream oncogenic pathways and a crucial role for repression of insulin-like growth factor binding protein 3. *Mol Cell Biol* 24(16):7275-7283.
113. Boro A*, et al.* (2012) Small-molecule screen identifies modulators of EWS/FLI1 target gene expression and cell survival in Ewing's sarcoma. *Int J Cancer* 131(9):2153-2164.
114. Marques Howarth M*, et al.* (2014) Long noncoding RNA EWSAT1-mediated gene repression facilitates Ewing sarcoma oncogenesis. *J Clin Invest* 124(12):5275-5290.
115. Sankar S*, et al.* (2013) Mechanism and relevance of EWS/FLI-mediated transcriptional repression in Ewing sarcoma. *Oncogene* 32(42):5089-5100.
116. Arvand A, Welford SM, Teitell MA, & Denny CT (2001) The COOH-terminal domain of FLI-1 is necessary for full tumorigenesis and transcriptional modulation by EWS/FLI-1. *Cancer Res* 61(13):5311-5317.
117. Deneen B & Denny CT (2001) Loss of p16 pathways stabilizes EWS/FLI1 expression and complements EWS/FLI1 mediated transformation. *Oncogene* 20(46):6731-6741.
118. Lessnick SL, Dacwag CS, & Golub TR (2002) The Ewing's sarcoma oncoprotein EWS/FLI induces a p53-dependent growth arrest in primary human fibroblasts. *Cancer Cell* 1(4):393-401.
119. Hu-Lieskovan S*, et al.* (2005) EWS-FLI1 fusion protein up-regulates critical genes in neural crest development and is responsible for the observed phenotype of Ewing's family of tumors. *Cancer Res* 65(11):4633-4644.

120. Braunreiter CL, Hancock JD, Coffin CM, Boucher KM, & Lessnick SL (2006) Expression of EWS-ETS fusions in NIH3T3 cells reveals significant differences to Ewing's sarcoma. *Cell Cycle* 5(23):2753-2759.
121. Riggi N*, et al.* (2008) EWS-FLI-1 expression triggers a Ewing's sarcoma initiation program in primary human mesenchymal stem cells. *Cancer Res* 68(7):2176-2185.
122. Matsumoto Y*, et al.* (2001) Downregulation and forced expression of EWS-Fli1 fusion gene results in changes in the expression of G(1)regulatory genes. *Br J Cancer* 84(6):768-775.
123. Matsunobu T*, et al.* (2004) The prognostic and therapeutic relevance of p27kip1 in Ewing's family tumors. *Clin Cancer Res* 10(3):1003-1012.
124. Li X*, et al.* (2005) Transactivation of cyclin E gene by EWS-Fli1 and antitumor effects of cyclin dependent kinase inhibitor on Ewing's family tumor cells. *Int J Cancer* 116(3):385-394.
125. Hu HM*, et al.* (2008) EWS/FLI1 suppresses retinoblastoma protein function and senescence in Ewing's sarcoma cells. *J Orthop Res* 26(6):886-893.
126. Dauphinot L*, et al.* (2001) Analysis of the expression of cell cycle regulators in Ewing cell lines: EWS-FLI-1 modulates p57KIP2and c-Myc expression. *Oncogene* 20(25):3258-3265.
127. Matsunobu T*, et al.* (2006) The possible role of EWS-Fli1 in evasion of senescence in Ewing family tumors. *Cancer Res* 66(2):803-811.
128. Pereira R*, et al.* (1999) FLI-1 inhibits differentiation and induces proliferation of primary erythroblasts. *Oncogene* 18(8):1597-1608.
129. Spahn L*, et al.* (2002) Interaction of the EWS NH2 terminus with BARD1 links the Ewing's sarcoma gene to a common tumor suppressor pathway. *Cancer Res* 62(16):4583-4587.
130. Embree LJ, Azuma M, & Hickstein DD (2009) Ewing sarcoma fusion protein EWSR1/FLI1 interacts with EWSR1 leading to mitotic defects in zebrafish embryos and human cell lines. *Cancer Res* 69(10):4363-4371.
131. Toretsky JA*, et al.* (2006) Oncoprotein EWS-FLI1 activity is enhanced by RNA helicase A. *Cancer Res* 66(11):5574-5581.
132. Erkizan HV*, et al.* (2009) A small molecule blocking oncogenic protein EWS-FLI1 interaction with RNA helicase A inhibits growth of Ewing's sarcoma. *Nat Med* 15(7):750-756.
133. Barber-Rotenberg JS*, et al.* (2012) Single enantiomer of YK-4-279 demonstrates specificity in targeting the oncogene EWS-FLI1. *Oncotarget* 3(2):172-182.
134. Petermann R*, et al.* (1998) Oncogenic EWS-Fli1 interacts with hsRPB7, a subunit of human RNA polymerase II. *Oncogene* 17(5):603-610.
135. Knoop LL & Baker SJ (2000) The splicing factor U1C represses EWS/FLI-mediated transactivation. *The Journal of biological chemistry* 275(32):24865-24871.
136. Yang L, Chansky HA, & Hickstein DD (2000) EWS.Fli-1 fusion protein interacts with hyperphosphorylated RNA polymerase II and interferes with serine-arginine protein-mediated RNA splicing. *The Journal of biological chemistry* 275(48):37612-37618.
137. Chansky HA, Hu M, Hickstein DD, & Yang L (2001) Oncogenic TLS/ERG and EWS/Fli-1 fusion proteins inhibit RNA splicing mediated by YB-1 protein. *Cancer Res* 61(9):3586-3590.
138. Knoop LL & Baker SJ (2001) EWS/FLI alters 5'-splice site selection. *The Journal of biological chemistry* 276(25):22317-22322.
139. Selvanathan SP*, et al.* (2015) Oncogenic fusion protein EWS-FLI1 is a network hub that regulates alternative splicing. *Proc Natl Acad Sci U S A* 112(11):E1307-1316.
140. Wasylyk B, Hahn SL, & Giovane A (1993) The Ets family of transcription factors. *Eur J Biochem* 211(1-2):7-18.
141. Laudet V, Hanni C, Stehelin D, & Duterque-Coquillaud M (1999) Molecular phylogeny of the ETS gene family. *Oncogene* 18(6):1351-1359.
142. Laudet V, Niel C, Duterque-Coquillaud M, Leprince D, & Stehelin D (1993) Evolution of the ets gene family. *Biochem Biophys Res Commun* 190(1):8-14.
143. Hollenhorst PC, McIntosh LP, & Graves BJ (2011) Genomic and biochemical insights into the specificity of ETS transcription factors. *Annu Rev Biochem* 80:437-471.

144. Nye JA, Petersen JM, Gunther CV, Jonsen MD, & Graves BJ (1992) Interaction of murine ets-1 with GGA-binding sites establishes the ETS domain as a new DNA-binding motif. *Genes Dev* 6(6):975-990.
145. Li R, Pei H, & Watson DK (2000) Regulation of Ets function by protein - protein interactions. *Oncogene* 19(55):6514-6523.
146. Muthusamy N, Barton K, & Leiden JM (1995) Defective activation and survival of T cells lacking the Ets-1 transcription factor. *Nature* 377(6550):639-642.
147. Sharrocks AD (2001) The ETS-domain transcription factor family. *Nat Rev Mol Cell Biol* 2(11):827-837.
148. Lelievre E, Lionneton F, Soncin F, & Vandenbunder B (2001) The Ets family contains transcriptional activators and repressors involved in angiogenesis. *Int J Biochem Cell Biol* 33(4):391-407.
149. Golub TR*, et al.* (1995) Fusion of the TEL gene on 12p13 to the AML1 gene on 21q22 in acute lymphoblastic leukemia. *Proc Natl Acad Sci U S A* 92(11):4917-4921.
150. Davidson B*, et al.* (2001) Ets-1 messenger RNA expression is a novel marker of poor survival in ovarian carcinoma. *Clin Cancer Res* 7(3):551-557.
151. Tomlins SA*, et al.* (2005) Recurrent fusion of TMPRSS2 and ETS transcription factor genes in prostate cancer. *Science* 310(5748):644-648.
152. Petrovics G*, et al.* (2005) Frequent overexpression of ETS-related gene-1 (ERG1) in prostate cancer transcriptome. *Oncogene* 24(23):3847-3852.
153. Kumar-Sinha C, Tomlins SA, & Chinnaiyan AM (2008) Recurrent gene fusions in prostate cancer. *Nat Rev Cancer* 8(7):497-511.
154. Seth A & Watson DK (2005) ETS transcription factors and their emerging roles in human cancer. *Eur J Cancer* 41(16):2462-2478.
155. Moriyama T*, et al.* (2015) Germline genetic variation in ETV6 and risk of childhood acute lymphoblastic leukaemia: a systematic genetic study. *Lancet Oncol* 16(16):1659-1666.
156. Ben-David Y, Giddens EB, & Bernstein A (1990) Identification and mapping of a common proviral integration site Fli-1 in erythroleukemia cells induced by Friend murine leukemia virus. *Proc Natl Acad Sci U S A* 87(4):1332-1336.
157. Klemsz MJ, Maki RA, Papayannopoulou T, Moore J, & Hromas R (1993) Characterization of the ets oncogene family member, fli-1. *The Journal of biological chemistry* 268(8):5769-5773.
158. Dhulipala PD, Lee L, Rao VN, & Reddy ES (1998) Fli-1b is generated by usage of differential splicing and alternative promoter. *Oncogene* 17(9):1149-1157.
159. Hu W, Philips AS, Kwok JC, Eisbacher M, & Chong BH (2005) Identification of nuclear import and export signals within Fli-1: roles of the nuclear import signals in Fli-1-dependent activation of megakaryocyte-specific promoters. *Mol Cell Biol* 25(8):3087-3108.
160. van den Akker E*, et al.* (2005) FLI-1 functionally interacts with PIASxalpha, a member of the PIAS E3 SUMO ligase family. *The Journal of biological chemistry* 280(45):38035-38046.
161. Asano Y, Czuwara J, & Trojanowska M (2007) Transforming growth factor-beta regulates DNA binding activity of transcription factor Fli1 by p300/CREB-binding protein-associated factor-dependent acetylation. *The Journal of biological chemistry* 282(48):34672-34683.
162. Asano Y & Trojanowska M (2009) Phosphorylation of Fli1 at threonine 312 by protein kinase C delta promotes its interaction with p300/CREB-binding protein-associated factor and subsequent acetylation in response to transforming growth factor beta. *Mol Cell Biol* 29(7):1882-1894.
163. Zhang XK & Watson DK (2005) The FLI-1 transcription factor is a short-lived phosphoprotein in T cells. *J Biochem* 137(3):297-302.
164. Lelievre E, Lionneton F, Mattot V, Spruyt N, & Soncin F (2002) Ets-1 regulates fli-1 expression in endothelial cells. Identification of ETS binding sites in the fli-1 gene promoter. *The Journal of biological chemistry* 277(28):25143-25151.
165. Kruse EA*, et al.* (2009) Dual requirement for the ETS transcription factors Fli-1 and Erg in hematopoietic stem cells and the megakaryocyte lineage. *Proc Natl Acad Sci U S A* 106(33):13814-13819.

166. Tamir A*, et al.* (1999) Fli-1, an Ets-related transcription factor, regulates erythropoietin-induced erythroid proliferation and differentiation: evidence for direct transcriptional repression of the Rb gene during differentiation. *Mol Cell Biol* 19(6):4452-4464.
167. Melet F, Motro B, Rossi DJ, Zhang L, & Bernstein A (1996) Generation of a novel Fli-1 protein by gene targeting leads to a defect in thymus development and a delay in Friend virus-induced erythroleukemia. *Mol Cell Biol* 16(6):2708-2718.
168. Ano S*, et al.* (2004) Erythroblast transformation by FLI-1 depends upon its specific DNA binding and transcriptional activation properties. *The Journal of biological chemistry* 279(4):2993-3002.
169. Truong AH & Ben-David Y (2000) The role of Fli-1 in normal cell function and malignant transformation. *Oncogene* 19(55):6482-6489.
170. Li Y, Luo H, Liu T, Zacksenhaus E, & Ben-David Y (2015) The ets transcription factor Fli-1 in development, cancer and disease. *Oncogene* 34(16):2022-2031.
171. Ben-David Y, Giddens EB, Letwin K, & Bernstein A (1991) Erythroleukemia induction by Friend murine leukemia virus: insertional activation of a new member of the ets gene family, Fli-1, closely linked to c-ets-1. *Genes Dev* 5(6):908-918.
172. Cui JW, Vecchiarelli-Federico LM, Li YJ, Wang GJ, & Ben-David Y (2009) Continuous Fli-1 expression plays an essential role in the proliferation and survival of F-MuLV-induced erythroleukemia and human erythroleukemia. *Leukemia* 23(7):1311-1319.
173. Paulo P*, et al.* (2012) FLI1 is a novel ETS transcription factor involved in gene fusions in prostate cancer. *Genes Chromosomes Cancer* 51(3):240-249.
174. Bonetti P*, et al.* (2013) Deregulation of ETS1 and FLI1 contributes to the pathogenesis of diffuse large B-cell lymphoma. *Blood* 122(13):2233-2241.
175. Bertolotti A, Lutz Y, Heard DJ, Chambon P, & Tora L (1996) hTAF(II)68, a novel RNA/ssDNA-binding protein with homology to the pro-oncoproteins TLS/FUS and EWS is associated with both TFIID and RNA polymerase II. *EMBO J* 15(18):5022-5031.
176. Tan AY & Manley JL (2009) The TET family of proteins: functions and roles in disease. *J Mol Cell Biol* 1(2):82-92.
177. Ohno T*, et al.* (1994) The EWS gene, involved in Ewing family of tumors, malignant melanoma of soft parts and desmoplastic small round cell tumors, codes for an RNA binding protein with novel regulatory domains. *Oncogene* 9(10):3087-3097.
178. Reeves BR, Fletcher CD, & Gusterson BA (1992) Translocation t(12;22)(q13;q13) is a nonrandom rearrangement in clear cell sarcoma. *Cancer Genet Cytogenet* 64(2):101-103.
179. Bridge JA, Sreekantaiah C, Neff JR, & Sandberg AA (1991) Cytogenetic findings in clear cell sarcoma of tendons and aponeuroses. Malignant melanoma of soft parts. *Cancer Genet Cytogenet* 52(1):101-106.
180. Andersson MK*, et al.* (2008) The multifunctional FUS, EWS and TAF15 proto-oncoproteins show cell type-specific expression patterns and involvement in cell spreading and stress response. *BMC Cell Biol* 9:37.
181. Ng KP*, et al.* (2007) Multiple aromatic side chains within a disordered structure are critical for transcription and transforming activity of EWS family oncoproteins. *Proc Natl Acad Sci U S A* 104(2):479-484.
182. Belyanskaya LL, Delattre O, & Gehring H (2003) Expression and subcellular localization of Ewing sarcoma (EWS) protein is affected by the methylation process. *Exp Cell Res* 288(2):374-381.
183. Olsen RJ & Hinrichs SH (2001) Phosphorylation of the EWS IQ domain regulates transcriptional activity of the EWS/ATF1 and EWS/FLI1 fusion proteins. *Oncogene* 20(14):1756-1764.
184. Klevernic IV, Morton S, Davis RJ, & Cohen P (2009) Phosphorylation of Ewing's sarcoma protein (EWS) and EWS-Fli1 in response to DNA damage. *Biochem J* 418(3):625-634.
185. Li H*, et al.* (2007) Ewing sarcoma gene EWS is essential for meiosis and B lymphocyte development. *J Clin Invest* 117(5):1314-1323.

186. Altmeyer M*, et al.* (2015) Liquid demixing of intrinsically disordered proteins is seeded by poly(ADP-ribose). *Nat Commun* 6:8088.
187. Park H*, et al.* (2014) Ewing sarcoma EWS protein regulates midzone formation by recruiting Aurora B kinase to the midzone. *Cell Cycle* 13(15):2391-2399.
188. Park JH*, et al.* (2013) A multifunctional protein, EWS, is essential for early brown fat lineage determination. *Dev Cell* 26(4):393-404.
189. Park JH & Lee SB (2015) An essential role for Ewing sarcoma gene (EWS) in early white adipogenesis. *Obesity (Silver Spring)* 23(1):138-144.
190. Cavazzana AO, Miser JS, Jefferson J, & Triche TJ (1987) Experimental evidence for a neural origin of Ewing's sarcoma of bone. *Am J Pathol* 127(3):507-518.
191. Coles EG, Lawlor ER, & Bronner-Fraser M (2008) EWS-FLI1 causes neuroepithelial defects and abrogates emigration of neural crest stem cells. *Stem Cells* 26(9):2237-2244.
192. Riggi N*, et al.* (2005) Development of Ewing's sarcoma from primary bone marrow-derived mesenchymal progenitor cells. *Cancer Res* 65(24):11459-11468.
193. Tirode F*, et al.* (2007) Mesenchymal stem cell features of Ewing tumors. *Cancer Cell* 11(5):421-429.
194. Potikyan G*, et al.* (2008) Genetically defined EWS/FLI1 model system suggests mesenchymal origin of Ewing's family tumors. *Lab Invest* 88(12):1291-1302.
195. Miyagawa Y*, et al.* (2008) Inducible expression of chimeric EWS/ETS proteins confers Ewing's family tumor-like phenotypes to human mesenchymal progenitor cells. *Mol Cell Biol* 28(7):2125-2137.
196. Kauer M*, et al.* (2009) A molecular function map of Ewing's sarcoma. *PLoS One* 4(4):e5415.
197. Tanaka M*, et al.* (2014) Ewing's sarcoma precursors are highly enriched in embryonic osteochondrogenic progenitors. *J Clin Invest* 124(7):3061-3074.
198. Lin PP*, et al.* (2008) EWS-FLI1 induces developmental abnormalities and accelerates sarcoma formation in a transgenic mouse model. *Cancer Res* 68(21):8968-8975.
199. Torchia EC, Boyd K, Rehg JE, Qu C, & Baker SJ (2007) EWS/FLI-1 induces rapid onset of myeloid/erythroid leukemia in mice. *Mol Cell Biol* 27(22):7918-7934.
200. Leacock SW*, et al.* (2012) A zebrafish transgenic model of Ewing's sarcoma reveals conserved mediators of EWS-FLI1 tumorigenesis. *Dis Model Mech* 5(1):95-106.
201. Stegmaier K*, et al.* (2007) Signature-based small molecule screening identifies cytosine arabinoside as an EWS/FLI modulator in Ewing sarcoma. *PLoS Med* 4(4):e122.
202. DuBois SG*, et al.* (2009) Phase II study of intermediate-dose cytarabine in patients with relapsed or refractory Ewing sarcoma: a report from the Children's Oncology Group. *Pediatric blood & cancer* 52(3):324-327.
203. Grohar PJ*, et al.* (2011) Identification of an inhibitor of the EWS-FLI1 oncogenic transcription factor by high-throughput screening. *J Natl Cancer Inst* 103(12):962-978.
204. Kofman S, Medrek TJ, & Alexander RW (1964) Mithramycin in the Treatment of Embryonal Cancer. *Cancer* 17:938-948.
205. Kofman S, Perlia CP, & Economou SG (1973) Mithramycin in the treatment of metastatic Ewing's sarcoma. *Cancer* 31(4):889-893.
206. Brenner JC*, et al.* (2011) Mechanistic rationale for inhibition of poly(ADP-ribose) polymerase in ETS gene fusion-positive prostate cancer. *Cancer Cell* 19(5):664-678.
207. Brenner JC*, et al.* (2012) PARP-1 inhibition as a targeted strategy to treat Ewing's sarcoma. *Cancer Res* 72(7):1608-1613.
208. Garnett MJ*, et al.* (2012) Systematic identification of genomic markers of drug sensitivity in cancer cells. *Nature* 483(7391):570-575.
209. Stewart E*, et al.* (2014) Targeting the DNA repair pathway in Ewing sarcoma. *Cell Rep* 9(3):829-841.
210. van Valen F, Winkelmann W, & Jurgens H (1992) Type I and type II insulin-like growth factor receptors and their function in human Ewing's sarcoma cells. *J Cancer Res Clin Oncol* 118(4):269-275.

211. Scotlandi K*, et al.* (1996) Insulin-like growth factor I receptor-mediated circuit in Ewing's sarcoma/peripheral neuroectodermal tumor: a possible therapeutic target. *Cancer Res* 56(20):4570-4574.
212. Toretsky JA, Kalebic T, Blakesley V, LeRoith D, & Helman LJ (1997) The insulin-like growth factor-I receptor is required for EWS/FLI-1 transformation of fibroblasts. *The Journal of biological chemistry* 272(49):30822-30827.
213. Scotlandi K*, et al.* (1998) Blockage of insulin-like growth factor-I receptor inhibits the growth of Ewing's sarcoma in athymic mice. *Cancer Res* 58(18):4127-4131.
214. Scotlandi K*, et al.* (2002) Expression of an IGF-I receptor dominant negative mutant induces apoptosis, inhibits tumorigenesis and enhances chemosensitivity in Ewing's sarcoma cells. *Int J Cancer* 101(1):11-16.
215. Scotlandi K*, et al.* (2002) Effectiveness of insulin-like growth factor I receptor antisense strategy against Ewing's sarcoma cells. *Cancer Gene Ther* 9(3):296-307.
216. McKinsey EL*, et al.* (2011) A novel oncogenic mechanism in Ewing sarcoma involving IGF pathway targeting by EWS/Fli1-regulated microRNAs. *Oncogene* 30(49):4910-4920.
217. Tolcher AW*, et al.* (2009) Phase I, pharmacokinetic, and pharmacodynamic study of AMG 479, a fully human monoclonal antibody to insulin-like growth factor receptor 1. *J Clin Oncol* 27(34):5800-5807.
218. Olmos D*, et al.* (2010) Safety, pharmacokinetics, and preliminary activity of the anti-IGF-1R antibody figitumumab (CP-751,871) in patients with sarcoma and Ewing's sarcoma: a phase 1 expansion cohort study. *Lancet Oncol* 11(2):129-135.
219. Olmos D, Tan DS, Jones RL, & Judson IR (2010) Biological rationale and current clinical experience with anti-insulin-like growth factor 1 receptor monoclonal antibodies in treating sarcoma: twenty years from the bench to the bedside. *Cancer J* 16(3):183-194.
220. Pappo AS*, et al.* (2011) R1507, a monoclonal antibody to the insulin-like growth factor 1 receptor, in patients with recurrent or refractory Ewing sarcoma family of tumors: results of a phase II Sarcoma Alliance for Research through Collaboration study. *J Clin Oncol* 29(34):4541-4547.
221. Pappo AS*, et al.* (2014) A phase 2 trial of R1507, a monoclonal antibody to the insulin-like growth factor-1 receptor (IGF-1R), in patients with recurrent or refractory rhabdomyosarcoma, osteosarcoma, synovial sarcoma, and other soft tissue sarcomas: results of a Sarcoma Alliance for Research Through Collaboration study. *Cancer* 120(16):2448-2456.
222. Borinstein SC*, et al.* (2011) Investigation of the insulin-like growth factor-1 signaling pathway in localized Ewing sarcoma: a report from the Children's Oncology Group. *Cancer* 117(21):4966-4976.
223. Garofalo C*, et al.* (2011) Efficacy of and resistance to anti-IGF-1R therapies in Ewing's sarcoma is dependent on insulin receptor signaling. *Oncogene* 30(24):2730-2740.
224. Scotlandi K*, et al.* (2011) Expression of insulin-like growth factor system components in Ewing's sarcoma and their association with survival. *Eur J Cancer* 47(8):1258-1266.
225. Juergens H*, et al.* (2011) Preliminary efficacy of the anti-insulin-like growth factor type 1 receptor antibody figitumumab in patients with refractory Ewing sarcoma. *J Clin Oncol* 29(34):4534-4540.
226. Tomazou EM*, et al.* (2015) Epigenome mapping reveals distinct modes of gene regulation and widespread enhancer reprogramming by the oncogenic fusion protein EWS-FLI1. *Cell Rep* 10(7):1082-1095.
227. Grohar PJ*, et al.* (2016) Functional Genomic Screening Reveals Splicing of the EWS-FLI1 Fusion Transcript as a Vulnerability in Ewing Sarcoma. *Cell Rep* 14(3):598-610.
228. Nakamura T*, et al.* (2007) The mechanism of cross-resistance to proteasome inhibitor bortezomib and overcoming resistance in Ewing's family tumor cells. *Int J Oncol* 31(4):803-811.
229. Houghton PJ*, et al.* (2008) Initial testing (stage 1) of the proteasome inhibitor bortezomib by the pediatric preclinical testing program. *Pediatric blood & cancer* 50(1):37-45.

230. Lu G, Punj V, & Chaudhary PM (2008) Proteasome inhibitor Bortezomib induces cell cycle arrest and apoptosis in cell lines derived from Ewing's sarcoma family of tumors and synergizes with TRAIL. *Cancer Biol Ther* 7(4):603-608.
231. Smith MA*, et al.* (2012) Initial testing of the investigational NEDD8-activating enzyme inhibitor MLN4924 by the pediatric preclinical testing program. *Pediatric blood & cancer* 59(2):246-253.
232. Carol H*, et al.* (2013) Initial testing of the MDM2 inhibitor RG7112 by the Pediatric Preclinical Testing Program. *Pediatric blood & cancer* 60(4):633-641.
233. Bachmaier R*, et al.* (2009) O-GlcNAcylation is involved in the transcriptional activity of EWS-FLI1 in Ewing's sarcoma. *Oncogene* 28(9):1280-1284.
234. Schlottmann S*, et al.* (2012) Acetylation Increases EWS-FLI1 DNA Binding and Transcriptional Activity. *Front Oncol* 2:107.
235. Elzi DJ, Song M, Hakala K, Weintraub ST, & Shiio Y (2014) Proteomic Analysis of the EWS-Fli-1 Interactome Reveals the Role of the Lysosome in EWS-Fli-1 Turnover. *J Proteome Res* 13(8):3783-3791.
236. Schaefer KL*, et al.* (2008) Microarray analysis of Ewing's sarcoma family of tumours reveals characteristic gene expression signatures associated with metastasis and resistance to chemotherapy. *Eur J Cancer* 44(5):699-709.
237. De Duve C, Gianetto R, Appelmans F, & Wattiaux R (1953) Enzymic content of the mitochondria fraction. *Nature* 172(4390):1143-1144.
238. Ciechanover A (2009) Tracing the history of the ubiquitin proteolytic system: the pioneering article. *Biochem Biophys Res Commun* 387(1):1-10.
239. Hershko A, Ciechanover A, & Rose IA (1979) Resolution of the ATP-dependent proteolytic system from reticulocytes: a component that interacts with ATP. *Proc Natl Acad Sci U S A* 76(7):3107-3110.
240. Wilkinson KD (2005) The discovery of ubiquitin-dependent proteolysis. *Proc Natl Acad Sci U S A* 102(43):15280-15282.
241. Ciechanover A (2005) Intracellular protein degradation: from a vague idea, through the lysosome and the ubiquitin-proteasome system, and onto human diseases and drug targeting (Nobel lecture). *Angew Chem Int Ed Engl* 44(37):5944-5967.
242. Hershko A & Ciechanover A (1992) The ubiquitin system for protein degradation. *Annu Rev Biochem* 61:761-807.
243. Hershko A & Ciechanover A (1998) The ubiquitin system. *Annu Rev Biochem* 67:425-479.
244. Glickman MH & Ciechanover A (2002) The ubiquitin-proteasome proteolytic pathway: destruction for the sake of construction. *Physiological reviews* 82(2):373-428.
245. Zhao J, Zhai B, Gygi SP, & Goldberg AL (2015) mTOR inhibition activates overall protein degradation by the ubiquitin proteasome system as well as by autophagy. *Proc Natl Acad Sci U S A* 112(52):15790-15797.
246. Driscoll J & Goldberg AL (1990) The proteasome (multicatalytic protease) is a component of the 1500-kDa proteolytic complex which degrades ubiquitin-conjugated proteins. *The Journal of biological chemistry* 265(9):4789-4792.
247. von Mikecz A (2006) The nuclear ubiquitin-proteasome system. *J Cell Sci* 119(Pt 10):1977-1984.
248. Finley D (2009) Recognition and processing of ubiquitin-protein conjugates by the proteasome. *Annu Rev Biochem* 78:477-513.
249. Hershko A, Leshinsky E, Ganoth D, & Heller H (1984) ATP-dependent degradation of ubiquitin-protein conjugates. *Proc Natl Acad Sci U S A* 81(6):1619-1623.
250. Hough R, Pratt G, & Rechsteiner M (1986) Ubiquitin-lysozyme conjugates. Identification and characterization of an ATP-dependent protease from rabbit reticulocyte lysates. *The Journal of biological chemistry* 261(5):2400-2408.
251. Hough R & Rechsteiner M (1986) Ubiquitin-lysozyme conjugates. Purification and susceptibility to proteolysis. *The Journal of biological chemistry* 261(5):2391-2399.

252. Hough R, Pratt G, & Rechsteiner M (1987) Purification of two high molecular weight proteases from rabbit reticulocyte lysate. *The Journal of biological chemistry* 262(17):8303-8313.
253. Tanaka K*, et al.* (1988) Proteasomes (multi-protease complexes) as 20 S ring-shaped particles in a variety of eukaryotic cells. *The Journal of biological chemistry* 263(31):16209-16217.
254. Arrigo AP, Tanaka K, Goldberg AL, & Welch WJ (1988) Identity of the 19S 'prosome' particle with the large multifunctional protease complex of mammalian cells (the proteasome). *Nature* 331(6152):192-194.
255. Eytan E, Ganoth D, Armon T, & Hershko A (1989) ATP-dependent incorporation of 20S protease into the 26S complex that degrades proteins conjugated to ubiquitin. *Proc Natl Acad Sci U S A* 86(20):7751-7755.
256. Armon T, Ganoth D, & Hershko A (1990) Assembly of the 26 S complex that degrades proteins ligated to ubiquitin is accompanied by the formation of ATPase activity. *The Journal of biological chemistry* 265(34):20723-20726.
257. Walz J*, et al.* (1998) 26S proteasome structure revealed by three-dimensional electron microscopy. *J Struct Biol* 121(1):19-29.
258. Lander GC*, et al.* (2012) Complete subunit architecture of the proteasome regulatory particle. *Nature* 482(7384):186-191.
259. Hoffman L, Pratt G, & Rechsteiner M (1992) Multiple forms of the 20 S multicatalytic and the 26 S ubiquitin/ATP-dependent proteases from rabbit reticulocyte lysate. *The Journal of biological chemistry* 267(31):22362-22368.
260. Dubiel W, Ferrell K, & Rechsteiner M (1995) Subunits of the regulatory complex of the 26S protease. *Mol Biol Rep* 21(1):27-34.
261. Orino E*, et al.* (1991) ATP-dependent reversible association of proteasomes with multiple protein components to form 26S complexes that degrade ubiquitinated proteins in human HL-60 cells. *FEBS Lett* 284(2):206-210.
262. Fu H*, et al.* (1998) Multiubiquitin chain binding and protein degradation are mediated by distinct domains within the 26 S proteasome subunit Mcb1. *The Journal of biological chemistry* 273(4):1970-1981.
263. Peth A, Besche HC, & Goldberg AL (2009) Ubiquitinated proteins activate the proteasome by binding to Usp14/Ubp6, which causes 20S gate opening. *Mol Cell* 36(5):794-804.
264. Haas AL & Rose IA (1982) The mechanism of ubiquitin activating enzyme. A kinetic and equilibrium analysis. *The Journal of biological chemistry* 257(17):10329-10337.
265. Waxman L, Fagan JM, & Goldberg AL (1987) Demonstration of two distinct high molecular weight proteases in rabbit reticulocytes, one of which degrades ubiquitin conjugates. *The Journal of biological chemistry* 262(6):2451-2457.
266. Ciechanover A, Finley D, & Varshavsky A (1984) Ubiquitin dependence of selective protein degradation demonstrated in the mammalian cell cycle mutant ts85. *Cell* 37(1):57-66.
267. Finley D, Ciechanover A, & Varshavsky A (1984) Thermolability of ubiquitin-activating enzyme from the mammalian cell cycle mutant ts85. *Cell* 37(1):43-55.
268. Jentsch S (1992) The ubiquitin-conjugation system. *Annual review of genetics* 26:179-207.
269. Hochstrasser M (2006) Lingering mysteries of ubiquitin-chain assembly. *Cell* 124(1):27-34.
270. Ye Y & Rape M (2009) Building ubiquitin chains: E2 enzymes at work. *Nat Rev Mol Cell Biol* 10(11):755-764.
271. Husnjak K & Dikic I (2012) Ubiquitin-binding proteins: decoders of ubiquitin-mediated cellular functions. *Annu Rev Biochem* 81:291-322.
272. Heride C, Urbe S, & Clague MJ (2014) Ubiquitin code assembly and disassembly. *Curr Biol* 24(6):R215-220.
273. Freemont PS, Hanson IM, & Trowsdale J (1991) A novel cysteine-rich sequence motif. *Cell* 64(3):483-484.
274. Huibregtse JM, Scheffner M, Beaudenon S, & Howley PM (1995) A family of proteins structurally and functionally related to the E6-AP ubiquitin-protein ligase. *Proc Natl Acad Sci U S A* 92(11):5249.

275. Johnson ES, Ma PC, Ota IM, & Varshavsky A (1995) A proteolytic pathway that recognizes ubiquitin as a degradation signal. *The Journal of biological chemistry* 270(29):17442-17456.
276. Petroski MD & Deshaies RJ (2005) Mechanism of lysine 48-linked ubiquitin-chain synthesis by the cullin-RING ubiquitin-ligase complex SCF-Cdc34. *Cell* 123(6):1107-1120.
277. Wiborg O*, et al.* (1985) The human ubiquitin multigene family: some genes contain multiple directly repeated ubiquitin coding sequences. *EMBO J* 4(3):755-759.
278. Varshavsky A (2005) Regulated protein degradation. *Trends Biochem Sci* 30(6):283-286.
279. Chau V*, et al.* (1989) A multiubiquitin chain is confined to specific lysine in a targeted short-lived protein. *Science* 243(4898):1576-1583.
280. Breitschopf K, Bengal E, Ziv T, Admon A, & Ciechanover A (1998) A novel site for ubiquitination: the N-terminal residue, and not internal lysines of MyoD, is essential for conjugation and degradation of the protein. *EMBO J* 17(20):5964-5973.
281. Bloom J, Amador V, Bartolini F, DeMartino G, & Pagano M (2003) Proteasome-mediated degradation of p21 via N-terminal ubiquitinylation. *Cell* 115(1):71-82.
282. Komander D & Rape M (2012) The ubiquitin code. *Annu Rev Biochem* 81:203-229.
283. Johnson ES, Bartel B, Seufert W, & Varshavsky A (1992) Ubiquitin as a degradation signal. *EMBO J* 11(2):497-505.
284. Finley D*, et al.* (1994) Inhibition of proteolysis and cell cycle progression in a multiubiquitination-deficient yeast mutant. *Mol Cell Biol* 14(8):5501-5509.
285. Thrower JS, Hoffman L, Rechsteiner M, & Pickart CM (2000) Recognition of the polyubiquitin proteolytic signal. *EMBO J* 19(1):94-102.
286. Boutet SC, Disatnik MH, Chan LS, Iori K, & Rando TA (2007) Regulation of Pax3 by proteasomal degradation of monoubiquitinated protein in skeletal muscle progenitors. *Cell* 130(2):349-362.
287. Shabek N*, et al.* (2012) The size of the proteasomal substrate determines whether its degradation will be mediated by mono- or polyubiquitylation. *Mol Cell* 48(1):87-97.
288. Baboshina OV & Haas AL (1996) Novel multiubiquitin chain linkages catalyzed by the conjugating enzymes E2EPF and RAD6 are recognized by 26 S proteasome subunit 5. *The Journal of biological chemistry* 271(5):2823-2831.
289. Xu P*, et al.* (2009) Quantitative proteomics reveals the function of unconventional ubiquitin chains in proteasomal degradation. *Cell* 137(1):133-145.
290. Matsumoto ML*, et al.* (2010) K11-linked polyubiquitination in cell cycle control revealed by a K11 linkage-specific antibody. *Mol Cell* 39(3):477-484.
291. Wickliffe KE, Williamson A, Meyer HJ, Kelly A, & Rape M (2011) K11-linked ubiquitin chains as novel regulators of cell division. *Trends Cell Biol* 21(11):656-663.
292. Arnason T & Ellison MJ (1994) Stress resistance in Saccharomyces cerevisiae is strongly correlated with assembly of a novel type of multiubiquitin chain. *Mol Cell Biol* 14(12):7876-7883.
293. Spence J, Sadis S, Haas AL, & Finley D (1995) A ubiquitin mutant with specific defects in DNA repair and multiubiquitination. *Mol Cell Biol* 15(3):1265-1273.
294. Galan JM & Haguenauer-Tsapis R (1997) Ubiquitin lys63 is involved in ubiquitination of a yeast plasma membrane protein. *EMBO J* 16(19):5847-5854.
295. Huang F, Kirkpatrick D, Jiang X, Gygi S, & Sorkin A (2006) Differential regulation of EGF receptor internalization and degradation by multiubiquitination within the kinase domain. *Mol Cell* 21(6):737-748.
296. Huang F*, et al.* (2013) Lysine 63-linked polyubiquitination is required for EGF receptor degradation. *Proc Natl Acad Sci U S A* 110(39):15722-15727.
297. Kulathu Y & Komander D (2012) Atypical ubiquitylation - the unexplored world of polyubiquitin beyond Lys48 and Lys63 linkages. *Nat Rev Mol Cell Biol* 13(8):508-523.
298. Kaiser SE*, et al.* (2011) Protein standard absolute quantification (PSAQ) method for the measurement of cellular ubiquitin pools. *Nat Methods* 8(8):691-696.
299. Zheng N*, et al.* (2002) Structure of the Cul1-Rbx1-Skp1-F boxSkp2 SCF ubiquitin ligase complex. *Nature* 416(6882):703-709.

300. Petroski MD & Deshaies RJ (2005) Function and regulation of cullin-RING ubiquitin ligases. *Nat Rev Mol Cell Biol* 6(1):9-20.
301. Cardozo T & Pagano M (2004) The SCF ubiquitin ligase: insights into a molecular machine. *Nat Rev Mol Cell Biol* 5(9):739-751.
302. Deshaies RJ & Joazeiro CA (2009) RING domain E3 ubiquitin ligases. *Annu Rev Biochem* 78:399-434.
303. Feldman RM, Correll CC, Kaplan KB, & Deshaies RJ (1997) A complex of Cdc4p, Skp1p, and Cdc53p/cullin catalyzes ubiquitination of the phosphorylated CDK inhibitor Sic1p. *Cell* 91(2):221-230.
304. Skowyra D, Craig KL, Tyers M, Elledge SJ, & Harper JW (1997) F-box proteins are receptors that recruit phosphorylated substrates to the SCF ubiquitin-ligase complex. *Cell* 91(2):209-219.
305. Geyer R, Wee S, Anderson S, Yates J, & Wolf DA (2003) BTB/POZ domain proteins are putative substrate adaptors for cullin 3 ubiquitin ligases. *Mol Cell* 12(3):783-790.
306. Xu L*, et al.* (2003) BTB proteins are substrate-specific adaptors in an SCF-like modular ubiquitin ligase containing CUL-3. *Nature* 425(6955):316-321.
307. Wu G*, et al.* (2003) Structure of a beta-TrCP1-Skp1-beta-catenin complex: destruction motif binding and lysine specificity of the SCF(beta-TrCP1) ubiquitin ligase. *Mol Cell* 11(6):1445-1456.
308. Liakopoulos D, Doenges G, Matuschewski K, & Jentsch S (1998) A novel protein modification pathway related to the ubiquitin system. *EMBO J* 17(8):2208-2214.
309. Mundt KE*, et al.* (1999) The COP9/signalosome complex is conserved in fission yeast and has a role in S phase. *Curr Biol* 9(23):1427-1430.
310. Naumann M, Bech-Otschir D, Huang X, Ferrell K, & Dubiel W (1999) COP9 signalosome-directed c-Jun activation/stabilization is independent of JNK. *The Journal of biological chemistry* 274(50):35297-35300.
311. Bech-Otschir D*, et al.* (2001) COP9 signalosome-specific phosphorylation targets p53 to degradation by the ubiquitin system. *EMBO J* 20(7):1630-1639.
312. Cope GA*, et al.* (2002) Role of predicted metalloprotease motif of Jab1/Csn5 in cleavage of Nedd8 from Cul1. *Science* 298(5593):608-611.
313. Yang X*, et al.* (2002) The COP9 signalosome inhibits p27(kip1) degradation and impedes G1-S phase progression via deneddylation of SCF Cul1. *Curr Biol* 12(8):667-672.
314. Schmidt MW, McQuary PR, Wee S, Hofmann K, & Wolf DA (2009) F-box-directed CRL complex assembly and regulation by the CSN and CAND1. *Mol Cell* 35(5):586-597.
315. Liu J, Furukawa M, Matsumoto T, & Xiong Y (2002) NEDD8 modification of CUL1 dissociates p120(CAND1), an inhibitor of CUL1-SKP1 binding and SCF ligases. *Mol Cell* 10(6):1511-1518.
316. Pierce NW*, et al.* (2013) Cand1 promotes assembly of new SCF complexes through dynamic exchange of F box proteins. *Cell* 153(1):206-215.
317. Zheng J*, et al.* (2002) CAND1 binds to unneddylated CUL1 and regulates the formation of SCF ubiquitin E3 ligase complex. *Mol Cell* 10(6):1519-1526.
318. Hwang JW, Min KW, Tamura TA, & Yoon JB (2003) TIP120A associates with unneddylated cullin 1 and regulates its neddylation. *FEBS Lett* 541(1-3):102-108.
319. Min KW*, et al.* (2005) CAND1 enhances deneddylation of CUL1 by COP9 signalosome. *Biochem Biophys Res Commun* 334(3):867-874.
320. Bai C*, et al.* (1996) SKP1 connects cell cycle regulators to the ubiquitin proteolysis machinery through a novel motif, the F-box. *Cell* 86(2):263-274.
321. Cenciarelli C*, et al.* (1999) Identification of a family of human F-box proteins. *Curr Biol* 9(20):1177-1179.
322. Smith TF, Gaitatzes C, Saxena K, & Neer EJ (1999) The WD repeat: a common architecture for diverse functions. *Trends Biochem Sci* 24(5):181-185.
323. Winston JT, Koepp DM, Zhu C, Elledge SJ, & Harper JW (1999) A family of mammalian F-box proteins. *Curr Biol* 9(20):1180-1182.

324. Kossatz U*, et al.* (2004) Skp2-dependent degradation of p27kip1 is essential for cell cycle progression. *Genes Dev* 18(21):2602-2607.
325. Emanuele MJ*, et al.* (2011) Global identification of modular cullin-RING ligase substrates. *Cell* 147(2):459-474.
326. Rotin D & Kumar S (2009) Physiological functions of the HECT family of ubiquitin ligases. *Nat Rev Mol Cell Biol* 10(6):398-409.
327. Scheffner M & Kumar S (2014) Mammalian HECT ubiquitin-protein ligases: biological and pathophysiological aspects. *Biochim Biophys Acta* 1843(1):61-74.
328. Wang M & Pickart CM (2005) Different HECT domain ubiquitin ligases employ distinct mechanisms of polyubiquitin chain synthesis. *EMBO J* 24(24):4324-4333.
329. Chen HI & Sudol M (1995) The WW domain of Yes-associated protein binds a proline-rich ligand that differs from the consensus established for Src homology 3-binding modules. *Proc Natl Acad Sci U S A* 92(17):7819-7823.
330. Bedford MT, Chan DC, & Leder P (1997) FBP WW domains and the Abl SH3 domain bind to a specific class of proline-rich ligands. *EMBO J* 16(9):2376-2383.
331. Ermekova KS*, et al.* (1997) The WW domain of neural protein FE65 interacts with proline-rich motifs in Mena, the mammalian homolog of Drosophila enabled. *The Journal of biological chemistry* 272(52):32869-32877.
332. Yaffe MB*, et al.* (1997) Sequence-specific and phosphorylation-dependent proline isomerization: a potential mitotic regulatory mechanism. *Science* 278(5345):1957-1960.
333. Lu PJ, Zhou XZ, Shen M, & Lu KP (1999) Function of WW domains as phosphoserine- or phosphothreonine-binding modules. *Science* 283(5406):1325-1328.
334. Bedford MT, Sarbassova D, Xu J, Leder P, & Yaffe MB (2000) A novel pro-Arg motif recognized by WW domains. *The Journal of biological chemistry* 275(14):10359-10369.
335. Ingham RJ, Gish G, & Pawson T (2004) The Nedd4 family of E3 ubiquitin ligases: functional diversity within a common modular architecture. *Oncogene* 23(11):1972-1984.
336. Moren A, Imamura T, Miyazono K, Heldin CH, & Moustakas A (2005) Degradation of the tumor suppressor Smad4 by WW and HECT domain ubiquitin ligases. *The Journal of biological chemistry* 280(23):22115-22123.
337. Wang X*, et al.* (2007) NEDD4-1 is a proto-oncogenic ubiquitin ligase for PTEN. *Cell* 128(1):129-139.
338. Salah Z, Cohen S, Itzhaki E, & Aqeilan RI (2013) NEDD4 E3 ligase inhibits the activity of the Hippo pathway by targeting LATS1 for degradation. *Cell Cycle* 12(24):3817-3823.
339. Pirozzi G*, et al.* (1997) Identification of novel human WW domain-containing proteins by cloning of ligand targets. *The Journal of biological chemistry* 272(23):14611-14616.
340. Huang K*, et al.* (2000) A HECT domain ubiquitin ligase closely related to the mammalian protein WWP1 is essential for Caenorhabditis elegans embryogenesis. *Gene* 252(1-2):137-145.
341. Zhi X & Chen C (2012) WWP1: a versatile ubiquitin E3 ligase in signaling and diseases. *Cell Mol Life Sci* 69(9):1425-1434.
342. Mosser EA*, et al.* (1998) Physical and functional interactions between the transactivation domain of the hematopoietic transcription factor NF-E2 and WW domains. *Biochemistry* 37(39):13686-13695.
343. Conkright MD, Wani MA, & Lingrel JB (2001) Lung Kruppel-like factor contains an autoinhibitory domain that regulates its transcriptional activation by binding WWP1, an E3 ubiquitin ligase. *The Journal of biological chemistry* 276(31):29299-29306.
344. Zhang X, Srinivasan SV, & Lingrel JB (2004) WWP1-dependent ubiquitination and degradation of the lung Kruppel-like factor, KLF2. *Biochem Biophys Res Commun* 316(1):139-148.
345. Komuro A*, et al.* (2004) Negative regulation of transforming growth factor-beta (TGF-beta) signaling by WW domain-containing protein 1 (WWP1). *Oncogene* 23(41):6914-6923.
346. Chen C*, et al.* (2008) The WW domain containing E3 ubiquitin protein ligase 1 upregulates ErbB2 and EGFR through RING finger protein 11. *Oncogene* 27(54):6845-6855.

347. Li Y, Zhou Z, & Chen C (2008) WW domain-containing E3 ubiquitin protein ligase 1 targets p63 transcription factor for ubiquitin-mediated proteasomal degradation and regulates apoptosis. *Cell Death Differ* 15(12):1941-1951.
348. Feng SM*, et al.* (2009) The E3 ubiquitin ligase WWP1 selectively targets HER4 and its proteolytically derived signaling isoforms for degradation. *Mol Cell Biol* 29(3):892-906.
349. Li Y, Zhou Z, Alimandi M, & Chen C (2009) WW domain containing E3 ubiquitin protein ligase 1 targets the full-length ErbB4 for ubiquitin-mediated degradation in breast cancer. *Oncogene* 28(33):2948-2958.
350. Yeung B, Ho KC, & Yang X (2013) WWP1 E3 ligase targets LATS1 for ubiquitin-mediated degradation in breast cancer cells. *PLoS One* 8(4):e61027.
351. Cao X*, et al.* (2011) WW domain-containing E3 ubiquitin protein ligase 1 (WWP1) delays cellular senescence by promoting p27(Kip1) degradation in human diploid fibroblasts. *The Journal of biological chemistry* 286(38):33447-33456.
352. Chen C*, et al.* (2007) Ubiquitin E3 ligase WWP1 as an oncogenic factor in human prostate cancer. *Oncogene* 26(16):2386-2394.
353. Chen C, Zhou Z, Ross JS, Zhou W, & Dong JT (2007) The amplified WWP1 gene is a potential molecular target in breast cancer. *Int J Cancer* 121(1):80-87.
354. Nguyen Huu NS*, et al.* (2008) Tumour-promoting activity of altered WWP1 expression in breast cancer and its utility as a prognostic indicator. *J Pathol* 216(1):93-102.
355. Chen C*, et al.* (2009) Overexpression of WWP1 is associated with the estrogen receptor and insulin-like growth factor receptor 1 in breast carcinoma. *Int J Cancer* 124(12):2829-2836.
356. Courivaud T*, et al.* (2015) Functional Characterization of a WWP1/Tiul1 Tumor-derived Mutant Reveals a Paradigm of Its Constitutive Activation in Human Cancer. *The Journal of biological chemistry* 290(34):21007-21018.
357. Zhang XF*, et al.* (2015) Overexpression of WWP1 promotes tumorigenesis and predicts unfavorable prognosis in patients with hepatocellular carcinoma. *Oncotarget* 6(38):40920-40933.
358. Hatakeyama S, Yada M, Matsumoto M, Ishida N, & Nakayama KI (2001) U box proteins as a new family of ubiquitin-protein ligases. *The Journal of biological chemistry* 276(35):33111-33120.
359. Pringa E, Martinez-Noel G, Muller U, & Harbers K (2001) Interaction of the ring finger-related U-box motif of a nuclear dot protein with ubiquitin-conjugating enzymes. *The Journal of biological chemistry* 276(22):19617-19623.
360. Skaar JR, Pagan JK, & Pagano M (2013) Mechanisms and function of substrate recruitment by F-box proteins. *Nat Rev Mol Cell Biol* 14(6):369-381.
361. Cyr DM, Hohfeld J, & Patterson C (2002) Protein quality control: U-box-containing E3 ubiquitin ligases join the fold. *Trends Biochem Sci* 27(7):368-375.
362. Hatakeyama S & Nakayama KI (2003) U-box proteins as a new family of ubiquitin ligases. *Biochem Biophys Res Commun* 302(4):635-645.
363. Nijman SM*, et al.* (2005) A genomic and functional inventory of deubiquitinating enzymes. *Cell* 123(5):773-786.
364. Fraile JM, Quesada V, Rodriguez D, Freije JM, & Lopez-Otin C (2012) Deubiquitinases in cancer: new functions and therapeutic options. *Oncogene* 31(19):2373-2388.
365. Quesada V*, et al.* (2004) Cloning and enzymatic analysis of 22 novel human ubiquitin-specific proteases. *Biochem Biophys Res Commun* 314(1):54-62.
366. Hu M*, et al.* (2002) Crystal structure of a UBP-family deubiquitinating enzyme in isolation and in complex with ubiquitin aldehyde. *Cell* 111(7):1041-1054.
367. Eytan E, Armon T, Heller H, Beck S, & Hershko A (1993) Ubiquitin C-terminal hydrolase activity associated with the 26 S protease complex. *The Journal of biological chemistry* 268(7):4668-4674.
368. Ventii KH & Wilkinson KD (2008) Protein partners of deubiquitinating enzymes. *Biochem J* 414(2):161-175.

369. VanderLinden RT*, et al.* (2015) Structural basis for the activation and inhibition of the UCH37 deubiquitylase. *Mol Cell* 57(5):901-911.
370. Komander D, Clague MJ, & Urbe S (2009) Breaking the chains: structure and function of the deubiquitinases. *Nat Rev Mol Cell Biol* 10(8):550-563.
371. Komander D*, et al.* (2009) Molecular discrimination of structurally equivalent Lys 63-linked and linear polyubiquitin chains. *EMBO reports* 10(5):466-473.
372. Wertz IE*, et al.* (2004) De-ubiquitination and ubiquitin ligase domains of A20 downregulate NF-kappaB signalling. *Nature* 430(7000):694-699.
373. Sowa ME, Bennett EJ, Gygi SP, & Harper JW (2009) Defining the human deubiquitinating enzyme interaction landscape. *Cell* 138(2):389-403.
374. Clague MJ, Coulson JM, & Urbe S (2012) Cellular functions of the DUBs. *J Cell Sci* 125(Pt 2):277-286.
375. Jacq X, Kemp M, Martin NM, & Jackson SP (2013) Deubiquitylating enzymes and DNA damage response pathways. *Cell Biochem Biophys* 67(1):25-43.
376. Sahtoe DD & Sixma TK (2015) Layers of DUB regulation. *Trends Biochem Sci* 40(8):456-467.
377. Borodovsky A*, et al.* (2001) A novel active site-directed probe specific for deubiquitylating enzymes reveals proteasome association of USP14. *EMBO J* 20(18):5187-5196.
378. Li T, Naqvi NI, Yang H, & Teo TS (2000) Identification of a 26S proteasome-associated UCH in fission yeast. *Biochem Biophys Res Commun* 272(1):270-275.
379. Lee MJ, Lee BH, Hanna J, King RW, & Finley D (2011) Trimming of ubiquitin chains by proteasome-associated deubiquitinating enzymes. *Mol Cell Proteomics* 10(5):R110 003871.
380. Hu M*, et al.* (2005) Structure and mechanisms of the proteasome-associated deubiquitinating enzyme USP14. *EMBO J* 24(21):3747-3756.
381. Renatus M*, et al.* (2006) Structural basis of ubiquitin recognition by the deubiquitinating protease USP2. *Structure* 14(8):1293-1302.
382. Hamazaki J*, et al.* (2006) A novel proteasome interacting protein recruits the deubiquitinating enzyme UCH37 to 26S proteasomes. *EMBO J* 25(19):4524-4536.
383. Yao T*, et al.* (2006) Proteasome recruitment and activation of the Uch37 deubiquitinating enzyme by Adrm1. *Nat Cell Biol* 8(9):994-1002.
384. Maiti TK*, et al.* (2011) Crystal structure of the catalytic domain of UCHL5, a proteasome-associated human deubiquitinating enzyme, reveals an unproductive form of the enzyme. *FEBS J* 278(24):4917-4926.
385. Hassink GC*, et al.* (2009) The ER-resident ubiquitin-specific protease 19 participates in the UPR and rescues ERAD substrates. *EMBO reports* 10(7):755-761.
386. Iphofer A*, et al.* (2012) Profiling ubiquitin linkage specificities of deubiquitinating enzymes with branched ubiquitin isopeptide probes. *Chembiochem* 13(10):1416-1420.
387. Mei Y, Hahn AA, Hu S, & Yang X (2011) The USP19 deubiquitinase regulates the stability of c-IAP1 and c-IAP2. *The Journal of biological chemistry* 286(41):35380-35387.
388. Lu Y*, et al.* (2009) USP19 deubiquitinating enzyme supports cell proliferation by stabilizing KPC1, a ubiquitin ligase for p27Kip1. *Mol Cell Biol* 29(2):547-558.
389. Nakamura N, Harada K, Kato M, & Hirose S (2014) Ubiquitin-specific protease 19 regulates the stability of the E3 ubiquitin ligase MARCH6. *Exp Cell Res* 328(1):207-216.
390. Altun M*, et al.* (2012) Ubiquitin-specific protease 19 (USP19) regulates hypoxia-inducible factor 1alpha (HIF-1alpha) during hypoxia. *The Journal of biological chemistry* 287(3):1962-1969.
391. Velasco K*, et al.* (2013) An N-terminal SIAH-interacting motif regulates the stability of the ubiquitin specific protease (USP)-19. *Biochem Biophys Res Commun* 433(4):390-395.
392. Lee JG, Kim W, Gygi S, & Ye Y (2014) Characterization of the deubiquitinating activity of USP19 and its role in endoplasmic reticulum-associated degradation. *The Journal of biological chemistry* 289(6):3510-3517.
393. Lu Y, Bedard N, Chevalier S, & Wing SS (2010) Identification of distinctive patterns of USP19-mediated growth regulation in normal and malignant cells. *PLoS One* 6(1):e15936.

394. Combaret L*, et al.* (2005) USP19 is a ubiquitin-specific protease regulated in rat skeletal muscle during catabolic states. *American journal of physiology* 288(4):E693-700.
395. Sundaram P, Pang Z, Miao M, Yu L, & Wing SS (2009) USP19-deubiquitinating enzyme regulates levels of major myofibrillar proteins in L6 muscle cells. *American journal of physiology* 297(6):E1283-1290.
396. Ogawa M*, et al.* (2011) 17beta-estradiol represses myogenic differentiation by increasing ubiquitin-specific peptidase 19 through estrogen receptor alpha. *The Journal of biological chemistry* 286(48):41455-41465.
397. Wiles B*, et al.* (2015) USP19 deubiquitinating enzyme inhibits muscle cell differentiation by suppressing unfolded-protein response signaling. *Mol Biol Cell* 26(5):913-923.
398. Schwartz AL & Ciechanover A (1999) The ubiquitin-proteasome pathway and pathogenesis of human diseases. *Annu Rev Med* 50:57-74.
399. Ciechanover A & Schwartz AL (2004) The ubiquitin system: pathogenesis of human diseases and drug targeting. *Biochim Biophys Acta* 1695(1-3):3-17.
400. Nakayama KI & Nakayama K (2006) Ubiquitin ligases: cell-cycle control and cancer. *Nat Rev Cancer* 6(5):369-381.
401. Gstaiger M*, et al.* (2001) Skp2 is oncogenic and overexpressed in human cancers. *Proc Natl Acad Sci U S A* 98(9):5043-5048.
402. Signoretti S*, et al.* (2002) Oncogenic role of the ubiquitin ligase subunit Skp2 in human breast cancer. *J Clin Invest* 110(5):633-641.
403. Yang G*, et al.* (2002) Elevated Skp2 protein expression in human prostate cancer: association with loss of the cyclin-dependent kinase inhibitor p27 and PTEN and with reduced recurrence-free survival. *Clin Cancer Res* 8(11):3419-3426.
404. Strohmaier H*, et al.* (2001) Human F-box protein hCdc4 targets cyclin E for proteolysis and is mutated in a breast cancer cell line. *Nature* 413(6853):316-322.
405. Spruck CH*, et al.* (2002) hCDC4 gene mutations in endometrial cancer. *Cancer Res* 62(16):4535-4539.
406. Cassia R*, et al.* (2003) Cyclin E gene (CCNE) amplification and hCDC4 mutations in endometrial carcinoma. *J Pathol* 201(4):589-595.
407. Kwak EL*, et al.* (2005) Infrequent mutations of Archipelago (hAGO, hCDC4, Fbw7) in primary ovarian cancer. *Gynecol Oncol* 98(1):124-128.
408. Lee JW*, et al.* (2006) Mutational analysis of the hCDC4 gene in gastric carcinomas. *Eur J Cancer* 42(14):2369-2373.
409. Luise C*, et al.* (2011) An atlas of altered expression of deubiquitinating enzymes in human cancer. *PLoS One* 6(1):e15891.
410. Jensen DE*, et al.* (1998) BAP1: a novel ubiquitin hydrolase which binds to the BRCA1 RING finger and enhances BRCA1-mediated cell growth suppression. *Oncogene* 16(9):1097-1112.
411. Harbour JW*, et al.* (2010) Frequent mutation of BAP1 in metastasizing uveal melanomas. *Science* 330(6009):1410-1413.
412. Testa JR*, et al.* (2011) Germline BAP1 mutations predispose to malignant mesothelioma. *Nature genetics* 43(10):1022-1025.
413. Mochel MC, Piris A, Nose V, & Hoang MP (2015) Loss of BAP1 Expression in Basal Cell Carcinomas in Patients With Germline BAP1 Mutations. *Am J Clin Pathol* 143(6):901-904.
414. Li M*, et al.* (2002) Deubiquitination of p53 by HAUSP is an important pathway for p53 stabilization. *Nature* 416(6881):648-653.
415. Pan J*, et al.* (2015) USP37 directly deubiquitinates and stabilizes c-Myc in lung cancer. *Oncogene* 34(30):3957-3967.
416. Schwickart M*, et al.* (2010) Deubiquitinase USP9X stabilizes MCL1 and promotes tumour cell survival. *Nature* 463(7277):103-107.
417. Peddaboina C*, et al.* (2012) The downregulation of Mcl-1 via USP9X inhibition sensitizes solid tumors to Bcl-xl inhibition. *BMC Cancer* 12:541.
418. Perez-Mancera PA*, et al.* (2012) The deubiquitinase USP9X suppresses pancreatic ductal adenocarcinoma. *Nature* 486(7402):266-270.

419. Ciechanover A & Kwon YT (2015) Degradation of misfolded proteins in neurodegenerative diseases: therapeutic targets and strategies. *Exp Mol Med* 47:e147.
420. Sukari A, Muqbil I, Mohammad RM, Philip PA, & Azmi AS (2016) F-BOX proteins in cancer cachexia and muscle wasting: Emerging regulators and therapeutic opportunities. *Semin Cancer Biol* 36:95-104.
421. Popovic D, Vucic D, & Dikic I (2014) Ubiquitination in disease pathogenesis and treatment. *Nat Med* 20(11):1242-1253.
422. Ciechanover A (2010) Intracellular protein degradation: from a vague idea through the lysosome and the ubiquitin-proteasome system and onto human diseases and drug targeting. *Medicina (B Aires)* 70(2):105-119.
423. Burger AM & Seth AK (2004) The ubiquitin-mediated protein degradation pathway in cancer: therapeutic implications. *Eur J Cancer* 40(15):2217-2229.
424. Ande SR, Chen J, & Maddika S (2009) The ubiquitin pathway: an emerging drug target in cancer therapy. *Eur J Pharmacol* 625(1-3):199-205.
425. Liu J*, et al.* (2015) Targeting the ubiquitin pathway for cancer treatment. *Biochim Biophys Acta* 1855(1):50-60.
426. Wilk S & Figueiredo-Pereira ME (1993) Synthetic inhibitors of the multicatalytic proteinase complex (proteasome). *Enzyme Protein* 47(4-6):306-313.
427. Rock KL*, et al.* (1994) Inhibitors of the proteasome block the degradation of most cell proteins and the generation of peptides presented on MHC class I molecules. *Cell* 78(5):761-771.
428. Vinitsky A, Cardozo C, Sepp-Lorenzino L, Michaud C, & Orlowski M (1994) Inhibition of the proteolytic activity of the multicatalytic proteinase complex (proteasome) by substrate-related peptidyl aldehydes. *The Journal of biological chemistry* 269(47):29860-29866.
429. Iqbal M*, et al.* (1995) Potent inhibitors of proteasome. *J Med Chem* 38(13):2276-2277.
430. Lee DH & Goldberg AL (1998) Proteasome inhibitors: valuable new tools for cell biologists. *Trends Cell Biol* 8(10):397-403.
431. Lee DH & Goldberg AL (1998) Proteasome inhibitors cause induction of heat shock proteins and trehalose, which together confer thermotolerance in Saccharomyces cerevisiae. *Mol Cell Biol* 18(1):30-38.
432. Gronostajski RM, Pardee AB, & Goldberg AL (1985) The ATP dependence of the degradation of short- and long-lived proteins in growing fibroblasts. *The Journal of biological chemistry* 260(6):3344-3349.
433. Adams J (2004) The development of proteasome inhibitors as anticancer drugs. *Cancer Cell* 5(5):417-421.
434. Adams J (2004) The proteasome: a suitable antineoplastic target. *Nat Rev Cancer* 4(5):349-360.
435. Adams J & Kauffman M (2004) Development of the proteasome inhibitor Velcade (Bortezomib). *Cancer Invest* 22(2):304-311.
436. Almond JB & Cohen GM (2002) The proteasome: a novel target for cancer chemotherapy. *Leukemia* 16(4):433-443.
437. Buac D*, et al.* (2013) From bortezomib to other inhibitors of the proteasome and beyond. *Curr Pharm Des* 19(22):4025-4038.
438. Yang Y*, et al.* (2007) Inhibitors of ubiquitin-activating enzyme (E1), a new class of potential cancer therapeutics. *Cancer Res* 67(19):9472-9481.
439. Ceccarelli DF*, et al.* (2011) An allosteric inhibitor of the human Cdc34 ubiquitin-conjugating enzyme. *Cell* 145(7):1075-1087.
440. Soucy TA*, et al.* (2009) An inhibitor of NEDD8-activating enzyme as a new approach to treat cancer. *Nature* 458(7239):732-736.
441. Soucy TA, Smith PG, & Rolfe M (2009) Targeting NEDD8-activated cullin-RING ligases for the treatment of cancer. *Clin Cancer Res* 15(12):3912-3916.

442. Liao H*, et al.* (2011) Quantitative proteomic analysis of cellular protein modulation upon inhibition of the NEDD8-activating enzyme by MLN4924. *Mol Cell Proteomics* 10(11):M111 009183.
443. Aghajan M*, et al.* (2010) Chemical genetics screen for enhancers of rapamycin identifies a specific inhibitor of an SCF family E3 ubiquitin ligase. *Nat Biotechnol* 28(7):738-742.
444. Orlicky S*, et al.* (2010) An allosteric inhibitor of substrate recognition by the SCF(Cdc4) ubiquitin ligase. *Nat Biotechnol* 28(7):733-737.
445. Green DR & Kroemer G (2009) Cytoplasmic functions of the tumour suppressor p53. *Nature* 458(7242):1127-1130.
446. Chene P (2003) Inhibiting the p53-MDM2 interaction: an important target for cancer therapy. *Nat Rev Cancer* 3(2):102-109.
447. Pavletich NP, Chambers KA, & Pabo CO (1993) The DNA-binding domain of p53 contains the four conserved regions and the major mutation hot spots. *Genes Dev* 7(12B):2556-2564.
448. Chen J, Marechal V, & Levine AJ (1993) Mapping of the p53 and mdm-2 interaction domains. *Mol Cell Biol* 13(7):4107-4114.
449. Momand J, Zambetti GP, Olson DC, George D, & Levine AJ (1992) The mdm-2 oncogene product forms a complex with the p53 protein and inhibits p53-mediated transactivation. *Cell* 69(7):1237-1245.
450. Vassilev LT*, et al.* (2004) In vivo activation of the p53 pathway by small-molecule antagonists of MDM2. *Science* 303(5659):844-848.
451. Shangary S*, et al.* (2008) Temporal activation of p53 by a specific MDM2 inhibitor is selectively toxic to tumors and leads to complete tumor growth inhibition. *Proc Natl Acad Sci U S A* 105(10):3933-3938.
452. Zhuang C*, et al.* (2012) Discovery, synthesis, and biological evaluation of orally active pyrrolidone derivatives as novel inhibitors of p53-MDM2 protein-protein interaction. *J Med Chem* 55(22):9630-9642.
453. Colland F*, et al.* (2009) Small-molecule inhibitor of USP7/HAUSP ubiquitin protease stabilizes and activates p53 in cells. *Mol Cancer Ther* 8(8):2286-2295.
454. Reverdy C*, et al.* (2012) Discovery of specific inhibitors of human USP7/HAUSP deubiquitinating enzyme. *Chem Biol* 19(4):467-477.
455. Chauhan D*, et al.* (2012) A small molecule inhibitor of ubiquitin-specific protease-7 induces apoptosis in multiple myeloma cells and overcomes bortezomib resistance. *Cancer Cell* 22(3):345-358.
456. Kapuria V*, et al.* (2010) Deubiquitinase inhibition by small-molecule WP1130 triggers aggresome formation and tumor cell apoptosis. *Cancer Res* 70(22):9265-9276.
457. Liu H*, et al.* (2015) WP1130 increases doxorubicin sensitivity in hepatocellular carcinoma cells through usp9x-dependent p53 degradation. *Cancer Lett* 361(2):218-225.
458. Sun H*, et al.* (2011) Bcr-Abl ubiquitination and Usp9x inhibition block kinase signaling and promote CML cell apoptosis. *Blood* 117(11):3151-3162.
459. D'Arcy P*, et al.* (2011) Inhibition of proteasome deubiquitinating activity as a new cancer therapy. *Nat Med* 17(12):1636-1640.
460. Tian Z*, et al.* (2014) A novel small molecule inhibitor of deubiquitylating enzyme USP14 and UCHL5 induces apoptosis in multiple myeloma and overcomes bortezomib resistance. *Blood* 123(5):706-716.
461. Nalepa G, Rolfe M, & Harper JW (2006) Drug discovery in the ubiquitin-proteasome system. *Nat Rev Drug Discov* 5(7):596-613.
462. Verma R*, et al.* (2004) Ubistatins inhibit proteasome-dependent degradation by binding the ubiquitin chain. *Science* 306(5693):117-120.
463. Shen M, Schmitt S, Buac D, & Dou QP (2013) Targeting the ubiquitin-proteasome system for cancer therapy. *Expert Opin Ther Targets* 17(9):1091-1108.
464. Lill JR & Wertz IE (2014) Toward understanding ubiquitin-modifying enzymes: from pharmacological targeting to proteomics. *Trends Pharmacol Sci* 35(4):187-207.

465. Zhang W & Sidhu SS (2014) Development of inhibitors in the ubiquitination cascade. *FEBS Lett* 588(2):356-367.
466. Hideshima T*, et al.* (2001) The proteasome inhibitor PS-341 inhibits growth, induces apoptosis, and overcomes drug resistance in human multiple myeloma cells. *Cancer Res* 61(7):3071-3076.
467. Guzman ML*, et al.* (2002) Preferential induction of apoptosis for primary human leukemic stem cells. *Proc Natl Acad Sci U S A* 99(25):16220-16225.
468. Stapnes C*, et al.* (2007) The proteasome inhibitors bortezomib and PR-171 have antiproliferative and proapoptotic effects on primary human acute myeloid leukaemia cells. *Br J Haematol* 136(6):814-828.
469. Bross PF*, et al.* (2004) Approval summary for bortezomib for injection in the treatment of multiple myeloma. *Clin Cancer Res* 10(12 Pt 1):3954-3964.
470. Herndon TM*, et al.* (2013) U.s. Food and Drug Administration approval: carfilzomib for the treatment of multiple myeloma. *Clin Cancer Res* 19(17):4559-4563.
471. Kane RC, Farrell AT, Sridhara R, & Pazdur R (2006) United States Food and Drug Administration approval summary: bortezomib for the treatment of progressive multiple myeloma after one prior therapy. *Clin Cancer Res* 12(10):2955-2960.
472. Richardson PG*, et al.* (2003) A phase 2 study of bortezomib in relapsed, refractory myeloma. *N Engl J Med* 348(26):2609-2617.
473. Richardson PG*, et al.* (2005) Bortezomib or high-dose dexamethasone for relapsed multiple myeloma. *N Engl J Med* 352(24):2487-2498.
474. Druker BJ*, et al.* (2001) Efficacy and safety of a specific inhibitor of the BCR-ABL tyrosine kinase in chronic myeloid leukemia. *N Engl J Med* 344(14):1031-1037.
475. Dou QP, McGuire TF, Peng Y, & An B (1999) Proteasome inhibition leads to significant reduction of Bcr-Abl expression and subsequent induction of apoptosis in K562 human chronic myelogenous leukemia cells. *J Pharmacol Exp Ther* 289(2):781-790.
476. Gorre ME, Ellwood-Yen K, Chiosis G, Rosen N, & Sawyers CL (2002) BCR-ABL point mutants isolated from patients with imatinib mesylate-resistant chronic myeloid leukemia remain sensitive to inhibitors of the BCR-ABL chaperone heat shock protein 90. *Blood* 100(8):3041-3044.
477. Tsukahara F & Maru Y (2010) Bag1 directly routes immature BCR-ABL for proteasomal degradation. *Blood* 116(18):3582-3592.
478. Thalhammer V*, et al.* (2015) PLK1 phosphorylates PAX3-FOXO1, the inhibition of which triggers regression of alveolar Rhabdomyosarcoma. *Cancer Res* 75(1):98-110.
479. Clark J*, et al.* (2007) Diversity of TMPRSS2-ERG fusion transcripts in the human prostate. *Oncogene* 26(18):2667-2673.
480. Tomlins SA*, et al.* (2008) Role of the TMPRSS2-ERG gene fusion in prostate cancer. *Neoplasia* 10(2):177-188.
481. Carver BS*, et al.* (2009) Aberrant ERG expression cooperates with loss of PTEN to promote cancer progression in the prostate. *Nature genetics* 41(5):619-624.
482. An J*, et al.* (2015) Truncated ERG Oncoproteins from TMPRSS2-ERG Fusions Are Resistant to SPOP-Mediated Proteasome Degradation. *Mol Cell* 59(6):904-916.
483. Gan W*, et al.* (2015) SPOP Promotes Ubiquitination and Degradation of the ERG Oncoprotein to Suppress Prostate Cancer Progression. *Mol Cell* 59(6):917-930.
484. Wang S*, et al.* (2014) Ablation of the oncogenic transcription factor ERG by deubiquitinase inhibition in prostate cancer. *Proc Natl Acad Sci U S A* 111(11):4251-4256.
485. Vitari AC*, et al.* (2011) COP1 is a tumour suppressor that causes degradation of ETS transcription factors. *Nature* 474(7351):403-406.
486. Rego EM, He LZ, Warrell RP, Jr., Wang ZG, & Pandolfi PP (2000) Retinoic acid (RA) and As2O3 treatment in transgenic models of acute promyelocytic leukemia (APL) unravel the distinct nature of the leukemogenic process induced by the PML-RARalpha and PLZF-RARalpha oncoproteins. *Proc Natl Acad Sci U S A* 97(18):10173-10178.

487. Yoshida H*, et al.* (1996) Accelerated degradation of PML-retinoic acid receptor alpha (PML-RARA) oncoprotein by all-trans-retinoic acid in acute promyelocytic leukemia: possible role of the proteasome pathway. *Cancer Res* 56(13):2945-2948.
488. Koken MH*, et al.* (1999) Retinoic acid, but not arsenic trioxide, degrades the PLZF/RARalpha fusion protein, without inducing terminal differentiation or apoptosis, in a RA-therapy resistant t(11;17)(q23;q21) APL patient. *Oncogene* 18(4):1113-1118.
489. Zhu J*, et al.* (1999) Retinoic acid induces proteasome-dependent degradation of retinoic acid receptor alpha (RARalpha) and oncogenic RARalpha fusion proteins. *Proc Natl Acad Sci U S A* 96(26):14807-14812.
490. He LZ*, et al.* (1998) Distinct interactions of PML-RARalpha and PLZF-RARalpha with co-repressors determine differential responses to RA in APL. *Nature genetics* 18(2):126-135.
491. Duprez E*, et al.* (1999) SUMO-1 modification of the acute promyelocytic leukaemia protein PML: implications for nuclear localisation. *J Cell Sci* 112 (Pt 3):381-393.
492. Rabellino A*, et al.* (2012) The SUMO E3-ligase PIAS1 regulates the tumor suppressor PML and its oncogenic counterpart PML-RARA. *Cancer Res* 72(9):2275-2284.
493. Zhu J*, et al.* (2005) A sumoylation site in PML/RARA is essential for leukemic transformation. *Cancer Cell* 7(2):143-153.
494. Lallemand-Breitenbach V*, et al.* (2008) Arsenic degrades PML or PML-RARalpha through a SUMO-triggered RNF4/ubiquitin-mediated pathway. *Nat Cell Biol* 10(5):547-555.
495. Tatham MH*, et al.* (2008) RNF4 is a poly-SUMO-specific E3 ubiquitin ligase required for arsenic-induced PML degradation. *Nat Cell Biol* 10(5):538-546.
496. Shen ZX*, et al.* (2004) All-trans retinoic acid/As2O3 combination yields a high quality remission and survival in newly diagnosed acute promyelocytic leukemia. *Proc Natl Acad Sci U S A* 101(15):5328-5335.
497. Wang ZY & Chen Z (2008) Acute promyelocytic leukemia: from highly fatal to highly curable. *Blood* 111(5):2505-2515.
498. Kovar H (2014) Blocking the road, stopping the engine or killing the driver? Advances in targeting EWS/FLI-1 fusion in Ewing sarcoma as novel therapy. *Expert Opin Ther Targets* 18(11):1315-1328.
499. Kronke J*, et al.* (2015) Lenalidomide induces ubiquitination and degradation of CK1alpha in del(5q) MDS. *Nature* 523(7559):183-188.
500. Kronke J*, et al.* (2014) Lenalidomide causes selective degradation of IKZF1 and IKZF3 in multiple myeloma cells. *Science* 343(6168):301-305.
501. Mullard A (2012) Next-generation proteasome blockers promise safer cancer therapy. *Nat Med* 18(1):7.
502. Lydeard JR & Harper JW (2010) Inhibitors for E3 ubiquitin ligases. *Nat Biotechnol* 28(7):682-684.
503. Cohen P & Tcherpakov M (2010) Will the ubiquitin system furnish as many drug targets as protein kinases? *Cell* 143(5):686-693.
504. Ito T*, et al.* (2010) Identification of a primary target of thalidomide teratogenicity. *Science* 327(5971):1345-1350.
505. Fischer ES*, et al.* (2014) Structure of the DDB1-CRBN E3 ubiquitin ligase in complex with thalidomide. *Nature* 512(7512):49-53.
506. Mistry H*, et al.* (2013) Small-molecule inhibitors of USP1 target ID1 degradation in leukemic cells. *Mol Cancer Ther* 12(12):2651-2662.
507. Buckley DL & Crews CM (2014) Small-molecule control of intracellular protein levels through modulation of the ubiquitin proteasome system. *Angew Chem Int Ed Engl* 53(9):2312-2330.
508. Neklesa TK*, et al.* (2011) Small-molecule hydrophobic tagging-induced degradation of HaloTag fusion proteins. *Nat Chem Biol* 7(8):538-543.
509. Neklesa TK*, et al.* (2013) A bidirectional system for the dynamic small molecule control of intracellular fusion proteins. *ACS Chem Biol* 8(10):2293-2300.

510. Sakamoto KM*, et al.* (2001) Protacs: chimeric molecules that target proteins to the Skp1-Cullin-F box complex for ubiquitination and degradation. *Proc Natl Acad Sci U S A* 98(15):8554-8559.
511. Sakamoto KM*, et al.* (2003) Development of Protacs to target cancer-promoting proteins for ubiquitination and degradation. *Mol Cell Proteomics* 2(12):1350-1358.
512. Rodriguez-Gonzalez A*, et al.* (2008) Targeting steroid hormone receptors for ubiquitination and degradation in breast and prostate cancer. *Oncogene* 27(57):7201-7211.
513. Schneekloth AR, Pucheault M, Tae HS, & Crews CM (2008) Targeted intracellular protein degradation induced by a small molecule: En route to chemical proteomics. *Bioorg Med Chem Lett* 18(22):5904-5908.
514. Lai AC*, et al.* (2016) Modular PROTAC Design for the Degradation of Oncogenic BCR-ABL. *Angew Chem Int Ed Engl* 55(2):807-810.
515. Toure M & Crews CM (2016) Small-Molecule PROTACS: New Approaches to Protein Degradation. *Angew Chem Int Ed Engl* 55(6):1966-1973.
516. Ablain J, Nasr R, Bazarbachi A, & de The H (2011) The drug-induced degradation of oncoproteins: an unexpected Achilles' heel of cancer cells? *Cancer Discov* 1(2):117-127.
517. Mori S*, et al.* (2015) Age and dPCR can predict relapse in CML patients who discontinued imatinib: the ISAV study. *Am J Hematol* 90(10):910-914.
518. Goto E*, et al.* (2011) Missense mutations in PML-RARA are critical for the lack of responsiveness to arsenic trioxide treatment. *Blood* 118(6):1600-1609.
519. Liu J, Zhu HH, Jiang H, Jiang Q, & Huang XJ (2016) Varying responses of PML-RARA with different genetic mutations to arsenic trioxide. *Blood* 127(2):243-250.
520. Zhu HH, Qin YZ, & Huang XJ (2014) Resistance to arsenic therapy in acute promyelocytic leukemia. *N Engl J Med* 370(19):1864-1866.
521. Wang X*, et al.* (2016) LG-362B targets PML-RARalpha and blocks ATRA resistance of acute promyelocytic leukemia. *Leukemia*.
522. Williamson A, Werner A, & Rape M (2013) The Colossus of ubiquitylation: decrypting a cellular code. *Mol Cell* 49(4):591-600.
523. Yen HC & Elledge SJ (2008) Identification of SCF ubiquitin ligase substrates by global protein stability profiling. *Science* 322(5903):923-929.
524. Yen HC, Xu Q, Chou DM, Zhao Z, & Elledge SJ (2008) Global protein stability profiling in mammalian cells. *Science* 322(5903):918-923.
525. Osula O, Swatkoski S, & Cotter RJ (2012) Identification of protein SUMOylation sites by mass spectrometry using combined microwave-assisted aspartic acid cleavage and tryptic digestion. *J Mass Spectrom* 47(5):644-654.
526. Kaypee S*, et al.* (2016) Aberrant lysine acetylation in tumorigenesis: Implications in the development of therapeutics. *Pharmacol Ther*.
527. Vaquerizas JM, Kummerfeld SK, Teichmann SA, & Luscombe NM (2009) A census of human transcription factors: function, expression and evolution. *Nat Rev Genet* 10(4):252-263.
528. Bhatia K*, et al.* (1993) Point mutations in the c-Myc transactivation domain are common in Burkitt's lymphoma and mouse plasmacytomas. *Nature genetics* 5(1):56-61.
529. Clark HM*, et al.* (1994) Mutations in the coding region of c-MYC in AIDS-associated and other aggressive lymphomas. *Cancer Res* 54(13):3383-3386.
530. Salghetti SE, Kim SY, & Tansey WP (1999) Destruction of Myc by ubiquitin-mediated proteolysis: cancer-associated and transforming mutations stabilize Myc. *EMBO J* 18(3):717-726.
531. Muratani M & Tansey WP (2003) How the ubiquitin-proteasome system controls transcription. *Nat Rev Mol Cell Biol* 4(3):192-201.
532. Reid G*, et al.* (2003) Cyclic, proteasome-mediated turnover of unliganded and liganded ERalpha on responsive promoters is an integral feature of estrogen signaling. *Mol Cell* 11(3):695-707.
533. Jaenicke LA*, et al.* (2016) Ubiquitin-Dependent Turnover of MYC Antagonizes MYC/PAF1C Complex Accumulation to Drive Transcriptional Elongation. *Mol Cell* 61(1):54-67.

534. Yao J, Munson KM, Webb WW, & Lis JT (2006) Dynamics of heat shock factor association with native gene loci in living cells. *Nature* 442(7106):1050-1053.
535. Kodadek T, Sikder D, & Nalley K (2006) Keeping transcriptional activators under control. *Cell* 127(2):261-264.
536. Hjerpe R, Thomas Y, & Kurz T (2012) NEDD8 overexpression results in neddylation of ubiquitin substrates by the ubiquitin pathway. *J Mol Biol* 421(1):27-29.
537. Yang WC & Shih HM (2013) The deubiquitinating enzyme USP37 regulates the oncogenic fusion protein PLZF/RARA stability. *Oncogene* 32(43):5167-5175.

9. Acknowledgements

First, I would especially like to thank Prof. Beat Schäfer for the opportunity to join his laboratory to perform my PhD work, for support and guidance in a project related to my two greatest interests in research. I very much appreciated all the great research possibilities in the laboratory and the freedom to follow all the ideas during the years.

Further, I would like to thank my thesis committee members and evaluators Prof. Wolfgang Dubiel, PD Stefano Ferrari and Prof. Felix Niggli for continuous support and helpful comments during the years. The meetings have been full of productive discussions and helpful advices for experiments and the structure of the project.

It has been a great pleasure to have guided such a talented Master student as Franziska Pfistner who later became my closest colleague in the ubiquitin research and in the laboratory. Many thanks for infinite discussions, helpful support and dreaming of what could be possible.

I would like to express my special gratitude to all the past and present Ewing laboratory members Dr. Aleksandar Boro, Chiara Giorgi, Franziska Pfistner, Gloria Pedot, Dr. Laura Lopez-Garcia, Dr. Lilian Quero, Natalie Streiff and Stefanie Lang for their contributions and creative environment. Especially over the last years, it has become such a supportive team. It has been a great honor to be one of the Ewing girls for so long now.

My sincere thanks also goes to my both friends and colleagues Patricia Jaaks and Nagjie Alijaj for always being there for me and for the support in the difficult and in the good times. I would also like to thank Dr. Marco Wachtel for all the great solutions he provided for any upcoming challenge. Moreover, I would like to acknowledge all my other colleagues from the Schäfer lab and the EICR department for all the help I received within the last years and every discussion during that time.

At the end I would like to express my deepest appreciation to the most important people in my life: to my parents, my brother and my boyfriend. My family has been a constant support and inspiration to me from the beginning till now.

10. Appendix

Curriculum vitae

Personal data

Name	Maria Elka Gierisch
Date/ place of birth	23rd July 1986 in Berlin, Germany
Nationality	German
Current position	PhD student Children's Hospital Zurich, Switzerland Department of Oncology
Working address	August-Forel-Strasse 1, 8008 Zurich, Switzerland
Private address	Baumackerstrasse 45, 8050 Zurich, Switzerland
E- Mail	maria.gierisch@gmail.com

Education and training

Since Nov 2011 **PhD student**
Group of Prof. Dr. Beat Schäfer
Department of Oncology, Children's Hospital Zurich, Switzerland
Cancer Biology PhD program, University of Zurich

Thesis: "Proteasomal turnover of EWS/FLI1 fusion protein in Ewing sarcoma: Implications as a novel therapeutic strategy"
Date of defense: July 2016

Oct 2009 - Sep 2011 **Master's Program of Molecular Medicine**
University Hospital Charité Berlin, Germany

Feb - Sep 11 **Master Thesis**
Group of Prof. Dr. Wolfgang Dubiel
Department of Experimental Surgery, University Hospital Charité, Germany

Title: "Influence of CAND1 on the composition of COP9 signalosome-based supercomplexes and regulators of adipogenesis"

Sep - Dec 10 3rd laboratory rotation at group of PD Dr. Savaskan
Institute for Cell- and Neurobiology, Charité, Germany
"Targeting the cancer metabolism: oxidative glycolysis and beyond"

Apr - Jul 10 2nd laboratory rotation at group of Prof. Dr. Herzel
Institute for Theoretical Biology, Humboldt University Berlin, Germany
"Analysis of ChIP data to elucidate transcriptional regulation of clock-controlled genes"

Oct 09 - Feb 10 1st laboratory rotation at group of PD Dr. Strowski
Clinic for Hepatology and Gastroenterology, Charité, Germany
"Orexin A stimulation of lipogenesis and adiponectin expression in adipocytes"

Oct 2006 - Sep 2009	**Biology, Bachelor of Science** Humboldt University Berlin, Germany
Feb - Aug 09	**Bachelor Thesis** Group of PD Dr. A. Lukowsky Department of Dermatology, Charité, Germany *Title:* "Clonality Analysis of Patients with Cutaneous T-Cell Lymphomas"
Aug 2000 - Jul 2006	Linus-Pauling-Gymnasium Berlin, Germany Abitur

Teaching experience

Jul 14 - Aug 15	Supervisor Master Thesis, Biology student, University of Zürich
Nov 12 + Nov 13	Course assistance "Cancer Cell Motility", University of Zurich
Oct 08 - Mar 11	Seminars "Mathematics in Biology", assistance with exam supervision and corrections, Institute for Theoretical Biology, Humboldt University, Germany

Competences

Languages	German (mother tongue), English (fluent), French (basic)
Computer competences	Good commands in Microsoft Office (Word, Excel, Powerpoint). Adobe Creative Suite (Photoshop, Illustrator), Clone Manger, PrismGraphpad, dChip, ImageJ Basic knowledge in GnuR, Latex
FELASA, category B	Course for Animal Experimentation, University of Zurich

Grants

Oct 15	Travel Grant Cancer PhD program, UZH, Zurich, Switzerland
	EMBO Conference "Ubiquitin and ubiquitin-like modifiers" Sep 2015
Aug 15	Travel Grant Hartmann-Müller-Stiftung, Zurich, Switzerland
	AACR Apr 2015

Conferences and talks

International conferences

Apr 2016 7th Proteasome and Autophagy Workshop, Clermont-Ferrand, France
Talk (selected short communication) + Poster: "Proteasomal turnover controls oncogenic activity of the EWS/FLI1 fusion protein: Implications as a novel therapeutic strategy"

Sep 2015 EMBO conference "Ubiquitin and ubiquitin-like modifiers: From molecular mechanisms to human diseases", Cavtat, Croatia
Poster: "Identification of deubiquitinating enzyme USP19 as a regulator of EWS/FLI1 protein turnover in Ewing sarcoma"

Apr 2015 AACR Annual Meeting, Philadelphia, USA
Poster: "Identification of deubiquitinating enzyme USP19 as a regulator of EWS/FLI1 protein turnover in Ewing sarcoma"

Aug 2014 Benzon Symposium "Nuclear Regulation by Ubiquitin", Copenhagen, Denmark
Poster: "Targeting the turnover: Diminish EWS/FLI1 protein level by ubiquitin-proteasome-system (UPS) dependent degradation in Ewing sarcoma"

Public communications:

March 2016 Joint Cancer Meeting, Cancer Network Zurich
Talk: "Proteasomal turnover of the EWS/FLI1 fusion protein: Implications for novel therapeutic strategies in Ewing sarcoma"

March 2016 Colloquium of Applied Cancer Research, University Hospital Zurich
Talk: "Proteasomal turnover of the EWS/FLI1 fusion protein: Implications for novel therapeutic strategies in Ewing sarcoma"

May 2015 Colloquium of Applied Cancer Research, University Hospital Zurich
Talk: "Understanding EWS/FLI1 fusion protein turnover and its impact in Ewing sarcoma pathogenesis"

Nov 2013 Colloquium of Applied Cancer Research, University Hospital Zurich
Talk: "Deregulated Turnover of EWS/FLI1 fusion protein in Ewing Sarcoma Pathogenesis"

Cancer Biology PhD program and Cancer Network retreats:

Feb 2014 Cancer Biology PhD retreat
Linh, Switzerland
Poster: "Involvement of components of the ubiquitin-proteasome-system in Ewing sarcoma pathogenesis"

Apr 2013 Cancer Network Zurich retreat
Grindelwald, Switzerland
Poster: "Deregulated Turnover of EWS/FLI1 fusion protein in Ewing Sarcoma"

Publication list:

1. **Gierisch ME**, Pedot G, Pfistner F, Lopez-Garcia LA, Jaaks P, Schäfer BW, Niggli FK
   "EWS-FLI1 protein destabilization by the deubiquitinating enzyme USP19 as a novel treatment strategy in Ewing sarcoma"
   Cancer Res. submitted 2016

2. **Gierisch ME**, Pfistner F, Lopez-Garcia LA, Harder L, Schäfer BW, Niggli FK
   "Proteasomal degradation of the EWS-FLI1 fusion protein is regulated by a single lysine residue"
   J Biol Chem. 2016 Nov 8. pii: jbc.M116.752063

3. Giorgi C, Boro A, Rechfeld F, Lopez-Garcia LA, **Gierisch ME**, Schäfer BW, Niggli FK
   "PI3K/AKT signaling modulates transcriptional expression of EWS/FLI1 through specificity protein 1"
   Oncotarget 2015 Oct 6;6(30):28895-910

4. Thalhammer V, Lopez-Garcia LA, Herrero-Martin D, Hecker R, Laubscher D, **Gierisch ME,** Wachtel M, Bode P, Nanni P, Blank B, Koscielniak E, Schäfer BW
   "PLK1 Phosphorylates PAX3-FOXO1, the Inhibition of Which Triggers Regression of Alveolar Rhabdomyosarcoma"
   Cancer Res. 2015 Jan 1;75(1):98-110

5. Humme D, Lukowsky A, **Gierisch M**, Haider A, Vandersee S, Assaf C, Sterry W, Möbs M, Beyer M
   "T-cell receptor gene rearrangement analysis of sequential biopsies in cutaneous T-cell lymphomas with the Biomed-2 PCR reveals transient T-cell clones in addition to the tumor clone"
   Exp Dermatol. 2014 Jul;23(7):504-8

6. Dubiel D**, Gierisch ME**, Huang X, Dubiel W, Naumann M
   "CAND1-dependent control of cullin 1-RING Ub ligases is essential for adipogenesis"
   Biochim Biophys Acta 2013 May;1833(5):1078-84